Thèse en cotutelle avec
L'Université de Borås, (Suède) et l' Université de Soochow (Chine)

Luminescent textiles using biobased products – A bioinspired approach

Textiles luminescents utilisant des produits biosourcés - Une approche bio-inspirée

Présentée par:

SWETA IYER

Pour obtenir le grade de Docteur de l'Université de Lille

Spécialité: Mécanique Energétique Matériaux

Soutenue le 25 septembre 2020 devant la commission d'examen composée de:

Georg GUBITZ	Professeur, BOKU University, Austria	Rapporteur
Bhuvanesh GUPTA	Professeur, IIT Delhi, India	Rapporteur
Renato ROIDEVEAUX	Professeur, University of Lille, France	Examinateur
Frank HOLLMANN	Professeur, TU Delft, Netherlands	Examinateur
Lieva Van LANGENHOVE	Professeur, Ghent University, Belgium	Examinateur
Chuanxiang QIN	Associate Professeure, Soochow University, China	Examinateur
Nemeshwaree BEHARY	Associate Professeure, HDR, ENSAIT, France	Directeur de thèse
Vincent NIERSTRASZ	Professeur, Universiry of Borås, Sweden	Co-directeur de thèse
Jinping GUAN	Associate Professeure, Soochow University, China	Invite

Luminescent textiles using biobased products – A bioinspired approach

Luminescent textiles using biobased products – A bioinspired approach

Abstract

Nature is the most exquisite thing around us with the existence of living organisms exhibiting different intrinsic properties such as water repellence, camouflage behavior, pine cone effect, and touch-sensitive plants. Transfer of knowledge inspired by nature to technological applications has enabled scientists to create sustainable solutions. Nature has designed a few biobased molecules that are responsible for bioluminescence and photoluminescence in some living species. In this thesis, the potential use of luminescence phenomena existing in nature toward the attainment of luminescent textiles was explored.

The primary focus of the thesis was to create a biomimetic design method to obtain luminescent textiles using biobased products. Thus, the design method was focused on the selection of optimum bioluminescent reaction systems to emulate on textiles. In the first part of the thesis, a detailed literature study on luminescence phenomena seen in nature was reviewed. The results of the literature study allowed to form the selection of luminous bacteria reaction system depending upon the availability, regeneration of the substrate, and cost. The selected 'luminous bacteria' bioluminescent system involves two enzyme(s) bacterial luciferase (Luc) and NAD(P)H: FMN oxidoreductase (FMN reductase), a biobased substrate flavin mononucleotide (FMN) along with co-factor such as NADH and long-chain aldehyde. Eco technologies such as air atmospheric plasma and cold remote plasma treatment were used for textile activation and enzyme immobilization. Primarily, the catalytic activity and luminescence efficiency of the luminous bacteria system were evaluated and optimized in the aqueous phase, by intensity measurements using a luminometer. Furthermore, the optimized reaction system was incorporated onto textiles to evaluate the bioluminescence effect. The evaluation of the bioluminescent system on textiles showed that the relative light intensity (RLU) as high as 60,000 RLU equivalent to that of LED light could be achieved. The study revealed its first successful attempt to utilize a biomimetic strategy for immobilization of enzyme(s) involved in the luminous bacteria reaction system onto a plasma-activated microfibrous nonwoven textile to attain biomimetic/bio luminescent materials that can be used for various applications such as biosensors, biomedical, safety and aesthetic use.

Furthermore, the inherent photoluminescence property of biobased molecules riboflavin (RF) and flavin mononucleotide (FMN) was explored with an aim to obtain multifunctional photoluminescent textiles. Hence, with the emulation and design to obtain biomimetic luminescent textiles/bioluminescent materials using FMN as a substrate in the enzymatic process, the potential use of native RF and its derivative FMN molecule to obtain photoluminescent textiles were also studied.

Cellulosic, polyester, silk, and wool-based photoluminescent textiles were obtained using traditional methods such as diffusion, screen printing, coating, and also using resource-efficient digital printing techniques. The study allowed to achieve biobased photoluminescent cellulosic textiles using the diffusion technique exhibiting greenish-yellow fluorescence on textiles, and corresponding quantum efficiencies were determined. In addition to the photoluminescent property, the RF and FMN treated textiles also exhibited multifunctional properties such as UV protection and coloration. Later, the ability of FMN to impart photoluminescent textiles was explored using inkjet and chromojet (digital printing techniques) on different textile materials such as cotton, mercerized cotton, and PET woven samples. The use of the digital printing technique allowed the textile to exhibit an antibacterial effect along with the photoluminescence, quantum efficiency, coloration, and UV protection properties. Furthermore, the photodegradation study of FMN on printed textiles resulted in varying fluorescence intensity from yellow, blue to white fluorescence. Thereafter, glow-in-dark patterned PET nonwoven panels were designed using screen printing and coating methods with which textile surface pattern designers may create light-emitting textiles and interesting aesthetic expressions. Hence, the study enabled to explore the use of biobased products to produce photoluminescent and bioluminescent textiles using functionalization and eco-technological methods.

Textiles luminescents utilisant des produits biosourcés - Une approche bio-inspirée

Résumé

La nature est la chose la plus exquise qui nous entoure avec l'existence d'organismes vivants présentant différentes propriétés intrinsèques telles que l'hydrofugation, le comportement de camouflage, l'effet de la pomme de pin et les plantes sensibles au toucher. Le transfert de connaissances inspirées par la nature vers des applications technologiques a permis aux scientifiques de créer des solutions durables. La nature a conçu quelques molécules biosourcées responsables de la bioluminescence et de la photoluminescence chez certaines espèces vivantes. Dans cette thèse, l'utilisation potentielle des phénomènes de luminescence existant dans la nature vers la réalisation de textiles luminescents a été explorée.

L'objectif principal de la thèse était de créer une méthode de conception biomimétique pour obtenir des textiles luminescents en utilisant des produits biosourcés. Ainsi, la méthode de conception s'est concentrée sur la sélection de systèmes de réaction bioluminescents optimaux à imiter avec les textiles. Dans la première partie de la thèse, une étude détaillée de la littérature sur les phénomènes de luminescence observés dans la nature a été revue. Les résultats de l'étude de la littérature ont permis de former la sélection du système de réaction des bactéries lumineuses en fonction de la disponibilité, de la régénération du substrat et du coût. La réaction bioluminescente des «bactéries lumineuses» sélectionnée implique deux enzymes, la luciférase bactérienne (Luc) et la NAD(P)H: FMN oxidoréductase (FMN réductase), un mononucléotide de flavine de substrat biosourcé (FMN) ainsi qu'un cofacteur tel que le NADH et l'aldéhyde à longue chaîne. Des écotechnologies telles que le plasma atmosphérique atmosphérique et le traitement plasma à distance à froid ont été utilisées pour l'activation textile et l'immobilisation enzymatique. Principalement, l'activité catalytique et l'efficacité de luminescence du système de bactéries lumineuses ont été évaluées et optimisées dans la phase aqueuse, par des mesures d'intensité à l'aide d'un luminomètre. De plus, le système de réaction optimisé a été incorporé aux textiles pour évaluer l'effet de bioluminescence. L'évaluation du système bioluminescent sur les textiles a montré que l'intensité lumineuse relative (RLU) aussi élevée que 60,000 RLU équivalente à celle de la lumière LED pouvait être atteinte. L'étude a révélé sa première tentative réussie d'utiliser une stratégie biomimétique pour l'immobilisation d'enzyme (s) impliquées dans le système de réaction des bactéries lumineuses sur un textile non tissé microfibreux activé par plasma pour atteindre des matériaux bioluminescents qui peuvent être utilisés pour diverses applications telles que les biocapteurs, biomédicaux , sécurité et usage esthétique.

En outre, la propriété de photoluminescence inhérente aux molécules biosourcées riboflavine (RF) et flavine mononucléotide (FMN) a été explorée dans le but d'obtenir des textiles photoluminescents

multifonctionnels. Par conséquent, avec l'émulation et la conception pour obtenir des textiles luminescents biomimétiques / des matériaux bioluminescents en utilisant le FMN comme substrat dans le processus enzymatique, l'utilisation potentielle de RF native et de sa molécule FMN dérivée pour obtenir des textiles photoluminescents a également été étudiée.

Les textiles photoluminescents cellulosiques, en polyester, en soie et en laine ont été obtenus en utilisant des méthodes traditionnelles telles que la diffusion, la sérigraphie, le revêtement ; mais aussi en utilisant des techniques d'impression numérique économes en ressources. L'étude a permis de réaliser des textiles cellulosiques photoluminescents biosourcés en utilisant une technique de diffusion présentant une fluorescence jaune verdâtre sur les textiles et les rendements quantiques correspondants ont été déterminés. En plus de la propriété photoluminescente, les textiles traités RF et FMN présentaient également des propriétés multifonctionnelles telles que la protection UV et la coloration. Plus tard, la capacité de la FMN à conférer des textiles photoluminescents a été explorée en utilisant le jet d'encre et le chromojet (techniques d'impression numérique) sur différents matériaux textiles tels que le coton, le coton mercerisé et les échantillons tissés en PET. L'utilisation de la technique d'impression numérique a permis au textile de présenter un effet antibactérien avec les propriétés de photoluminescence, d'efficacité quantique, de coloration et de protection UV. De plus, l'étude de photodégradation du FMN sur les textiles imprimés a entraîné une variation de l'intensité de fluorescence de la fluorescence jaune, bleue à blanche. Par la suite, des panneaux non tissés en PET à motifs luminescents ont été conçus en utilisant des méthodes de sérigraphie et de revêtement avec lesquelles les concepteurs de motifs de surface textile peuvent créer des textiles émettant de la lumière et des expressions esthétiques intéressantes. Par conséquent, l'étude a permis d'explorer l'utilisation de produits biosourcés pour produire des textiles photoluminescents et bioluminescents en utilisant des méthodes de fonctionnalisation et éco-technologiques.

Mots-clés: Bioinspiré, biosourcé, bioluminescent, photoluminescent, textile, bactéries lumineuses, enzymes, immobilisation, plasma, riboflavine, flavine mononucléotide, durable, d'impression digitale, fonctionnalisation.

Luminiscens textilier med biobaserade produkter - En bioinspirerad strategi

Abstrakt

Naturen är det mest enastående omkring oss med förekomsten av levande organismer som uppvisar olika inneboende egenskaper så som vattenavvisning, kamouflerande beteende, "pine cone" effekt, och växter känsliga för beröring. Överföringen av kunskap inspirerad av naturen till tekniska applikationer har gjort det möjligt för forskare att skapa hållbara lösningar. Naturen har utformat biobaserade molekyler som ansvarar för bioluminescens och fotoluminiscens i vissa levande arter. I den här avhandlingen utforskades den potentiella användningen av luminiscensfenomen som existerar i naturen för att uppnå luminiscens/självlysande textilier.

Avhandlingens främsta fokus var att skapa en biomimetisk designmetod för att erhålla självlysande textilier genom användningen av biobaserade produkter. Därför var designmetoden inriktad på valet av optimala bioluminiscerande reaktionssystem för att reproducera på textilier. I avhandlingens första del granskades de luminiscensfenomen som finns i naturen i en detaljerad litteraturstudie. Resultaten från litteraturstudien möjliggjorde valet av bakteriereaktionssystem baserat på tillgängligheten, substratets regeneration och kostnaden. Det utvalda bioluminiscens systemet för "lysande bakterier" involverar två enzym, bakteriell luciferas (Luc) och NAD(P)H: FMN oxidoreduktas (FMN reduktas) och ett biobaserat substrat flavin mononukleotid (FMN) tillsammans med en samfaktor som NADH och långkedjig aldehyd. Ekoteknologier såsom atmosfärisk plasma och kall fjärr-plasmabehandling användes för aktiveringen av textilen och för enzym immobilisering. Primärt utvärderades och optimerades den katalytiska aktiviteten och luminescenseffektiviteten hos bakteriesystemet i vätskefas genom intensitetsmätningar med hjälp av en luminometer. Vidare inkorporerades det optimerade reaktionssystemet på textilier för att utvärdera bioluminescenseffekten. Utvärderingen visade att den relativa ljusintensiteten (RLU) så hög som 60000 RLU kunde uppnås, vilket motsvarar den för LED-ljus. Studien visade det första lyckade försöket att utnyttja en biomimetisk strategi för att immobilisera enzym(er) i bakteriereaktionssystemet av luminiscens applicerat på en plasma-aktiverad mikrofibrös nonwoven textilie för att åstadkomma biomimetisk/bioluminiscens material som kan användas för en rad applikationer som biosensorer, biomedicin eller inom säkerhet och estetik.

Vidare undersöktes den inneboende fotoluminescensegenskapen av biobaserade molekyler riboflavin (RF) och flavinmononukleotid (FMN) med syftet att erhålla multifunktionella fotoluminescerande textilier. Med emulering och design för att erhålla biomimetiska självlysande textilier / bioluminescerande material med användning av FMN som ett substrat i enzymatisk process studerades följaktligen också den potentiella användningen av nativ RF och dess derivat FMN-molekyl för att erhålla fotoluminescerande textilier.

Textilier med fotoluminiscens kunde uppnås på cellulosa, polyester, silke och ull baserade material genom traditionella metoder som diffusion, screen tryck, beläggning och även genom att använda resurseffektiva digitalprint metoder. Studien gjorde det möjligt att uppnå textilier av cellulosa med biobaserad fotoluminiscens genom diffusion som uppvisar grön-gul flourescens på textilier och motsvarande kvantum effektivitet kunde fastställas. Utöver fotoluminiscens visade de RF och FMN behandlade textilierna även multifunktionella egenskaper som UV skydd och färgning. Senare utforskades möjligheten att använda FMN med inkjet och chromojet (digitalprint metoder) för att åstadkomma textilier med fotoluminiscens på olika vävda material såsom bomull, merceriserad bomull och PET. Genom att använda digitala printmetoder kunde textilen uppvisa en antibakteriell effekt jämsides dess fotoluminiscens, "quantum" effektivitet, färgning och UV skyddande egenskaper. Därutöver visade studien om fotodegredation av FMN på tryckta textilier att det fanns varierande intensitet i flourescens, från gul till blå till vit flourescens. Därefter designades självlysande i mönster på paneler av nonwoven PET genom screen tryck och beläggningsmetoder genom vilka mönsterdesigners kan skapa ljustemitterande textilier och intressanta estetiska uttryck. Därför har studien kunnat utforska användningen av biobaserade produkter för att producera textilier med fotoluminiscens och bioluminiscens genom funktionalisering och ekotekniska metoder.

Nyckelord: Bioinspirerade, biobaserade, bioluminescerande, fotoluminescerande, textil, lysande bakterier, enzymer, immobilisering, plasma, riboflavin, flavin mononucleotide, hållbart, digitaltryck, funktionalisering.

基于生物基物质的发光纺织品仿生设计

摘要

大自然中存在着具有不同内在特征的生物，如疏水、伪装行为、松果效应和触敏植物等，是我们身边最精美的事物。而且自然界还设计了一些可以产生光的生物。所有这些自然界存在的现象激发了科学家将自然启发的知识应用到可持续发展技术中。本论文主要涉及自然界存在的生物发光现象在发光纺织品制备中的潜在应用。

本研究主要通过仿生设计法制备生物基发光纺织品。为此，本研究主要筛选合适的生物发光反应体系以制备仿真纺织品。论文第一部分主要对自然界的发光现象作了详细综述，为后续研究中"发光细菌"反应体系的选择从基材的可得性、再生性及成本角度提供了依据。所采用的"发光细菌"生物发光系统主要包括细菌荧光素酶（Luc）、NAD(P)H: FMN 氧化还原酶(FMN 还原酶)、生物质黄素单核苷酸（FMN）及 NADH 和长链醛等辅因子。将空气等离子和冷远程等离子处理等生态技术用于纺织品活化和生物酶处理。首先，通过采用发光对光强度进行测试，评价并优化水相中发光细菌系统的催化活性和发光效率。此外，将优化的反应系统应用于纺织品并评估其生物发光效率。通过评估纺织品的生物发光系统，表明发光强度高达60,000 RLU，相当于 LED 灯光的强度。研究结果表明成功地通过仿生策略将发光细菌酶固定于等离子体激活的微纤维非织造布上，从而得到生物发光材料。这些发光材料可应用于生物传感器、生物医疗领域以及安全及美学设计。

此外，黄素单核苷酸的另一个名称 FMN 为人们广泛熟知，它是核黄素的一种衍生物。核黄素及FMN上的异咯嗪环为光致发光现象的原因，细菌荧光素中的FMN分子及其辅因子如NADH，长链醛可致使生物荧光反应的发生。因此，可通过仿真和设计酶促过程采用 FMN 基质制备仿生发光纺织品或生物发光材料，并探索 FMN 分子在制备发光纺织品中应用性能。

现有研究主要通过传统方法如扩散、丝网印刷、涂层和高效先进的数码印花技术制备发光纤维素、聚酯、蚕丝和羊毛等纺织品。本研究主要采用扩散技术制备生物基发光纤维素纺织品，该技术使得纺织品上显示出绿光黄的荧光，并确定了相应的量子效率。除了发光性能外，经 RF 和 FMN 处理的纺织品还具有抗紫外和着色等性能。然后，通过喷墨和数码喷印技术将 FMN 应用于不同纺织材料如棉、丝光棉及聚酯机织物，以赋予织物发光性能。数码喷印技术可赋予织物抗菌性能、发光性能、量子性能、着色和抗紫外性能。而且，经光降解后 FMN 印花织物的荧光强度从黄色、蓝色变为白色荧光。此后，采用丝网印刷和涂层方法设计了在黑暗中发光的图案化 PET 无纺织物，因此纺织品表面图案设计者可以使用它们来制造发光的纺织品和有趣

的美学表现形式。综上，本研究主要采用生物基材料制备通过功能化和生态技术制备光致发光和生物发光纺织品。

关键词：生物灵感，生物基，生物发光，光致发光，纺织品，发光细菌，酶，固定化，等离子体，核黄素，黄素单核苷酸，可持续，数码喷印，功能化

Acknowledgments

The journey of these four years of my Ph.D. has been a period of immense learning, not only in the scientific front but also in terms of personal development. Exploring different countries and cultures will forever remain as a beautiful memory. Firstly, I thank God Almighty for the shower of blessings, giving me strength and wisdom to achieve my dream.

I would like to express my sincere gratitude to my supervisors, Assoc. Prof. Nemshwaree Behary in ENSAIT (France), Prof. Dr. ir. Vincent Nierstrasz at University of Borås (Sweden), Assoc. Prof. Jinping Guan and Prof. Guoqiang Chen at Soochow University (China) for their continuous support at all the time of my Ph.D. study and research activities. Their patience, motivation, enthusiasm, and immense knowledge acted as driving forces for the completion of my thesis, and I am deeply thankful to all of them.

I am grateful to Prof. Philippe Vroman, Assoc. Prof. Thomas Chaffraix, Prof. Anne Perwuelz, Prof. Brigitte Mutel, research engineer Luc Boussekey, Assoc. Prof. Martina Vikova for their scientific support, as well as Prof. Xianyi Zeng, Dr. Eva Gustafsson, Department head Magnus Bratt and Prof. Yan Chen for their administrative support along the way. I would also like to especially thank Marie Hombert, Camila Oberg, Petri Granoth, Christian Catel, and Haike for constant administrative and lab support during my mobility period at respective countries.

Thank you to all my friends with whom I made life memories; firstly, special thanks to my wonderful SMDTex Ph.D. mates Sheenam, Marzeih, Nett for constant help and inspiration, and also Mulat (mon ami), Molla, Daniele. Special thanks to my ex-colleague and senior SMDTex mate Neeraj and Ph.D. colleague Dr.Yuyang, Tuser and Dr. Mehmet for scientific support, advice, and motivation. I am also thankful to several Ph.D. colleagues Melissa, May, Prisca, Razieh, Balkis, Chanda, Mengru, Shukla, Sara, Yanni, Natalie, Sina, Veronica, Carin, Katarina, Niina, Felicia, Sarah, Jyoti, Vijay, Parag, Sohail, Tarun, Jagadish, Melkie, Ajinkya, Ashik, Neaz, Shahood, Xiang, Zhenglei, Vivien, Nitin, Emanuel, Junchun, Milad, Claude, Maneesh, Ke Ma and friends, Rushab, Jamila, and Noopur, Ankit.

My deepest appreciation to dear friends Martina, Meenakshi, Mayuri, Anita, Apparao, Pondurai, Monika, Vivek, Venkat, Raj, Bhaskar, Santosh, Chandu, Sanooj, Tushar, and Subu. I would also like to acknowledge and extend my thanks to my professional career seniors and mentors, Neelkanth sir, Dr. Parag, Dr. Anil, Dr. Babu, Nitin sir, Vibhor and Muthuswamy sir.

I am so grateful to have the most loving and supporting family, firstly, my mother, Pushpa, and father Narayan, whose guidance, motivation, and support was always persistent and helpful in pursuing my dream. The blessings of my grandparents, my father and mother-in-law Bibhu Prasad and Geeta, the unconditional love, support, and encouragement of my sister Sapna, my jiju Vinod, my princess niece Anisha, my uncle Kannan and Mohan, and all my close family members in India has stood as a pillar in completion of this journey.

Last but certainly not the least, I would like to thank the most beloved person of my life, Biswajeet, for his full support and patience to walk with me throughout this journey of peaks and valleys.

Borås, Sweden – July 2020

Sweta Iyer

List of Publications:

Journal publications:

This thesis is based on the work presented in the following publications,

    I.   **Iyer S.N.**, Behary N., Nierstrasz V., Guan J., "Study of photoluminescence property on cellulosic fabric using multifunctional biomaterials riboflavin and its derivative Flavin mononucleotide", *Sci Rep* **9**, 8696 (2019).

    II.   **Iyer S.N.**, Behary N., Nierstrasz V., Guan J., "Towards bioluminescent materials by plasma treatment of microfibrous nonwovens followed by immobilization of one or both enzyme (Luciferase and FMN Reductase) involved in luminescent bacteria", *ACS Appl. Bio Mater.* (2020), 3, 5, 3401–3412.

    III.   **Iyer S.N.**, Behary N., Nierstrasz V., Guan J., "Color-changing intensified light-emitting multifunctional textiles via digital printing of biobased flavin, Sweta Iyer, Behary Nemeshwaree, Jinping Guan, Mehmet Orhan, Vincent Nierstrasz", *Manuscript submitted.*

    IV.   **Iyer S.N.**, Behary N., Nierstrasz V., Guan J., "Glow-in-Dark patterned PET nonwoven using air-atmospheric plasma treatment and Vitamin B2- derivative (FMN)", *Manuscript submitted.*

    V.   **Iyer S.N.**, Behary N., Nierstrasz V., Guan J., "Dyeing and digital printing of silk and wool fabric with biobased flavin dyes: Study of fluorescence property", *Manuscript submitted.*

Contribution report:

- Paper I and II: **Iyer S.N.** conceived the idea, conducting the experiment and writing the paper. Iyer S.N., Behary N. conceived and designed the project and methodology. All the co-authors have participated and contributed in the refinement of the manuscript.

- Paper III: **Iyer S.N.** conceived the idea, conducting the experiment and writing the paper. Iyer S.N., Nierstrasz V. conceived and designed the project and methodology. All the co-authors have participated and contributed in the refinement of the manuscript.

- Paper IV and V: **Iyer S.N.** responsible for planning, experimental work, data analysis and article writing. All the co-authors have participated and contributed in the refinement of the manuscript.

Conference presentations and proceedings:

I.   **Iyer S.N.**, Behary N., Nierstrasz V., Guan J., "Bio-Inspired approaches to design Bio-luminescent textiles", *Designer Biology, Symposium Conference,* Vienna (2017).

II. **Iyer S.N.**, Behary N., Nierstrasz V., Guan J., "Photoluminescent textile using biobased riboflavin derivative (FMN)", *18th AUTEX World Textile Conference,* Istanbul (2018), p. 1 - 4, article id 3471.

III. **Iyer S.N.**, Behary N., Nierstrasz V., Guan J., "Measurement of luminescence intensity on textiles using luminous bacterial biocatalytic system", *12th TZG - Textile Science and Economy French-Croatian Forum, Z*agreb (2019).

IV. **Iyer S.N.**, Behary N., Nierstrasz V., Guan J., "Influence of plasma treatment on luminescence intensity of biomimetic luminescent textile", *19th AUTEX World Textile Conference,* Ghent (2019).

V.   **Iyer S.N.**, Behary N., Nierstrasz V., "The Potential Use of Flavin Mononucleotide for Photoluminescent and Bioluminescent Textile", *International Conference on Luminescent Materials,* London (2019), 108376.

VI. **Iyer S.N.**, Behary N., Nierstrasz V., Eutionnat-Diffo P., Cayla A., Campagne C., "Incorporation of flavin mononucleotide molecule into polymers for development of photoluminescent textiles using 3D printing", *Aachen Dresden international textile conference,* Dresden (2019), (Work not included in the thesis).

The papers and proceedings are not included in this version of the thesis but can be found on the particular publisher's print or electronic databases.

List of abbreviation

RF	Riboflavin
FMN	Flavin mononucleotide
PL	Photoluminescence
BL	Bioluminescence
CRP	Cold remote plasma treatment
CRPNO	Cold remote plasma treatment (N_2 and O_2)
ATMP	Air atmospheric plasma treatment
RLU	Relative light units
LED	Light emitting diode
FTIR	Fourier transform infrared spectroscopy
SEM	Scanning electron microscope
AFM	Atomic force microscopy
ESCA	Electron spectroscopy for chemical analysis
UVI	Ultraviolet light irradiated
VISI	Visible light irradiated
QE	Quantum efficiency
FQE	Fluorescence quantum efficiency
Luc	Bacterial luciferase
FMN reductase	NAD(P)H:FMN oxidoreductase
CD	Cotton duck white
MC	Mercerized cotton
PET	Polyester
DBD	Dielectric barrier discharge
WCA	Water contact angle
HTHP	High Temperature and High Pressure/Beaker Dyeing Machines
owf	On weight of fabric
UPF	Ultraviolet protection factor

Table of Contents

List of figures

List of Tables

List of chemical schemes

GENERAL INTRODUCTION

General introduction

Nature consists of distinct living organisms that have evolved over billions of years to develop sustainable solutions such as self-cleaning, superhydrophobicity, energy conservation, adaptive growth, and so on, possessing abundant functionalities with time [1]. Some of these solutions existing in nature inspired scientists to achieve magnificent outcomes. Among all these different inherent functionalities seen in nature, bioluminescence is one such phenomenon exhibited abundantly by marine and terrestrial living organisms. The transfer of knowledge inspired by nature into technology to create sustainable solutions is widely termed as biomimetics. Biomimetics can also be defined as the science of systems that possess or represent some characteristics of natural systems or their analogs. Generally, the development which is inspired by nature from a biological perspective or living nature into design and engineering or technological perspectives, all of these are categorized and named either as biomimetics, bionics, biomorphic, or as biomimeses.

In recent years, biomimetic research studies have gained attention with an increase in the number of publications and patents [2][3][4]. With the increase in demand for functionalized and high-performance textile materials, a steep rise in research for application and development of sustainable functionalized textiles based on biomimetics has been ongoing. Various research studies based on the application of biomimicry reviews the possibilities to obtain functional textiles [5][6][7]. Although interdisciplinary technological innovations using bioinspired strategies exist for the development of smart and intelligent textiles [8], in particular, this thesis focuses on bioinspired strategy for the development of luminescent textiles.

Fundamentally, the essential use of textile being considered only for clothing purposes evolved with the growth and development of society. Hence, textile clothing with protection emerged, and thereby research studies seeking solutions for adding functionalities on textiles increased. With the continuous research and development of functional textiles, its application did not remain limited to clothing industries. Massive growth in the use of functional textiles for various application fields was seen. Textile being flexible, breathable, and cost-effective, have gained attention for its use in almost all fields, which include aeronautics, defense, aesthetics, interiors, among others. Such a revolutionized increase in the use of textiles for different applications could eventuate due to the added functionalities on textiles [9]. Thus, the changing dynamics in the use of textiles beyond fashion has increased the demand for functional textiles [10]. Luminescent textile is one such functional textile, which could be used for different purposes such as warning, safety, and aesthetics [11][12][13][14][15]. In recent years, the use of luminescent textiles has increased along with the expansion of application fields such as smart textiles, anti-counterfeiting, biomedical, and medical fields [16][17][18].
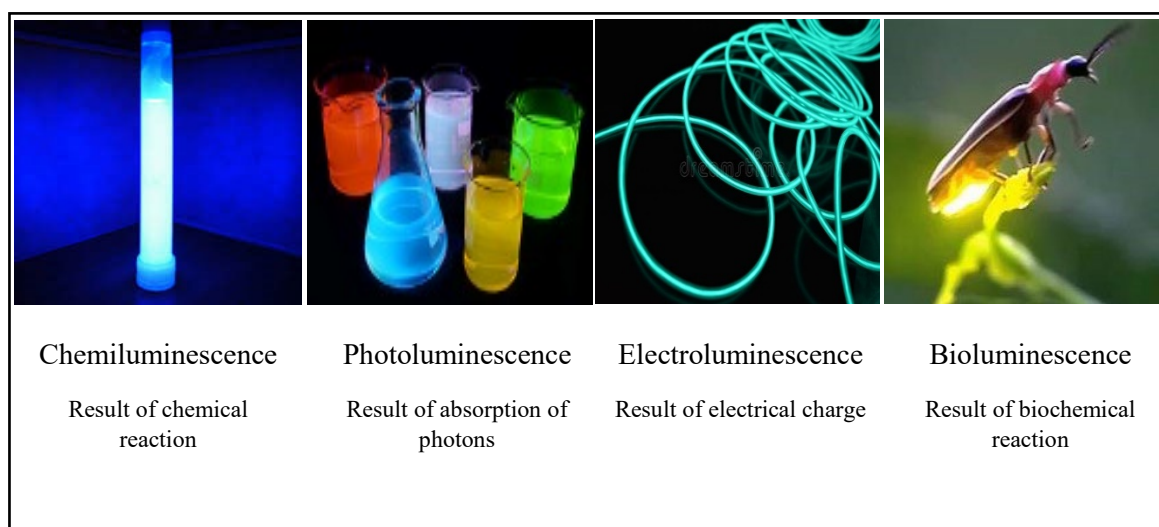
Figure 1. Different kind of luminescence depending upon the type of energy transformed into light (images from[19][20][21][22])

The objective of this thesis was to investigate the development of luminescent textiles based upon existing biochemical reaction study of the bioluminescence system occurring in nature [23][24][25]. In addition to luminescence, textiles modified with these bio-based products can possess multifunctional properties (antibacterial, UV protection) [26], which were also explored in this study. Due to the fast growth, addressing new technology and approach to fulfill the demand of functional textile with the requirement of sustainable solutions concerning economy, environmental, and social aspects is very important. Thus, it is necessary to conceptualize and design bioinspired as well as eco-efficient concepts for the development of luminescent textiles.

Luminescence, in general, is a light-emitting phenomenon, and when seen in nature, it is termed as bioluminescence. Bioluminescence, seen widely in marine as well as terrestrial living organisms, can impart light in the visible region of wavelength wherein the luminescence occurs due to the biochemical reaction process [27]. Researchers can produce garments using a light-emitting device with electronic textile engineering and using rare earth elements such as strontium aluminate. However, due to cost, flexibility constraints, as well as a certain level of toxicity involved in the use of rare-earth metals, an alternative or sustainable approach to obtain luminescent textiles becomes essential. Hence, the biochemical reaction occurring in a bioluminescent living organism provides the inciting motivation to attempt designing glowing clothes in the dark that would add valuable assets to the fabrics and textile industry. Furthermore, along with biomimetic or bioinspired strategy, the choice of eco-technologies to study the bioluminescence phenomenon for its application in textile technology would be a sustainable approach.

The development of bioluminescence is a natural phenomenon occurring in living organisms, which imparts visible light due to its in-vivo biochemical reaction [27] [28]. The identification of such an organism illuminating visible light have been studied during the early '90s, and the term 'bioluminescence' came into existence due to its biochemical reaction ability to produce light [29]. There are different types of luminescence based upon the different sources of energy and fundamental reaction aspects such as electroluminescence, photoluminescence, chemiluminescence, and mechanoluminescence [30]. Consequently, the light is emitted through either of the processes such as chemical, electrical, or absorption of photons, as shown in Figure 1.

Bioluminescence, in general, is light emitted by a substance, not because of heat, and hence also termed as cold light. Further, after the identification of different bioluminescence generating living organisms, many studies were done to understand the reaction mechanism occurring in the living organism that enables them to produce the light [31][32][33][34][35][36]. There are various studies about the biochemistry existing in the living organism, which allowed scientists to continue research and identify the application based upon the biochemical principle. The continuous research in the field of bioluminescence was at the peak until early 2000; however, the leap in the research work took place after 2010 when the application research based upon the bioluminescence increased [37][38] [39][40][41][42][43]. Hence, the field is gaining much attention due to the application research activity in the field of bioluminescence.

Luminescence in itself co-exists in various fields of applications, however pertaining to the field of textile applications, there exists a total record of 120 according to the web of science study combining AND / OR with keywords luminescence, textiles. Bioluminescence is a form of chemiluminescence whereby the light is emitted due to chemical reaction. The major leap of the work on luminescence began from the year of 2000. The sudden drop in between 2004 and 2015 might be due to the lack of knowledge of the luminescence reaction mechanism that is widely seen in many living organisms. Exploration of the same has been carried out widely and is still an ongoing process.

In context to the development of luminescent textiles using bioinspired biobased multifunctional products, it was important to go through a literature study focused on the four quadrants of keywords such as luminescence, bioluminescence, and its respective combine results with the keyword textile as shown in Figure 2. Following these four quadrants of keywords, according to the web of science study, the total number of records exceeded 39,593 for luminescence and 13,929 for bioluminescence. However, interestingly the combination of luminescence AND textiles OR luminescent textile search resulted in 120 records only. Also, the combination of bioluminescence AND textiles yielded a mere 22 records in total. The results include parallel interaction of both bioluminescence and textiles, which do not implicate or consist of publication resulting in bioinspired luminescent textiles.

Further, the literature study also reveals that rapid attention was gained during the previous decade (2010) for various applied research activities based on both luminescence and bioluminescence.
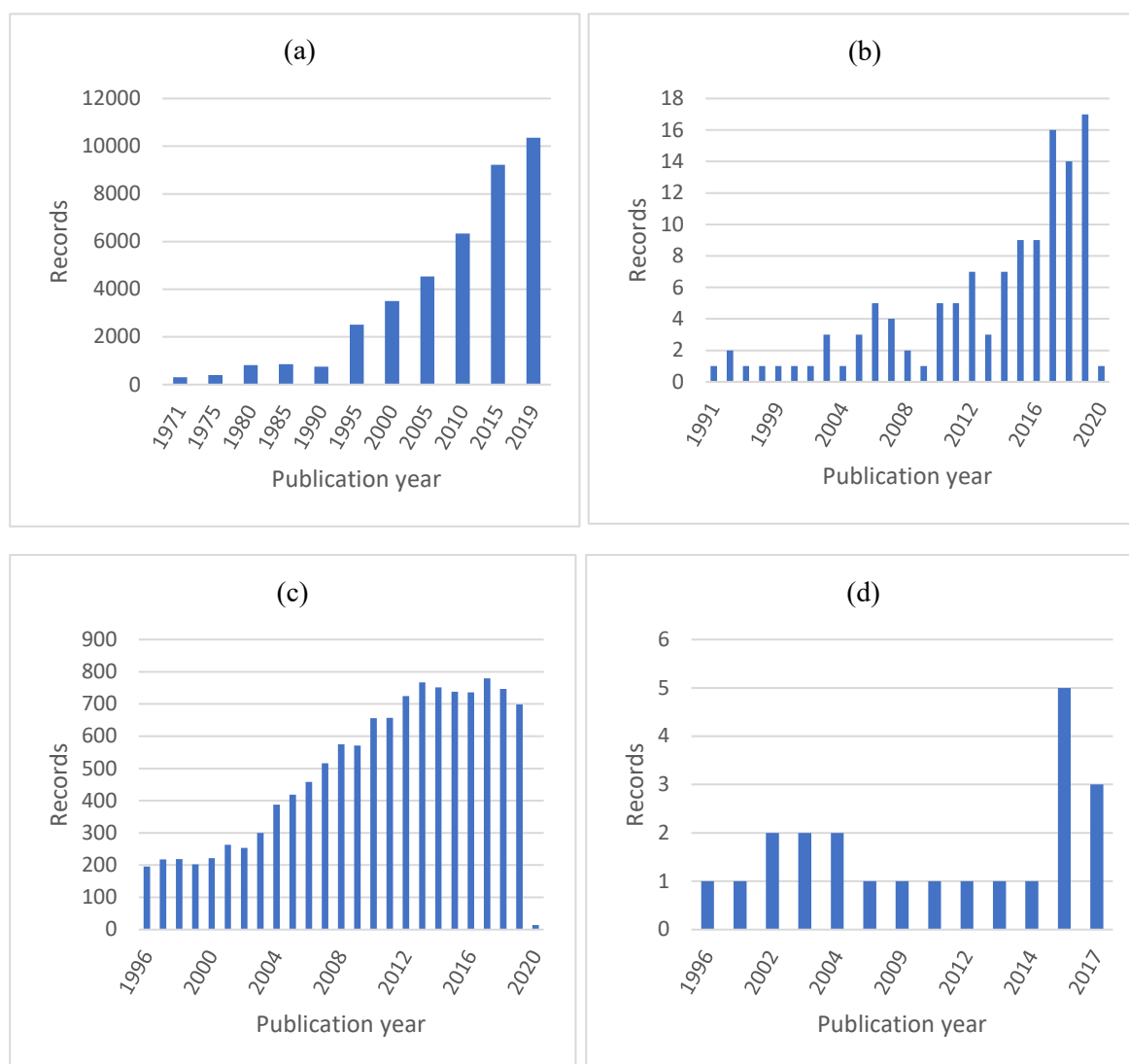
Figure 2. Web of science analysis study of documents by year (a) search keyword ' luminescence' (b) search keyword ' luminescence AND textile OR luminescent textile' (c) search keyword ' bioluminescence' (d) search keyword ' bioluminescence AND textile'

Therefore, the aim was to investigate developing textiles based on bioluminescence as a proof of concept. The sustainable approach towards attaining the biobased luminescent textiles will strengthen the scope to develop functional textiles

Thesis Purpose and Objectives

The primary aim of this thesis work was to find possible proof of concept by biomimicking the natural phenomena to produce biobased luminescent textiles. The literature study allowed to identify the appropriate bioluminescent system as well as a potential biobased substrate molecule flavin mononucleotide (FMN) that can exhibit both bioluminescence and photoluminescence emission spectrum depending upon the absence or presence of enzymes and co-factors in the reaction system. The potential use of FMN depending upon the choice of bioluminescence reaction system consecutively allowed captivating the thesis outline 'Toward sustainable luminescent textiles from nature to emerging materials' into two main objectives,

- ❖ Proof of concept towards biomimetic/bio luminescent textile
- ❖ The potential scope of biobased riboflavin (RF) and its derivative flavin mononucleotide (FMN) as a fluorescent molecule to produce photoluminescent textiles with the multifunctional property.

Research framework and thesis outline

This Ph.D. thesis discusses the development of luminescent textiles using biobased resources. Biobased molecule riboflavin and its derivative FMN was considered as a key molecule to develop two types of luminescent textiles, photoluminescent and bioluminescent textile. Under the framework of the SMDTex program, the research work aims at focusing the sustainability of management and design for textiles contributing towards sustainable goals concerning the environment, society, and human factors. The Ph.D. thesis work was conducted at three designated universities involved in the project; first mobility was at ENSAIT-GEMTEX in France, second mobility was at the University of Borås in Sweden, and finally at Soochow University in China. The main objectives were to identify the biobased resource based upon the literature study and implement the biobased molecule onto textiles to obtain luminescent textiles.

The outline of the thesis was designed based on the initial literature study. The results of the literature study allowed to form the selection of luminous bacteria/ bioluminescent bacterial reaction systems depending upon the availability, regeneration of the substrate, and cost. After, selection of the system, the thesis research framework was unfolded into two main objectives, firstly an attempt to make biomimetic/bio luminescent textile using the bioluminescent bacterial system and secondly, the potential use of biobased molecule FMN to obtain photoluminescent textiles along with multifunctional potential such as UV protection, antibacterial, etc. The research study resulted in providing scope to obtain biomimetic luminescent textiles by enzyme immobilization and spiking of the substrates involved in the bioluminescent bacterial system. Thus, the luminescence intensity of the immobilized textile system was

studied using luminometer equipment for availing the new possibilities of biolighting textiles. The study also allowed to explore the potential use of FMN to obtain multifunctional photoluminescent textiles. Sustainable eco-technologies such as plasma treatment and digital printing techniques such as inkjet and chromojet printing were used to obtain biomimetic/bio luminescent and photoluminescent textiles, respectively.

The thesis structure is mainly organized into five different chapters.

Chapter 1 deals with state of the art, focusing on luminescence in general and describing different bioinspired luminescence system. Further, the chapter reviews in brief biomimetics and its role for material development with an overview of riboflavin and FMN molecule exhibiting both photoluminescence and bioluminescence phenomena. Besides, it highlights the concepts of functionalization methods and eco-technologies mainly used in the thesis framework. Finally, the selected system for the thesis study and strategies to obtain luminescent textiles using the bioinspired luminescence system is summarized.

Chapter 2 mainly includes a description of the materials and methods used for the thesis study. Furthermore, the chapter presents a description of characterization techniques used to assess and evaluate the performance of treated textiles in terms of bioluminescence and photoluminescence, along with the assessment of multifunctional properties.

Chapter 3 presents the results obtained in context to the development of biomimetic/bio luminescent textiles. The two-folded study (a) aqueous phase study (b) textile phase study involving immobilization of enzyme(s) are described, and the resulting luminescence properties are analyzed and discussed.

Chapter 4 presents the results obtained within this thesis, using different functionalization and eco-technologies to produce photoluminescent textiles. Further, the analysis and discussions of the resulting photoluminescent phenomena observed on different textile substrates are described in detail, with respect to the different approaches used.

Chapter 5 derives the primary outcome and general conclusions based on results and discussion in the previous presented chapters. Also, the insights into future perspectives within the presented area of research, along with challenges and limitations, are described in this chapter.

Thus, the overall schematic representation of the thesis research aim is illustrated below in Figure 3
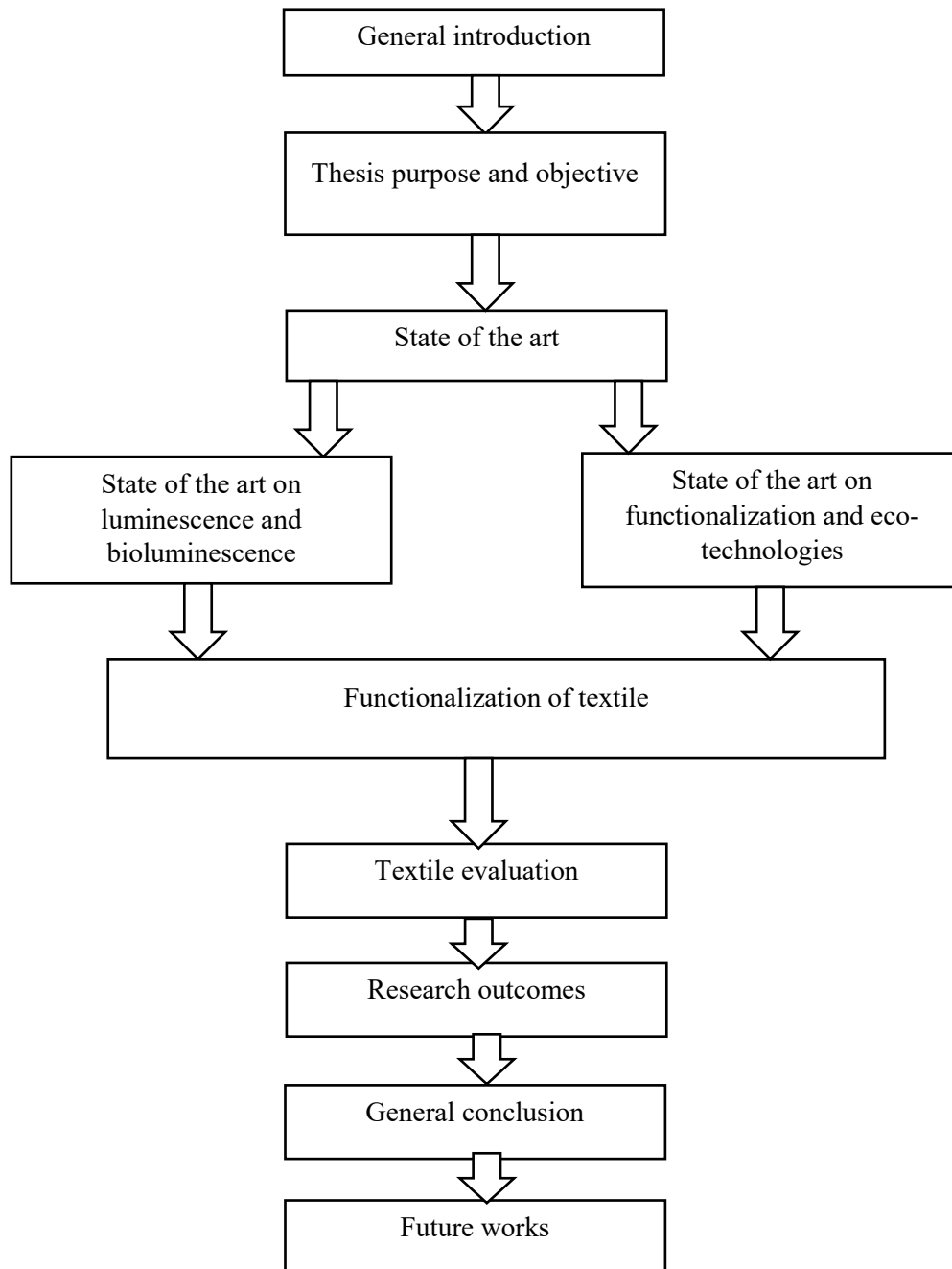
Figure 3. Schematic illustration of the thesis framework

CHAPTER 1: STATE OF THE ART

1.1. Luminescence and luminescent textiles

This section presents at first, a brief historical background on the study of luminescent materials, which is the main objective of the thesis. Further, a general overview of luminescence and an overview of different types of luminescence phenomena are described. Later, various luminescent materials exhibiting the luminescence properties and its application on textiles are briefed.

1.1.1. Historical background of luminescent materials

Luminescence and luminescent materials research studies have been ongoing for more than 100 years. Moreover, 1000 publications have been published describing different aspects of luminescence and a wide variety of materials based on the luminescence effect. The emission of light by a material after it has been exposed to either ultraviolet or infrared radiation, electron bombardment, X-rays, and other potential sources of radiation has driven scientists research interest in this field since the early 1900s [44]. Thus, overall, a luminescent material emits light because of energy absorption at moderate temperatures, and the energy absorption can be attained by a different source.

1.1.2. Luminescence in general

Although luminescence related phenomena have been observed for thousands of years, systematic study and understanding have been undertaken only since the last century. Stokes reported the phenomena exhibiting strong photoluminescence under ultraviolet (UV) light in the year 1852. Later, Wiedmann, in the year 1888, proposed 'luminescence' as a term named for all broad class of materials exhibiting light emission [30]. The phenomenon in which the energy is explicitly channeled to the molecule, to produce an excited state and return to a lower energy state by the release of photon 'hν', is known as luminescence, as represented in Figure 4.

$$A + B \rightarrow C^* + D \rightarrow C + h\nu,$$

where, C^* is an electronically excited molecule

'hν' represents light emission upon return of C^* to a lower energy state.¨

A, B are participating molecules and D is the product.
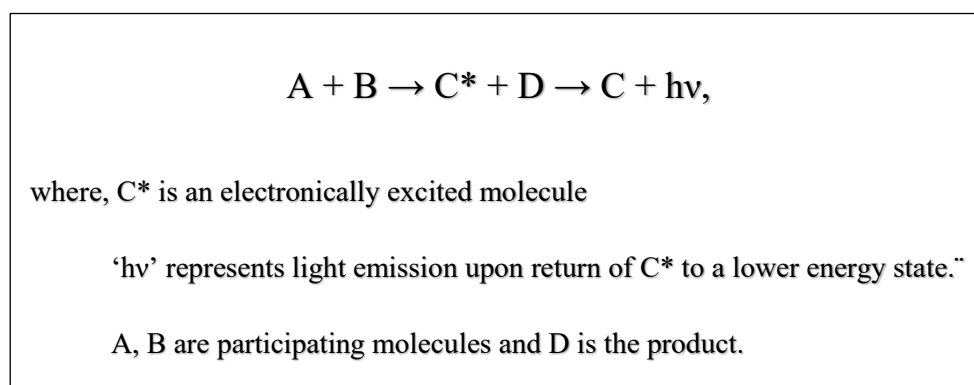
Figure 4. Illustration of luminescence reaction in general

The general phenomena of luminescent materials are a consequence of energy absorption, which re-emits part of it as light, either infrared-IR, visible or ultraviolet-UV light, and such light emission process is termed as 'luminescence' by Wiedemann in the year 1888. The energy absorption or excitation of luminescent material can be attained in various ways, and depending upon the source, luminescence effects are expressed accordingly. For example, if the excitation energy may be provided by moderate heat, it is termed as thermoluminescence (TL). This light emission process includes a wide range of luminescence depending upon the type of source, as mentioned in the earlier example. Apart from TL, there exist chemiluminescence (CL) produced as a result of chemical reaction, electroluminescence (EL) as a result of electrical charge, photoluminescence (PL) as a result of the absorption of photons, and bioluminescence (BL), which is part of CL [30]. However, in the case of BL, the light emission is due to the chemical reaction occurring in a living organism in contrast to synthetic luminol chemical reaction producing luminescence, also called chemiluminescence [45][46]. Photoluminescence mainly includes two types of light-emitting reactions (i) fluorescence and (ii) phosphorescence.

Photoluminescence

Photoluminescence is a kind of luminescence, which involves the absorption of energy, thereby emitting light. Broadly, the photoluminescence can be further classified into fluorescence and phosphorescence, depending upon the singlet and triplet state of luminescent species. They are radiative emission transitions from higher to lower energy states and are categorized upon the persistence of emission after the source of excitation energy is removed. Materials that show delayed emission wherein continuous luminescence is observed for an extended period even after the excitation energy is removed is generally termed as phosphorescence. Contrarily, materials which showed emission during the time of excitation is known as fluorescence. The electronic states of a photoluminescent molecule and the transitions between them are illustrated in Figure 5 [47].
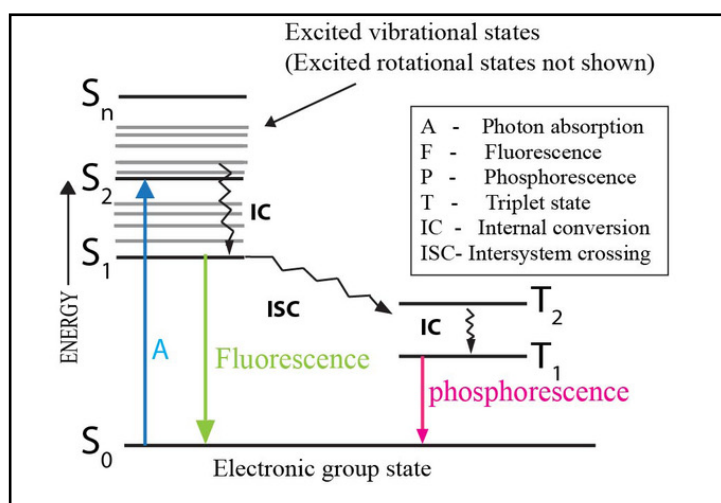
Figure 5. Jablonski diagram explaining photoluminescence.

Fluorescence is the immediate emission of radiation, usually visible light depending on the absorption of radiation such as ultraviolet light. In contrast, phosphorescence is similar to fluorescence, except that the emission of radiation occurs slowly over an extended period in the case of phosphorescence [48]. Apart from these, there are various other existing luminescence phenomena.

Types of luminescence

Different types of luminescence are summarized in Table 1. depending upon their origin and different applications [49][50][51].

Table 1. Types of luminescence, their origin, and its applications, based on Harvey.

Phenomena/type of luminescence	Origin / mode of excitation/ excitation source	Applications
Bioluminescence	Excitation due to a chemical reaction in biological matter	Biotechnology, environmental, bioimaging
Photoluminescence	Irradiation by UV or visible light	Purity and defects in minerals and crystals, forensic science, counteraction detection
Thermoluminescence	Emission from previously absorbed electromagnetic or ionizing radiation upon heating of the material	Environmental and personal dosimeters, archeological pottery dating, irradiated food identification
Electroluminescence	Excitation due to electric field	LED, lighting, displays, medical applications
Pyroluminescence	Emission from excited atoms, ions, and molecules in flames	Lamps, fireworks, flames
Candoluminescence	Emission from incandescent solids at shorter wavelengths than that expected from their blackbody emission	Photography, outside lamps/lighting

Radioluminescence	Irradiation by high energy photons such as X-rays, γ-rays or particles (e.g., neutrons)	Scintillators, X-ray film radiography
Cathodoluminescence	Excitation from electron impact on solids or gases	TV screen, impurity mapping, discharge lamps
Ionoluminescence	Excitation produced from alpha particles emitted by radioactive elements	Early clock dials

The color of the emitted light depends mainly on the inherent characteristics such as purity and defect content of material along with other factors such as temperature, external magnetic, electric field, and particle size. The exploitation of luminescent materials for applications in different fields, as elaborated in Table 1. provides the insights of science in our everyday life and continuous growth of research and development in the luminescence field. Hence, luminescent materials, depending upon the excitation source, exhibit corresponding different luminescence behavior; subsequently, the applications of luminescent material also vary. The interaction occurring between the luminescent center and the atomic transition from either singlet to singlet or triplet to singlet transitions displays luminescence behavior [51].

1.1.3. Light spectrum in general

In general, light refers to visible radiant energy, although it may also refer to sources of illumination such as natural sunlight and artificial light sources such as lamps. The evolution of humankind over the past century has led to electrically powered lamps from ancient natural forms of light, such as candles, flame torches, and oil lamps. Open flames and incandescent sources are rich in longer visible (orange, red) and infrared to near-infrared irradiation. Fluorescent lamps evolved in the 1950s, commonly rich in green light and line spectra. Later, LEDs were developed capable of emitting broad wavelength bands and blue-violet fluorescent LEDs producing white light [52]. The relative spectral power distributions of LED lamps constitute range from 380 nm to 780 nm, as represented in Figure 6.
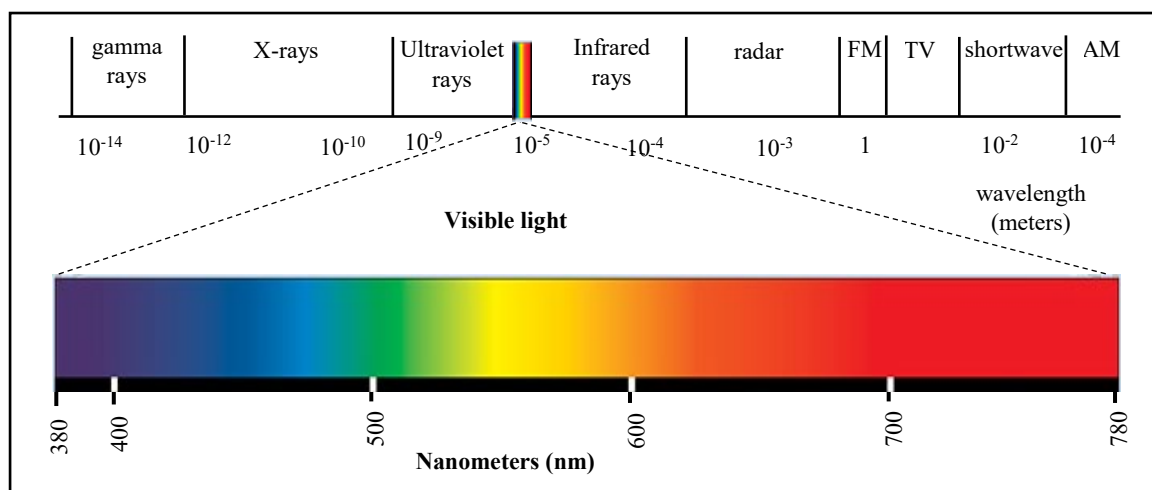
Figure 6. Illustration of the light spectrum in general.

1.1.4. Existing luminescent materials and luminescent textiles

This section mainly describes the evolution and research on different types of luminescent materials, which include inorganic, rare earth ions, organic, chemiluminescent, and bioluminescent materials. Depending upon the luminescent properties of these inorganic and organic luminescent materials, the emission wavelength varies, and this tendency is also observed in the case of the different bioluminescent systems depending on the biochemical reaction [53]. In ancient times, there existed mainly two classes of luminous pigments (i) zinc and zinc cadmium sulfides exhibiting mainly fluorescence property and (ii) alkaline earth sulfides, which possess phosphorescence property [54]. Luminescent materials are substances that can emit electromagnetic radiation in the ultraviolet (UV), visible or infrared regions of the spectrum upon excitation produced by either absorption of photons, by application of an electric field, by cathode rays or electrons [44][55]. A variety of materials such as rare-earth ions, transition metal ions give rise to luminescence. The type of luminescence varies depending upon the interaction between the electronic system of the luminescent centers and the vibrations of the atoms or ions surrounding the environment [56]. Further, depending upon the luminescent material properties such as the spectral position of the absorption and emission bands as well as the decay time of the emission, there exist different application fields. In the case of inorganic luminescent materials such as Ce^{3+} and Eu^{2+} phosphors, various strategies and optimization of luminescent properties led to the development of light sources such as LEDs and fluorescent lamps. Certain radiation sources are used for disinfection purposes, and many light-emitting devices or light-emitting properties are used in biomedical devices, and medical imaging [57], and these techniques have gained a lot of attention concerning COVID-19 lately [58]. There are also organometallic compounds such as metal carbonyl complex, vanadium, chromium, molybdenum, tungsten, rhodium, ruthenium complexes, etc., and their

14

photophysical behavior with emission phenomena has been studied widely [59]. Although the inorganic phosphors are produced widely, some specific fields also utilize organic luminescent materials. The advantage of organic materials is its ability to exhibit luminescence both in dissolved and in the molten state is contrary to inorganic materials, which shows a luminescent effect due to crystal lattice structure [60]. Organic light-emitting diodes from anthracene crystals, 8-hydroxyquinoline aluminum, and a diamine have been designed for material applications [61][62].

Although scientist Boyle performed the scientific investigations of luminescence in 1672 [29], the biochemical reaction occurring in nature was studied in late 1800. However, progressive studies provided the concept of bioluminescent reactions and found different practical applications in recent years due to its high luminescence efficiency [31]. Later in the year 1928, the understanding and awareness about the biochemical origin of light and basic properties such as cold light emission lead to the development of synthetic compounds such as luminol, referred to as efficient chemiluminescent materials. Strong blue chemiluminescence can be observed due to oxidation of the luminol compound. Based on these assorted luminescent materials, there exist different fields of application. Textiles is one such application field which integrates various luminescent materials onto textiles for its use in smart textiles [63][11], medical and biomedical field, protection, and safety. Photoluminescent textile based on strontium aluminate via spray coating was developed that could bring benefit for safety enhancement [64]. Furthermore, electroluminescent layers were coated on PET woven textiles for its use as alternative light therapy for medical care applications [65]. Moreover, fluorescein treated cotton fibers were developed for anti-counterfeiting applications [16]. Depending upon the type of luminescent materials, various techniques such as dyeing, coating, screen printing, electrospinning, weaving, etc., have been explored to develop luminescent textiles [64][66][67].

1.1.5. Environmental concern and sustainability

LED and electronic textiles were emerging trends for luminescent textiles. However, photoluminescent dyes and pigments later played a role in developing glow in dark patterned textiles, which were then used for various applications such as medical sectors apart from fashion and aesthetic applications [68]. The application of luminescent materials broadened with its use in buildings and safety sectors, hence increasing the demand. However, with the increase in demand, the awareness of the luminescent textile manufacturing ways and its sustainability issue also increased. Thus, it is important to develop and focus on sustainable luminescent textiles with growing environmental concerns. There exist different kinds of photoluminescent dyes and pigments, as well as LED and electronic textiles. Consequently, the urge to the development of potential new photoluminescent pigments also continued. In the case of inorganic pigments, the development of luminescent materials focuses on either high intensities and development of nanoparticles to adhere to host material for vivid applications, but have environmental concerns [57].

In the case of the optical fibers, there exist limitations in context to the property of bending and mechanical stress, also bending radius being minimum. LEDs, on the other hand, are of high cost and have the limitation of the mechanical property. Hence, the urge for the development of a more sustainable solution is essential.

1.2. Luminescence seen in nature

In concern with the environmental issues, toxicity, and high cost of different luminescent materials, a bioinspired strategy was aimed to obtain luminescent textiles in this thesis. Accordingly, in this section, the luminescence phenomena seen in nature and the taxonomical distribution, along with its role in the living system, are summarized. Further, with the scope of using biomimetic products, it was important to carry out a literature review to understand the different biochemical reaction mechanisms occurring in bioluminescent organisms. Detailed literature review allowed to identify the extreme diversity of chemistries seen in bioluminescent living organisms such as fireflies, fungi, earthworm that are found on land and jellyfish, shrimp, dinoflagellates, corals found in the marine environment. The reaction mechanism was studied for different categories of a luminous organism to make the right choice of the bioluminescent reaction system that can be studied for textile applications.

1.2.1. Bioluminescence

The term 'cold light' refers to chemical reaction producing light without the generation of heat. Bioluminescence seen in nature is termed as 'cold light' because the luminescence phenomena are seen due to the biochemical reaction occurring in the living organisms. The existence of self-luminescence in nature was already reported by Aristotle (384-322 BCE), and the term bioluminescence came into existence. This light-emitting phenomenon seen in various animals and plants has inspired the interest of humanity and remains a crucial area of investigation by several renowned physicists, naturalists, and physiologists. The anatomy and histology of various luminous organisms were studied predominantly in the 19th century; however, the chemistry of bioluminescence was revealed and uncovered only in the 20th century. It was Aristotle and Pliny the elder who mentioned that damp wood and fish produced light [69]. It was the scientist Wiedmann who created the term 'luminescence' in 1888, and Harvey, in 1916, used the term 'bioluminescence' indicating luminescence from living organisms [53].

The identification of bioluminescence exhibiting organisms, mostly in marine and few terrestrial environments, led to detailed research on the quantification of bioluminescence in nature. The bioluminescence quantification from the surface to the deep sea demonstrates bioluminescence predominance as an ecological trait. In context to literature descriptions on BL exhibiting ability, more than 350,000 observations were classified, accounting for 76 % of living organisms having bioluminescence capability [27]. The natural characteristics of bioluminescence are elaborated in

various segments, indicated by the different sections, such as depth, the traits, and taxonomically different levels. The existence and distribution of bioluminescence in living organisms have been studied and elaborated in detail by biologists and marine scientists [70]. Nature is the best inspiration of science, which can be seen in these existing bioluminescent organisms that integrate mechanisms of various disciplines such as chemistry, physics, physiology, and morphology [71]. Boyle then stated that oxygen is required for the systems to carry out the reaction to produce light and can also be seen in a worm known as glow worm [38]. The significant benefit of using the bioluminescence system is their high luminescence specificity due to the *in-vivo* biochemical reaction, without the requirement of any bulky excitation source.

1.2.2. Light spectrum seen in nature

Although today, artificial lighting is the primary source of illumination for almost the whole array of the visible spectrum as described in section 1.1.3, a spectrum of color can also be seen in nature, broadly in bioluminescent marine and terrestrial organisms, as shown in Figure 7.
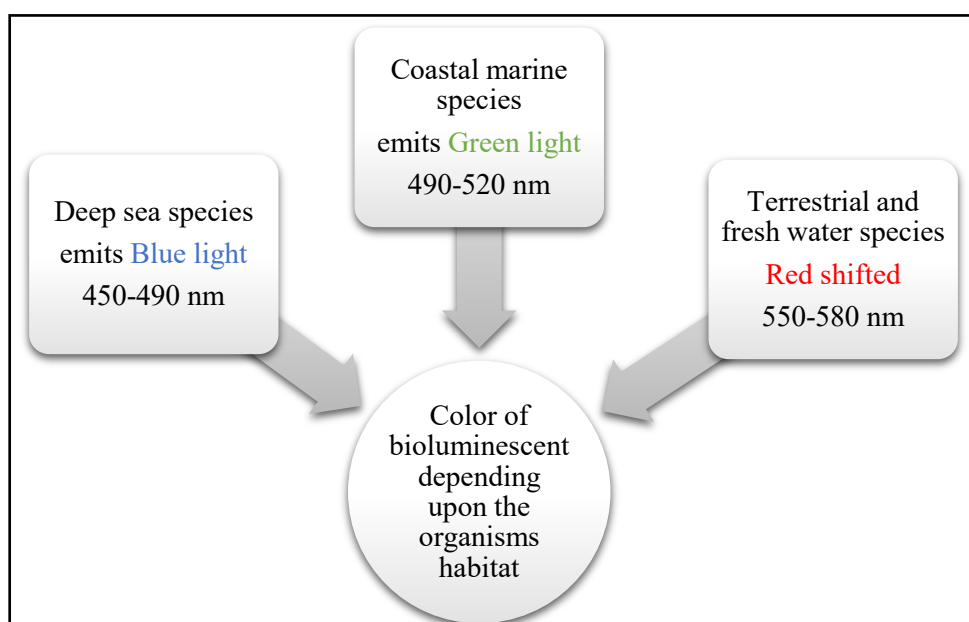
Figure 7. Bioluminescent wavelengths depending upon the habitat of the organism.

These organisms evolve independently numerous times, thus providing a broad spectrum of luminescence with a tangible advantage in bioresearch, as shown in [72]. The web of science literature study based on keyword search broadly on 'bioluminescence terrestrial' and bioluminescence marine' provided a comprehensive total of 82 and 757 articles, respectively. The marine bioluminescence being the major in the taxonomical group of the division, was further searched with keywords 'marine shallow water', 'marine deep sea' and 'marine sea' giving total 12, 54, and 164 literature articles.
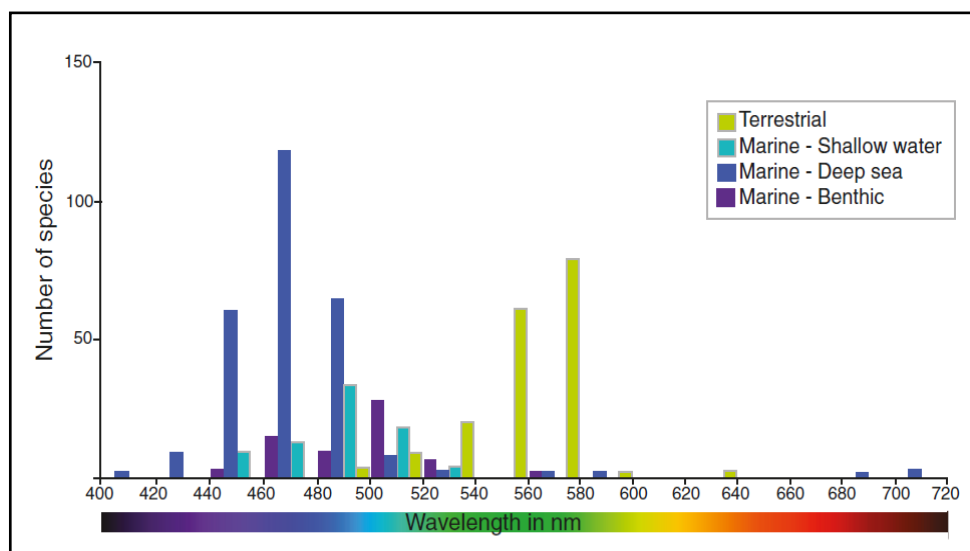
Figure 8. Light spectrum in nature [72].

1.2.2.1. Role of bioluminescence in nature

In nature, living organisms have evolved over millions of years to provide light, and the purpose of giving off light varies depending upon the environment. In the case of marine organism, creatures move to the deep water wherein natural light do not penetrate easily. Hence, the organisms emit light to communicate, to attract food, and for mating purposes. The majority of all deep-sea vertebrates and invertebrates living organisms (estimated 80 – 90 %) living in the dark depths are bioluminescent wherein the most common use of bioluminescence is a defense against predators. For example, some species of shrimps vomit out brightly luminescent blue-green slime at enemies when they are threatened [73][74].

1.2.2.2. Bioluminescence reaction mechanisms in general

Dubois demonstrated the fundamental chemical study of bioluminescence in 1885. He concluded that a relatively stable substrate termed as 'luciferin' and necessary enzyme 'luciferase' reaction mixture results in the emission of light as represented in Figure 9. Harvey later than discovered the 'luciferin-luciferase' reaction system occurring in various living organisms, which further provided more clarification of the reaction mechanism system producing light. A great variety of luminous organisms was studied underlying the fundamental aspects of the bioluminescence chemistry converging the belief that almost all phenomena of bioluminescence were due to luciferin-luciferase reaction. However, Shimomura discovered bioluminescent protein aequorin in 1962 [75]. The protein named 'aequorin' was found in jellyfish, and the light emission phenomena occurred due to the intramolecular reaction of protein in the presence of co-factor such as calcium (Ca^{2+}). Although most of the luminous organisms

exhibit enzyme-catalyzed, namely luciferin-luciferase reaction, exception for non-enzyme catalyzed based reaction was also found, which can emit light due to bioluminescent protein also termed as 'photoprotein' triggered by co-factors. In general, a bioluminescent reaction is a chemiluminescent reaction, in which an organic compound luciferin in the presence of a specific luciferase can emit photons under standardized conditions. However, a complete understanding of the bioluminescence phenomenon requires multidisciplinary studies, including genetics, physiology, spectroscopy, cell biology, morphology, biochemistry, and organic chemistry [53].
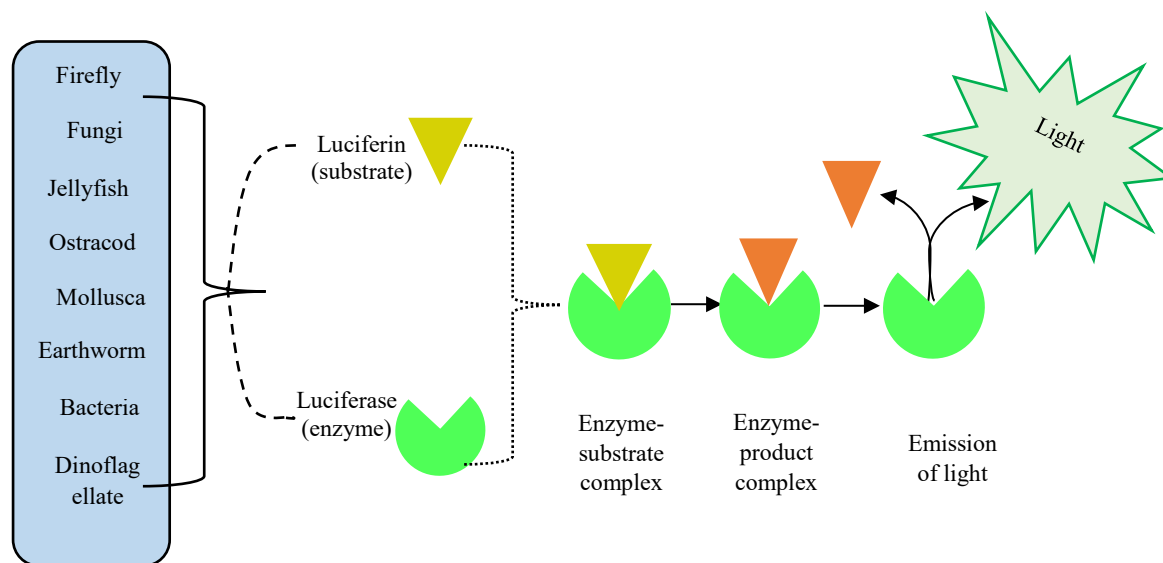
Figure 9. Schematic representation of the bioluminescence reaction mechanism in general

1.2.3. Bioluminescence classification

The bioluminescence seen in nature can be broadly classified as an enzyme-catalyzed and non-enzyme catalyzed reaction system, as shown in Figure 10. However, most of the bioluminescent organisms exhibit enzyme-catalyzed, with the luciferin-luciferase reaction system. In general, the enzyme luciferase catalyzes the reaction of the substrate luciferin with oxygen, producing an excited state molecule. The excited molecule then returns to the ground state with the release of energy in the form of light. Based on the literature study, the organisms exhibiting bioluminescence were classified depending upon their reaction mechanism.
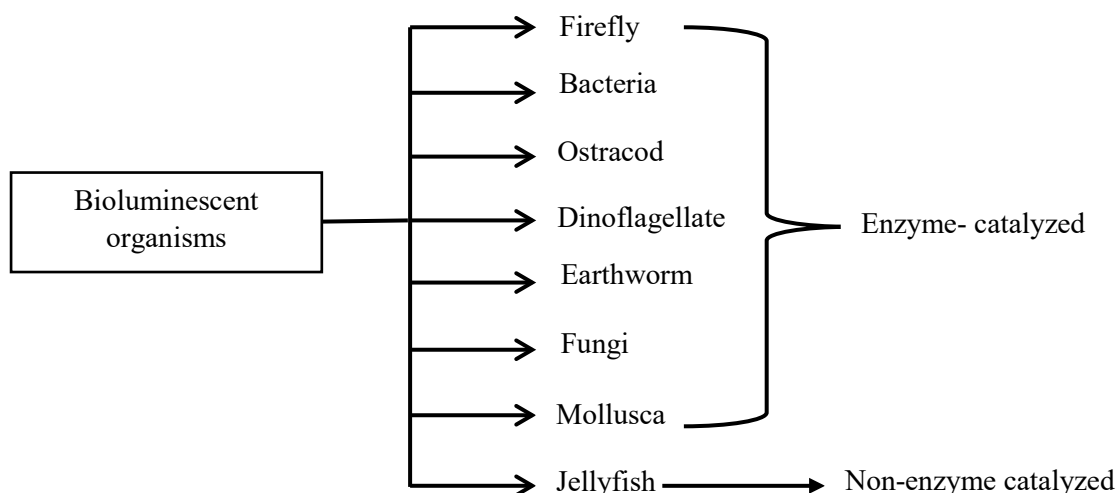
Figure 10. Classification of organisms exhibiting luminescence.

Non-enzyme catalyzed reaction

Among all these luminescent organisms present in nature, the molecular mechanisms of few organisms are studied widely. As represented in Figure 10, the non-enzyme catalyzed reaction was found in jellyfish, wherein the aequorin protein in the presence of an excess amount of Ca^{+2} produces (Scheme 1) a blue light. Aequorin molecule consists of coelenterazine moiety in peroxide form. Aequorin protein, together with the photoluminescent green fluorescent protein (GFP), emits green light when it receives blue light from aequorin activation. The initial process of light emission in the presence of photoprotein is a fast reaction, whereas the regeneration process is slow that inhibits the continuous light emission process [76]. The slow regeneration process essentially requires apoaequorin, coelenterazine, and molecular oxygen, while calcium must be absent [36].
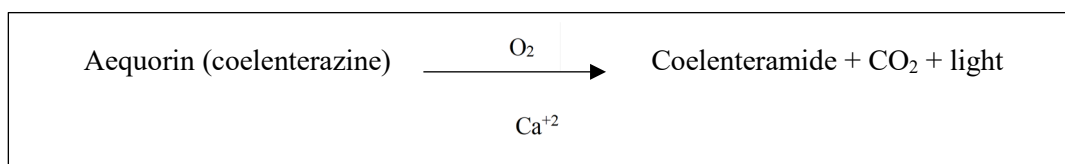
Scheme 1. Reaction mechanism of luminous aequorin

Enzyme-catalyzed reaction

Further, the **enzyme-catalyzed bioluminescence** system as shown in Figure 11, based on the enzyme(s) (luciferase) / substrate(s) (luciferin) can be classified into,

- ❖ <u>Multistep enzyme-catalyzed reaction</u> – The multistep enzyme-catalyzed reaction system consists of one or more substrate(s) and enzyme(s) along with co-factors to produce luminescence in nature.
- ❖ <u>Single-step enzyme-catalyzed reaction</u> – In this type of reaction, the substrate (a luciferin) molecule emits light in the presence of a single enzyme (luciferase).

Firefly

Bacteria

Ostracod
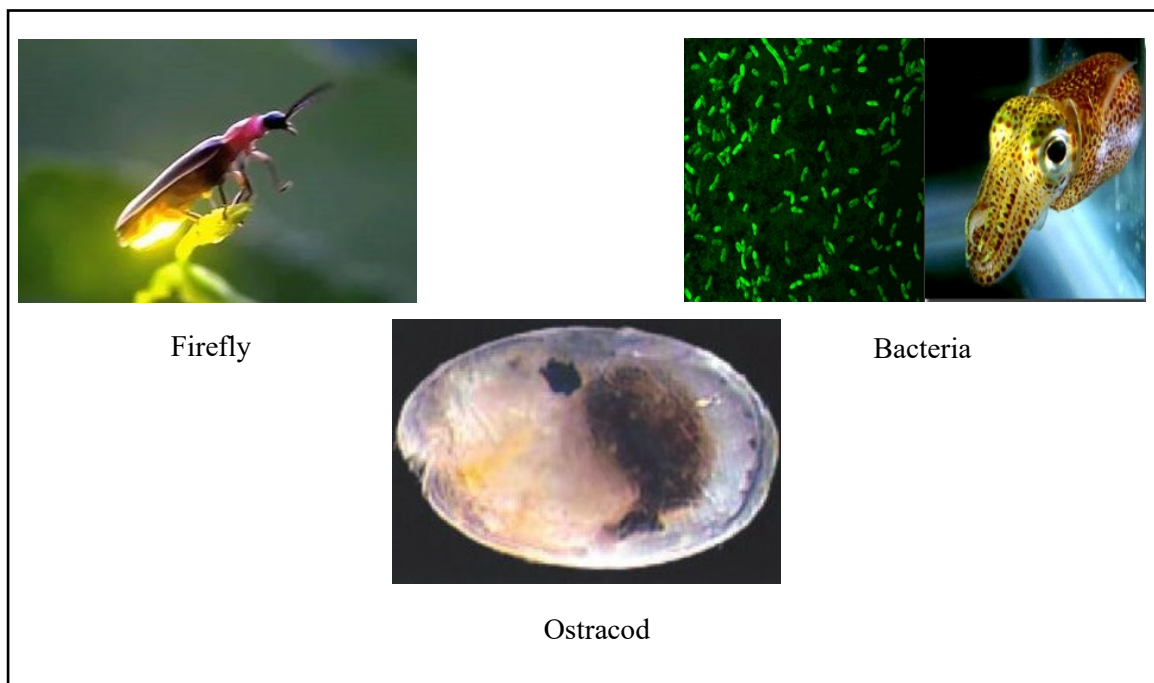
Figure 11. Enzyme catalyzed bioluminescent organisms (images from [77] [78][79])

Luminous firefly

The biochemical mechanism of firefly typically consists of D-luciferin (L) substrate and firefly luciferase enzyme (E) obtained from different species and hence can also produce a wide range of colors when catalyzed by different luciferases, having emission wavelength ranging from 535 nm, i.e., yellow-green color to 638 nm, i.e., red color

$$E + L + ATP + Mg^{2+} \longrightarrow E.L\text{-}AMP + PP + Mg^{2+} \ (1)$$

$$E.L\text{-}AMP + O_2 \longrightarrow E.OL + CO_2 + AMP + Light \ (2)$$
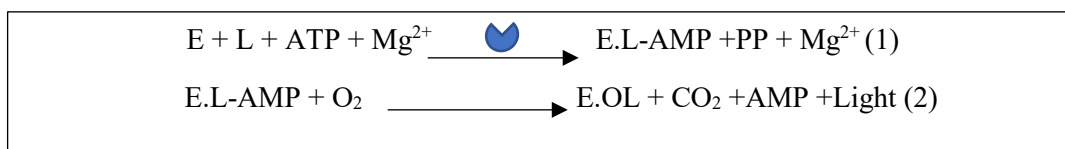
Scheme 2. Reaction scheme of a luminous firefly

In the above reaction mechanism (Scheme 2), reaction (1) is an enzyme-catalyzed reaction wherein firefly luciferin gets adenylated in the presence of enzyme firefly luciferase and co-factors ATP and Mg^{2+}. The adenylated molecule is then quickly oxygenated at a tertiary carbon atom, forming a hydroperoxide intermediate. The intermediate formed is a very unstable 4-membered di-oxetanone ring,

splitting off AMP, which then decomposes, yielding the keto or enol form of oxyluciferin. The formation of keto/enol form of oxyluciferin emits red and yellow-green light, respectively [80].

Luminous bacteria

Luminous bacteria, also termed as bioluminescent bacteria in this thesis, are widely distributed in the marine environment and have been isolated from various sources such as light organs of the squid, as shown in Figure 11. In luminous bacteria reaction system, the bacterial luciferase catalyzes the oxidation of reduced flavin mononucleotide ($FMNH_2$) by molecular oxygen in the presence of a long-chain aldehyde, yielding an excited state of hydroxyflavin-luciferase complex along with the formation of fatty acid, which returns to its ground state, emitting light and the FMN as shown in step (1) of Scheme 3. Moreover, the enzyme NAD(P)H: FMN oxidoreductase (FMN reductase) catalyzes the reduction of FMN in the presence of NADH to form $FMNH_2$, as shown in step (2) of Scheme 3.

$$FMNH_2 + O_2 + RCHO \xrightarrow{\text{Bacterial luciferase (Luc)}} FMN + RCOOH + H_2O + light \quad (1)$$

$$FMN + NADH + H^+ \xrightarrow{\text{NAD(P)H: FMN oxido reductase (FMN reductase)}} FMNH_2 + NAD^+ \quad (2)$$
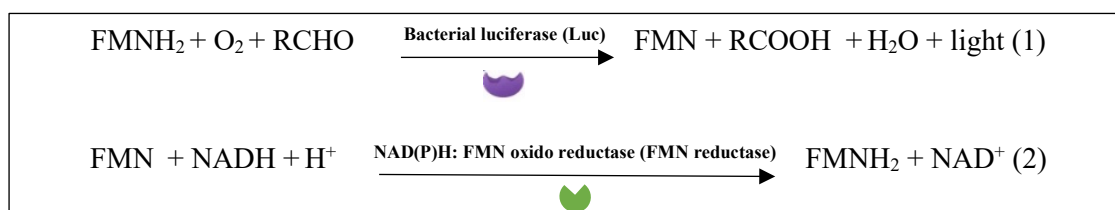
Scheme 3. Reaction mechanism of luminous bacteria

Thus, FMN formed can be readily reduced to $FMNH_2$ making continuous reaction processes until the exhaustion of aldehyde and NADH [71][81]. Unlike other bioluminescent reaction system wherein the substrate either has to be regenerated using another enzyme(s) or slow regeneration occurs, the luminous bacteria system is a continuous process due to its cyclic reaction system.

Luminous ostracod

In luminous ostracod, the luciferin (LnH) gets easily oxygenated by O_2, and in the presence of enzyme luciferase (E-Luc), peroxide is formed, which then cyclizes to form a dioxetanone ring and decomposes by splitting of the 4-membered ring into CO_2 and excited state of oxyluciferin (OLnH) as illustrated in Scheme 4.

$$LnH \xrightarrow{\text{E-Luc}} OLnH + CO_2 + light$$
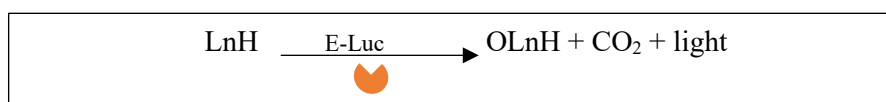
Scheme 4. Reaction mechanism of luminous ostracod

Luminous ostracod enzyme-catalyzed reaction also involves a side reaction whereby 85-90% of luciferin is converted into oxyluciferin, and the rest 10-15% converted to ethioluciferin, which is not the light emitter [70].

Comparing bioluminescence reaction mechanisms in different organisms

Light wavelength and intensity vary from one living organism to another depending upon the chemical structures. The study of most living organisms showed the presence of two components, luciferin and luciferase. However, the luciferin of one category would not necessarily interact with the luciferase of another, leading to the presence of many kinds of luciferins and luciferase in the living organisms. Illumination time varies from several seconds to minutes depending upon the reaction mechanism and its concentration. For example, a flashlight can be seen in jellyfish, and glow light can be seen in the case of luminous bacteria. Another vital aspect to consider is the regeneration of the substrate for the continuous reaction process to increase the duration of luminescence, as in the case of luminous bacteria. Thus, Table 2 summarizes the different reaction mechanisms based on commercially available substrates, enzymes, and co-factors required for the generation of light in different bioluminescent living organisms.

Table 2. Summary of bioluminescent living organisms

Categories	Substrate	Requirement for light production		Enzyme/Co-factor/ substrate for regeneration	Wave-length (nm) λmax
		Enzyme for reaction	Co-factors		
Insects (Firefly)	Luciferin (Benzothiozole)	Luciferase (Firefly)	ATP/Mg^{+2}	D-Cysteine + Light regenerating enzyme(LRE-not identified)	560 - 615 nm flashlight(can be extended if the substrate is regenerated)
Bacteria (*Photo bacterium fischeri*)	Riboflavin ($C_{17}H_{20}N_4O_6$) / flavin mononucleotide i.e.FMN ($C_{17}H_{21}N_4O_9P$)	a. Bacterial luciferase b. NADH: FMN oxidoreductase	Long chain aldehyde such as dodecanal ($CH_3(CH_2)_{10}CHO$)	No enzyme (Cyclic process because of the regeneration cycle)	490 nm Glow light intensity possible due to the substrate regeneration process
Crustaceans (Ostracod)	Cypridina Luciferin ($C_{22}H_{27}N_7O$)	Cypridina Luciferase	Not Required	Regeneration of Oxyluciferin is a challenge	465 nm flashlight

| Aequorea Victoria (Jellyfish) | Aequorin | Not required | Calcium | No enzyme/ Coelenterazine | 453-455 nm Flashlight (can be extended if substrate is regenerated) |

Other light-emitting organisms

In the mucus of the marine worm *Chaetopterus* (Figure 12), in the dark, a blue glow is produced in the mucus. It involves a photoprotein, iron, and flavins, wherein both ferric and ferrous irons were found, thus, indicating the presence of oxidase and reductase activity. However, the exact mechanism of bioluminescence is not yet completely known. Once Fe^{+3} of ferritin is secreted, it can be reduced in the presence of riboflavin and molecular oxygen, allowing the reactive ferrous ions to associate with chromophore or photoprotein leading to light production [82].
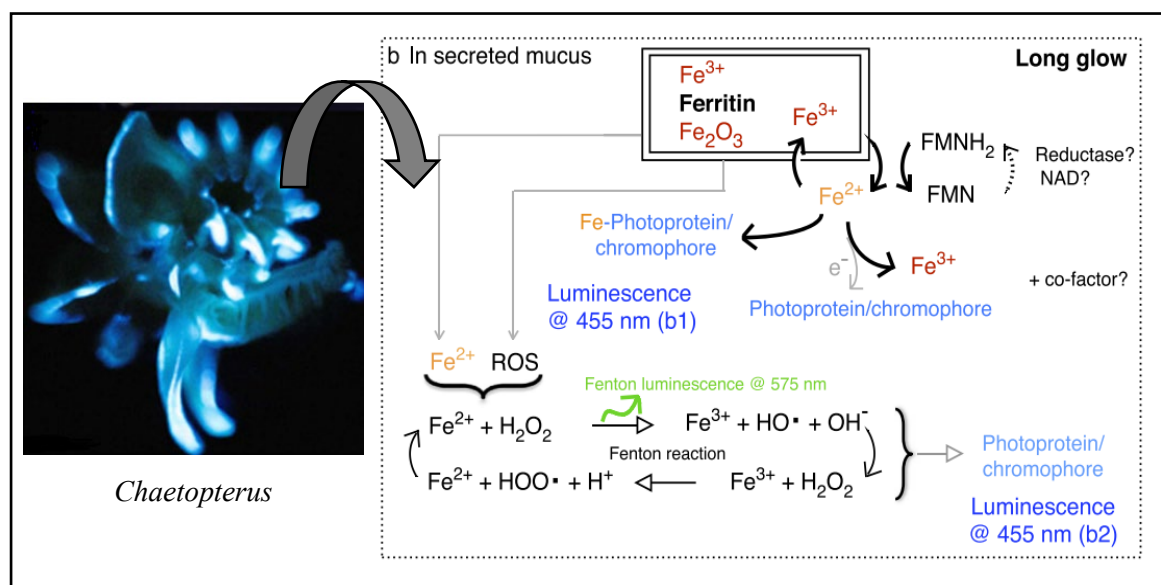
Figure 12. Schematic representation of the possible mechanisms for marine worm *Chaetopterus* [82]

1.2.4. Photoluminescence and fluorescence along with bioluminescence

In addition to the bioluminescence phenomenon, nature also exhibits photoluminescence and biofluorescence phenomena due to the presence of the chromophore group and photoprotein, respectively. The biofluorescence phenomenon occurs, wherein an organism absorbs blue light and emits different colors, usually red, orange, or green. However, they possess similar aims as bioluminescence (camouflage, communication, or mating) [83]. Further, the photoluminescence phenomenon occurring in plants has been studied widely [84][85][86]. Fluorescence of plant dyes has been studied mainly during the past decade, and several have been used for application to textiles. Some

naturally occurring fluorophores in plants are coumarins [87] and their derivatives (occurring in Arabidopsis), anthraquinones [88] (9,10-anthraquinones), cyanidin 3-O-β-(2-glucopyranosyl-O-β-galactopyranoside occurring in red and white flowers of *Plumeria Rubra* and carotenoid pigments (such as lutein occurring in marigold flower) [89][90][91]. Further, various GFP (green fluorescent protein) in nature are briefed. Moreover, in this thesis, a special focus will be made on molecules that are involved in bioluminescence reactions in certain organisms. These involve mainly the riboflavin (RF) and its derivative (FMN).

1.2.4.1. Biofluorescence and its role in nature

As discussed in section 1.2.2, with the discovery of green fluorescent protein (GFP) widely termed as photoproteins (PPs) (Figure 13) or fluorescent proteins (FPs) from Aequorea Victoria, it has been studied that organisms such as crustaceans and cephalochordates as well as various other marine organisms also possess FPs [83].
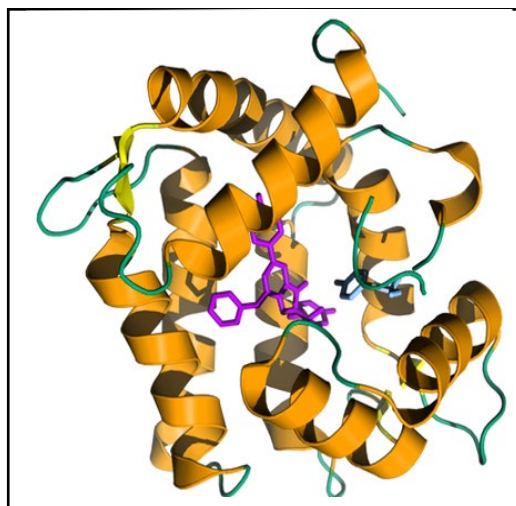
Figure 13. Green fluorescent protein from *Aequorea Victoria*

In Aequorea Victoria, the GFP allows producing an intense green light (508 nm) when illuminated by the blue light (470 nm) [76] produced by bioluminescence (see section 1.2.3). The green fluorescent protein contains a naturally built chromophore that consists of a unique sequence of amino acids. The fluorescence emission maxima for most of the natural GFPs are identical at around 508-509 nm and the excitation peak in a range of 450 – 500 nm [71]. Furthermore, researchers have shown photoluminescence behavior in certain organisms, such as in earthworm Eisenia lucens due to the presence of riboflavin or its derivative flavin mononucleotide (FMN). Indeed these are involved in organisms such and the marine earthworm Chaetopterus (as shown in Figure 12). The earthworm Eisenia lucens exhibits green fluorescence under UV irradiation. However, blue-green bioluminescence is observed when placed in the dark region. The measured bioluminescence system seen in earthworm

resembled the bioluminescence observed in the luminous bacteria system. Fluorescence seen in earthworm is due to the presence of a high quantity of riboflavin. Thus, riboflavin plays a vital role in the glowing bioluminescence reaction, and the proposed reaction mechanism, as illustrated in Figure 14, was reported in the study of photoluminescent and bioluminescent based earthworm [92].
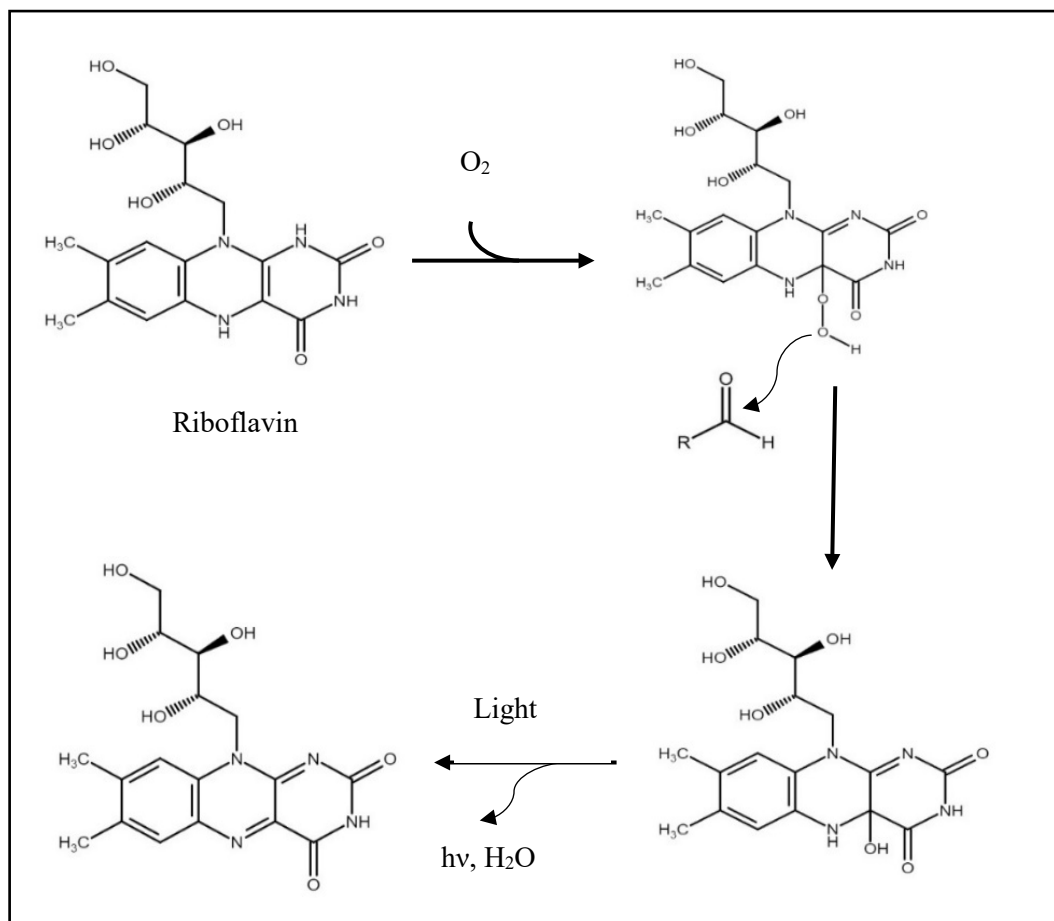
Figure 14. Proposed reaction mechanism of earthworm *Eisenia lucens* [92].

Thus, the improved knowledge of the reaction mechanism for different bioluminescent and photoluminescent based organisms increased research study for its application in various fields developed. Bioluminescence being the unique source of light based on the enzyme-substrate or luciferin-luciferase reaction, tends to have significant applications in the field of bioresearch. The diversity of reactions in bioluminescent organisms wherein the structure and biochemical reaction in between luciferin-luciferase have been identified and are now utilized broadly in environmental monitoring[93] [94], diagnostics [95], in vitro and in vivo food testing [96], drug screenings [97] [98], biomedical research [38][99][100]. On the contrary, photoluminescent applications have also evolved in recent years. E.g., development of photoluminescent functional textiles using photoluminescent nanomaterials such as tris (8-hydroxyquinoline) aluminum complex [14]. Further, most of the photoluminescent pigments are used in paints, coatings, laminates, incorporation in polymer dope stage to obtain

photoluminescent filaments and have found applications in safety, warnings, and aesthetics of textile for its use as ambient lighting as well as design and fashion is the trending scope [101].

Conclusion on literature work carried on bioluminescence and biofluorescence:

Based on the literature work carried, the selected bioluminescence system chosen was that of the bioluminescent bacteria/luminous bacteria. This choice was made based on economic considerations such as availability and affordable price, and also the possibility of regenerating the FMN substrate molecule in the bioluminescence reaction, which can potentially allow for continuous illumination. As described in the previous section 1.2.3, two enzymes are involved, together with FMN as a substrate, which is regenerated. Furthermore, as discussed in section 1.2.4.1, with the use of riboflavin and its derivative FMN in bioluminescence, these molecules also exhibit photoluminescence behavior, more specifically, biofluorescence. Hence, both riboflavin and FMN can be used to functionalize textiles to produce luminescent textiles.

1.2.5. Platforms for luminescence detection

Most of the chemiluminescence and bioluminescence reactions are monitored using a luminometer. The advantage of the luminometer analytical technique is its sensitivity and wide dynamic working range. Two components of light reach the detector, first, are equivalent or proportional to the concentration of reactants in the chemiluminescent reaction. The second component is known as a background act as constant light due to different factors such as the phosphorescence of plastics, impurities in the reagents, etc. In the luminometer, this background light component is much lower than in other analytical techniques such as spectrophotometry and fluorometry. Samples can be measured across decades of concentration without dilution or modification of the sample cell [102].

1.3. Bioinspiration to textile application

As described earlier, the transfer of knowledge inspired by nature into technology to create sustainable solutions is widely termed as biomimetics. In general, biomimetics can be achieved via different modes or levels, such as molecular, structural, ecological, and nanoscopy levels [4][8][103]. In general, biomimetics can be achieved via different modes or levels, such as molecular, structural, ecological, and nanoscopy levels [4][8][103].

Different strategies of biomimetics, as stated below has been used to obtain various functionalities on textiles,

- ❖ Transferring chemicals to technologies to obtain hydrophobic textiles – Using the biomimetic approach (lotus effect), various techniques such as sol-gel have been used to create roughness, hence attaining the hydrophobic effect on textiles.
- ❖ Structural design transfer – By understanding the chameleon effect seen in nature due to its structural design, textiles are modified by either weaving or knitting techniques to create structural fabric. Hence, the single dyed fabric can attain different colors due to the reflectance of light on the structurally modified fabric.

This study emphasizes the molecular level of biomimetics wherein the molecules participating in the bioluminescence chemical reaction are aimed to functionalize on the textile substrate.

Hence, the bioinspired strategy can be defined as a transfer of knowledge from nature to technological application for creating sustainable solutions. However, considering different biomimetic approaches and principles to achieve materials as a result of bioinspiration, it is important to consider that the outcome and results of concept to materials can take a minimum of 20 years to come from idea to market. For example, based on a literature study for the development of bioinspired self-repairing materials [104], similar principles were envisaged in this study to obtain luminescent textiles mainly studying in three phases, (i) understanding the luminescence mechanisms occurring in nature, either in plants or animals. (ii) transfer and integration of biological knowledge with technology. (iii) to obtain biomimetic or bioinspired luminescent materials. Further, various eco-technologies were studied and implemented to obtain eco-efficient luminescent materials.

Thus, to achieve the luminescence effect inspired by nature, a detailed literature study was carried out, as mentioned earlier. Among different bioluminescent organisms, which are identified and studied, bioluminescence bacteria have been widely studied. Bioluminescent bacteria widely exist in the marine environment, and the isolation processes have been studied widely; thus, the availability of enzyme(s) participating in the reaction system is higher as compared to other bioluminescent organisms. Furthermore, other bioluminescent reaction systems would require an additional substrate regenerating enzyme, also termed as LRE (light regenerating enzyme), contrary to the cyclic luminous bacteria system, which plays a crucial role for the longevity of luminescence. Also, the cost of the enzyme(s) and substrate(s) for the bioluminescent bacteria system is preferable among other bioluminescent organisms, as mentioned in Table 2.

Therefore, the choice of bioluminescent bacterial system for the current research study is due to its availability, low cost as compared to other enzymes of other bioluminescent living organisms, and mainly due to cyclic reaction system that retains the substrate molecule back in the system, thus can possess prolonged luminescence.

Thus, the overall strategy was to use FMN based bioluminescence and photoluminescence system to produce luminescent textiles/materials. In the case of FMN based bioluminescence pathway, the strategy was to immobilize the enzyme(s) on textiles. Previous studies of enzyme immobilization system on PET nonwoven textile surface provided the overview and the immobilization techniques that can be implemented for the thesis experimental study [105]. On the other hand, in the case of FMN based photoluminescence approach, the molecules were introduced using different functionalization methods as well as some advanced eco-technologies were explored to obtain photoluminescent textiles. The choice of eco-technologies yielding the biolighting /biofluorescence effect was important to create eco-efficient and sustainable solutions.

1.4. Functionalization and eco-technologies

To obtain bioluminescent textiles through luminous bacteria, system immobilization of enzyme(s) onto textiles was a necessary step. Previous research has revealed that plasma treatment can be an effective way to assist the immobilization of enzyme, more specifically, a single enzyme [105]. However, the challenge involving the luminous bacteria system was the immobilization of two different enzyme(s) on the textile surface. Hence, state of the art about different enzyme immobilization process and functionalization using eco-technologies are elaborated in this section.

On the other hand, to identify the potential use of biobased RF and FMN to obtain photoluminescent textiles, initial screening using the diffusion technique was a necessary step. Furthermore, a technology-driven approach with resource-efficient solutions was also aimed, such as the use of digital printing methods, inkjet, and chromojet printing. Therefore, state of the art of various eco-technologies is also described in this section.

1.4.1. Functionalization methods

In this section, different methods to incorporate the functional molecules to the textile material are described. Typically, the functional molecules are introduced either inside the fiber by diffusion (e.g., dyeing) or during the spinning process [106] or fixed at the fiber surface through chemical grafting, fiber surface activation [107] or using a cross-linker [108]. Functional molecules can be of various sizes, in the form of small molecules (e.g., dyes), or bigger molecules such as oligomers, polymers, macromolecules (such as enzymes), or the form of nanoparticles. While most of them can be incorporated into microcapsules before applications to textile [109][110], other functionalization methods are used depending on the size and chemistry of the functional molecule. Functional molecules of small size with a solubility parameter close to that of polymer fiber can functionalize a textile fiber by diffusion method, where the transport vector is either water or supercritical carbondioxide, an

anhydrous dyeing technology [111][112]. Functional molecules can also be deposited on the fabric fiber surface using padding or printing. These molecules can diffuse inside the fiber (depending on their size and fiber affinity, and temperature used) or graft on the fiber surface depending on chemical moieties present on the fiber surface as well in the functional molecule. Screen printing requires a higher viscosity formulation than padding, which can be achieved using an additional thickener such as a biopolymer. However, in the case of inkjet and chromojet printing, this viscosity has to be very low. Further, depending upon the textile nature, various interactions can occur between the fiber and the functional molecules; cellulose possesses hydroxyl moiety and exhibits hydrophilicity, in contrast to hydrophobic PET which does not allow easy surface functionalization. Hence, surface activation of polyester fabric to create reactive functional groups at the fiber surface, plays a key role in surface functionalization, and can be achieved using various techniques such as plasma technology.

1.4.1.1. Diffusion method

In the diffusion method through the exhaustion process, the textile is immersed in a water bath containing the functional species, such as a dye. The process generally involves adsorption, i.e., transfer of dye from the aqueous solution onto the textile surface to form a boundary layer, followed by diffusion wherein the dye gets diffused from this layer into the textile fiber. The method requires a temperature above the glass transition temperature (Tg) of the fiber that induces the segmental motion of polymer chains in textile material. Once the polymer chains are mobile, the dye begins to diffuse and are gradually embedded into the fiber, until equilibrium is attained between the dye concentration in the fiber surface and that in the dye bath solution. After equilibrium is reached and the system temperature is decreased, the dye molecules are trapped inside the textile material [113][114]. However, in this thesis, the objective is not to determine or demonstrate any theory of dyeing kinetics or thermodynamics. The study mainly focuses on the investigation of the potential use of these methods for yielding photoluminescent textiles using FMN and riboflavin molecules.

1.4.2. Eco-technologies

The term 'eco-technology' was first proposed in 1971 to describe combinations of practices related to the environment and technological intervention. With the increasing concerns related to environmental changes, the search for solutions in terms of managing resources, design, and use of technology that provide services of value to the society has become a need for action [115]. Each of these technologies contributes to one or more of the following attributes: decreasing the amount of added chemicals and solvents, minimizing treatment time and energy, reducing health hazards, reducing waste and wastewater production, and minimizing the environmental impact overall.

In this thesis work, two of the advances in eco-technologies, such as plasma treatment and digital printing, were used to facilitate the immobilization of functional molecules on textiles.

1.4.2.1. Plasma technique

Plasma technology applied to textiles is a surface modification process. It has gained tremendous importance among other available processes such as wet surface modification, physical and chemical vapor deposition [107]. Plasma, the 4th state of matter, is an electrically charged particles, and free electric charges make plasma electrically conductive and strongly responsive to the electromagnetic field. In nature, there exist plenty of plasmas; however, plasmas can also be effectively produced in the lab-scale and at the industrial level. All these different kinds of plasma are broadly classified into two categories: thermal and non-thermal. However, due to high temperature and possessing thermal equilibrium between all species contained in the gas of thermal plasma, it turns out to be destructive for nature, particularly for textiles. Hence, non-thermal plasma, also termed as cold plasma, is widely used, wherein the temperature of the electrons is much higher while the gas temperature remains near room temperature. Cold plasmas such as vacuum and atmospheric plasma can be created either by excitation of gas between two electrodes, either corona discharge or dielectric barrier discharge (DBD) electrode. Cold plasma can also be created by the excitation of gas by electrodeless microwave discharge with high frequency (2450 MHz), like cold, remote plasma (CRP), which is the type of plasma used within the frame of this thesis [116].

Further, depending upon the treatment conditions and type of textile material, different effects can be obtained using the plasma technique. Increase wettability, surface roughness, generation of free radicals, and plasma polymerization are some of the effects that can be attained. The major advantage is chemical and morphological surface modification without altering the bulk properties of textile material. The other significant advantage in context to eco-technology is the application method being a dry, environmental, and user-friendly process [117]. In this thesis, air atmospheric plasma (ATMP) and cold remote plasma with a mixture of N_2 and O_2 gases (CRPNO) treatment were used.

1.4.2.2. Digital printing technology

Textile printing has evolved rapidly over the last few decades, especially in terms of technology advancement, offering various methods of obtaining a design printing on textiles. Currently, inkjet printing technologies exhibit many advantages in terms of its process efficiency, simplicity, flexibility, cost-effectiveness, and environmental impact benefits. Due to the development and advancement in inkjet printing technologies, it has gained tremendous attention in various fields for its application use, such as in biotechnology, solar cells, sensors, bioprinting, etc. [118][119][120]. Inkjet printing

technology can be widely categorized into two main methods of printing, continuous method and drop-on-demand method. The commercialization of the continuous inkjet printer started from the year 1976 and is widely used for textile printing and labeling[120]. Further advances and background on digital printing technology, inkjet, and chromojet can be seen as described in the literature [121][118][122]. In the textile industry, inkjet printing techniques have been adapted for rapid production cycles maintaining the resolution and pattern quality as compared to conventional printing techniques [123][124]. The emerging use of digital printing techniques has advantages such as multi-color registration built-in systems, quick response to personalization and customization of products, non-contact printing, hence eliminating image distortion as well as low water and energy consumption is one of the key advantages of using advanced printing technologies [118].

1.4.3. Functionalization of textiles with immobilized enzymes

Enzyme immobilization can be defined as the confinement of enzymes in support/matrix. The support or matrix on which the enzymes are immobilized allows the exchange of medium containing substrate or inhibitor molecules [125]. In general, there are five methods for immobilization of enzymes; physical adsorption, covalent bonding, entrapment, encapsulation, and crosslinking. There are several advantages of enzyme immobilization, such as retaining enzyme activity and its reusability, stability of enzymes, ability to stop the reaction rapidly by removing the enzyme [126].
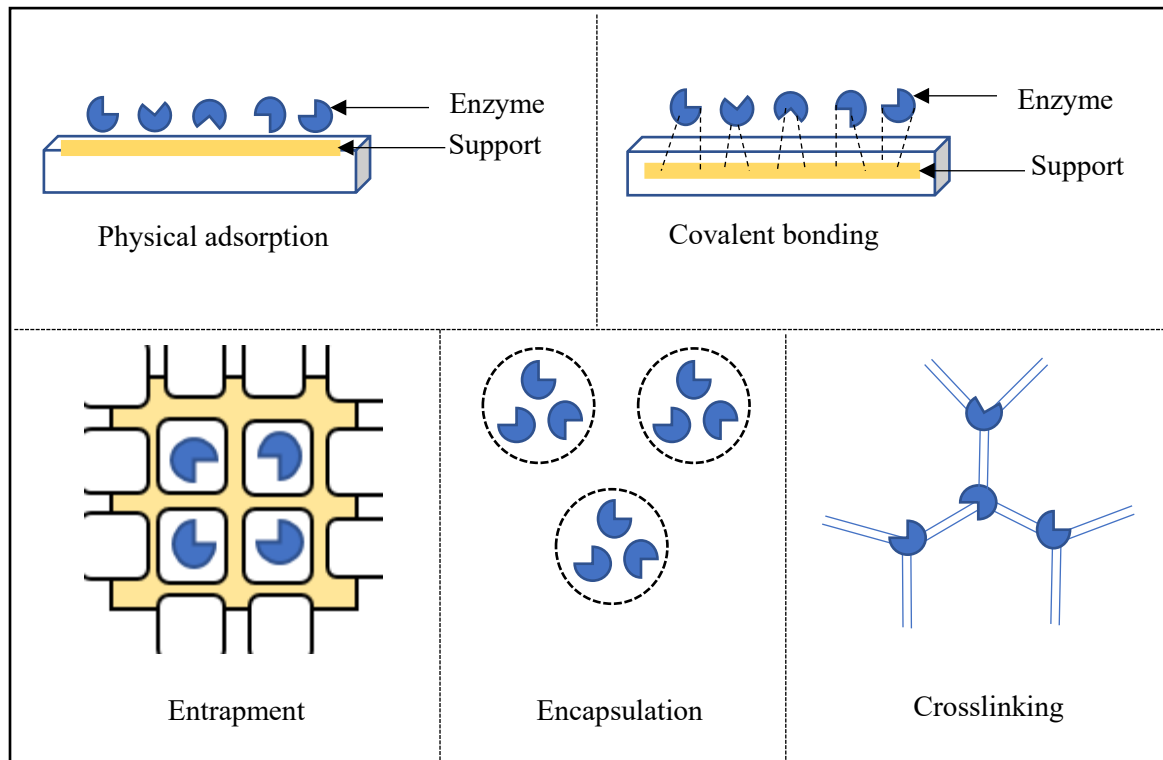
Figure 15. Illustration of immobilization methods of enzymes

Various methods, as mentioned in Figure 15, are used in literature and prevails in different chemistry between the proteins and the support materials. *Physical adsorption* is one of the most commonly used methods for enzyme immobilization, which is achieved by weak physical interaction between the adsorbed enzyme and the support material such as hydrogen bonding, Van der Waals bonds, or stronger ionic bonding. Although the forces are weak, they are sufficiently large in number to enable reasonable binding. *Covalent bonding* provides a direct chemical bonding between the enzyme and the support material via functional groups. The functional groups such as amino groups (NH_2), carboxylic (COOH), hydroxyl (OH), and sulfhydryl (SH) groups on the surface of the enzyme can form a covalent bond between the functional groups present on the surface of the support.

Polysaccharide polymers such as cellulose, starch, and agarose are known to support materials consisting of hydroxyl groups for covalent bond formation. *Entrapment* involves the inclusion of an enzyme in a polymer matrix such as an organic polymer. There exist significant entrapment methods such as gelation of macromolecules with multivalent cations (e.g., alginate), temperature-induced gelation, and organic polymerization reaction using chemical (e.g., polyacrylamide). *Encapsulation* of enzymes can be attained by entrapping the enzymes within a semipermeable membrane, a sol-gel, or a microcapsule. Different materials, such as nylon and cellulose nitrate, have been utilized to form microcapsules. Crosslinking can be achieved either chemically or physically. The chemical crosslinking involves the formation of a covalent linkage between the cells using a multifunctional reagent such as glutaraldehyde and toluene diisocyanate. Further, for the crosslinking of a single enzyme, both gelatin and albumin have also been used [127] [126] [128].

Furthermore, several factors, such as temperature, pH, and concentration of the enzyme, can influence enzyme activity. Thus, an optimization of the conditions to be used for enzyme immobilization should be considered to avoid denaturation of enzyme and loss of their activity. As for Luc used in this thesis, the optimum pH range is 6 - 8.5 and is inactivated at a temperature above $30 - 35°C$. Furthermore, the chemical modification of the sulfhydryl or imidazole group also causes inactivation, particularly in the case of Luc. Multivalent anions such as phosphate, sulfate, pyrophosphate, etc. at 0.1 M concentrations or higher significantly protect Luc from inactivation by heat [129].

1.5. Conclusion and strategy

The background of luminescence and existing luminescent materials, along with its environmental concerns, were elaborated in the first section. The bioinspired strategies to develop various functional textiles are the changing research trend and interests for all scientists. Thus, the luminescence phenomena seen in nature were reviewed and summarized in the consecutive section. It was found that the bioluminescent bacteria reaction system in nature has been widely studied concerning its extraction,

reaction mechanism, comparatively lower cost of enzyme, availability, and potential applications, and that is why this system was selected for experimental work to create a bioluminescent textile.

The further literature study revealed that both riboflavin (RF) and its derivate flavin mononucleotide (FMN), which are key substrate molecules for the luminous bacteria reaction system, exhibit photoluminescence and bioluminescence phenomena as seen in the biochemical reaction of individual organisms such as earthworm. Thus, the bioinspired strategy was also focused on developing photoluminescent textiles. In this context, the purpose of the study is the development of photoluminescent textiles using biobased products. Thus, riboflavin and its role in nature were reviewed, and the molecule being biobased interests the research more along with its ability to possess both photoluminescence and bioluminescence by itself and in the presence of enzyme(s) respectively. Hence, the potential use of RF and FMN with/without enzyme(s) to attain luminescent textiles using functionalization and eco-technological methods were investigated

The overall purpose of the study was unfolded into two main objectives

- ❖ Development of biomimetic/bioluminescent textiles or materials
- ❖ Development of photoluminescent textiles or materials

Thus, to fulfill the objectives mentioned above, the schematic illustration of the thesis framework was followed, as shown in Figure 3. The detailed descriptions of materials, methods, experimental study, and conclusions are discussed in the subsequent chapters.

CHAPTER 2: MATERIALS AND METHODS

2.1. Materials

2.1.1. Textiles

The textile industry is an ever-growing market due to its development in applications such as the industrial and technical sectors apart from clothing and household applications. Currently, the textile materials mainly being produced and consumed are synthetic, natural, silk, and wool materials with industrial footprints across the globe. The global fiber production in the year 2018 was around 107 million metric tons and expected to reach 145 million metric tons by 2030 [130]. In this thesis, textile materials such as PET woven and nonwoven, cotton and mercerized cotton, silk, and wool was used for the research study.

2.1.1.1 Polyester (PET)

PET fiber is the most produced and consumed fiber in the world, having global production of around 55 million mt in 2018 [130]. PET is the ester of ethylene glycol and terephthalic acid and has the chemical structure as represented in Figure 16.
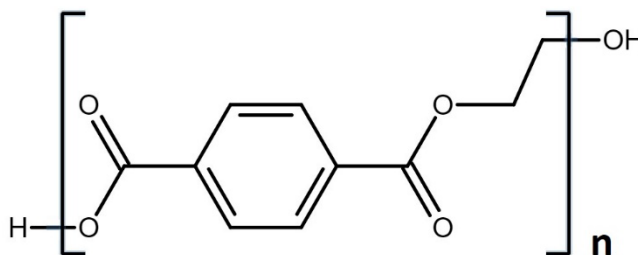
Figure 16. PET

In general, PET fiber possesses the right combination of properties for a wide variety of products. The density of PET fiber is typically 1.39 gcm^{-3} and usually is hydrophobic due to few polar interactions. Thus the moisture regains value is as low as 0.4 %. The structure of the fiber is semi-crystalline with partially amorphous and crystalline regions. The thermal properties generally depend on the method of manufacture; however, the typical glass transition temperature is in the range of 75 to 80°C with crystallization and melting ranges around 130°C and 260°C respectively. PET possesses a rigid structure, well-developed crystallinity, and lack of reactive sites; hence for further fiber treatment processes such as coloration, various methods for modification of dyes have been reported to employ the dye. [131] Recently, with the growing concerns and environmental problems, the use of plasma treatments for sustainable textile processing such as pretreatment of PET, dyeing, digital printing, and finishing of synthetic fiber has been studied [132]. Further, a new segment of fabrics, such as nonwoven

fabrics, has become an important part of the textile industry in recent years. Nonwoven fabrics are usually produced as sheet materials from randomly linked synthetic fibers such as PET as well as natural fibers. With the growing demand for environmentally friendly fibers for nonwoven, producers of polyesters are moving towards sustainable initiatives such as PET bio recycling [133]. The PET nonwoven can be engineered using a different manufacturing process and due to properties such as porosity and permeability, a significant increase in its use for smart textiles [133], and enzyme immobilization [121].

In the current thesis, both PET woven and nonwoven textiles were used for the experimental study to obtain photoluminescent and bioluminescent textiles, respectively. The microfibrous nonwoven PET structure of 100% PET fibers was formed by carding and hydroentanglement process ((i.e., entangling with water jets). The textile was manufactured at the European nonwoven platform, CENT (Tourcoing, France). It possessed a thickness of 950 µm, the areal density of 230 g/m^2 along with porosity of 93% and an air permeability of 645 mm/sec. The average fiber diameter was observed to be 12 µm using microscopic images. The specific surface area is 50 cm^2 of fiber surface per cm^2 of nonwoven. Besides, for photoluminescent molecule functionalization, a 100 % plain woven polyester textile of 160 g/m^2 provided by FOV Fabrics AB, Borås, Sweden, was also used in the research study.

2.1.1.2 Cellulose

Cellulose is the second most important fiber in terms of production volume. Its global production is around 26 million mt in the year 2018. Cellulose, as shown in Figure 17, is a condensation polymer formed by bio-synthesis from carbon dioxide and water along with glucose as an intermediate monomer.
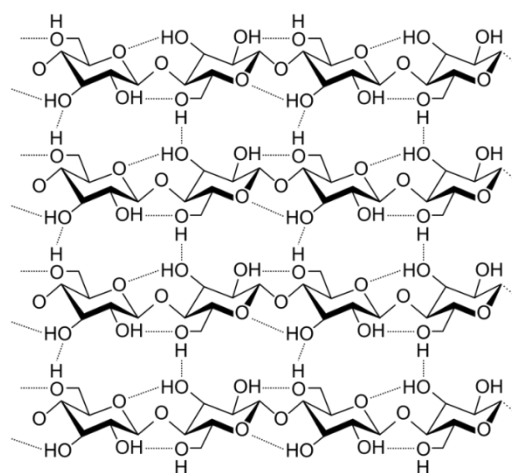
Figure 17. Cellulose

It is a long-chain polymer with a natural degree of polymerization (DP) over 10,000 and 70 % of crystallinity. Mercerization is a treatment of cotton fiber using sodium hydroxide solution that disrupts the crystals due to swelling of fibers. Importantly, it converts the fibers from bean shaped into round shaped cross-sections with a small central lumen, hence increasing the fiber luster, tensile strength, dyeability, color depth, etc. [134][135].

In this thesis, cellulosic woven material such as viscose fabric 40 g/m^2 was primarily used, and most of the evaluation of different functional properties was carried out on viscose fabric. Moreover, the cotton fabric of 70 g/m^2 was also studied. Before dyeing, both viscose and cotton fabric samples were cleaned using non-ionic detergent with subsequent hot and cold-water wash treatment. Further, the substrate material used for printing was mercerized cotton (MC), cotton duck white (CD) purchased from Whaleys (Bradford Ltd.) having textile weight 170 and 270 g/m^2, respectively.

2.1.1.3   Silk and wool

Silk and wool are proteinic fibers made from amino acids, and contribute to 0.1 to 1 % of global textile production, major being wool fiber production of around 1 million mt followed by silk having 0.1 million mt global production in 2018 [130]. Silk varies from other natural fibers, and due to its unique qualities such as the fiber shape, bulk, and surface properties, it's market demand can be seen. Wool, on the contrary, is more resilient and durable, which can be made into warm, attractive clothing. Wool possesses the most complex structure of the fiber, and the structural features determine the specific properties of wool [135]. Thus, in this thesis, both silk and wool woven fabrics having 85 g/m^2 and 265 g/m^2 textile weight were used respectively.

2.1.2. Chemicals

All chemicals such as riboflavin, riboflavin 5′-monophosphate sodium salt hydrate, widely known as flavin mononucleotide (FMN), sodium phosphate monobasic dehydrate and sodium phosphate dibasic dihydrate, citric acid, tannic acid, calcium chloride, β-Nicotinamide adenine dinucleotide disodium salt (NADH), dodecanal were purchased from Sigma Aldrich and used as received without any further pre-treatment. Further biopolymers such as starch, gelatin, and sodium alginate, and bovine serum albumin (BSA) were used for an experimental research study. Table 3 summarizes the properties of the biopolymers as per the analysis sheet of Sigma Aldrich.

Table 3. Properties of biopolymers (Source: Sigma Aldrich material data)

Properties	Starch	Gelatin from porcine skin	Sodium alginate
Appearance	White powder	Faint yellow powder	Off white solid
Water solubility	Soluble	50 mg/ml, H_2O	Soluble
Viscosity/ gel strength*	-	300*	24.4 cps (1% at 5°C)
Formula weight/*Protein	342.30 g/mol	77*	-

2.1.3. Enzymes

2.1.3.1 Bacterial luciferase (Luc)

Luciferase extracted from *Vibrio* (*photobacterium*) *fischeri* EC 1.14.14.3 was purchased from Sigma Aldrich. As per the supplier details, the luciferase is a lyophilized powder protein partially purified, which may contain certain soluble extracts of FMN reductase. The structure of the bacterial luciferase has been reported, as shown in Figure 18. The enzyme consists of a β-strand-loop-α helix-loop having active centers located at the carboxyl end of the barrel. The 'N' and 'C' terminals are usually adjacent in enzymes, the carboxyl-terminal residing at the end of the loop beside the amino ends of the β strands [136].
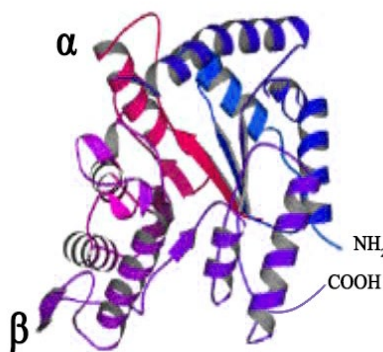
Figure 18. Bacterial luciferase enzyme from *Vibrio* (*photobacterium*) *fischeri*

2.1.3.2 NAD(P)H: FMN oxidoreductase (FMN Reductase)

It is also known as FMN reductase, extracted from Photobacterium fischeri EC.1.6.8.1, and was purchased from Sigma Aldrich. FMN reductase is a flavoprotein possessing FMN as a prosthetic group and acts as a dimer in the solution. The overall structure of FMN reductase represented by the ribbon

model and the yellow-colored FMN molecules at the interface of the two polypeptide chains can be seen in Figure 19 [137].
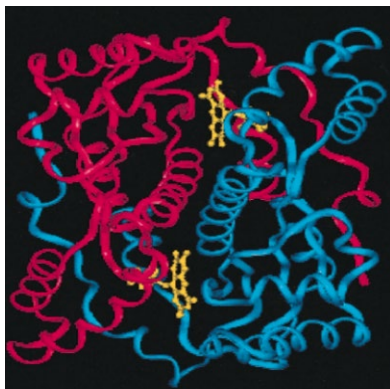
Figure 19. FMN reductase from *Vibrio* (*photobacterium*) *fischeri* [137]

2.2. Methods

2.2.1 Textile surface treatment / functionalization and characterization

2.2.1.1 Surface treatment and functionalization

2.2.1.1.a Textile surface treatment using plasma

A 100 % nonwoven PET was modified for the immobilization of enzyme using two different plasma treatments, air atmospheric plasma (ATMP) and cold remote plasma with a mixture of nitrogen and oxygen gases (CRPNO). The nonwoven was cleaned as the textile surface need to be free from any surface impurities and spinning oil before the surface plasma activation [138]. PET sample cleanliness was then confirmed by measuring the surface tension of final rinsing water, which indeed was equivalent to the surface tension of pure water that is 72.6 mN/m.

Air atmospheric plasma treatment (ATMP) conditions:

The plasma treatment was performed using an air atmospheric plasma machine called ¨Coating Star¨ manufactured by the Ahlbrandt system (Germany), as shown in Figure 20. A `50 x 50 cm´ PET nonwoven was cut into square pieces according to the electrode length of the plasma machine. The machine parameters were set as follows, electrical power at 1 kW, frequency of 26 kHz, speed set at 2 m/min having an interelectrode distance of 1.5 mm, and treatment power of 45 kJ/m^2. The textile was treated at the same condition on both sides. After plasma treatment, each treated nonwoven PET was kept away from light [138].
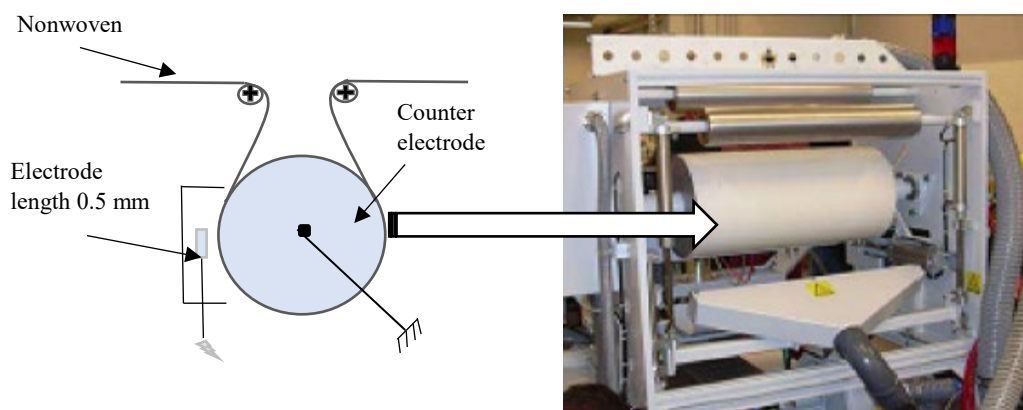
Figure 20. Air atmospheric plasma equipment

Cold remote plasma with N_2 and O_2 (CRPNO) treatment conditions:

In the cold remote plasma treatment equipment (France), plasma discharge was created using the mixture of oxygen and nitrogen gases and are subjected to microwave (as shown in Figure 21). As the discharge was located far from the samples to be treated (0.9 meters), the plasma reaching the textile sample, were free of any UV radiations or charged particles. The principal reactive species are atomic nitrogen, atomic oxygen, and vibrationally electronically excited nitrogen molecules. The experimental set up for cold remote plasma treatment has been illustrated previously [105]. The nonwoven PET was cut into square pieces and subjected to the specified conditions. The gaseous flow of $(N_2 + O_2)$ mixture with N_2 flow 1250 Ncm^3 / min and O_2 flow set at 45 Ncm^3/min was achieved by continuous pumping using a mechanical rotary pump (33 $m^3.h^{-1}$). The gas flow was excited by an electrodeless microwave discharge (800 W - 2450 MHz) produced in a quartz tube with an inner diameter of 30 mm, coupled to a cylindrical Pyrex treatment chamber with a diameter of 150 mm and a volume of 15 L [139].
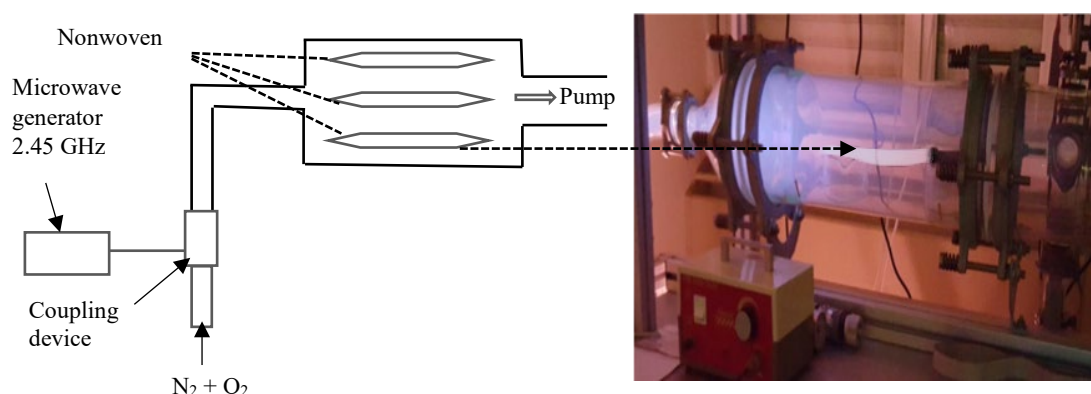
Figure 21. Cold remote plasma equipment

2.2.1.1.b Textile functionalization using inkjet/chromojet

Inkjet printer: The printing process was carried out using a Xennia Carnelian 100 inkjet printer, as shown in Figure 22. For textile printing, the printer was set up using a piezoelectric print head from Dimatix Sapphire QS-256/80 AAA (Fujifilm, USA) having a printable drop size of 80 pL and 100 dpi resolution.
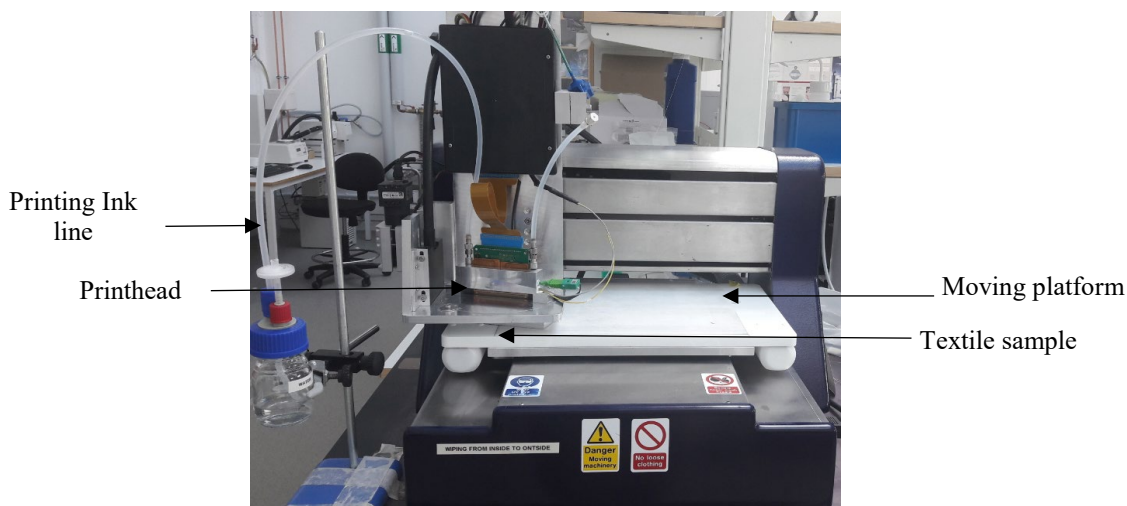
Figure 22. Inkjet printer set up (Xennia Carnelian 100)

Chromojet printer: The electromagnetic type print head known as chromojet printer by Zimmer (Austria) is based on jetting fluid using a switchable electromagnetic valve combined with pressurized air (Figure 23). The chromojet printer is a digital printing technology wherein an electromagnet activates a plunger allowing opening and closing of the nozzle. The quantity can be controlled by coverage, nozzle diameter, viscosity, pressure, and head speed. In this study, 150 µm of nozzle diameter at 2 bar pressure with the head speed of 1 m/s having 50 dpi resolution was used.
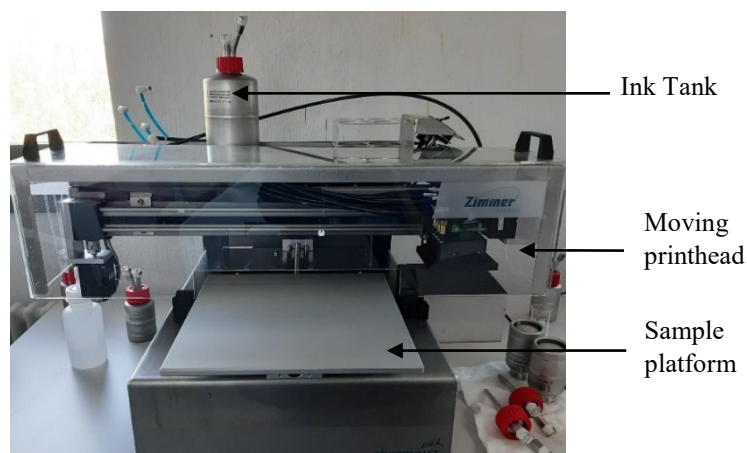
Figure 23. Chromojet printer set up (Zimmer, Austria)

Several parameters influence drop size, ejection speed, coverage, and total pick up. The easiest way to control pick up is to rasterize the coverage. The raster can be in a range between 10% and 100% depending upon the textile type and pick up.

2.2.1.2 Characterization methods after surface treatment/functionalization of textiles

2.2.1.2.a Capillary measurement and contact angle

Traditionally, the water contact angle of PET film remains within the range of 75-80° [140][141]. While the water contact angle (WCA) is an important characteristic parameter used to describe the wetting processes related to surface energies of solid material, the measured value is not only dependent on the material chemistry, but the surface roughness of the material can also influence this value. In the case of hydrophobic PET nonwoven with a contact angle higher than $90°$, the sample was measured using a sessile drop method in 'Digidrop' equipment from GBX instruments (France). To measure water contact angle < 90°, a wicking test was performed with a 3S scale tensiometer (GBX instruments) to measure capillary uptake and water contact angle of plasma treated PET nonwoven samples. A rectangular piece of the size of 3×5 cm was used, wherein the edge of one end connected to the tensiometer at weighing position, and the other end edge was bought in contact with the surface of distilled water placed in a glass beaker. As soon as the sample was in contact with the water surface, a sudden increase in weight (Wm) the meniscus weight was noted, and the water contact angle was then calculated using Eq.1,

$$W_m . g = \gamma_L . cos\theta . p \qquad \text{(Eq.1)}$$

Where W_m = Meniscus weight

g = 9.81 g s^{-2}

γ_L = surface tension of liquid water in `mN m^{-1}´

p = sample perimeter in contact with the liquid (mm) and

θ = water contact angle (°)

The time of contact with water was set to 3 min. The capillary weight was noted after the removal of the nonwoven sample from the water surface [142].

2.2.1.2.b SEM and AFM

The SEM micrographs were obtained using a Hitachi S 4800 cold field emission scanning electron microscope. Before the SEM analysis, each textile sample was sputtered with gold. The samples were prepared by cutting textiles into 5×5 mm size and placing it to the electron microscope stage with conductive adhesive. Further, to obtain the topographical images of textile samples, an AFM Dimension

Icon instrument from Bruker was used, and the images were analyzed using a contact mode method, as shown in Figure 24.
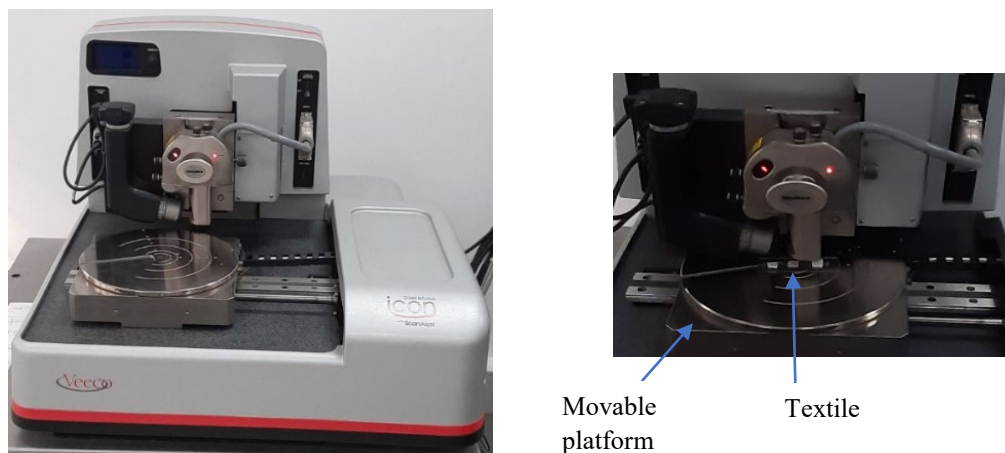
Figure 24. AFM equipment

2.2.1.2.c ESCA

The surface chemistry of the nonwoven was characterized using ESCA. Results reported here are measured using the PHI5500 ESCA instrument equipped with a monochromated aluminum (Al) source (Photon energy = 1486.6 eV). Beam size or the analyzed area during the measurement was kept around 800 μm in diameter. The samples were analyzed in duplicates from different portions of the nonwoven. Electron neutralizer was used for charge compensation on the insulating material. The survey scan was run in the range between 0 and 1330 eV with the pass energy 93.5 eV, and the energy step was 0.40 eV in the spectrum.

2.2.1.2.d FTIR

FTIR analyses were carried out using Nicolet is10 spectrophotometer (ThermoFisher Scientific) using the KBr pellet technique within the scan range of $4000 - 400$ cm^{-1} (64 scans at 4 cm^{-1} optical resolution). Before analyzing the samples, the background correction of CO_2 from the air was performed. The identification was based on the characteristic absorption peak indicating the chemical compound. Spectra are evaluated and presented as absorbance values versus wavelength (cm^{-1}) in arbitrary units.

2.2.1.3 Printing paste/ ink characterization

2.2.1.3.a Rheometer

The rheological properties were measured using a modular compact Anton Paar rheometer (Physica MCR500, Austria). The viscosity was recorded at the highest measurable shear rate of the instrument 10000 s^{-1} with a set temperature range depending upon the samples. Viscosity is an important parameter to measure the jettability of fluid in a specific print head [124]. The viscosity range for the inkjet printer

is in the range of 8 – 14 mPa.s [124], and the viscosity range for the chromojet printer is 0 – 500 mPa.s [143].

2.2.1.3.b Surface tension

The surface tension was measured using an optical tensiometer (Attension theta, Biolin scientific). A pendant drop method was used with an ink drop volume of 4 µL, and an average of three independent measurements are reported.

2.2.2 Characterization methods for the development of biomimetic/bio luminescent textiles

2.2.2.1 Luminometer

Luminometer equipment was used for the detection and measurement of the emitted light or the luminous signal obtained during the experimental study. The detector in the luminometer devices is generally a photomultiplier tube. In order to measure the smallest quantities of light, a photomultiplier tube (PMT) is commonly used due to its fast amplification and quick response for bacterial bioluminescence detection, as shown in Figure 25.
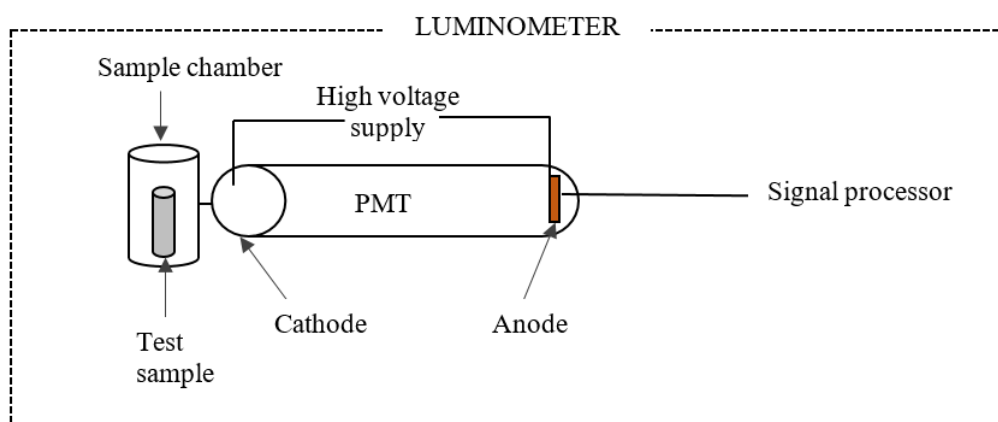
Figure 25. Schematic representation of PMT detector

It greatly amplifies incoming signals so that even the weak signals are detectable. PMT is an extremely sensitive detector for light detection in a broad spectrum ranging from ultraviolet to near-infrared regions or wavelength. Thus, it can analyze the bacterial bioluminescent, which appears as a blue-green light with a center wavelength at 490 nm. After PMT, more advanced silicon photomultiplier tubes with more sensitivity has been developed. There are also few imaging techniques, which are developed with the principle of charge coupling device. Also, electrochemical detection of bioluminescence phenomena has been developed [102]. However, in the current research work, measurements were performed on a Luminometer MicrolumatPlus LB 96V (France). A photodetector PMT known as

photomultiplier tube was used where the detecting signal is photon counts. The equipment detector consists of an ultra-fast single-photon counter system along with a spectral sensitivity range from 380 – 630 nm. The light emission was measured in terms of relative light units (RLU).

2.2.2.1.a Lab-scale analysis method

Table 4 and Table 5 represents analysis methods for the determination of light intensity using a luminometer of the bioluminescent bacterial system in the aqueous phase and on immobilized nonwoven textile samples.

Table 4. Aqueous phase study
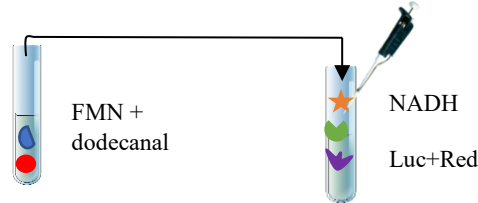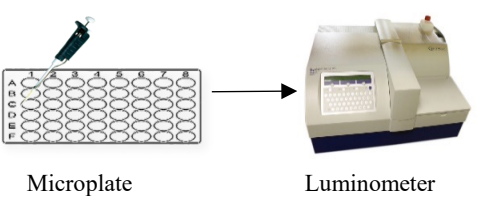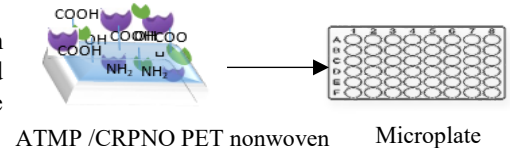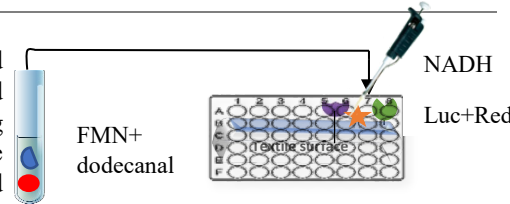
Step 1:	Weighing freshly prepared Luc enzyme (with/without buffer, biopolymer, and BSA) and mixing with Red enzyme	Luc Red
Step 2:	Preparation of mixture using the substrate as FMN and freshly prepared dodecanal as a co-factor and introducing in enzyme mixture prepared as in Step 1 followed by the initiation of reaction by injection of NADH to the reaction mixture and mixing for about a minute	FMN + dodecanal NADH Luc+Red
Step 3:	Injection of 200 µl from the total reaction mixture and analyzing solution after 2 minutes using Luminometer equipment. The samples were also analyzed every 2 minutes for approximately 60 – 80 minutes to study the luminescence variation	Microplate Luminometer

Table 5. Textile phase study

Step 1:	Placing the 1×1 cm^2 PET nonwoven with immobilized Luc enzyme only, or co-immobilized with both Luc and Red enzymes, in a vial of the microplate.	ATMP /CRPNO PET nonwoven Microplate
Step 2:	Preparation of mixture using FMN as substrate and freshly prepared dodecanal as a co-factor and injecting in vials of a microplate containing enzyme immobilized nonwoven followed by the initiation of reaction by injecting NADH and mixing it for about a minute	FMN+ dodecanal NADH Luc+Red

| Step 3: | The treated textile placed in microplate was then analyzed every 2 minutes for approximately 60 – 80 minutes using a luminometer to study the luminescence variation. | Luminometer |

2.2.2.2 UV/visible spectroscopy

The activity of the FMN reductase enzyme was measured by VWR UV- visible (UV-Vis) spectrophotometer, Model UV-3100 PC. The spectrophotometric studies were also carried to follow variations in the concentration of FMN substrate, co-enzyme NADH, and to monitor the formation of $FMNH_2$ in the presence of FMN reductase enzyme.

2.2.3 Characterization methods for the development of photoluminescent textiles

2.2.3.1 Experimental set up for treated sample observation

The fluorescence effect of FMN on treated textile samples was qualitatively analyzed by observing them under UV light (370 nm) in a closed chamber, keeping the setup, as shown in Figure 26. The visual images of printed textiles under the UV chamber were captured using a phone camera, keeping flashlight in the ´OFF´ mode.

Figure 26. Schematic diagram of the UV chamber.

2.2.3.2 Photoluminescence spectroscopy

The photoluminescence characteristics of dyed fabric samples were analyzed by a triple monochromator Dilor RT 30 and then detected using a Hamamatsu R943 photomultiplier in the photon-counting mode. Photoluminescence spectra were recorded at room temperature, and the emission spectra were obt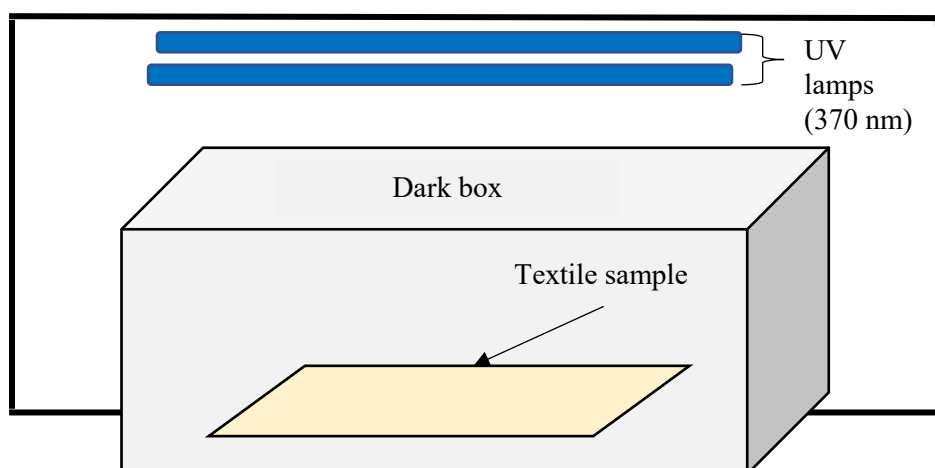ained by scanning with the analyzing spectrometer using fixed illumination at wavelengths of 364 nm and 470 nm line with 30 mW argon laser. The laser beam was focused with a 100-mm focal length lens to produce a 50-micron diameter with an average exposure time of 4 seconds spot on the sample. The incident power on the fabric sample was kept at 3 Mw. Further, a quantitative analysis of fluorescent properties for all printed textile samples was analyzed using a Horiba Fluorolog-3 fluorescence spectrophotometer, wherein a monochromated Xenon arc lamp was used as an excitation source. The slit width of both excitation and emission was set at 1 nm, and the scan wavelength speed at 1200 nm min^{-1}. The fluorescence spectra were scanned in the wavelength range from 385 nm to 700 nm with an increment of 1 nm wavelength having an integration time of 0.1 s. During sample measurement, the excitation wavelength was kept 15 nm low because if the fluorescence on the samples is high (high % intensity), it can quench the fluorescence. The corrected emission curves were recorded in the CPS / MicroAmps unit and analyzed. The excitation wavelength was kept 10 nm below the range of wavelength that needs to be analyzed. Thus, mainly there were two excitation wavelengths to be analyzed at 445 and 370 nm, the wavelengths are depending upon the absorption wavelength of the fluorescent dye molecule used.

2.2.3.3 Quantum efficiency theoretical evaluation

In addition to spectroscopy analysis measuring the emission spectra and photoluminescence intensity, the photoluminescence property was further investigated theoretically by quantifying the quantum efficiency of the dyed and printed samples. The method involves measurement of spectral reflectance curve obtained using illuminant D65, 10° standard observer in Konica-Minolta CM3610A spectrophotometer. The spectral reflectance measurements of the dyed samples, along with the undyed sample, were recorded. The measured values were substituted in extended Kubelka Munk [144], [145] Eq.2 stated below, and quantum efficiency value was obtained, respectively.

$$R_{f(\lambda')} = \frac{K_f}{S}\varphi(\lambda')\frac{(1+R_{\infty(\lambda')})(1+R'_\infty)}{\left(\frac{1}{R_{\infty(\lambda')}}-R_{\infty(\lambda')}\right)+\left(\frac{1}{R'_\infty}-R'_\infty\right)}$$

$$\frac{K_f}{S} = \frac{(1-R_{\infty(\lambda')})^2}{2R_{\infty(\lambda')}} - \frac{(1-R_{S(\lambda')})^2}{2R_{S(\lambda')}} \qquad (Eq.2)$$

Where,

λ' is an absorption wavelength

$\varphi(\lambda')$ is quantum efficiency at λ' wavelength

$R_{\infty(\lambda')}$ is spectral reflectance of the treated sample at λ' wavelength

R'_{∞} is spectral reflectance of substrate at λ' wavelength

$R_{f(\lambda')}$ is the difference in spectral reflectance value between forward and reverse measurement at the absorption wavelength

K_f is the absorption coefficient of the dyed samples minus that of the undyed samples

S is the scattering coefficient of the undyed sample in the emission region

2.2.3.4 Spectrophotometer

The aqueous solution of FMN was analyzed using the UV Visible spectrophotometer of Make-VWR, Model No. UV-3100 PC. Further, the absorption spectrum of FMN solutions irradiated with UV and visible light sources were analyzed using Thermo scientific (Evolution 201, USA) UV-visible spectrophotometer.

2.2.3.5 Color evaluation

The color strength of the dyed fabrics was evaluated using a Konica-Minolta CM3610A spectrophotometer (illuminant D65, 10° standard observer). The measurement data provided the K/S, L*, a*, b* color coordinates, which are lightness (L*), redness-greenness value (a*), yellowness-blueness value (b*). Consequently, to describe the depth of color on the textile substrate, the Kubelka-Munk theory was used (Eq.3). Thus, the K/S value was determined from reflectance values (R) measured for different wavelengths varying between 360 to 740 nm,

$$\frac{K}{S} = \frac{(1 - R)^2}{2R} \qquad (Eq.3)$$

Where R is the diffused reflectance, K is the absorption coefficient of the sample, and S is the scattering coefficient.

The color characteristics of the printed textile samples were evaluated using a Datacolor Check II reflectance spectrophotometer. Reflectance measurements were conducted under the condition of D65 illuminant and 10° standard observers on the folded samples (four layers). The color strength was then determined using the Kubelka-Munk Eq.3.

2.2.4 Antibacterial test

The antibacterial activity was evaluated against gram-negative Escherichia coli (E-coli, ATCC 25922), according to ASTM 2149. The bacterial concentration of about 10^5 CFU/ml was prepared and applied to samples for testing. Samples were placed in 50 ml bacterial suspension and were shaken in a wrist-action shaker for 24 hours at $37\,°C$. The viable colonies were counted (in CFU/mL), and the bacterial reduction was determined. The antibacterial activity was expressed in % reduction of the organisms after contact with the test sample at time '0' compared to the number of bacterial cells surviving after contact with the sample after 24 hours. The reduction rate (R %) of bacteria was calculated using Eq.4.

$$R(\%) = \left[\frac{B\text{-}A}{B}\right] \times 100 \qquad \text{(Eq. 4)}$$

Where `A´ is the number of bacteria recovered from inoculated treated test sample in a jar incubated for 24 hours, and `B´ is the number of bacteria recovered from inoculated treated test sample at '0' contact time.

2.2.5 UV protection test

UV protection performance values were evaluated for the dyed and printed fabric samples. Labsphere UV 1000F ultraviolet transmittance analyzer (USA) was used to determine the ultraviolet protection factor (UPF) and UV transmittance of the sample. Each sample was tested in quadrate, and the obtained results were then averaged. The measurements were conducted according to the standard GB/T 18830-2009. Transmission measurement was evaluated in the range of 250-450 nm. Consequently, the UPF ratings for all the treated fabric samples were obtained. The UPF value can be calculated using the following Eq.5,

$$UPF = \frac{\sum_{250\,nm}^{450\,nm} E(\lambda)S(\lambda)\Delta\lambda}{\sum_{250\,nm}^{450\,nm} E(\lambda)S(\lambda)T(\lambda)\Delta\lambda} \qquad \text{(Eq.5)}$$

Where E (λ) is the relative erythemal spectral effectiveness, S (λ) is solar spectral irradiance, T (λ) is the spectral transmittance of each fabric, and $\Delta\lambda$ is the wavelength step in nm.

CHAPTER 3: DEVELOPMENT OF BIOMIMETIC/BIO LUMINESCENT TEXTILES

3.1. Introduction

The extreme diversity of bioluminescence chemistries can be seen in living organisms (as summarized in Table 2). In this work, among all of the reaction mechanisms summarized, the bioluminescent bacteria (also mentioned as luminous bacteria in the thesis) reaction system was investigated. In addition to the extensive study done for isolation of the bioluminescent bacteria system from marine sources, various studies have been undertaken to pertain to its applications. However, the native bioluminescent enzymes are generally subject to inactivation in-vitro and hence not suitable for applications. Immobilized enzymes largely resolve the instability issue, thus enabling the development in practical applications such as luminescent biosensors [146], in medical diagnosis, biotechnology, environmental protection as well as for high sensitivity enzymatic assay determination [38][41][147][148][149][150]. Thus to create a biomimetic/bio luminescent textile using enzyme immobilization, a specific pathway involving the following details was studied.

Firstly, detailed bibliography on bioluminescent bacterial system

The bioluminescent bacterial system being non-toxic, has been a subject of research interest for the development of different applications such as toxicity measurement [95][150]. In the bioluminescent bacterial system, flavin mononucleotide (FMN) functions as a substrate in the light emission mechanism, wherein the 'isoalloxazine' nucleus is the chromophoric group that gets excited. The FMN molecule reduced using NAD(P)H: FMN-oxidoreductase (FMN reductase), and NADH as a reducing agent forms reduced flavin mononucleotide ($FMNH_2$), which in the presence of oxygen and long-chain aldehyde form intermediate FMN-peroxyhemiacetal. Further, the intermediate in the presence of bacterial luciferase (Luc) forms an excited state of FMN hydroxide, which, when relaxes to the ground state, light is emitted at around 490 nm along with the release of fatty acid [151]. However, the ground state FMN hydroxide after the release of one water molecule retains its state back to the FMN substrate. The source of the enzyme becomes an important factor in determining the color of the light emitted. Since it is possible that different source of enzyme catalyzes differently and produce tautomerism form of excited state which when released can produce a different state of light varying from blue-green light (490 nm) to yellow-red light (530 nm) [14]. When NADH binds to FMN reductase, two 'H' electrons are transferred by an enzymatic reaction to FMN yielding $FMNH_2$, which then causes immediate dissociation of $FMNH_2$ from the enzyme [16]. Thus, the bioluminescent bacterial system, as represented in Figure 27, is a cyclic reaction process. The excitation mechanism and energetics of bioluminescence vary from one species to another, depending upon the ecological presence and physiology behavior of different luminous organisms. The bacterial coupled enzyme system: NAD(P)H:FMN-oxidoreductase (FMN reductase) + bacterial luciferase (Luc) involves two step reactions:

$$Luc + FMNH_2 + RCHO + O_2 \rightarrow FMN + RCOOH + H_2O + h\nu \text{ [Reaction (1)]}$$

$$\text{FMN reductase} + \text{NAD(P)H} + \text{FMN} + \text{H}^+ \rightarrow \text{NAD(P)}^+ + \text{FMNH}_2 \text{ [Reaction (2)]}$$

In reaction (1), the oxidation of long-chain aliphatic aldehyde (RCHO) involving $FMNH_2$ is catalyzed by Luc. One of the products of this reaction is a quantum of light (hv) in the blue-green spectrum. However, to provide Luc with $FMNH_2$, Luc is coupled with the reaction catalyzed by FMN reductase, as elaborated in reaction (2) [14].
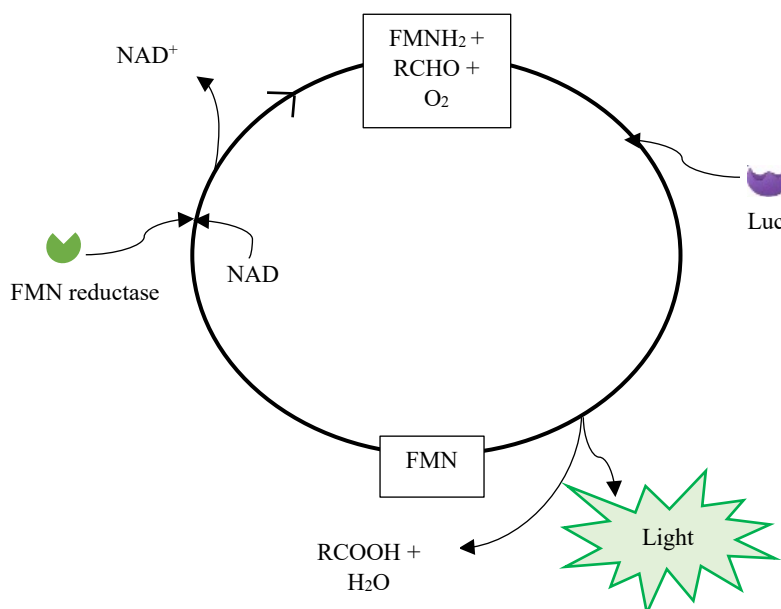
Figure 27. Reaction cycle of the bioluminescent bacterial system

Strategy to create biomimetic/bio luminescent textiles through enzyme immobilization

Figure 28 represents the overall strategy adopted for the immobilization of enzymes on textiles. Further, the choice of the fibrous matrix and the surface activation using plasma treatment are described.
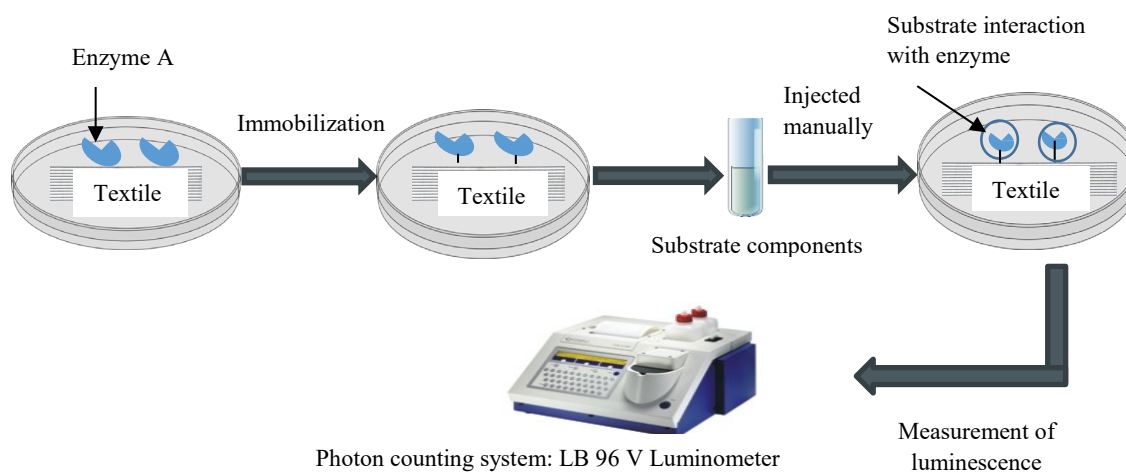

Figure 28. A general strategy for immobilization of the enzyme(s) on the textile surface.

In the case of the bioluminescent bacteria enzyme system, there are three categories of immobilization techniques used which are chemical modification, physical adsorption, and gel entrapment on support matrix such as on glass rods, in polymer gels such as starch (polysaccharide) and gelatin (polypeptide) matrix [152] [153][129]. However, no work has been carried on plasma-activated polyester fibrous nonwoven. Nonwoven protein binding study through physical adsorption technique requires soaking of support into a solution of enzyme and incubating to allow time for adsorption to occur, pH of the solution, and isoelectric point. The single enzyme immobilization has been explored [105], although it is very challenging to efficiently drive the multistep reaction toward the desired direction, which is especially true when reactive intermediates are present, specific material-based approaches to multi-enzyme co-localization have also been reviewed [154]. Also, the properties of the coupled enzyme system involved in the luminous bacteria reaction system were studied [129].

Choice of fibrous matrix and fiber surface activation using plasma

In this work, the enzyme(s) involved in the bioluminescent bacteria system were immobilized on plasma-activated microfibrous nonwovens, and the optimized luminescence activity on textiles are reported. Fibrous nonwoven is porous materials that have low-pressure drop and high surface-to-volume ratio for enzyme immobilization and high porosity, enabling easy diffusion of reactant mixture (substrates and products). PET (polyethylene terephthalate) fibrous nonwoven, which is a non-toxic and biocompatible material, has successfully been described as an appropriate support material to immobilize various enzymes (β galactosidase, glucose oxidase) [105]. Furthermore, the presence of favorable functional groups created by plasma activation of the PET fiber surface can favor the biocatalytic activity of enzymes, as well as the increase in capillary uptake increases microfluidics flow inside the fibrous nonwoven, through micropores [117][138]. Two different types of plasma were used: air atmospheric plasma treatment (ATMP) and cold, remote plasma treatment with N_2 and O_2 (CRPNO). The different modifications of the PET fiber surface were monitored using various techniques, including AFM, SEM, ESCA, water contact angle, and capillary uptake measurements.

Study of the bioluminescent bacteria system in aqueous form and after enzyme(s) immobilization of polymer matrix

Thus, the present work considers the conditions and substrates/enzymes concentrations that affect the luminescence. The study involved a lab-scale reaction study in two phases; the first phase was focused on the study of luminescence of the reactional mixture (involving substrates and enzymes) in the aqueous state using a luminometer. The second phase aimed at physical adsorption of only one or both enzyme(s) on a porous fibrous nonwoven support, followed by the manual introduction of various substrates (FMN, NADH, and dodecanal) and the activity was quantified by the measurement of photons of light emitted in terms of relative light units (RLU) using a luminometer.

Hence, this study aims to obtain bioluminescent materials by analyzing bacterial bioluminescence activity onto a microfibrous nonwoven PET textile surface. The research work has been extensively published in Paper-II [68].

3.2. Experimental section

3.2.1. Enzyme immobilization on nonwoven using adsorption technique

The activities of the single enzyme and coupled enzyme system were analyzed by immobilization of Luc singly and in association with FMN reductase on both ATMP and CRPNO treated nonwoven PET using physical adsorption technique at 4°C for 18 hours as shown in Figure 29. The nonwoven sample size of 1×1 cm^2 was immersed in a petri dish containing 50 µl of a phosphate buffer solution with 1 mg of dissolved Luc or a mixture of 1 mg Luc with 50 µl FMN reductase. Each nonwoven sample with the immobilized enzyme was then placed in the microplate. The other components of reactional mixture [NADH: 7 x10^{-8} moles (50 µl), FMN: 1x10^{-9} moles (50 µl), dodecanal: 2.71x10^{-8} moles (50 µl), FMN reductase: 0.2 U (50 µl)] were then injected into the vial successively and mixed quickly, thereafter the measurement plate was placed into luminometer to measure the RLU values (as illustrated in section 2.2.2.1.a).

The lyophilized powder of Luc was weighed (1 mg) directly during the analysis and stored on ice. NADH stock solution of concentration 1.4×10^{-2} M was prepared and refrigerated at 4°C. FMN and dodecanal solutions were always prepared freshly using a phosphate buffer solution pH 7 (prepared using sodium phosphate monobasic and dibasic dihydrate) at room temperature and analyzed.
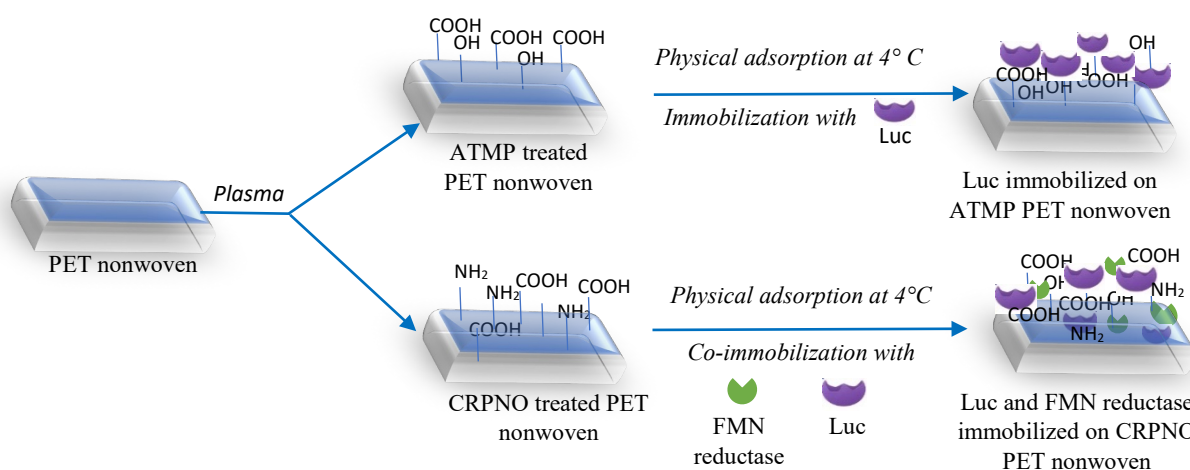

Figure 29. Schematic representation of the immobilization of enzymes on different plasma treated textile surfaces [68].

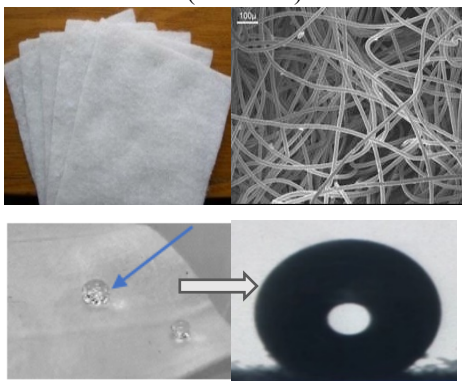## 3.2.2. Enzyme immobilization on nonwoven using biopolymers and BSA protein

1 mg of Luc was dissolved individually in 50 µl of aqueous solutions of bovine serum albumin (1% and 3% BSA), gelatin (2%, 5%), and starch (1%, 2%) respectively. Each enzyme solution was placed in a separate petri dish, and then the nonwoven of 1×1 cm^2 was immersed in each, respectively. Samples were immobilized in the prepared system and analyzed using methods described in the previous section 3.2.1. and 2.2.2.1.a.
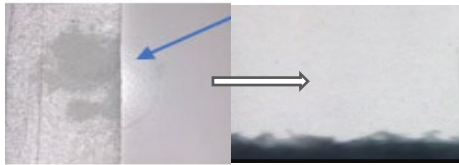
3.3. Results and Discussion

3.3.1. Physico-chemical analysis of untreated and plasma treated nonwoven

The water contact angle and capillary uptake for untreated and both of the plasma treated (ATMP and CRPNO) are summarized as shown in Table 6. The increase in surface energy of plasma treated PET fiber can be seen by a reduction in water contact angle and an increase in capillary uptake. The capillary uptake of untreated nonwoven PET was null. It increased up to 1460 mg and 1648 mg for the ATMP and CRPNO treated PET, respectively. In parallel, the water contact angle of the nonwoven PET reached 0° for both types of plasma treatment used compared to 141° for the untreated PET nonwoven. The decrease in WCA down to 0° indicates the treatment of fiber surface at the outer surface of the nonwoven. In contrast, the high capillary uptake (1460 mg, 1648 mg) is related to the water uptake after treatment of the fiber surface inside the PET nonwoven fabric [117].

Table 6. Water contact angle (WCA), capillary uptake and chemical functional group (ESCA) analyses for nonwoven PET samples [68]

Sample Description	WCA	Capillary uptake	ESCA
PET (untreated)	141°	0 mg	O/C = 0.3

PET treated by air atmospheric plasma treatment (ATMP)			
	0°	1460 mg	Carboxylic groups (COOH) O/C = 0.5 N= 0%
PET treated cold remote plasma (CRPNO)	0°	1648 mg	Carboxylic and amino groups O/C = 0.3 N=1.1 %

Scissions of ester bonds, in the case of ATMP, led to the integration of O (oxygen atoms) and thus an increase in O/C ratio up to 0.5 as confirmed by ESCA analysis, with hydrophilic terminal carboxyl and hydroxyl ends as confirmed by previous works [105][142][155].

Another previous work also reports the effect of a CRPNO plasma on a PET nonwoven when the volume ratio of nitrogen/oxygen gases used was 1250/89 cm^3/min. Both amino and carboxylic groups were detected with the O/C ratio of 0.3 and 'N' atomic content of 0.5%. However, in this work, when the volume ratio of nitrogen/oxygen gases used for CRPNO plasma was 1250/45 cm^3/min, the O/C slightly increased to 0.34, while the atomic content of 'N' increased to 1% (ESCA spectra as shown in Figure 30) implying a further increase in the number of terminal amino groups formed. Both carboxylic and amino groups led to a hydrophilic PET fiber surface with the water contact angle reaching 0°.
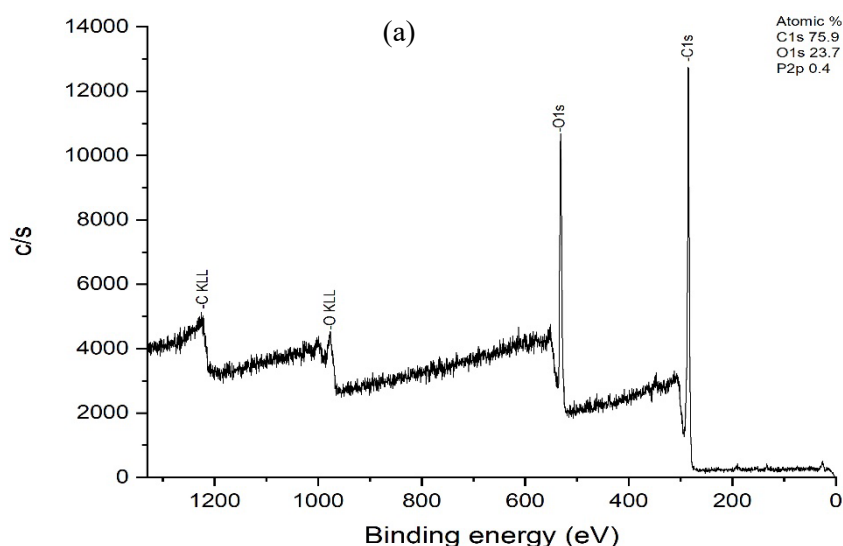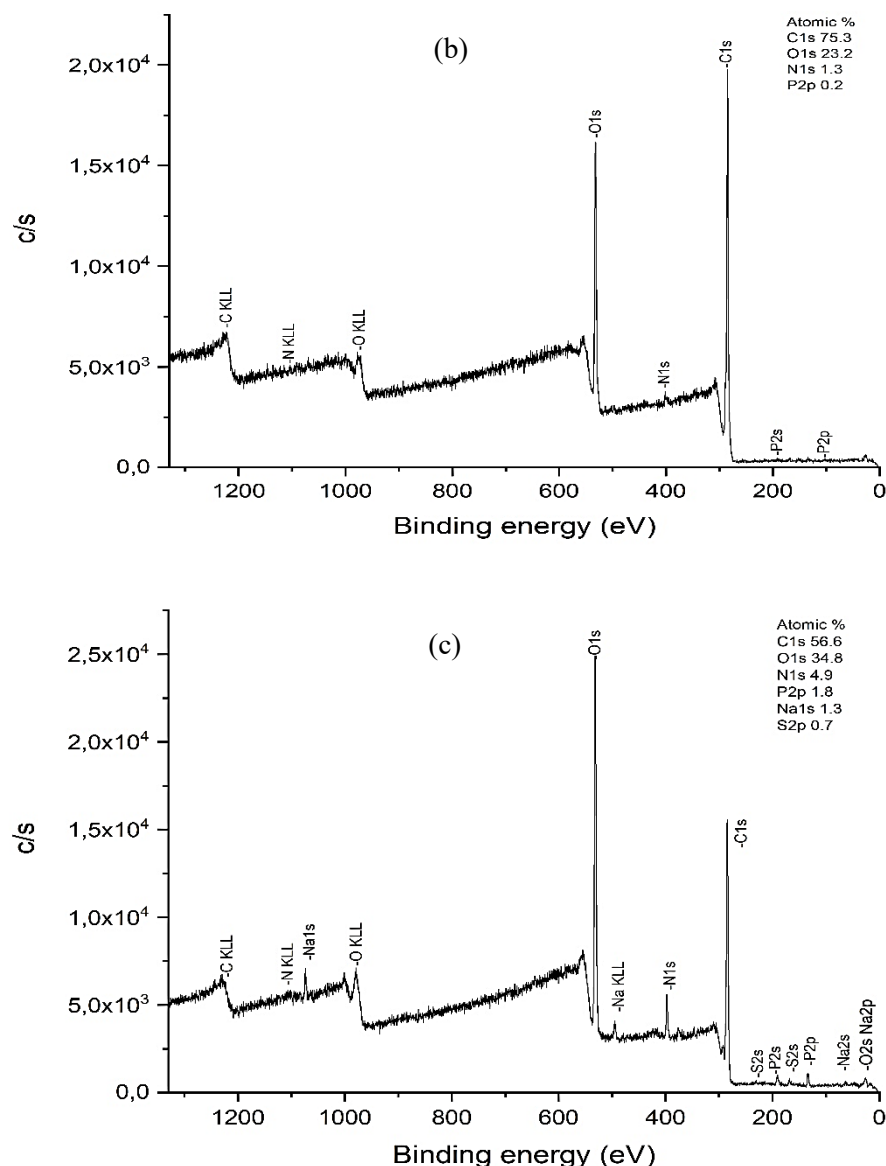
Figure 30. ESCA data of (a) 100 % PET nonwoven untreated, (b) 100 % PET nonwoven CRPNO treated, (c) 100 % PET nonwoven CRPNO treated with immobilized enzyme

AFM topographical images (1μm x 1μm) of PET fiber surface before and after the two plasma treatments are illustrated in Figure 31. The fiber surface of the untreated nonwoven textile is smooth and homogeneous Figure 31 (a). In contrast, the fiber surface subjected to both plasma treatments has increased surface roughness Figure 31 (b, c) with the appearance of scale-like surface structures. Both plasma treatments lead to changes in chemical properties and morphological changes of the PET fiber surface.

58

| (a) Untreated PET | (b) ATMP treated PET | (c) CRPNO treated PET |
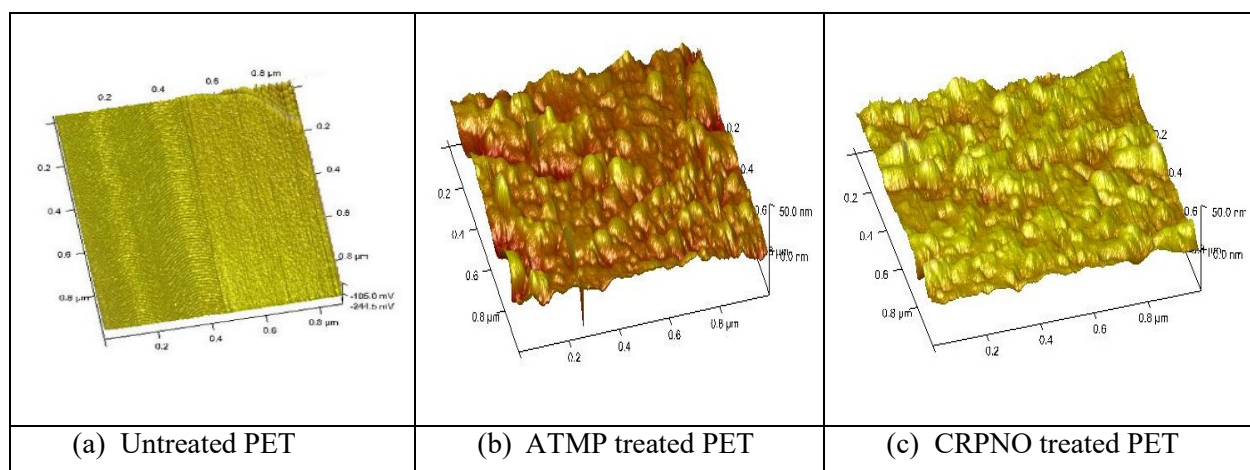
Figure 31. AFM images of (a) untreated PET, (b) ATMP & (c) CRPNO plasma treated fiber surface of nonwovens [68].

3.3.2. Enzymatic reaction and assay monitoring using UV/Visible spectrophotometer method

Reaction (1) analysis in the presence of enzyme FMN reductase

$FMNH_2$ required for the bioluminescent bacterial system was produced using FMN reductase, and the corresponding reaction (2) illustrated in section 3.1 was monitored by UV-visible spectroscopy analysis.

Figure 32. UV-visible spectra of (a) FMN $5x10^{-5}$ M red curve, (b) NADH $1x10^{-4}$ M black curve, (c) mixture of FMN $5x10^{-5}$ M and NADH $1x10^{-4}$ M along with 0.2 U of FMN reductase enzyme.

The ultraviolet-visible (UV/Vis) spectra of 5×10^{-5} M aqueous solution of FMN showed absorbance peaks at 373 nm and 445 n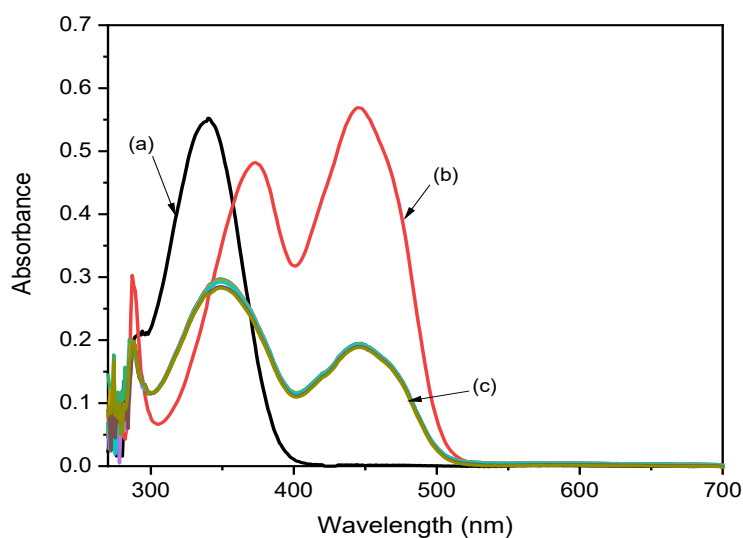m, as represented in Figure 32 (b), whereas 1×10^{-4} M NADH co-enzyme showed a sharp absorbance peak at 340 nm, as shown in Figure 32 (a). After the addition of the NADH and FMN reductase enzyme in the FMN solution, the peak at about 445 nm diminished. An increase in absorbance peak at about 348 nm was observed confirming the reaction (i) of the bioluminescent bacterial system, which was monitored for 30 minutes at an interval of 5 min. and the combined spectra can be seen in Figure 32 (c).

Assay monitoring of enzyme FMN reductase

The activity of the FMN reductase was analyzed using a spectrophotometer, and the difference in the absorbance was calculated for the determination of its activity. Absorbance was measured at 340 nm for blank and test samples by maintaining the conditions of the spectrophotometer at 25°C and light path distance of 1 cm. As shown in Eq.6, the calculation was carried out based upon the total volume of the assay (3 ml), dilution factor (df), the millimolar extinction coefficient of NADH at 340 nm (6.22 mM), for 0.1 ml of the enzyme used.

$$\text{Units/ml enzyme} = \frac{A_{340nm}Sample - A_{340nm}Blank * 3 * df}{6.22 * 0.1} \qquad \text{(Eq.6)}$$

$$\text{Units/mg protein} = \frac{\text{units/ml enzyme}}{\text{mg protein}}$$

Thus, the enzyme activity of FMN reductase was confirmed to be 0.2 unit/ml enzyme as expected from the data provided by the supplier.

3.3.3. Luminescence study

3.3.3.1 Aqueous based

The study focused its principal attention to the choice of optimum concentration for enzymes FMN reductase and Luc. Two factors were considered, the light intensity and the duration of the maximum light intensity. The latter factor is important for the activity of the enzyme and dependent substrates in the reaction system. The aqueous phase study of bioluminescent bacteria was studied using a luminometer, and the mean value of 3762 RLU was obtained on activation of reaction using NADH, as shown in Table 7.

Table 7. Stimulation of flavin reductase activity on the addition of FMN, Luc enzyme and co-factors

Conditions	Enzyme activity in terms of relative light units (RLU) (Mean Value)	Standard deviation
Luc + FMN reductase	5	0.58
Luc + FMN reductase + FMN	7	1.15
Luc + FMN reductase + FMN + dodecanal	7	0.58
Luc + FMN reductase + FMN + dodecanal + NADH	3762	24.98

Furthermore, the results of numerous experiments carried out using enzyme(s) and substrates in aqueous solution form (using a lab-scale analysis method described in section 2.2.2.1.a) are presented.

Effect of total reactional mixture volume

The luminescence of the reactional mixture was monitored with the addition of a different volume of phosphate buffer solution. The reactional mixture content without additional buffer was as follows: NADH: $7x10^{-8}$ moles (50 μl), FMN: $0.1x10^{-9}$ moles (50 μl), 0.1% dodecanal (50 μl), FMN reductase: 0.2 U (50 μl) mixed with 1 mg Luc enzyme, i.e., 200 μl of total reactional mixture 'a'. Another mixture 'b' was prepared by adding 200 μl of phosphate buffer to the mixture 'a'. Thus, the volume of the mixture 'b' was 400 μl, and both mixture 'a' and 'b' were analyzed using the luminometer equipment. Higher luminescence of about RLU 9500 was observed in case of mixture 'a' containing 200 μl reactional volume as compared to RLU 1100 obtained for the 400 μl mixture 'b'. Hence, luminescence intensity seems to depend upon the total volume of the reactional mixture at fixed quantities of substrate and enzymes in the mixture. As shown in Figure 33, the maximum optimized RLU value of 9500 was achieved using the equivalent volume of enzyme and substrate with the specified concentration of reaction mixture 'a'.
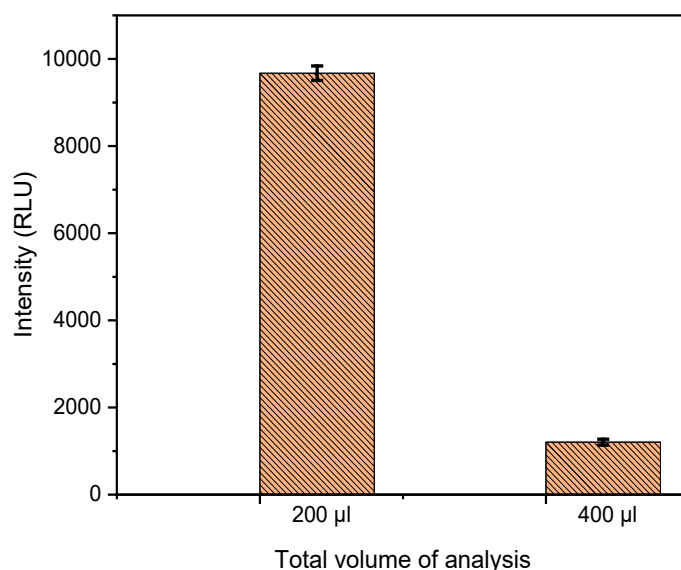
Figure 33. Relative luminescence values (RLU) measured as a function of total reactional mixture volume

Study of luminescence intensity with varying enzyme concentration versus time

The luminescence intensities were measured at varying enzyme concentrations, and simultaneously the effect of time on luminescence was also studied. Initially, luminescence was monitored for three different quantities of Luc enzyme (0.1 mg, 0.3 mg, and 0.5 mg) for a fixed volume of the total reactional mixture. Fixed quantities of FMN reductase and substrates used were the same as mentioned in section 3.2.1. The comparative analysis with increasing Luc concentration revealed that the maximum intensity was attained within 8 minutes of reactional mixture analysis, as shown in Figure 34. The RLU values remained more or less the same until 30 minutes. A gradual decrease in the luminescence intensity was observed after 30 minutes of measurements, as shown in Figure 34 (a). The intensity variation with respect to time was studied by conducting a reproducibility study, measuring luminescence of two identical reactional mixtures at fixed Luc enzyme (0.3 mg) concentration containing the same amount of FMN reductase enzyme and substrates as used earlier in this experiment. As observed in Figure 34 (b), the analysis of the luminescence variation with time reveals three plateau stages of steady luminescence intensity. The first plateau stage of steady intensity was observed from 8–14 minutes, followed by a sudden drop in luminescence intensity until 20 minutes. The second plateau of steady intensity was observed from 20 to 44 minutes. Finally, the luminescence intensity dropped, and the third plateau stage was then observed from 52 minutes until 1 hour 40 minutes. The drop in RLU value seen after 30 minutes could be due to the total consumption of dodecanal and NADH. NADH and dodecanal can be the two limiting factors, which have to be in excess concerning the enzyme concentration [69]. Thus, with respect to the analysis data obtained in this experimental study, the amount of NADH and dodecanal that would be required for an hour prolonged luminescence intensity would be three times higher [NADH: 2.1×10^{-9} moles (50 μl), 0.3 % dodecanal (50 μl)] to that required for 20 minutes of steady luminescence intensity.
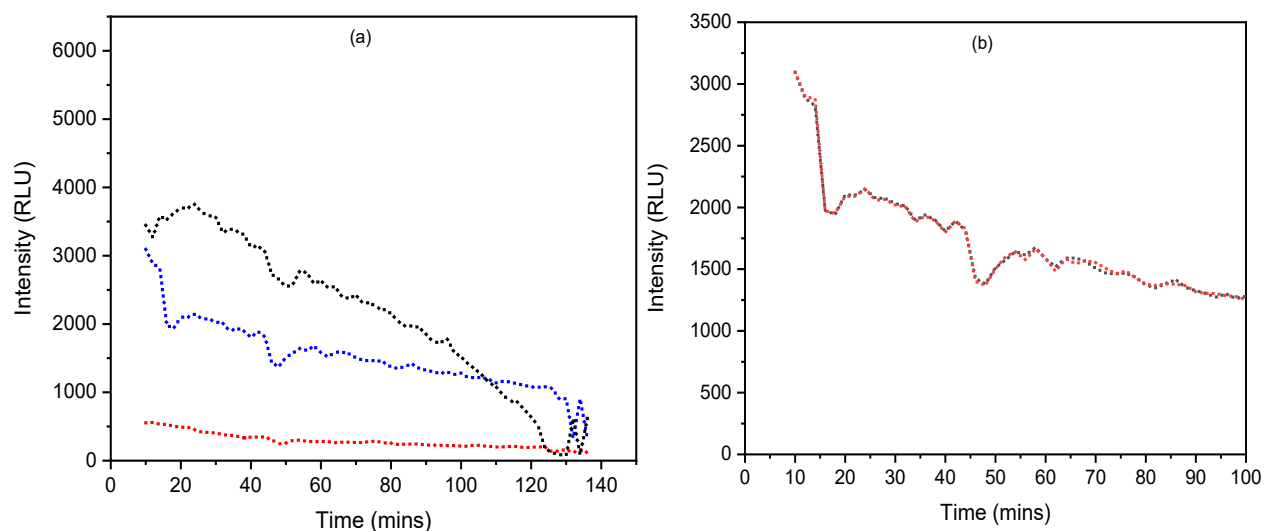
62

Figure 34. (a) Luminescence intensity w.r.t enzyme concentration: 0.1 mg (red curve), 0.3 mg (blue curve), 0.5 mg (black curve) vs time (mins), (b) Luminescence intensity vs time in mins (reproducibility study).

Calibration curve

A calibration curve was obtained using the bioluminescent bacterial system in the aqueous phase under the optimum conditions of substrate and enzyme concentration. The calibration graph was found to be linear over the range of 0.1, 0.5, and 1 mg enzyme concentration. The linear fit equation obtained was I= 9861.8c– 18.29, with R^2 value of 0.9841, where 'I' refers to the intensity, and 'c' is Luc enzyme concentration, as represented in Figure 35.
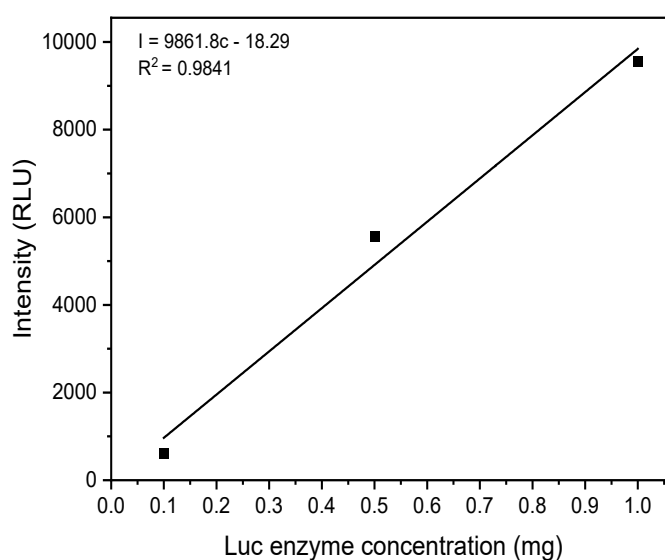

Figure 35. Calibration curve w.r.t enzyme concentration of bioluminescent bacterial system in the aqueous phase

63

3.3.3.2 Textile based

Comparative analysis of Luc immobilized by adsorption method on-air atmospheric plasma (ATMP) and cold remote plasma (CRPNO) treatment.

1 mg Luc in 50 μl phosphate buffer was immobilized onto the plasma-activated PET nonwoven, using the method described in section 2.2.2.1.a. The reaction was monitored in the presence of following co-enzyme, substrate, co-factor and enzyme quantities: NADH: $7x10^{-8}$ moles (50 μl), FMN: $0.1x10^{-9}$ moles (50 μl), 0.1% dodecanal (50 μl), FMN reductase: 0.2 U (50 μl). The bioluminescent bacterial system reaction study on ATMP and CRPNO plasma treated textile (Figure 36) showed relative light intensity at about 470 and 1800 RLU, respectively, as compared to 9500 RLU obtained in case of bioluminescent bacterial aqueous phase study. The decrease in the light intensity for textile samples could be due to the loss in Luc activity after its immobilization on the textile substrate. Thus, further studies were conducted to enhance the immobilized enzyme activity using stabilizers and biopolymers.
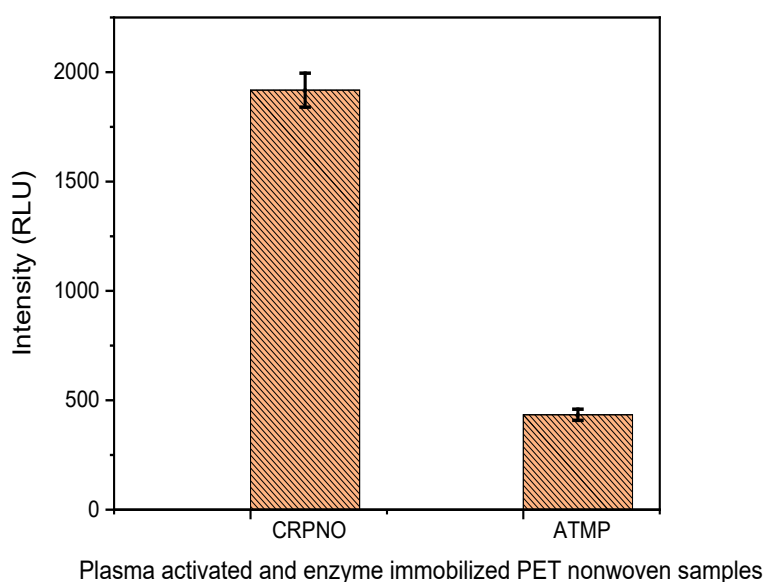

Figure 36. Luminescence intensity study for enzyme immobilized on ATMP and CRPNO plasma treated textile surface.

Analysis of Luc immobilized on-air atmospheric plasma treated nonwovens using biopolymers as stabilizers

Luc was immobilized on-air atmospheric plasma-activated nonwoven PET textile using BSA (bovine serum albumin), gelatin, and starch; luminescence was measured upon addition of substrates and the FMN reductase enzyme. BSA is a well-known activator of Luc [156], and it also leads to the stability of the enzyme. Further experimental studies were conducted to determine the effect of BSA on enzyme stability

by measuring the RLU values. Luc (1mg) was immobilized on nonwoven textile in the presence of 1%, and 3% of aqueous BSA and luminescence was measured after all the components of the reactional mixture were injected. The co-enzyme, substrate, co-factor and enzyme quantities used were, [NADH: 7×10^{-8} moles (50 µl), FMN: 0.1×10^{-9} moles (50 µl), 0.1% dodecanal (50 µl), FMN reductase: 0.2 U (50 µl)]. The highest luminescence, more than 3000 RLU (relative light units) was observed within 5 minutes in the case of 1% BSA (Table 8). Immobilization of the Luc enzyme on the ATMP treated nonwoven PET using BSA significantly increased the luminescence.

Table 8. Luminescence measured for Luc enzyme immobilized using stabilizers (BSA, gelatin, starch) on air-plasma treated PET nonwoven compared to that measured for Luc enzyme in aqueous solution form in the presence of the stabilizers.

Bacterial luciferase (1 mg Luc) on textiles with 50 µl of biopolymer	RLU value (± 100) on textiles	RLU value (± 100) in aqueous
1 % BSA	3354	3790
3 % BSA	2178	2747
2 % gelatin	289	467
5 % gelatin	146	413
1 % starch	854	791
2 % starch	756	578

Note: (± 100) indicates the variability of values observed for the individual samples, which are analysed in duplicates.

The immobilized coupled system Luc + FMN reductase does not require special storage conditions to save high enzymatic activity when immobilized in starch or gelatin gel as the biopolymer enzyme mixture leads to stabilization. Also, thermal stability could be attained in the coupled enzyme system immobilized in the starch gel. Previous studies have shown that in addition to BSA, stabilizers such as gelatin and starch can also be used to maintain the enzyme stability [157]. Thus, different concentrations of gelatin (2 %, 5%) and starch solutions (1%, 2%) were used for Luc (1 mg) stabilization. The analyses were done both in its aqueous phase and the textile phase (Table 8) using the same concentration of the reactional mixture, as mentioned earlier in this section. The luminescence intensities observed in the presence of each biopolymer, gelatin, and starch were low as compared to those with BSA, as shown in Figure 37. Both aqueous and textile phase study showed almost similar and highest luminescence values (RLU) in the presence of BSA, followed by starch and gelatin (as tabulated in Table 8).
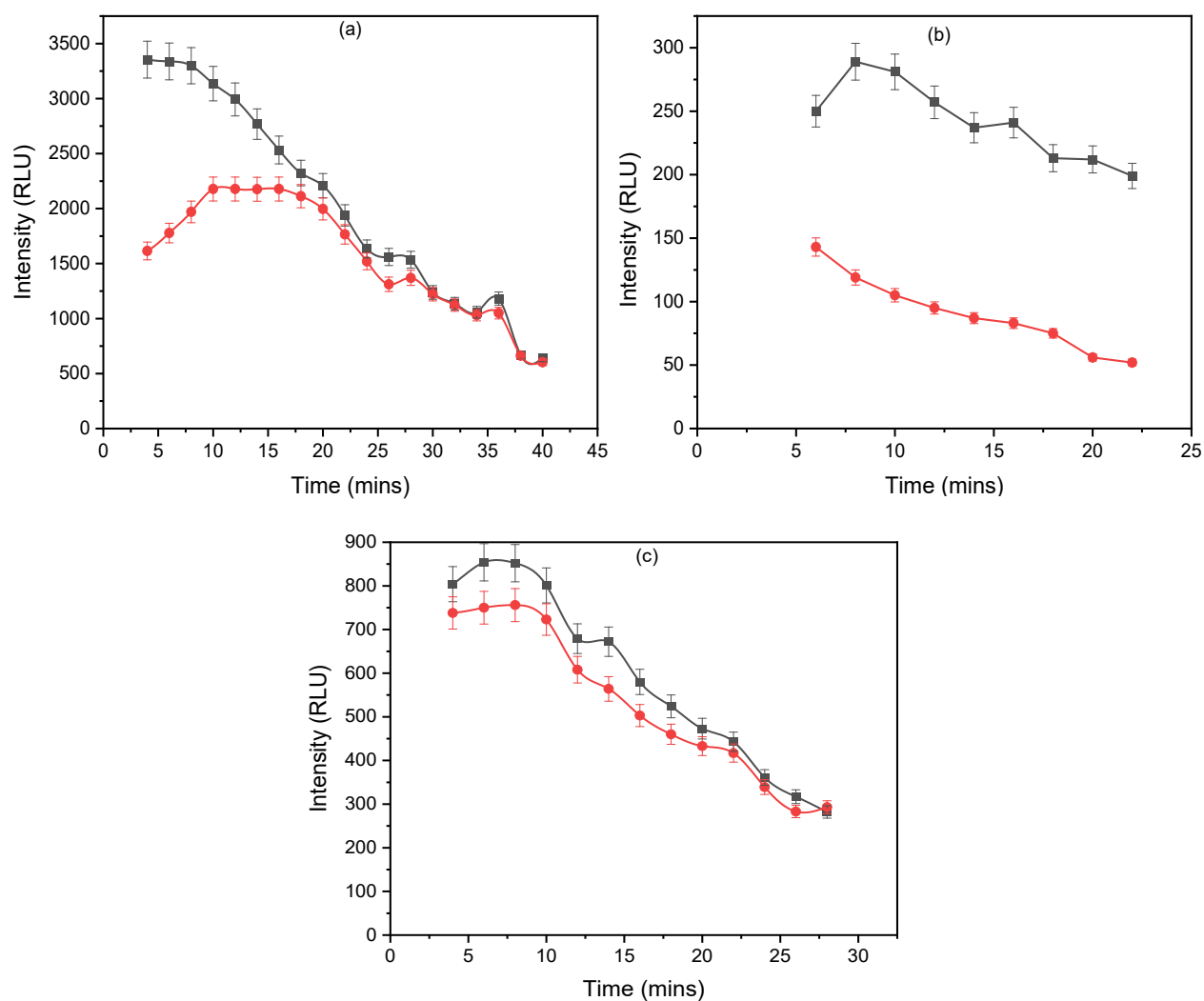
Figure 37. Effect of biopolymer used for Luc enzyme immobilization on nonwovens v/s luminescence (a) 1 % BSA -black box, 3 % BSA-red dot (b) 2 % gelatin -black box, 5% gelatin -red dot (c) 1 % starch - black box, 2 % starch-red dot

At a higher concentration of biopolymers (starch or gelatin) and BSA-protein, luminescence seems to decrease, probably because a denser gel entrapping the Luc is formed, which slows down the rate of movement of the substrate towards the active site of the Luc. Thus, for further studies, a 1% BSA stabilizer was selected for enzyme immobilization on PET nonwoven.
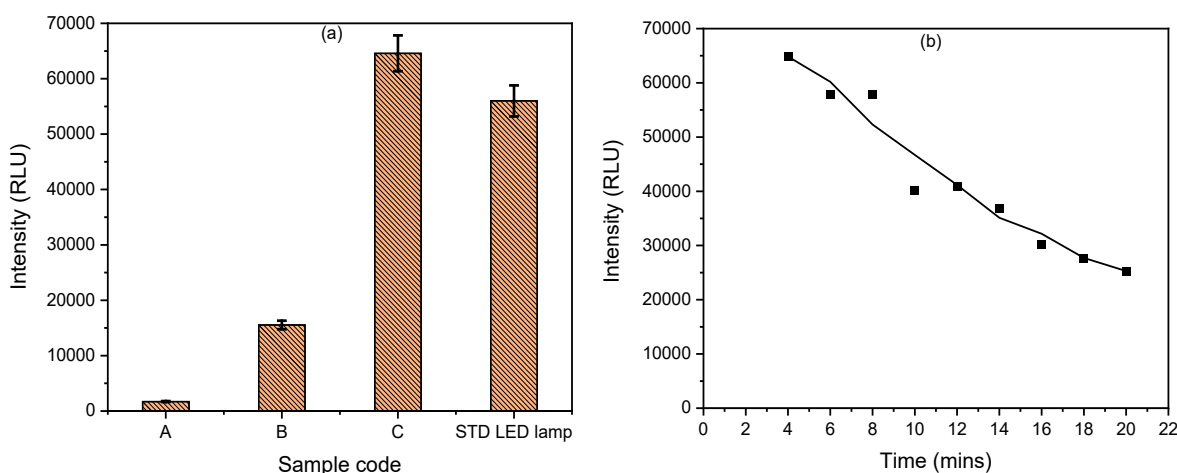
Analysis of co-immobilized Luc and FMN reductase on CRPNO plasma-activated PET nonwoven, using BSA.

Different quantities of Luc and FMN reductase (as mentioned in Table 9) were first co-immobilized on 1 cm x 1 cm PET nonwoven using 1% BSA.

Table 9. Quantities of Luc and FMN reductase enzymes used for immobilization on CRPNO plasma treated nonwoven PET

Sample	Luc (mg)	Volume of 0.2 U of FMN reductase (µl)
A	1	100
B	10	100
C	10	200

Luminescence values were measured on the addition of other components (NADH: 7×10^{-8} mol/50 µl; FMN: 0.1×10^{-9} mol/50 µl; and dodecanal: 2.71×10^{-8} mol/50 µl). Figure 38 showed the RLU values measured for samples A, B, and C. When the quantity of Luc was increased 10 times, from 1 mg to 10 mg. In comparison, the FMN reductase quantity was kept constant (samples A and B), and the RLU value also increased almost 8-10 times (from 1700 to 15500). However, when the quantity of the FMN reductase was multiplied by two (sample C) while maintaining the quantity of Luc to 10 mg. The RLU value reached was as high as 65000 and remained stable until 6 minutes with a sudden drop observed around 40,000 RLU with a gradual change in intensity w.r.t time, as shown in Figure 38 (b). The initial stable value was obtained at around 60000 RLU, as high as light emission generated by a temperature stabilized green LED (56000 RLU) of the luminescence test plate. Hence, a higher amount of enzyme provided increased RLU values, which could be compared with standard LED light intensity.
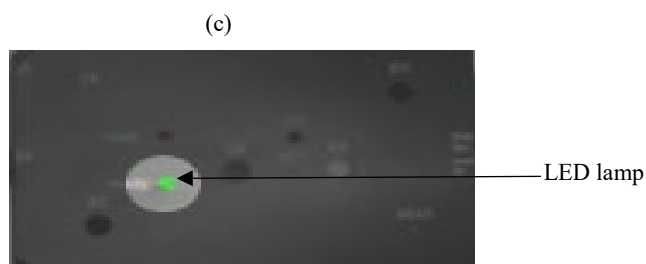
LED lamp

Figure 38. (a) the luminescence intensity of co-immobilized Luc and FMN reductase (sample A, B, C) on CRPNO plasma treated nonwoven PET compared with luminescence intensity of standard LED lamp (b) luminescence intensity of sample C w.r.t to time. (c) Luminescence test plate LB 9515 with standard LED lamp for testing the performance of the luminometer.

3.3.4. SEM image analysis

SEM images were taken before and after the co-immobilization of both Luc and FMN reductase. The enzyme immobilized on the fiber surface of the nonwoven PET could not be analyzed accurately using AFM in contact mode. However, SEM pictures show more appropriately morphological changes occurring before (Figure 39 a) and after enzyme immobilization (Figure 39 c), wherein the CRPNO plasma treatment alone affect the surface morphology of the cylindrical PET fiber (Figure 39 b), showing some surface etching as compared to the initial smooth PET fiber surface (as shown in AFM images in Figure 31). Moreover, after enzyme immobilization, irregular patches were observed on the fiber surface, probably due to deposits of the enzyme(s) and BSA mixture (Figure 39 c). However, these patches could not be analyzed in AFM contact mode, most likely due to scattered deposition, and adhesion between biopolymer and AFM tip should be too high to allow appropriate AFM image scanning in topographic mode.
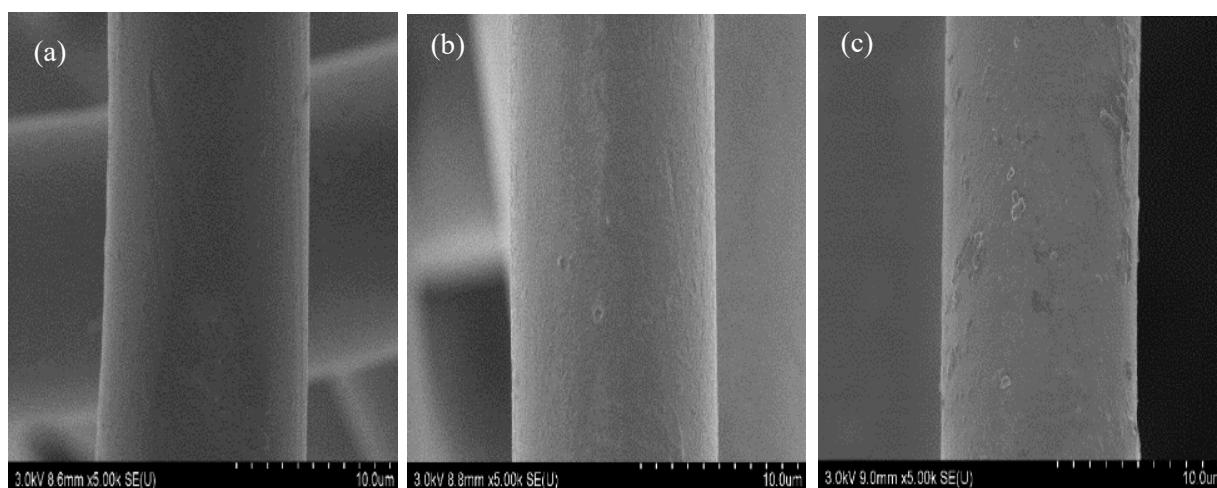

Figure 39. SEM images of (a) PET untreated, (b) CRPNO plasma treated, (c) enzyme immobilized

3.3.5. Chemical analysis ESCA

Further, ESCA analysis (Table 10) showed a significant increase in both 0/C ratio (from 0.34 to 0.61) and atomic N content (from 1.1% to 4.9%), after enzymes and BSA immobilization, confirming immobilization of 'N-nitrogen' containing enzymes which are protein by nature.

Table 10. ESCA analysis of untreated, CRPNO treated and enzyme treated nonwoven samples

Sample	ESCA analysis			
	C %	O %	N %	O/C
Untreated nonwoven PET	75.9	23.7	-	0.31
CRPNO PET nonwoven PET surface	73.6	24.9	1.1	0.34
CRPNO PET nonwoven PET surface with enzymes	56.6	34.8	4.9	0.61

3.4. Conclusion

The Luc catalyzes reaction (1) generating light in the visible region, as mentioned in the introduction section of the current chapter. However, for the activation of reaction (2), $FMNH_2$ is an essential intermediate substrate and was obtained by the reduction of FMN directly in the reaction mixture using enzymatic reaction [23]. As described in section 3.3.2, the reduction of FMN was monitored using a UV/Visible spectrophotometer. The aqueous phase study revealed that luminescence intensity measured in RLU depends on enzyme concentration and volume of the total reactional mixture. Luminescence stability was observed during the first 20 minutes after mixing of all components of the bacterial luminescence system. Both ATMP and CRPNO plasma treatments used to activate nonwoven PET were effective in enhancing the capillary uptake, hence allowing easier reactional mixture flow through the nonwoven.

Thus, either only Luc or both Luc and FMN reductase were immobilized on the plasma treated nonwoven with total reactional injection volume fixed to 200 µl. The luminescence intensity on plasma treated textiles was lower as compared to the aqueous phase study. Thus, the use of a stabilizer, such as bovine serum albumin protein (BSA) for Luc immobilization increased the luminescence value, better than starch and gelatin biopolymers. Immobilization of both Luc and FMN reductase on the CRPNO treated nonwoven using BSA could lead to high luminescence value (RLU 60,000) equivalent to that of a LED lamp used in luminescence test plate for testing and calibrating the luminometer performance.

The maximum light intensity was shown to depend on the FMN reductase and Luc concentrations. Enzymes have a globular structure with plenty of functional groups able to participate in the adsorption or covalent immobilization on activated supports such as plasma treated nonwoven. Carboxyl and amino groups obtained using CRPNO plasma treatment were observed to be interesting for adsorption, and the primary amino groups are the most suitable ones for covalent immobilization [158], thus resulting in higher luminescence intensity. Although maintaining the stability of both Luc and FMN reductase in the reactional system is an essential aspect for luminescence in an aqueous phase, properties of porous fibrous media such as nonwoven is also an important parameter determining the quantity and activity of immobilized enzymes, as well as the luminescence intensity measured in textile phase. The Luc immobilized on the nonwoven exhibited catalytic activity in the presence of FMN reductase with increased RLU value after the introduction of individual reaction components such as aldehyde, FMN, and NADH.

The experimental study revealed that the peak intensity/RLU value was attained immediately on the enzyme immobilized nonwoven with the subsequent addition and mixing of the substrate. The nature of functional groups created at the PET fiber surface (end-terminal amino and carboxylic groups) with CRPNO plasma and (the carboxylic and hydroxyl groups) by air atmospheric plasma seems to be an important factor that may cause a change in the orientation of enzymes at the PET fiber surface. Thus, allowing the availability

of the active site of the enzyme towards the corresponding substrate. End-terminal amino and carboxylic groups on PET fiber surface are more favorable, probably because enzymes, which are proteins, are also mainly composed of these terminal groups. The increase in RLU value was observed for the Luc immobilized in the presence of albumin on the air atmospheric plasma treated nonwoven that might be due to Luc activation and its interaction with BSA (protein-protein interaction). This interaction would improve Luc stability and activity. Furthermore, in comparison to starch and gelatin used as a stabilizer, it was found that in the presence of starch, the RLU values were higher as compared to gelatin, which can be correlated with the recent study that showed for better thermodynamic and kinetic stability of enzymes, starch is more preferable than gelatin [159].

The SEM images revealed uneven patches around the cylindrical-shaped PET fiber, comprising of BSA and the two enzymes. The introduction of the functional terminal groups such as amino–NH_2, and carboxylic -COOH on the PET fiber surface with CRPNO plasma, would enhance the adhesion of protein-based enzymes (without loss of its activity) and BSA on the fiber surface. Due to the property of nonwovens, such as porous structure and high surface area, PET nonwoven textile allowed easy diffusion of reactional mixture and co-immobilization of higher amounts of both Luc and FMN reductase enzymes.

Further, the improved enzyme stability provided with BSA would explain such good results. High porosity, low-pressure drop, and high mechanical strength of nonwoven PET provides interesting characteristics for its use in bioprocesses. Typically, the application of a luminous bacteria system has been explored for use in environmental biosensors and bioassays based on reaction system and immobilization of enzymes on polymer gels, microfluidic chip, and polymer beads [94][157][160]. However, in the current study, the luminous bacteria reaction system was activated through the enzyme(s) immobilization on the textile surface, and the corresponding light intensity was measured and discussed.

Luminous bacteria reaction system study in aqueous phase allowed determining the parameters affecting the luminescence intensity in terms of relative light units (RLU). The optimized enzyme and substrate concentration obtained in the aqueous phase were beneficial for its study on microfibrous PET nonwoven. Further, the microfibrous nonwoven PET surface was activated by two different plasma treatments for immobilizing one or both enzyme of bacterial bioluminescence system. Appropriate functional groups were created due to plasma treatments on the fiber surface, that led to an increase in surface roughness as well as capillary uptake increased, which in turn was beneficial for better enzyme activity. The detection of luminescence intensity (RLU) demonstrated catalytic activity and efficiency of the enzyme(s) immobilized on microfibrous PET nonwoven. Notably, the co-immobilized Luc and FMN reductase enzymes on CRPNO plasma treated nonwoven in the presence of bovine serum albumin (BSA) revealed the highest luminescence. Textile luminescence equivalent to the light intensity value of a LED lamp of the luminescence test plate was attained.

However, the study and subsequent luminescence values obtained here are indicative analysis or a proof of concept, of the possibility to create bioluminescent materials. The coupled immobilized enzyme system of luminous bacteria, both Luc and FMN reductase on the nonwoven PET substrate material, can be used to develop analysis methods for different metabolites and determination of enzyme activity. Further, it can also serve as a test substrate material for determining the integral environment toxicity. Luminous bacteria reaction systems can be very beneficial and useful as they are highly sensitive to pollution and are often used to detect toxins in water, often in place of animal tests. Hence, luminescent textiles based on the luminous bacteria reaction system can preferably work as an alarm for air pollution over different public places, etc.

CHAPTER 4: DEVELOPMENT OF PHOTOLUMINESCENT TEXTILES

4.1. Study of photoluminescence property of RF and FMN on cellulosic, silk and wool fabric using diffusion technique

4.1.1. Introduction

The functional molecule riboflavin and its derivative FMN are the key molecules in this thesis, due to its integration and ability to possess both photoluminescence and bioluminescence light-emitting phenomena. Riboflavin is one of the naturally occurring macromolecules in plants and trees. Plants and many microorganisms in nature produce riboflavin, widely known as Vitamin B_2, as shown in Figure 40. Riboflavin (RF) is the precursor of the flavin cofactors such as flavin mononucleotide (FMN) and flavin adenine dinucleotide (FAD). It has powerful antioxidant properties and is one of the essential hydrosoluble vitamins [161]. FMN and FAD serve as redox cofactors in all organisms, particularly in plants; these cofactors are required for many biochemical processes such as citric acid cycle, fatty acid oxidation, etc. [162] [163] and also DNA photo repair [164].

Moreover, these flavin based molecules are also involved in various other physiological processes. They also participate in different processes such as light sensing, as a photosensitizer, and also in bioluminescence phenomena. The use of RF as a redox mediator for anaerobic degradation of colorants by either hydrogen peroxide formation or UV induced microbial treatment. FMN can also act as a chromophore in certain plants and animals. The extensive use of RF also leads to a focus on the biosynthesis of riboflavin, which started in the 1950s. The chemical synthesis of RF has been replaced by the fermentation process using bacteria and yeast, which yield more amount of riboflavin. The industrial production of RF involves the biotechnical process performed using microorganisms. Hence, different strains of microorganisms were also developed and studied to compare the biotechnical process of RF production, in contrast to the chemical process, as well as the advantage of the biotechnical process, which meets the green demands [165].
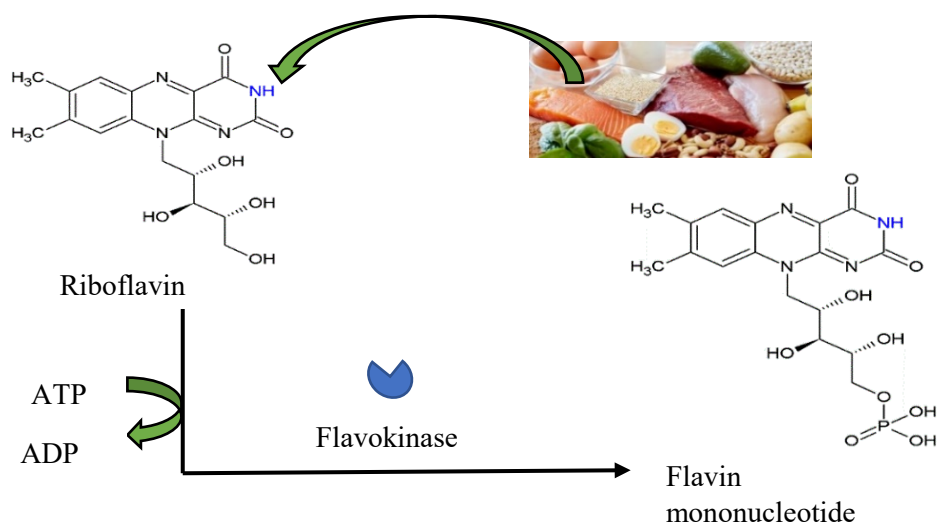
Figure 40. The natural resource of riboflavin and its enzymatic process to produce FMN

The photophysics and spectroscopy of alloxazine and related compounds in solution and the solid-state have been studied. The absorption, emission spectra, fluorescence lifetimes, and quantum yields of alloxazines have been measured in a nonpolar solvent, a polar aprotic, and a polar protic solvent. The UV- visible absorption and emission spectra reveal that in an aprotic solvent, the redshift in the absorption spectra can be observed, and comparative analysis of the spectral data in nonpolar show similar shifts. The difference in the fluorescence quantum yield depends on the alloxazine and its derivative. The longer fluorescence lifetime and quantum yield can be attributed to significantly slower rates of radiationless relaxation in the excited alloxazines and its substituted derivatives [166][167].

In particular, the study of the photo, thermal, and chemical degradation of riboflavin (RF) has been studied and discussed. Several factors are affecting the photodegradation of RF that are reviewed in the literature [168]; however, some of them are discussed and described below,

The radiation source, intensity, and wavelength

Several studies have been conducted by introducing low and high-intensity radiation sources emitting at different wavelengths in the UV and visible regions for the photolysis of RF. The photoproducts formed were the same irrespective of the radiation source; however, the rate of reaction was higher on UV irradiation as compared to that of visible irradiation.

Effect of solvent polarity and viscosity

The RF photolysis rate is affected due to solvent polarity as it causes changes in the conformation of the ribityl side chain to undergo degradation. The effect of aqueous and organic solvents on the photolysis has

been studied using a UV-visible spectrophotometer. Attempts have been made to correlate the rate constant of anaerobic photolysis with solvent viscosity, such as in the presence of ascorbic acid.

Effect of stabilizers and quenchers

Several methods with the use of stabilizers, quenchers, and also some complexing agents have been studied to stabilize the RF from photodegradation. Borate and citrate buffers have been found to exert a stabilizing effect on the photodegradation of RF. Ascorbic acid and sodium azide are widely studied external quenchers for RF photoreactions.

Overall, RF participates in various biochemical reactions. However, it is highly photosensitive, with optimum pH and addition of stabilizers, quenchers, and complexing agents that can provide better photostability.

Furthermore, recent focus has been on the spectroscopy, and photophysical study of organic dyes adsorbed onto different kinds of a solid substrate. E.g. the study was undertaken to characterize the spectral and photophysical properties of lumichrome adsorbed onto cellulose.

Riboflavin is a potential biomolecule, and to the best of knowledge, until now, no work has been carried out to determine the photoluminescence property on the textile substrate. Both RF and FMN was selected as a fluorophore for the photoluminescence study on cellulosic fabric using the diffusion technique. The study involved the determination of color performance and evaluation of luminescence property of the dyed fabric using a UV-visible spectrophotometer, monochromatic UV lamp (emitting at 370 nm), and photoluminescence spectroscopy. In addition to the determination of photoluminescence property using spectroscopy methods, quantum efficiency was calculated theoretically on textile fabric. The influence of biomordants on the dyed fabric was assessed. The work aimed to explore the photoluminescence property of RF and FMN for their application in the field of textiles producing photoluminescent textiles along with multifunctional properties. The research work has been extensively published in Paper-I [169].

4.1.2. Experimental section

Diffusion technique was used to dye the pre-cleaned cellulosic fabric samples using 200 ml beakers in a HTHP (High Pressure and High Temperature/Beaker Dyeing Machines) as depicted in Figure 41. Dye solutions of 4% and 20% of the weight of the fabric (owf) were prepared using phosphate buffer at pH 7. The temperature of the exhaustion bath was set to rise at about 1.5°C/min up to 60°C and maintained at the same temperature for about 45 min, followed by cooling of the dye bath to 45°C temperature. The dyed fabrics were air-dried at ambient temperature overnight. In the process, replicated dyed fabrics of 4% and 20% owf were generated for assessment of properties for both washed and unwashed fabric samples after

dyeing. The dyed fabrics were rinsed and washed using warm and cold water subsequently. The treated fabrics were assessed for color strength value (K/S) and other functional properties such as photoluminescence and UV protection ability.

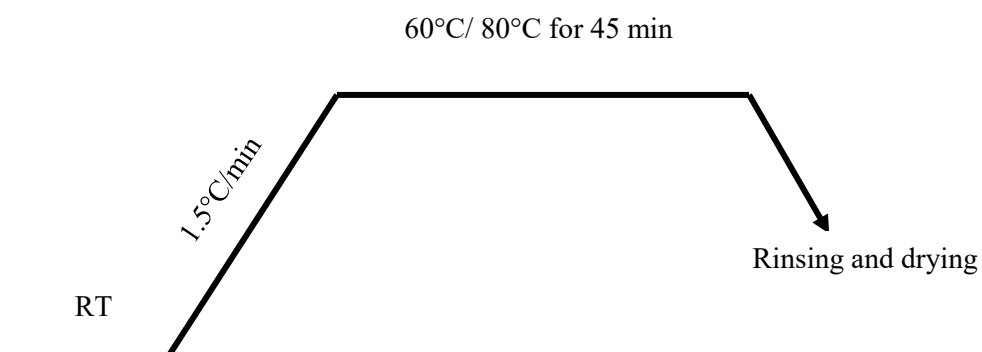60°C/ 80°C for 45 min

1.5°C/min

RT

Rinsing and drying

Figure 41. Condition for dyeing of textile with RF and FMN

The dyeing of the silk and wool fabric was also performed in accordance with the general dyeing method using the diffusion method in a HTHP (High Pressure and High Temperature/Beaker Dyeing Machines), at 60°C and 80°C using FMN solution prepared in distilled water (pH 7). A design of experiment was conducted using the following parameters as tabulated below.

Table 11. Silk and wool dyeing conditions

5 gm Fabric	0.2 gm Active agent	Max temp	Liquor (H_2O) volume
Silk	FMN	60 °C	20 ml
Wool	FMN	80 °C	20 ml
Silk	RF	80 °C	20 ml
Wool	RF	60 °C	20 ml

Drying and washing of the treated samples

The dyed samples were kept overnight for drying at room temperature and analyzed for the functional properties. Later, all samples were washed with water 3 to 4 times at 30°C and rinsed using cold water. Mainly the color strength and photoluminescence properties were evaluated.

4.1.3. Results and Discussion

4.1.3.1   UV-visible spectroscopy analysis

The UV-visible spectra of 2×10^{-4} M RF and FMN solutions are depicted in Figure 42 with absorption plotted against wavelength ranging from 200 to 700 nm at room temperature. The absorption peaks obtained for both RF and FMN solutions were similar, with maximum peaks at 270, 373, and 444 nm for RF solution and 271, 374, and 445 nm for FMN solution, respectively. The RF aqueous solution was dark yellow in comparison to the appearance of FMN, which was a transparent yellow color. However, a bright yellow-green fluorescence was seen for both RF and FMN under exposure to UV light at 370 nm.
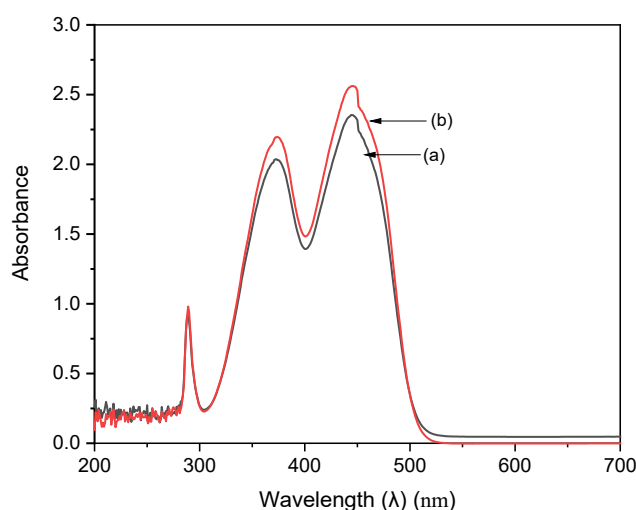
Figure 42. UV Visible spectroscopy of RF (a) and FMN (b) solution

4.1.3.2   Color strength evaluation

The color performance of both RF and FMN dyed viscose and cotton fabrics before and after wash was evaluated. The K/S spectral curves of all the dyed fabrics revealed two main absorption peaks at around 360 to 370 nm and 450 nm, similar to absorption peaks observed in aqueous solutions. A shift of 10 nm in maximum absorbance (360 nm) was observed for RF dyed fabric in comparison to the absorbance peak of aqueous riboflavin solution observed at 370 nm. A significant increase in K/S value from 13 to 28 (at wavelength 370 nm) with an increase in dye owf from 4 % to 20 % for FMN viscose and cotton dyed fabric, respectively. However, there was only a minor shift or increase in K/S from 7 to 9 observed for RF dyed viscose and cotton fabric samples at wavelength 360 nm, as shown in Figure 43 (a) and (a). The color coordinates depicted in Figure 45 reveal that both a* and b*are positive. However, the b* coordinate value was higher than a*, which shows that the yellow color predominates over red. All the treated fabric samples possess yellow coloration, which appears to be the same color as that of the flavin moiety. Hence, the photoluminescence behavior could be evaluated under UV exposure. Both molecules RF and FMN have the

same isoalloxazine ring structure, however, the water solubility of FMN is higher due to the presence of phosphate group, and hence the diffusion of FMN in cellulosic fabric was seen to be more predominant in comparison to RF.
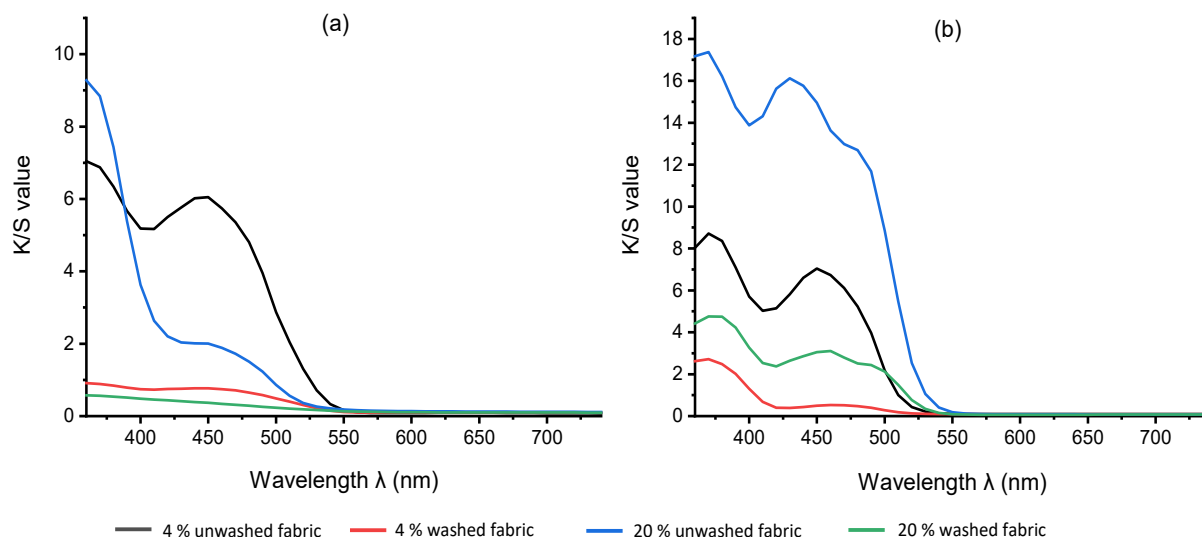

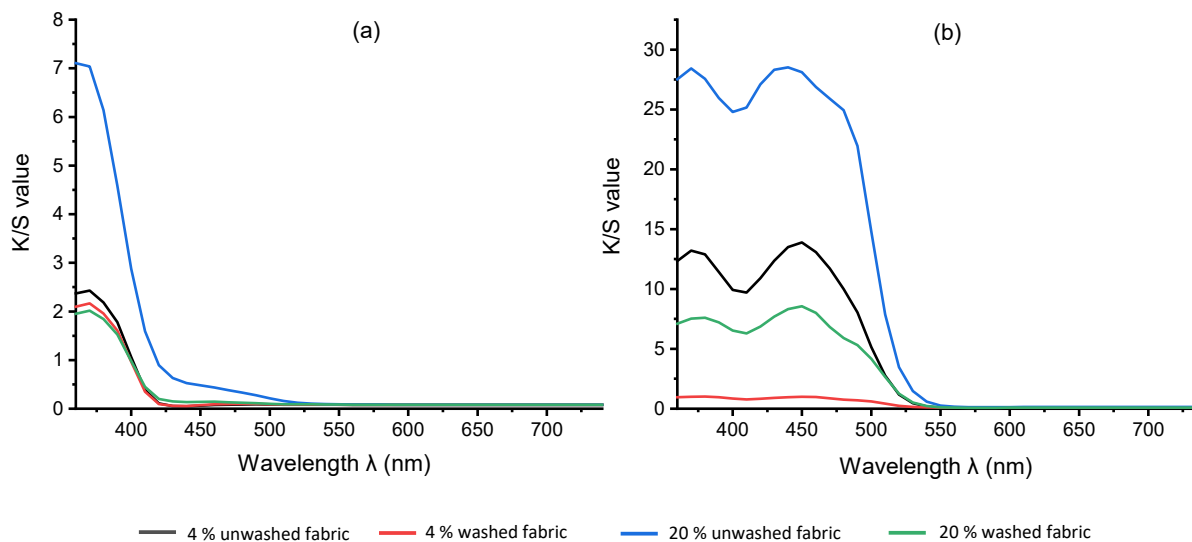Figure 43. K/S value of viscose dyed fabric using 4% and 20% owf (a) RF (b) FMN [169].

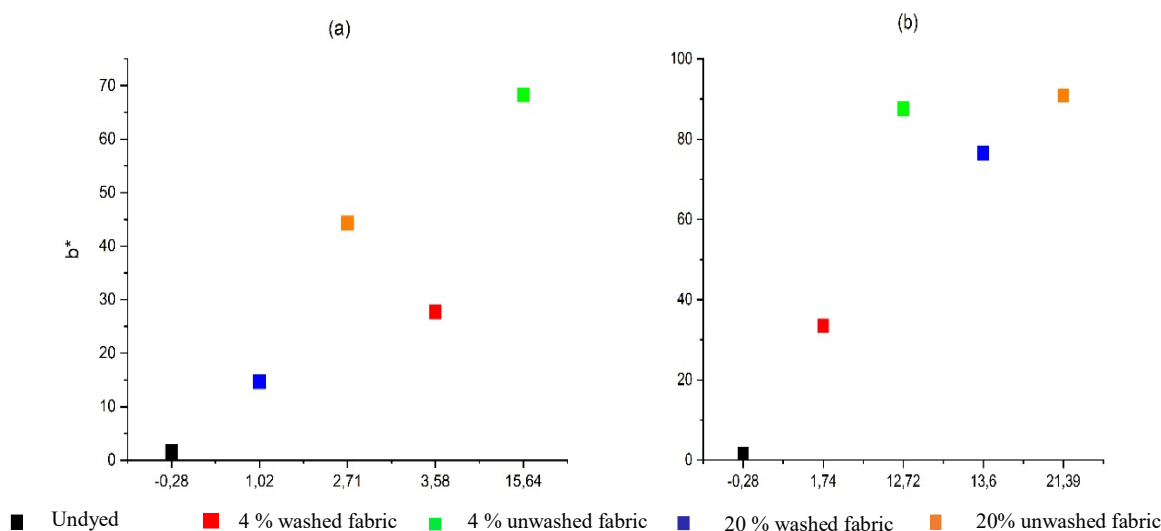Figure 44. K/S value of cotton dyed fabric using 4% and 20% owf (a) RF and (b) FMN [169].

Figure 45. Color coordinate of 4 % and 20 % owf viscose dyed fabric samples (a) RF and (b) FMN [169].

Moreover, the K/S values of silk and the wool dyed fabric showed relatively similar color strength values for both RF and FMN dyed fabric, as shown in Figure 46 and Figure 47. The maxima absorbance values were observed at 370 nm and 450 nm for all dyed fabric samples except for wool dyed using riboflavin, which showed a shift of 10 nm in maxima absorbance at 360 nm. The wool dyed fabric using both RF and FMN after wash showed better color strength values as compared to silk, which showed a comparatively higher loss in K/S values after wash.
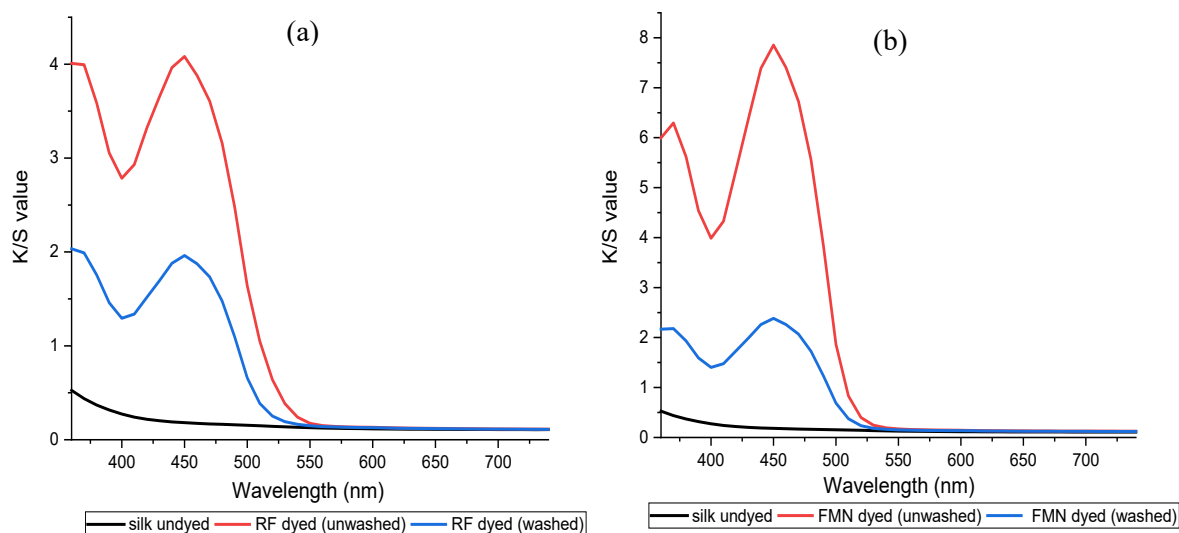
Figure 46. K/S value of silk undyed and dyed fabric using 4% owf (a) RF and (b) FMN.
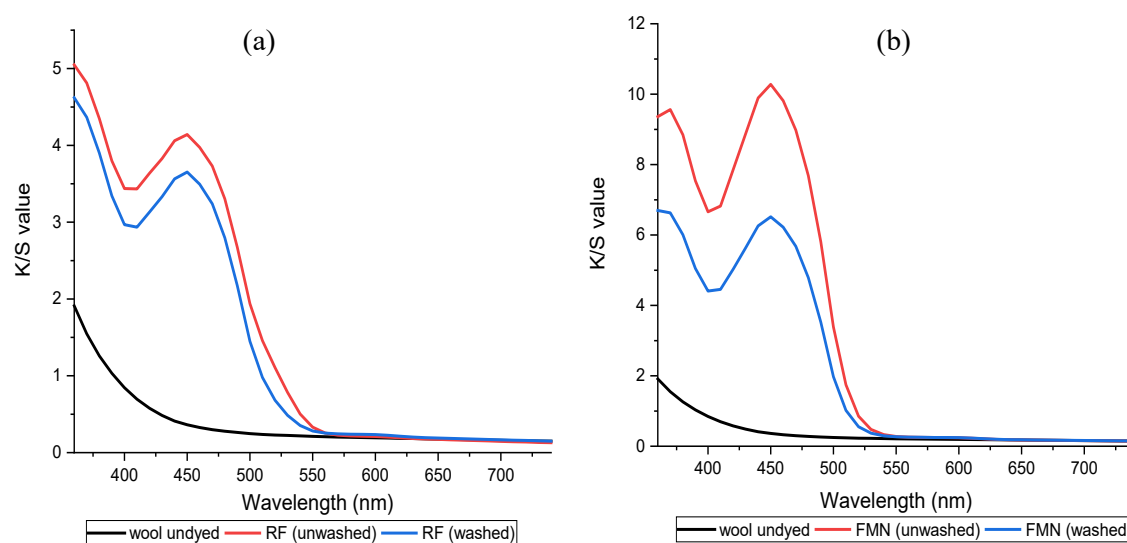
Figure 47. K/S value of wool undyed and dyed fabric using 4% owf (a) RF and (b) FMN.

4.1.3.3 Effect of mordants

The color strength evaluation of both RF and FMN on cellulosic (viscose and cotton) fabric showed a decrease in the K/S value after washings as expected. Hence, different biobased mordants such as tannic acid and citric acid as well as calcium chloride, which are nontoxic, were evaluated for the ability to enhance color strength value in 4% owf viscose dyed fabric. Mordanting was carried out after dyeing the samples by rinsing in 0.5 % calcium chloride or 0.1 % tannic acid or 0.5 % citric acid. For comparison analyses, the dyed sample was also rinsed with water, and the color strength of all the fabric samples was analyzed.

The RF dyed fabrics showed an increase in the color strength value with K/S values from 2 to 3 for citric acid and up to 6 for tannic acid (at 360 nm), as depicted in Figure 48 and Figure 49, whereas calcium chloride had no significant impact. In the case of FMN dyed fabric, calcium chloride yielded higher color strength, and the K/S value increased from 1 to 5 (at 370 nm). Moreover, even citric acid mordanting led to slightly increased K/S values at both the wavelengths 450 nm and 370 nm followed by tannic acid mordanting, which led to an increase in K/S values at 350 nm only. The visual image analysis in Table 20 and Table 21 showed the coloration of dyed fabric under normal daylight and the UV light (370 nm). Yellowish fluorescence was observed for calcium chloride mordanted FMN dyed fabric samples. In contrast, pale yellowish-green fluorescence was observed for citric acid, and tannic acid mordanted FMN dyed fabrics. Cellulosic viscose dyeing using FMN with calcium chloride mordanting leads to the most probable occurrence of electrostatic binding of at least two FMN molecule. The metal ion affinity governs the stability in the case of FMN dyed viscose fabric with calcium chloride as mordant. The alkalinity of the negatively charged phosphate group (PO_3^{2-}) in FMN with the positively charged bivalent Ca^{2+} ion provides more stable

binding of the dye complex to the cellulosic fabric. Fluorescence depicted in calcium mordanted dyed fabrics was yellowish in the case of the FMN and pale yellow fluorescence in the case of the RF. Probably, the calcium ions did not bind to the RF, but the ions did probably fix to the viscose fiber [170]. Indeed tannic acid was able to bind proteins due to the formation of multiple hydrogen bonds between the phenolic groups of tannins and the carbonyl functions of the peptide linkages of proteins [171]. Moreover, in case of dyeing of cellulosic viscose with RF along with tannic acid mordanting, numerous hydrogen bonding may occur between a tannic acid molecule and hydroxyl groups of the cellulose and of the RF dye. The kinetics of photolysis of both RF and FMN are influenced by the use of citrate buffers, hence, decreasing the fluorescence quenching leading to a stabilize RF solution [172]. Thus, the yellowish fluorescence was observed after wash for RF dyed fabric mordanted with citric acid. However, the photostability of riboflavin solutions increases by the introduction of certain acids such as sulphuric along with different metal ions, whereby the phenomena of decrease in photo destruction rate could occur due to protonation. Along with the formation of a complex in between the metal ions and the hydroxyl group of riboflavin, respectively [173].
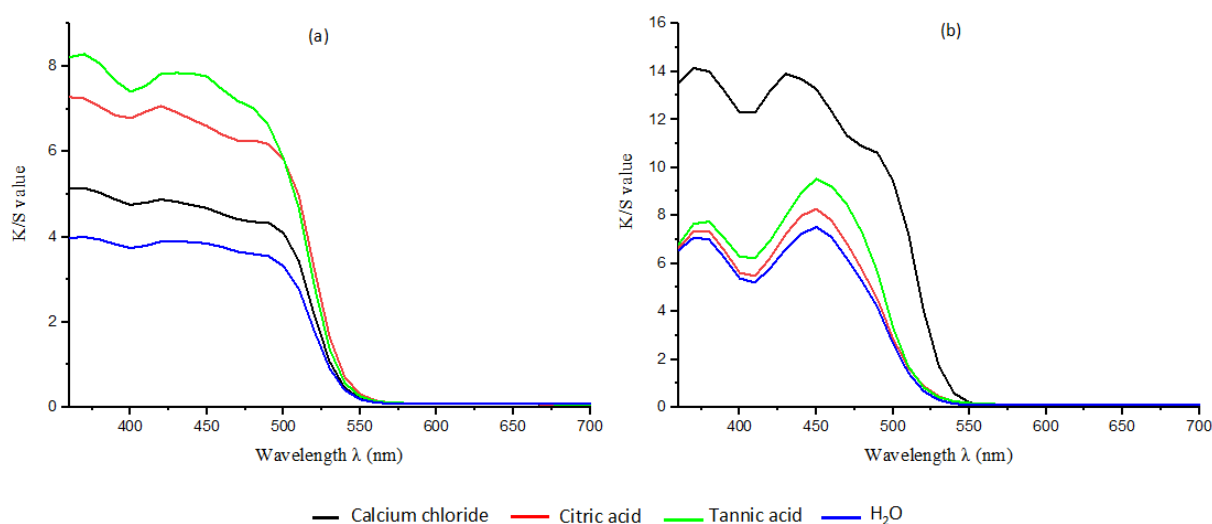
Figure 48. K/S value of (unwashed) viscose dyed fabric with different mordants using RF (a) and FMN (b)
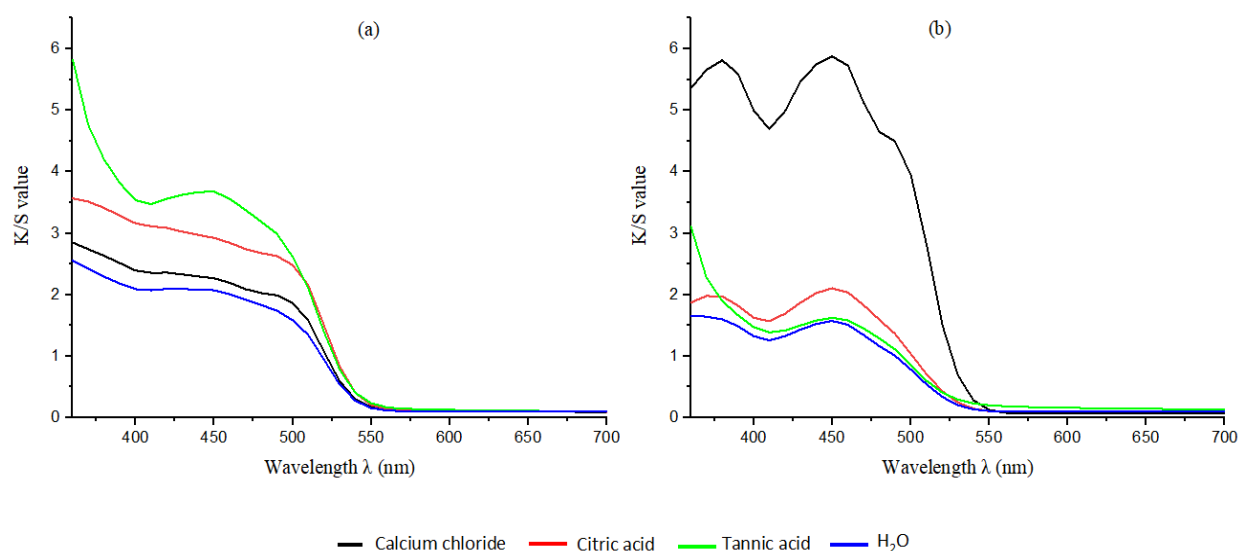
Figure 49. K/S value of (washed) viscose dyed fabric with different mordants (washed) using RF (a) and FMN (b).

4.1.3.4 Photoluminescence intensity

The photoluminescence of the dyed viscose fabrics was measured using photoluminescence spectroscopy to quantify the fluorescence observed under a UV lamp at 370 nm. Photoluminescence spectra were recorded using fixed illumination at two wavelengths of 364 nm and 470 nm line of a 30mW argon, and the emission spectra were obtained at room temperature. The luminescence spectra for both the dyed fabric using RF and FMN with 4% owf (unwashed) are illustrated in Figure 50. The maximum photoluminescence intensity of the RF and FMN dyed viscose fabric was observed at an emission wavelength of 570 nm for both excitation wavelengths at 364 nm and 470 nm. Immediate photoluminescence at a higher wavelength of 570 nm confirmed the fluorescence behavior of the dyed fabrics [174].

Table 12 provides detailed photoluminescence values of 4% and 20% owf RF and FMN dyed viscose fabrics, for excitation wavelengths of 364 nm and 470 nm, before and after washing. At excitation 470 nm, maximum photoluminescence was observed at 570 nm with values as high as 22000, and 27000 a.u was recorded for the RF and FMN dyed fabrics, respectively. At an excitation wavelength of 470 nm, the undyed viscose fabric also showed a value of 8000 a.u, but at an emission wavelength of 560 nm was observed. However, the undyed fabric emitted at 500 nm at an excitation wavelength of 370 nm, with luminescence intensity 15000 a.u, which can occur due to the use of optical brighteners in the cellulosic fabric making process [175]. The dyed samples intensities varied depending upon the photoluminescent moiety, concentration, and the excitation wavelength. At excitation wavelength of 364 nm, the FMN dyed fabric samples with 4 % and 20 % owf showed an intensity of about 9000 a.u and 11000 a.u, respectively, and an increase in the photoluminescence intensity value was observed for the washed samples.

The intensity value observed was 27000 a.u for FMN (4 % owf) and 19000 a.u for FMN (20 % owf) at the excitation wavelength of 470 nm, indicating a decrease in intensities with an increase in FMN concentration. Moreover, the intensity decreased for the FMN treated washed samples at the excitation wavelength of 470 nm. In the case of RF dyed fabric samples, the intensity value remained the same at about 22000 even after the increase in concentration from 4 % to 20 % owf at both the excitation wavelength of 364 nm and 470 nm. The intensity value corresponds to the maximum emission energy absorbed by the sample, which emits back at 570 nm. A fluorescence shift to higher wavelength (570 nm) on dyed fabrics compared to RF and FMN aqueous solution (530 nm) may be explained by the excitation wavelengths (364 nm and 470 nm), which are different from the wavelengths of maximum absorption peaks of the RF and FMN aqueous solution (350 -370 nm and 444 - 445 nm as shown in Figure 42). The stimulated intensity observed at a higher wavelength of 570 nm for the fabric samples might be due to the intensity spectrum and energy difference of the laser beam, which also leads to a narrow emission peak [176]. The increase in the concentration of RF influences the fluorescence intensity, wherein ionic strength log k quenches the fluorescence intensity [177]. As the concentration of riboflavin solution increased, there was a decrease in the intensity resulting in the quenching of fluorescence. However, the riboflavin dyed fabric samples did not result in a decrease in intensity; they remained almost equivalent, even with the increase in concentration. Depending upon the mechanism of monomer-dimer energy transfer for FMN in water along with steady-state and time-resolved technique, there exhibit a decrease in fluorescence intensity decay with an increase in the concentration of FMN solution at λexc = 473 nm [178]. Thus, the decreases in fluorescence intensity at an excitation wavelength of 470 nm was observed with an increase in the concentration of FMN dyed fabric samples.

Table 12. Photoluminescence intensity of RF and FMN dyed fabric after excitation at 364 and 470 nm (Results based on data analysis with proper baseline detection).

Sample Description	Intensity observed at 570 nm for Excitation wavelength (364 nm)	Intensity observed at 570 nm for Excitation wavelength (470 nm)	Intensity observed at 500 nm for Excitation wavelength (364 nm)	Intensity observed at 560 nm for Excitation wavelength (470 nm)
Viscose Undyed fabric	-	-	15000	8000
4 % FMN dyed (unwashed)	9000	27000		
4 % FMN dyed (washed)	12000	15000		
20 % FMN dyed (unwashed)	11000	19000		
20 % FMN dyed (washed)	17000	10000		
4 % RF dyed (unwashed)	22000	19000		
4 % RF dyed (washed))	23000	22000		
20 % RF dyed (unwashed)	22000	19000		
20 % RF dyed (washed)	23000	18000		

In accordance with the Stokes law, for a molecule to have fluorescence, it must first absorb the radiation, and generally, only 5 to 10 % of molecules that absorb the radiation eventually exhibit the fluorescence phenomenon. The Jablonski diagram provides an explicit representation of some processes involved in the electronic energy transitions of the molecule. The wavelength of emitted radiation is independent of the excitation wavelength. Fluorescence intensity and concentration are co-related, wherein the fluorescence quenching phenomenon occurs at higher concentrations, thereby decreasing the intensity. Three major factors are influencing the quenching of fluorescence, such as quantum efficiency, the intensity of incident radiation, and molar absorptivity. RF and FMN exhibit the fluorescence property; the absorbed light promotes the molecule to the excited singlet state. Then the excited state eventually returns to the ground state by emitting fluorescence. The undyed viscose fabric showed maximum intensity at 500 nm for excitation wavelength 364 nm. Although the photoluminescence intensity was measured at two wavelengths, 364 nm and 470 nm, the maximum intensity observed for both RF and FMN dyed fabric samples was at 570 nm, which significantly correlates with the observation of fabric samples under UV light irradiation at 370 nm as shown in Figure 50.
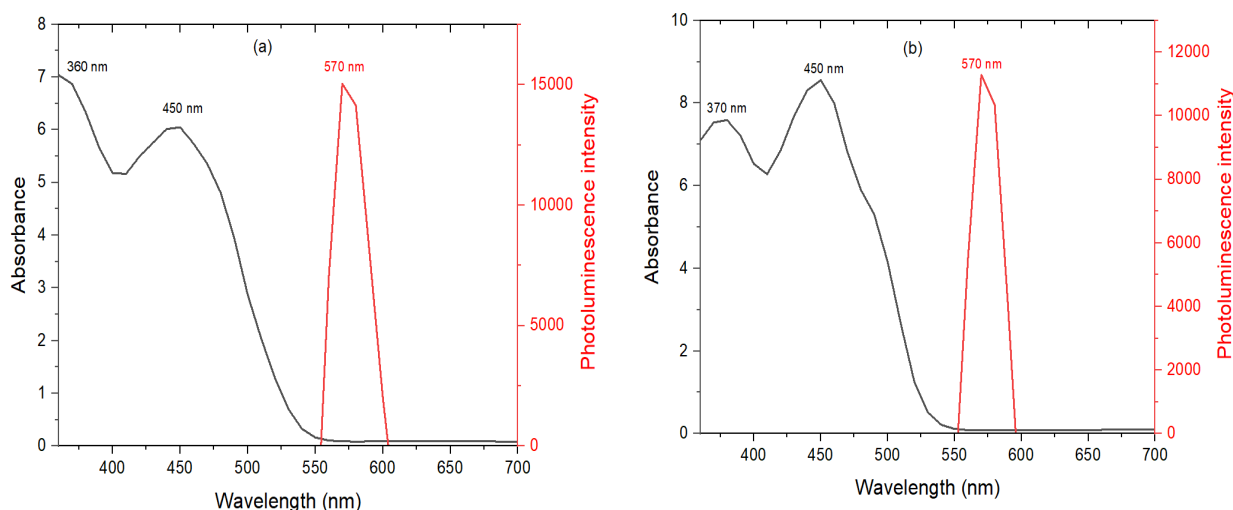
Figure 50. Photoluminescence and absorbance of (a) Riboflavin dyed viscose fabric and RF solution (b) FMN dyed viscose fabric and FMN solution

Similarly, the silk and wool dyed fabric revealed a maximum fluorescence intensity at a wavelength ranging from 535 nm to 555 nm, as represented in Figure 51. Although the K/S value decreased after wash, the photoluminescence intensity increased in the case of silk dyed fabric. In the case of wool dyed fabric, the K/S values remained similar after wash to that before wash. However, low-intensity value was observed after the wash of wool dyed fabric at 4% owf.
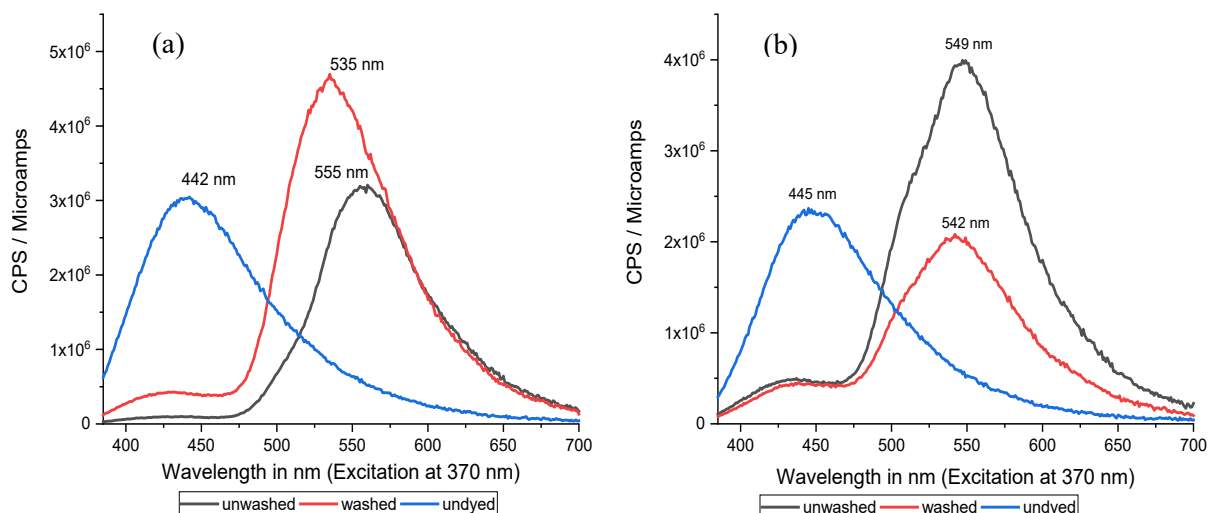
Figure 51. Photoluminescence intensity of undyed and dyed fabric samples (a) silk and (b) wool

4.1.3.5 Quantum efficiency

As shown in Table 12, the photoluminescence phenomenon was confirmed by the measurement of spectroscopy data wherein emitted radiation was observed at a longer wavelength than that of the impinged wavelength on the photoluminescent materials. As discussed in the Jablonski diagram, the molecule undergoes a chain of photophysical events such as internal conversion or vibrational relaxation, intersystem crossing, fluorescence, and phosphorescence [174]. Among the different events, the study revealed the classical visual observation of fluorescence phenomena, wherein the material stopped emission of light immediately after the removal of UV light. Thus, in addition to spectroscopy analysis, fluorescence quantum efficiency on the textile surface was measured for the various concentration of dyed samples, which also pertains to the lifetime measurement of the fluorescence sample [174] [179]. Fluorescence lifetime being the intrinsic property, does not depend on the method of measurement. It is independent of intensity measurement and concentration of fluorescence moiety. The lifetime function can be considered as state function due to its dependent factors such as excitation wavelength and the light exposure duration [174]

Quantum efficiency (QE) can be measured briefly, either using the two-monochromator method and two-mode method or one-monochromator method. However, the use of a two-monochromator method involves high-cost and is commonly inaccessible. Thus, using extended Kubelka-Munk theory (Eq.2), a one-monochromator method was used to measure the quantum efficiency [144] [145]. The quantum efficiency (QE) of RF and FMN molecule has been reported, which varies from 0.24 to 0.32 depending upon the solvent water or ethanol [180] [181]. In this study, the QE of the molecule diffused in fabric samples was determined. The QE value was evaluated at both the absorption wavelength of 360 and 470 nm, respectively. With the assumption that the difference between the forward and reverse spectral reflectance being 0.1, as

both the spectral reflectance band do not overlap, the QE of dyed textile was calculated using extended Kubelka-Munk theory and tabulated in Table 13.

The values varied with the increase in the dye concentration as well as the washed fabric samples, showED an increase in quantum efficiencies. In the case of 4 % RF and FMN dyed fabric samples, the unwashed samples showed a QE value of about 0.13 and 0.14, respectively. At the same time, both RF and FMN washed samples showed an increase in quantum efficiency, and 0.28 QE value was obtained for each. Further, quantum efficiency values at both the wavelengths 360 and 470 nm were calculated, which was observed to be invariant for FMN and RF dyed fabric samples. However, only in the case of 20% RF dyed fabric (unwashed), there was a difference in the quantum efficiency values at the respective wavelength.

Table 13. Quantum efficiency values for RF and FMN dyed fabric at a respective excitation wavelength (Photoluminescence results based on data analysis with proper baseline detection)

Excitation wavelength (nm)	360	470
Sample description	Quantum efficiency at an emission wavelength of 570 nm	
4 % FMN dyed (unwashed)	0.127	0.128
4 % FMN dyed (washed)	0.274	0.255
20 % FMN dyed (unwashed)	0.131	0.131
20 % FMN dyed (washed)	0.138	0.137
4 % RF dyed (unwashed)	0.14	0.143
4 % RF dyed (washed)	0.286	0.287
20 % RF dyed (unwashed)	0.144	0.206
20 % RF dyed (washed)	0.164	0.157

Furthermore, the QE values were studied for textiles dyed at varied concentrations of RF and FMN to evaluate the effect of concentration on the QE values, which varied for 4% and 20% owf dyed fabric samples, dyeing was carried out at 4%, 10%, 16%, and 20% owf respectively. Initially, the reflectance curves of the dyed textile fabric samples at different dye concentrations were measured to calculate the quantum efficiency.

The quantum efficiency for the dyed fabric samples at various concentrations was calculated and values tabulated, as shown in Table 14 and Table 15. The QE value of FMN and RF dyed fabric revealed a gradual increase in QE value with an increase in dye concentration from 4%, 10% to 16% (unwashed) samples, and drops at 20% owf dyed fabric (unwashed sample). However, for the washed fabric samples, the quantum efficiency was observed to be high at 0.28 for 4% owf, which then eventually dropped from 10% to 20% owf. The average quantum efficiency for both 4% and 20% owf FMN dyed fabric sample shows 0.13, a significant increase in quantum efficiency can be seen for samples after washing in the case of 4% owf dyed fabric, whereas 20% owf dyed fabric shows an only minor increase. However, in the case of RF dyed fabric

samples, a significant increase in quantum efficiency can be seen for both 4% and 20% owf dyed fabric samples.

Table 14. Quantum efficiency at the various concentration for FMN dyed fabric samples

Sample description	FMN dyed fabric (unwashed)		FMN dyed fabric (washed)	
Excitation wavelength(nm)	360	470	360	470
Dye %owf	Quantum efficiency calculated at a fluorescent emission wavelength of 570 nm			
4 %	0.12897	0.12842	0.27386	0.25553
10 %	0.13699	0.13947	0.15755	0.1562
16 %	0.14723	0.14971	0.15428	0.14804
20 %	0.12621	0.12755	0.15166	0.14253

Table 15. Quantum efficiency at the various concentration for RF dyed fabric samples

Sample description	RF dyed fabric (unwashed)		RF dyed fabric (washed)	
Excitation wavelength(nm)	360	470	360	470
Dye concentration %owf	Quantum efficiency calculated at a fluorescent emission wavelength of 570 nm			
4 %	0.14012	0.14342	0.28605	0.28793
10 %	0.18036	0.19093	0.15755	0.16694
16 %	0.14794	0.15606	0.15428	0.16335
20 %	0.14224	0.15011	0.15166	0.16077
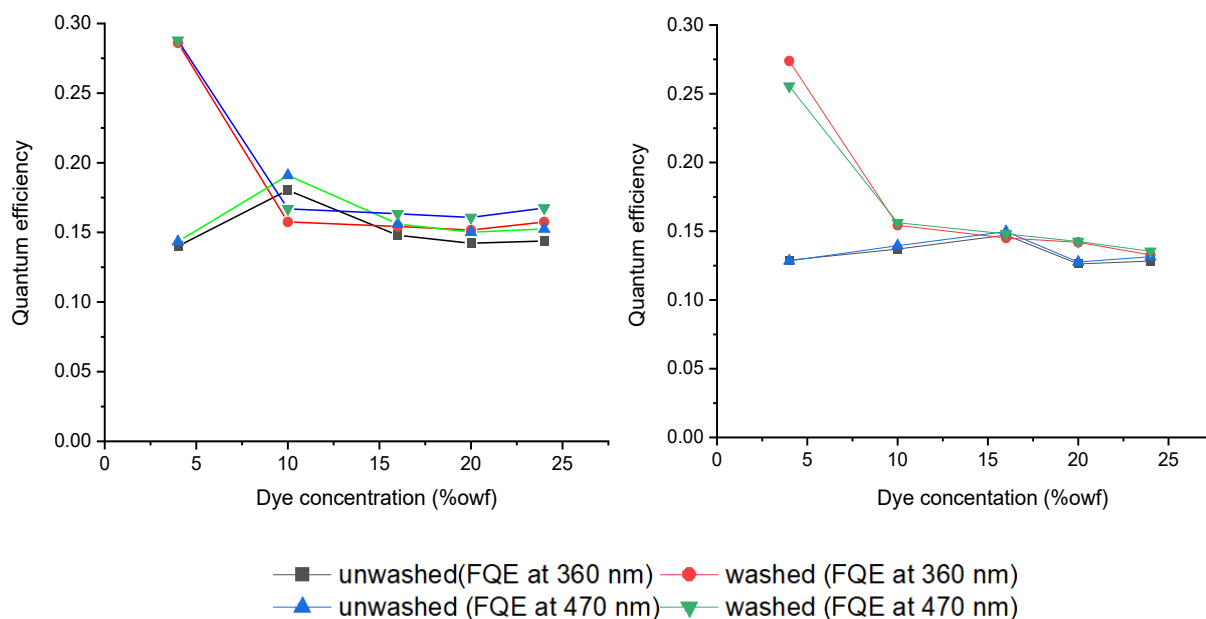
Figure 52. Quantum efficiency of dyed fabric (unwashed and washed at 360 and 470 nm) at different dye concentrations (a) RF (b) FMN.

As shown in Figure 52, the QE or fluorescence quantum efficiency (FQE) value drops with the increase in dye concentration; thus, the quenching phenomenon of riboflavin and flavin mononucleotide can be seen. The FQE values varied depending upon the concentration of dye. The decrease in quantum efficiency value could occur due to molecule aggregation on the textile surface. The quenching concentration of riboflavin and FMN exists whereby the fluorescence quantum efficiency drops, and the QE is invariant with the exciting wavelength. Hence, with the increase in the concentration of RF and FMN dye, quenching of fluorescence can be seen when measured the quantum efficiency, which drops at the concentration where the quenching effect begins. For both RF and FMN washed fabric samples, the QE value dropped from 10% owf dyed sample and was seen to be almost stable, possessing 0.15 QE value. For RF and FMN dyed (unwashed) fabric samples, the QE attains stability from 16% owf dyed sample showing 0.14 QE value. The dyed fabric sample (unwashed) shows molecules physical adsorbed on the textile surface, as molecules were on the fiber surface low quantity of reflectance was yielded, and quantum efficiency was seen low. After washing, there was an increase in quantum efficiency due to the quenching effect concerning the molecules on the surface and its effect in yielding fluorescence. Quantum efficiency can vary at different pH, the dyeing using riboflavin and FMN was carried out at pH 7, and hence the molecule could be rigid. Thus the quantum efficiency was seen to be high. An increase in rigidity yields an increase in fluorescence emission because of more conjugation in the isoalloxazine ring of RF and FMN molecule. Fluorophore has an absorption spectrum, which is the excitation spectrum to study the fluorescence. In the case of RF and FMN, the absorption was seen at wavelength 364 nm and 470 nm.

Moreover, the wavelength at which the emission light obtained was at 570 nm, and the maximum quantum efficiency value of 0.28 was determined. Besides, the silk and wool dyed fabric also exhibited FQE values in the range of 0.17 to 0.33 at 4% owf.

Table 16. Quantum efficiency values of silk and wool RF dyed fabric samples

Fabric	Sample description	RF dyed (unwashed)		RF dyed (unwashed)	
	Excitation wavelength(nm)	360	470	360	470
	Dye concentration %owf	Quantum efficiency calculated at a fluorescent emission wavelength of 570 nm			
Silk	4 %	0.2144	0.2003	0.2584	0.2223
Wool	4 %	0.3352	0.2459	0.3240	0.2286

Table 17. Quantum efficiency values of silk and wool FMN dyed fabric samples

Fabric	Sample description	FMN dyed (unwashed)		FMN dyed (unwashed)	
	Excitation wavelength(nm)	360	470	360	470
	Dye concentration %owf	Quantum efficiency calculated at a fluorescent emission wavelength of 570 nm			
Silk	4 %	0.1740	0.1602	0.2460	0.2054
Wool	4 %	0.2100	0.1738	0.2343	0.1817

4.1.3.6 Image analysis

The dyed fabric samples observed under UV chamber and tabulated below,

Table 18. Image of Viscose untreated fabric under daylight and UV light.

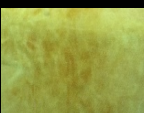Table 19. Images of viscose dyed fabric under daylight and UV light.

Biomaterial	Dyed fabric under daylight (unwashed)	Dyed fabric under UV light (unwashed)	Dyed fabric under daylight (washed)	Dyed fabric under UV light (washed)
Riboflavin				
Flavin mononucleotide				

Table 20. Images of Riboflavin dyed viscose fabric samples treated with different mordants.
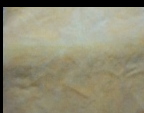
Effect of mordants	Dyed fabric under daylight (unwashed)	Dyed fabric under UV light (unwashed)	Dyed fabric under daylight (washed)	Dyed fabric under UV light (washed)
Tannic acid				
Calcium chloride				
Citric acid				
H_2O				

Table 21.Images of FMN dyed viscose fabric samples treated with different mordants.
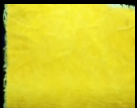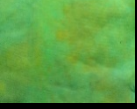
Effect of mordants	Dyed fabric under daylight (unwashed)	Dyed fabric under UV light (unwashed)	Dyed fabric under daylight (washed)	Dyed fabric under UV light (washed)
Tannic acid				
Calcium chloride				
Citric acid				
H_2O				

Table 22. Images of Silk and wool untreated fabric under daylight and UV light.

Fabric	Under daylight	Under UV light
Silk untreated fabric		
Wool untreated fabric		

Table 23. Images of FMN dyed silk and wool fabric samples
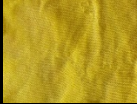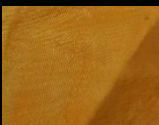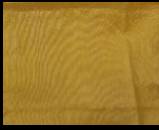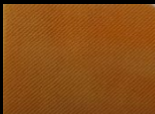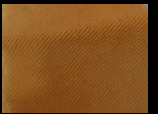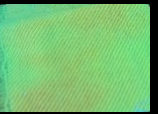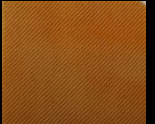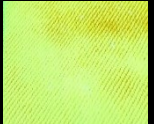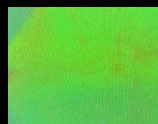
Fabric	Dyed fabric under daylight (unwashed)	Dyed fabric under UV light (unwashed)	Dyed fabric under daylight (washed)	Dyed fabric under UV light (washed)
Silk				
Wool				

Table 24.Images of Ribofalvin dyed silk and wool fabric samples

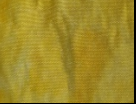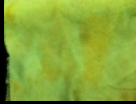| Fabric	Dyed fabric under daylight (unwashed)	Dyed fabric under UV light (unwashed)	Dyed fabric under daylight (washed)	Dyed fabric under UV light (washed)
Silk				
Wool				

4.1.3.7 UV PROTECTION

Ultraviolet radiation ranges from near UV (290-400 nm), far UV (180-290 nm), and vacuum UV (below 180 nm). The term UVA represents the region 320-400 nm, UVB represents 290-320 nm, and the UVC region represents below 290 nm. The undyed viscose fabric showed a UPF value of 5, revealing no effect to block UV radiation. However, an improved UPF rating was observed for the dyed cellulosic fabric with both FMN and RF.

The UPF value was greater than 50 for the RF dyed fabric samples. It remained> 50 even after a wash, which is highest when compared to FMN dyed fabric with UPF value of 35 and 30 for unwashed and washed fabric, respectively. The FMN and RF absorption maximum can be seen in the visible region at 440 nm and 370 nm in the UV region, hence improved UV protection effect was observed for both FMN and RF, as shown in Table 25. Various factors such as physical/chemical type of fiber, fabric construction, thickness, and porosity influence different types of interactions between the textile material and the ultraviolet radiation hitting the substrate, thus, affecting the ultraviolet protection ability [182]. The research study shows the impact of the UV rays on various living organisms, such as premature aging and a significant reason for malignant cutaneous melanoma, which is a skin disease. Studies have been carried out to cure the melanoma using RF [183]. Overall, the assessment provided the ultraviolet protection ability for both RF and FMN dyed fabric samples.

Table 25. UPF analysis of FMN and RF viscose dyed fabric samples

Sample Description	UPF	UV A	UV B
Viscose Undyed fabric	7.32	23.68	11.55
4 % FMN dyed (unwashed)	42.92	2.08	2.28
4 % FMN dyed (washed)	35.96	2.59	2.62
4 % RF dyed (unwashed)	138.1	0.72	0.72
4 % RF dyed (washed)	85.33	1.17	1.15

Table 26. UPF analysis of FMN and RF silk dyed fabric samples

Sample Description	UPF	UV A	UV B
Silk undyed fabric	25.18	0.11	0.03
4 % FMN dyed (unwashed)	25.61	0.04	0.03
4 % FMN dyed (washed)	25.43	0.05	0.04
4 % RF dyed (unwashed)	40.17	0.03	0.02
4 % RF dyed (washed)	23.9	0.06	0.04

Table 27. UPF analysis of FMN and RF viscose dyed fabric samples

Sample Description	UPF	UV A	UV B
Wool undyed fabric	259	0.02	0.00
4 % FMN dyed (unwashed)	500	0.00	0.00
4 % FMN dyed (washed)	496	0.00	0.00
4 % RF dyed (unwashed)	500	0.00	0.00
4 % RF dyed (washed)	496	0.00	0.00

4.1.4. Conclusion

The study confirmed the potential use of diffusion method to impart photoluminescence on textiles along with multifunctional properties to the cellulosic fabric. The spectroscopic properties of RF and FMN largely depend upon the local environment, concentration, and temperature; hence, it was important to detect the fluorescence property exhibited by the molecule on textiles. The photoluminescence and UV protection analyses data revealed that most of the properties of both RF and FMN are transferred to the fabric. The K/S data showed that high dye uptake was observed in the case of FMN, as compared to RF treated fabric samples. Wash fastness increased using tannic acid and citric acid in the case of riboflavin. However, tannic acid leads to a duller shade and less fluorescence when observed visually under UV illumination. Viscose fabric dyed using FMN and calcium chloride as mordant increases the wash fastness and the fluorescence property enhanced. The mordanting effect has to be further investigated to understand the phenomenon occurring between the RF and FMN moiety. The visual observance of photoluminescence allowed determining the intensity of dyed samples quantitatively. The theoretical evaluation of quantum efficiency on the textile fabric revealed approximately the same quantum efficiency as that of RF and FMN molecule. It is well known that the riboflavin solution exhibits antibacterial property; however, due to the probability of low deposition of molecules on the fabric samples, the effect could not be observed. Interestingly high UPF factors were observed for RF, and FMN treated fabrics.

The work allowed to explore the photoluminescence property of RF and FMN, along with multifunctional properties, for its application in the field of textiles as a new scope of producing photoluminescent textiles. However, further studies in case of dye fixation would be interesting in perspective to obtain other functionalities such as antibacterial property along with the attainment and stability of photoluminescence effect on textiles. The study also enabled to explore the potential use of RF and FMN for dyeing silk and wool fabric showing color strength and enhanced fluorescence properties with their corresponding quantum efficiencies. Overall, the functionalization of FMN on cellulosic as well as silk and wool fabric widen the scope and application use of photoluminescent textiles obtained using RF and FMN.

4.2. Photoluminescent textile on plasma treated PET nonwoven using biopolymers and FMN

4.2.1. Introduction

In fluorescence, the emission of a photon is rapid, while in the case of phosphorescence, the light emitted is delayed. Indeed, photoluminescent pigments used to produce photoluminescent textiles fall onto the category of "Glow in Dark". The concept of "Glow in Dark" is the process of light emission when a fluorescent dye absorbs blue light emitted either by a phosphorescent material or by UV light from the atmosphere (example. sunsets, sunrise, and UV lamp). Photoluminescent textiles are also obtained either by fixing pigments in the fiber or onto the polymer fibrous surface using chemical binders by coating or printing, producing a glow in dark patterns on textiles. Accordingly, they can give textile a softer quality by emitting light without using any wires. Presently, photoluminescent molecules or particles such as rare earth doped strontium aluminate ($SrAl_2O_4$: Eu^{2+}, Dy^{3+}) are used to produce photoluminescent textiles are high-cost rare earth luminescent and seem to have health impacts on workers [184][185][15]. In this study, biobased FMN was printed and coated on PET nonwoven to create aesthetic panels with photoluminescent designs. PET being non-toxic, cheap, and biocompatible [186], is interesting to use for printing and coating.

A biopolymer/FMN mixture was used for coating and printing, as PET cannot be functionalized using the diffusion method these bio-based photoluminescent molecules. Biopolymers such as gelatin and alginate were used and previous studies using alginate as a thickener for cotton printing. Alginate has been already used as a thickener for cotton printing with reactive dyes [187]. However, in a previous study, alginate was used to immobilize bio-based peptides on plasma-activated polyester woven fabric [105].

In this study, FMN as a fluorescent dye on textiles has been explored to discover the new scope for photoluminescent and glow-in-the-dark textiles, like those produced by Kooroshnia [12], but using a biobased resource. Indeed FMN exhibits fluorescence that can be observed in the dark while a UV-light shines. The main aim of this work is, therefore, to study the application of flavin mononucleotide (FMN) on textiles using printing and coating methods to produce glow-in-the-dark patterns on polyester nonwoven, with the possibility of one expression in daylight and another in darkness. Previous studies [169] already revealed that FMN could diffuse inside cellulosic fibers textile and produce photoluminescent textile materials. As the FMN could not dye the polyester to produce photoluminescent materials, in this study, the combined use of biopolymers based and FMN has been investigated using coating and printing with prior surface activation of nonwoven PET to produce either uniform luminescent PET nonwoven panels or glow-in-the-dark patterns.

Coatings in textiles are either protective or decorative compositions that dry to a cohesive, adherent film when applied. Different types of coating formulations exist, such as hydrophobic, hydrophilic, organic, and inorganic, functional or aesthetic coatings. Further, the coating mechanism varies depending on the nature of formulations and the substrate material. Among various types of coating techniques such as chemical and physical vapor deposition, UV coating, sol-gel coating, and so on, direct coating and screen printing methods were used in the thesis study. The direct coating is a widely used technique for textile coatings, wherein the printing formulation is spread and pass through the frame of the screen using a squeegee. Hence, the set up mainly deals with the penetration of the coating formulation into the textile substrate. Further, the basic principle of screen printing also resonates with coating, wherein the formulation is pressed through a flatbed screen onto the textile substrate. A magnetic table is used beneath the textile, and a squeegee (or a metal rod) placed over the fixed screen on the top of the table is used to squeeze out the print through the flat screen mesh. However, the screen is usually printed with some desired pattern [188].

In the first part of the study, air atmospheric plasma activation of PET nonwoven was carried to produce hydrophilic PET nonwoven. AFM and wettability/capillarity measurements are already described in chapter 3 of the luminescence study on PET nonwoven but also described briefly in this section. In parallel, films were formed on polystyrene (PS) petridishes using biopolymer/FMN mixtures. Two biopolymers (gelatin and alginate) were tested, and the rheological study of aqueous solutions of biopolymers as a function of temperature and shear rate applied was carried. Fluorescence/photoluminescence of the films and the plasma nonwoven PET coated or printed with polymer/FMN mixture were then visualized under UV light and evaluated using photoluminescence spectroscopy.

4.2.2. Experimental section

Preparation of biopolymer film

Gelatin and alginate gels of 5% concentration were prepared, and the viscosities were measured using the rheoplus equipment at 20 °C. Based on the gelatinization temperature of the respective biopolymer, as mentioned in Table 28, the gel was prepared using distilled water. The gels were then introduced with 1ml of 1% and 5% FMN solution mixing it homogeneously on the magnetic stirrer for 5-10 minutes. The homogeneously mixed biopolymer FMN mixture was used to prepare films in polystyrene (PS) petridish.

Table 28. Details of biopolymer film preparation and conditions.

Biopolymer (5%)	Active agent (1, 5 %)	Max temp	(H_2O) volume
Gelatin	FMN	60 °C	100 ml
Alginate		80 °C	100ml

Application of biopolymer/FMN mixture on plasma-activated PET using screen printing and coating methods.

The biopolymer/FMN mixture was applied onto plasma treated nonwoven using the screen printing and coating techniques. The biopolymer/FMN mixture was screen printed on plasma treated nonwoven using the laboratory's flatbed screen-printer. The printing formulation was spread across the frame of the screen and squeezed using a squeegee to pass through the screen onto the textile substrate. Further, a metal rod was placed over the fixed screen and continuously coated onto the textile substrate. The textile was then dried and cured at 120°C for 30 seconds.

4.2.3. Results and Discussion

4.2.3.1 Plasma effect on PET nonwoven

The capillary uptake of untreated nonwoven PET was observed to be null, which then increased up to 1460 mg for the plasma treated PET nonwoven. Thus, the increase in capillary uptake and reduction in water contact angle to 0° as compared to 141° of the untreated PET nonwoven, thereby reveals the increase in surface energy of plasma treated PET fiber. Due to the scission of ester bonds, oxygen atoms were integrated. Thus an increase in O/C ratio up to 0.5 was confirmed by XPS analysis. Thus, hydrophilic terminal carboxyl and hydroxyl functional groups were introduced on the fiber surface, as confirmed in prior studies [105]. The SEM images of untreated PET showed a relatively smooth PET fiber surface (Figure 53). However, the plasma treatment PET fiber surface showed few surface etching on the cylindrical PET fiber, as shown in Figure 53b.
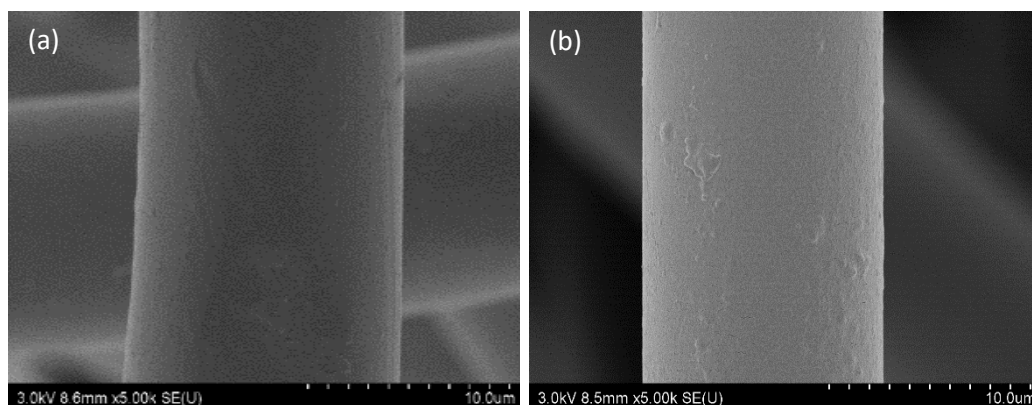
Figure 53. SEM images of (a) untreated PET, (b) ATMP plasma treated fiber surface of nonwovens

Moreover, the AFM topographical images (1µm x 1µm) of PET fiber surface before and after the plasma treatment reveals that the untreated nonwoven textile show smooth and homogeneous fiber surface; while the fiber surface subjected to both plasma treatments increased the surface roughness with the appearance of scale-like surface structures, similar to our previous studies discussed in section 3.3.1.

4.2.3.2　　Rheological properties

Mixtures of alginate and gelatin with FMN were studied by rheology at two different temperatures from 20 to 60°C at varying shear rates of 100, 200, 300, 400, and 500 s^{-1}. The rheological properties of the printing paste play one of the essential roles in the process of textile printing. The analysis revealed that gelatin and alginate mixture (Figure 54 and Figure 55) displays non-Newtonian pseudoplastic behavior [189][190], thus facilitating the coating and the printing process.
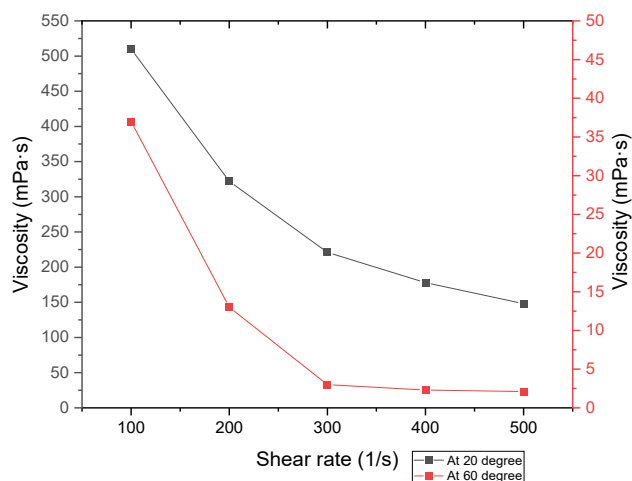
Figure 54. Viscosity of 5% gelatin with varying shear rate at 20 °C (black line) and 60 °C (red line)

Figure 55. Viscosity of 5% sodium alginate with varying shear rate at 20 °C (black line) and 60 °C (red line)

4.2.3.3 Visual observation under daylight and UV chamber

FMN-biopolymer films, coated and screen printed fabric

The biopolymer film formed with FMN was observed under daylight and under the UV chamber to see the fluorescence effect of FMN.
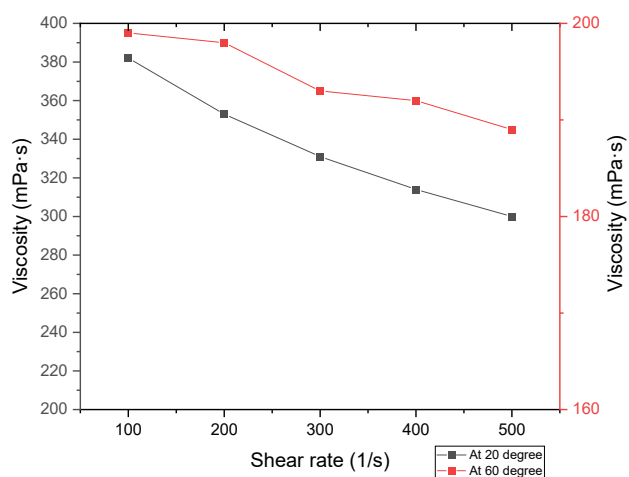
Sample A	Sample B	Sample C	Sample D
5% alginate + 1 ml of 5%FMN	5% alginate + 5 ml of 5%FMN	5% gelatin + 1 ml of 5%FMN	5% gelatin + 5 ml of 5%FMN
Under daylight			
Under UV light			
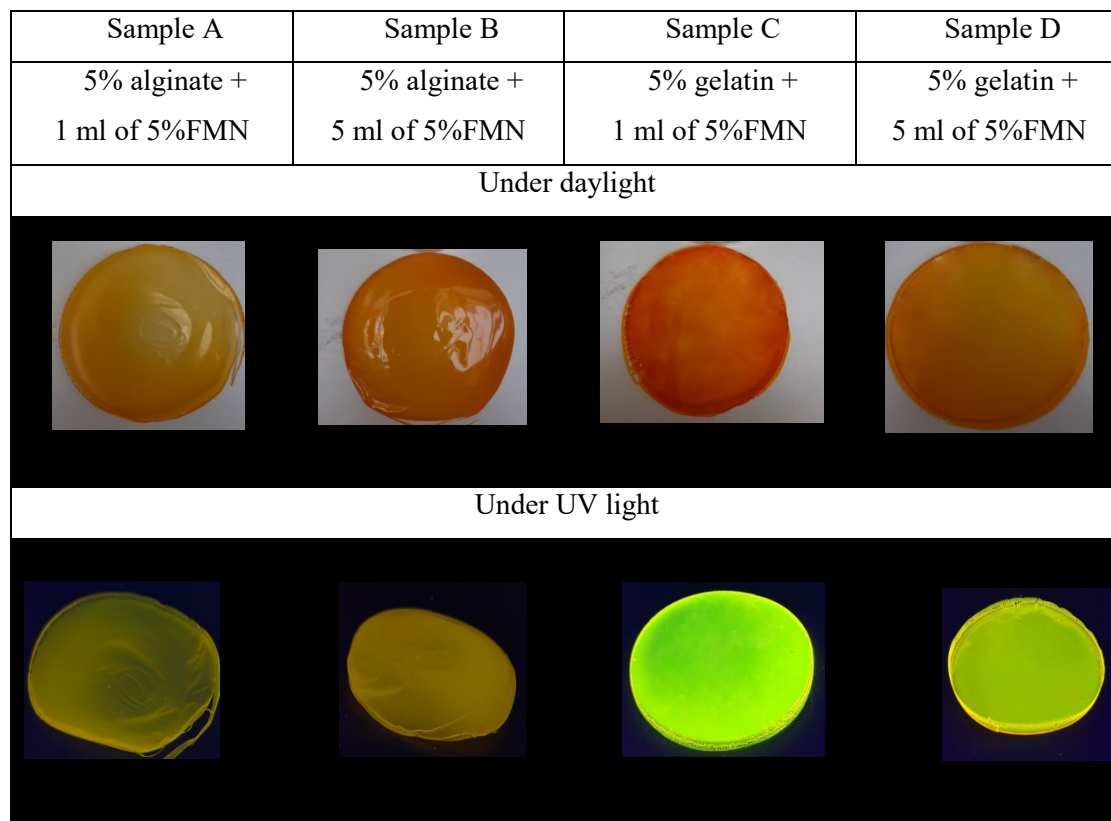
Figure 56. Biopolymer film images under UV and daylight

In the absence of FMN, alginate and gelatin formed transparent films when the corresponding solutions were dried at room temperature in different petridishes. These films did not adhere to the hydrophobic polystyrene petri dish. On the addition of FMN in each biopolymer solution, homogeneous films were formed and observed under the UV chamber for the FMN fluorescence effect. As shown in Figure 56, under daylight, all the films exhibited pale brown color, however under the UV light chamber, a prominent yellow-green fluorescence was observed only in the case of gelatin and FMN mixture, the alginate FMN mixture did not exhibit prominent fluorescence characteristics. Hence, for further screen printing and coating purpose, only gelatin and FMN mixture was used (Figure 57 and Figure 58). As shown in Figure 57(a to c), the biopolymer films were observed under daylight, and correspondingly Figure 57 (d to e) represents the untreated nonwoven and FMN coated nonwoven observed under daylight and UV light.
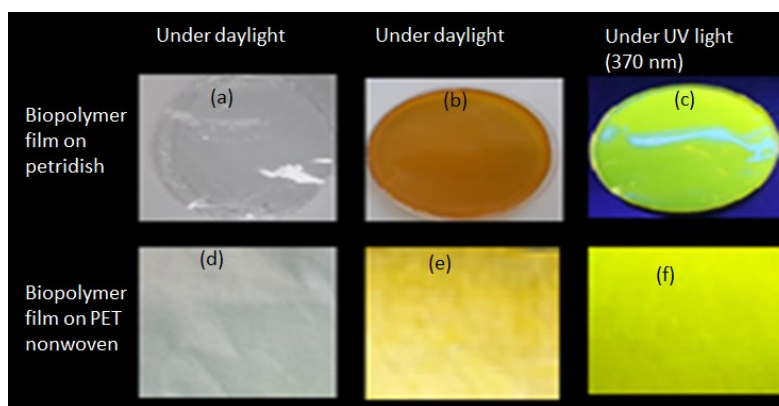
Figure 57. Coated nonwoven PET with gelatin and FMN mixture
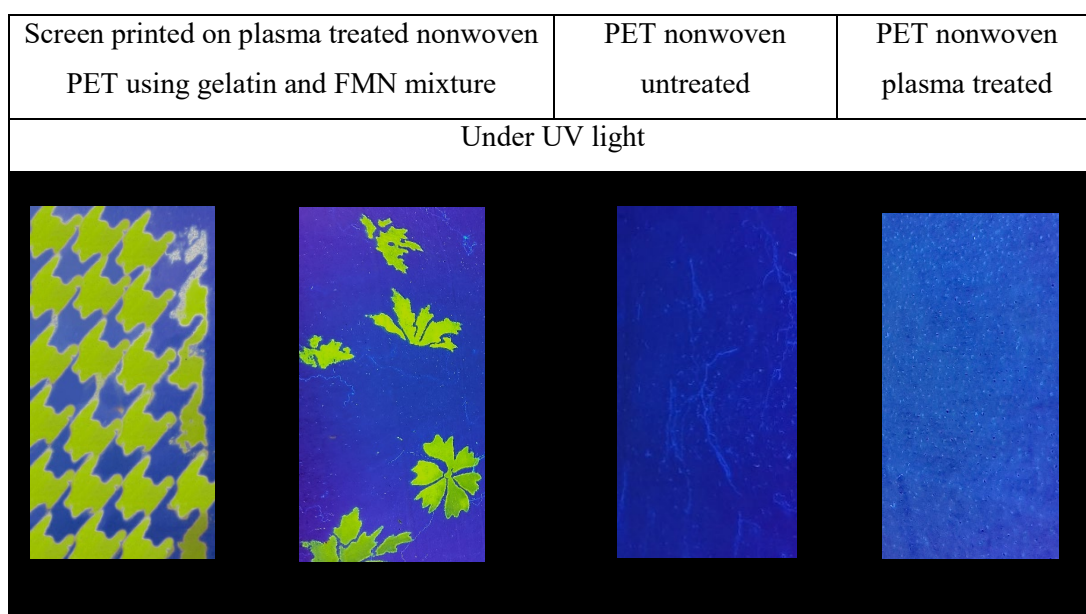
Figure 58. Screen printed nonwoven PET with gelatin and FMN mixture

4.2.3.4 K/S and photoluminescence intensity evaluation

Gelatin and FMN coated on PET nonwoven before and after plasma treatment

A uniform mixture of FMN moiety in gelatin was prepared using 5% gelatin mixed with 5 ml of 5% FMN solution during heating of gelatin solution at 80°C. This mixture was then coated onto untreated, and plasma treated PET fabric. The photoluminescence intensity and the color strength of all the treated fabrics were evaluated, as shown in Figure 59.

The characteristic fluorescence property of the FMN was observed onto PET coated textiles, and the maximum fluorescence intensity was observed at 530 to 540 nm for FMN coated on untreated PET nonwoven. In contrast, the intensity maxima were at 570 nm for the FMN coated on plasma treated PET fabric samples. The untreated PET nonwoven coated sample revealed similar fluorescence maximum wavelength as that observed for FMN solution. However, a shift of 40 nm wavelength was observed for the plasma PET coated sample, which might be due to the intensity spectrum and energy difference of the laser beam [176].

Besides, the maxima absorbance for FMN coated on untreated PET nonwoven was observed at 360 and 450 nm with K/S value around 5. Although after washing, the K/S value decreased drastically while the photoluminescence intensity was observed to be increased from 5×10^3 a.u. (unwashed) to 1.4×10^4 a.u. (washed). However, the FMN coated on plasma treated PET nonwoven showed coloration even after washing with K/S values around 8. The fluorescence intensity was also increased after washing from 1.7×10^4 to 2.2×10^4 a.u. The variation in intensity observed was due to the concentration of FMN, which influences the fluorescence intensity where ionic strength log k quenches the fluorescence intensity [168].
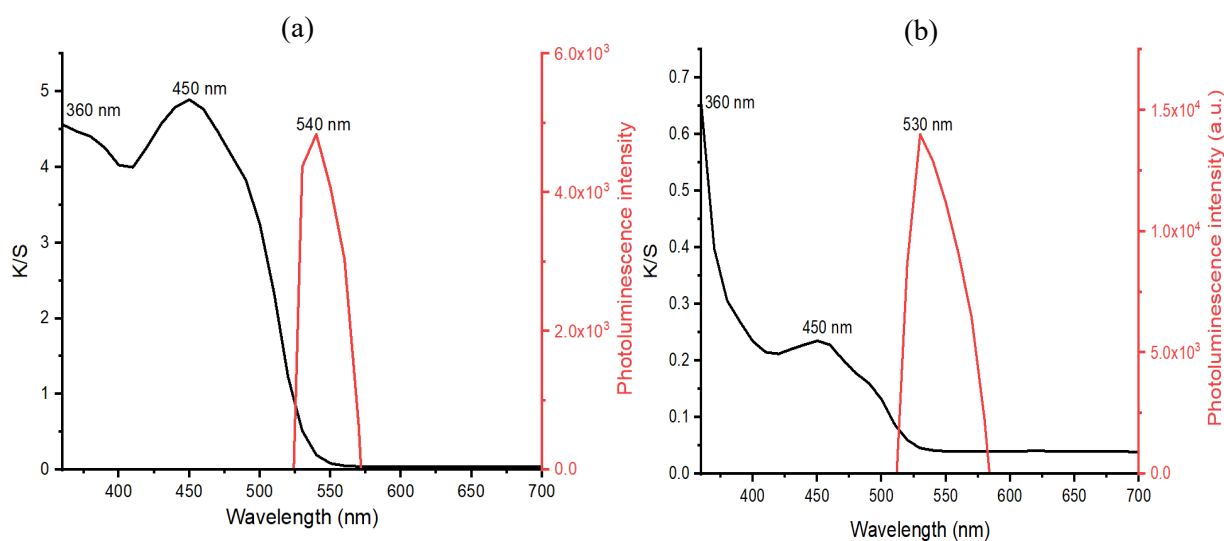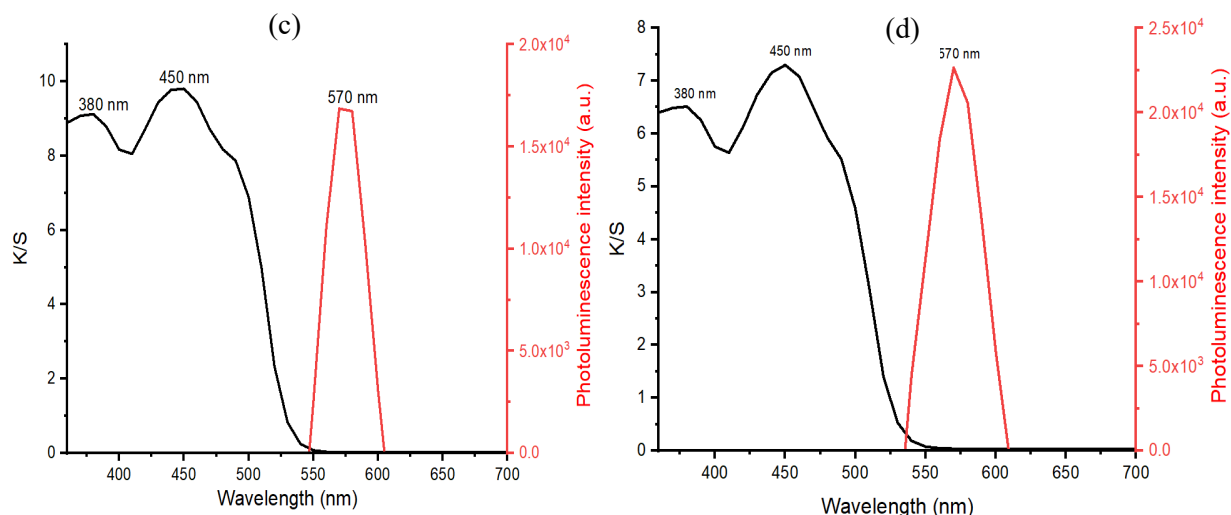
Figure 59. K/S and photoluminescence of FMN gelatin mixture coated on (a) untreated PET nonwoven coated unwashed sample, (b) untreated PET nonwoven coated washed sample, (c) plasma treated PET nonwoven coated unwashed sample, (d) plasma treated PET nonwoven coated washed sample

4.2.4. Conclusion

In printing and pad dyeing of polyester-based fabrics, generally disperse dyes which can sublimate readily are used, which are deposited at the surface and then subjected to thermosol process for the diffusion of dyes inside the polyester fiber. The polar nature of the fluorescent FMN molecule does not allow its diffusion inside the hydrophobic polyester fiber, using the dye exhaustion process. Hence hydrophilic biopolymers (gelatin, alginate) were selected for proper dispersion of FMN and used as a thickener in a screen printing process. They can also act as a binder to fix FMN on the PET fiber surface. However, the hydrophilic polymers need to be bound to the PET fiber surface to immobilize the FMN efficiently at the PET fiber surface. The gelatin and FMN films formed each a yellowish-brown layer, which exhibited green-yellow fluorescence under the blue UV light (370 nm). Without plasma, the hydrophilic polymers have no adhesion on the untreated hydrophobic polyester, and they are therefore washed easily. Air atmospheric plasma treatment increases the hydrophilic behavior of the PET nonwoven, with reduced contact angle and increased capillary uptake, as polar functional groups such as carboxylic and hydroxyl are formed due to scissions of ester bonds by the plasma discharge. This increase hydrophilic behavior allows a more homogeneous fabric and fiber coating (through coating and printing) and also improved adhesion of the hydrophilic films onto the PET plasma-activated fiber surface. Polar group creation, as well as the increased surface roughness of the polyester fiber, after plasma treatment, would explain the increased adhesion of

the hydrophilic polymers onto the plasma treated polyester fibers. The gelatin/FMN was completely washed out from the untreated hydrophobic PET.

Indeed different films were formed from aqueous solutions of each biopolymer and FMN by drying the FMN-biopolymer solution in a petridish. However, only gelatin showed greenish-yellow fluorescence of the FMN. No prominent yellow-green fluorescence was seen with alginate. Hence, only gelatin was used for coating of plasma treated polyester nonwoven, to produce an entire panel of green-yellow fluorescence under UV light. The use of gelatin paste allowed to create green-yellow fluorescent patterns on the PET nonwoven. Both gelatin/FMN coating and printing produced glow-in-the-dark panels of the polyester nonwoven. With the gelatin, however, a more rigid photoluminescent panel was obtained. The plasma treatment enhanced color strength. After washing, K/S decreases slightly; however, the photoluminescence increases.

From the above work, it can be concluded that vitamin B2 derivative- Flavin mononucleotide can exhibit fluorescence property and yield biobased photoluminescent textiles as well as the glow-in-the-dark pattern on polyester nonwoven, using coating and printing techniques after plasma activation of the PET nonwoven. Gelatin is an ideal polymer coating and binder to observe the fluorescence properties of FMN in printed patterns and hence to create and design glow-in-the-dark patterns on the PET nonwoven. Application of the coating on plasma treated PET nonwoven results in a photoluminescent polyester nonwoven with improved wash fastness properties. The screen printing technique used for the study allowed to create a glow-in-the-dark pattern on textiles with the possibility of one expression in daylight and another in darkness. Bio-based natural products such as the FMN are potentially interesting photoluminescent molecules with which textile surface pattern designers may create light-emitting textiles and interesting aesthetic expressions. Further work should focus on the influence of time and light irradiation on the luminescence intensity and coloration.

4.3. Photoluminescent textiles using digital printing techniques on cellulose and PET fabrics.

4.3.1. Introduction

The use of the fluorescent dyes has focused on application in textiles using conventional dyeing, coating, and printing techniques. However, all these techniques do not necessarily fulfill the criteria of green production due to the massive consumption of resources such as water, energy, and waste emissions in water. Thus, it is necessary to move towards more sustainable textile coloration techniques and acquire modification of textiles through ultrasonic radiation, microwave radiation, plasma treatment, and digital printing techniques [191][192][193][194][195][196]. The efficient use of raw materials as well as energy resources in the manufacture and application of ink or chemicals can attribute to green chemistry [197]. Although the use of biobased RF and FMN was explored using the diffusion technique as discussed in section 4.1, in this study, only the more soluble molecule FMN was studied.

The FMN was used as a photoluminescent molecule on different textile materials such as cotton duck white (CD), mercerized cotton (MC), and woven polyester (PET) using advanced printing techniques such as inkjet and chromojet printing as a sustainable approach. The ink formulations and their stability were determined using surface tension and viscosity measurements to study the jettability behavior before printing on textiles. Different concentrations of inks were formulated, and Fourier transform infrared spectroscopy (FTIR), UV visible spectroscopy analyses were performed. Primarily the photoluminescence property and color strength of the printed textile were evaluated; moreover, even the fluorescence quantum efficiency (FQE) values were determined theoretically. Besides, multifunctional properties such as UV protection and antibacterial properties were explored. Several scientists have studied the degradation properties of the riboflavin solution [167]. Thus all the printed textiles were induced under UV and visible light to study the degradation properties of the photoluminescent FMN printed on textiles.

4.3.2. Experimental section
4.3.2.1 Preparation of ink formulation

The ink solution was formulated for both inkjet and chromojet printing, respectively. Initially, for inkjet printing, the ink solution of 0.1% FMN was prepared using 50% glycerol in an aqueous solution containing 0.3% Triton X 100. Chromojet printing included the preparation of glycerol-based and water-based formulations. FMN solution at different concentration: 0.1%, 0.3%, 0.5%, 0.8% and 1% were prepared using deionised water (water-based formulations) referred as A, B, C, D, E samples for CD, MC and PET textile respectively. Further, 0.1%, 0.3%, 0.5%, 0.8% and 1% solution were prepared using composition of 50%

glycerol in aqueous solution containing 0.3% Triton X 100 (glycerol-based formulations) referred as F, G, H, I, J samples for CD, MC and PET textile respectively.

4.3.2.2 Set up for inkjet printing on textile

A solid square pattern was inkjet printed using the ink formulation on PET, MC, and CD textile surface at a resolution of 100 dpi by consecutive passes of 2,4,6,8 and 10, respectively. The textile samples were then air-dried and conditioned at room temperature for 24 hours for further analysis. The textile was placed in the adjustable platform, and the inks were supplied directly into printhead from glass bottles via inert plastic tubing. Thorough cleaning of the printhead and tubing was ensured to prevent choking. The initial 30 ml of ink solution was purged out to remove any previous traces of ink. The jetting was performed at temperature 25°C. Consequently, multiple printhead passes were printed, keeping the jetting voltage and waveform constant.

4.3.2.3 Set up for chromojet printing on textile

The set parameters for chromojet printing on the different textile were pressure set at 2 bar, coverage by raster set as 100 %, the printhead having nozzle diameter of 150 µm was used.

4.3.3. Results and Discussion
4.3.3.1   Surface tension and Viscosity analysis

The surface tension and viscosity are essential characteristics of the printing solution and are closely connected to the printing performances [34]. The analysis result for viscosity and surface tension (Figure 60) fulfilled the printhead specifications for inkjet printing and chromojet printing, respectively [35]. The viscosity of 0.1% FMN (glycerol-based formulation) showed no significant change with an increase in temperature from 20 to 30°C. The viscosity and the surface tension of ink was 8.2 mPa·s and surface tension of 27.42 mN/m. Further, the viscosity was measured at 20°C and 10000 s^{-1} shear rate for all the ink formulations used for chromojet printing. The average viscosity of 8.1 mPa·s for glycerol-based and 3.1 mPa·s for water-based formulations were obtained, and viscosity remained the same irrespective of varying concentrations. The surface tension of all water-based ink formulations, as expected, were 72 mN/m equivalent to that of surface tension of pure water.
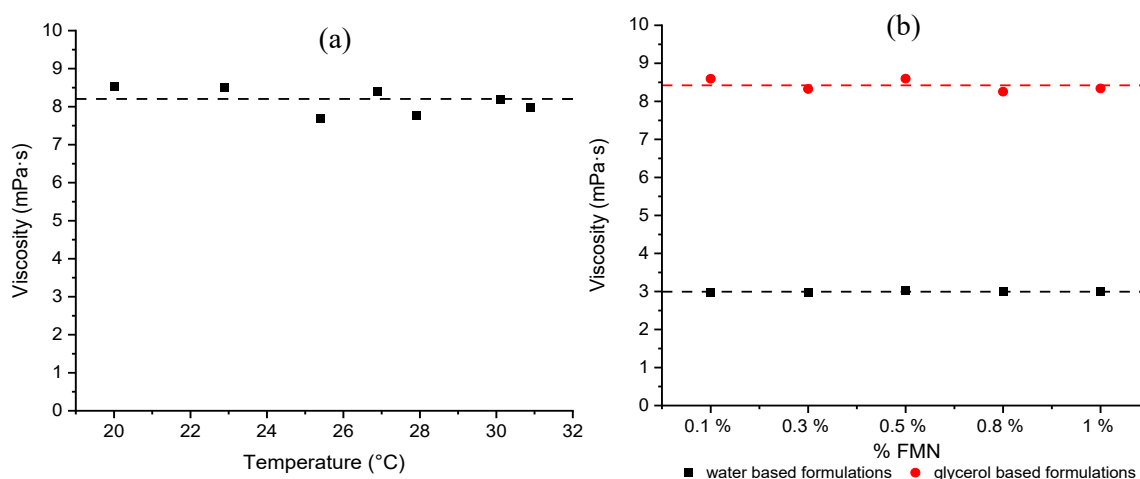
Figure 60. Rheological properties of FMN ink formulations: (a) viscosity of 0.1% FMN (glycerol-based) measured in the temperature range from 20 to 32°C (b) viscosity at 20°C

4.3.3.2   FTIR analysis

The Fourier transform infrared (FTIR) spectrum of FMN solution and FMN inkjet printed textiles CD, MC, and PET revealed absorption bands at 1031, 1315, and 1430 cm^{-1} corresponding to C-N, C-C, and N-H band respectively. The absorbance bands at 1647, 3337 cm^{-1} can be attributed to stretching bands of C = 0 and C-H stretching, respectively, in agreement with the literature data [37]. The absorbance peak values increased with an increase in the number of the print pass for all the inkjet-printed textile samples. However, only the mercerized cotton (MC) showed an absorbance value equivalent to that of FMN solution even after 10 print passes. Thus, it can be concluded that a higher number of the print pass would be required for a higher amount of FMN deposition on the different textile surfaces.

Hence, to avoid the number of passes, a chromojet printer was used for the further research study. The FTIR spectra of CD, MC, and PET printed textile samples were evaluated as absorbance values versus wavelength (cm^{-1}), same as represented for inkjet printed textiles. The absorbance value represents the intensity of the associated peak due to the bonding vibration of covalent bonds, and the wave number represents the infrared energy absorbed by the bonds during the analysis. Thus, the absorbance intensities of chromojet printed textiles were compared to that of inkjet printed samples with the maximum print pass. Overall, the FMN chromojet printed textile using glycerol-based formulations showed higher absorbance values as compared to water-based formulations. In the case of chromojet printed cotton textile samples (CD and MC), the absorbance intensities did not vary with an increase in FMN concentrations, as shown in Figure 61.

However, in the case of PET printed textile samples, both water-based and glycerol-based prints showed equivalent absorbance values, but the intensities varied slightly for lower FMN concentrations.
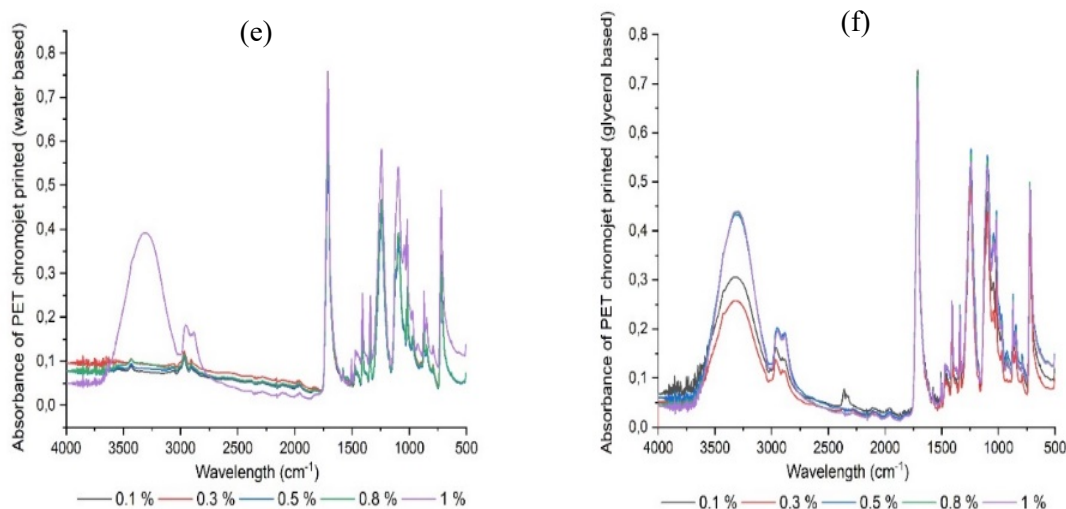
(a)

(b)

(c)

(d)
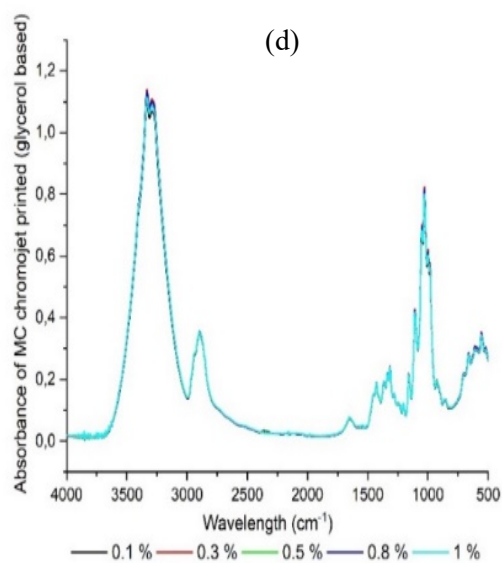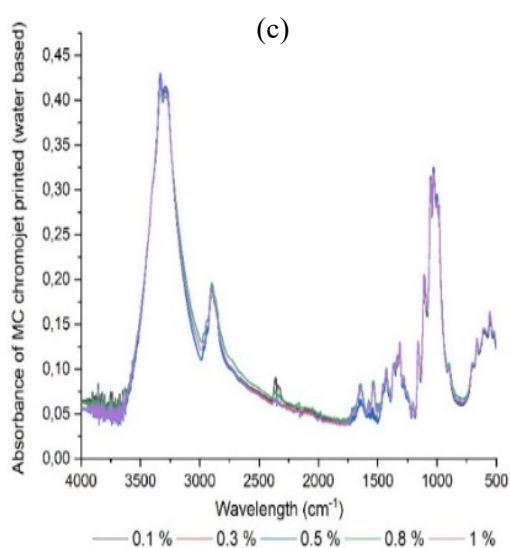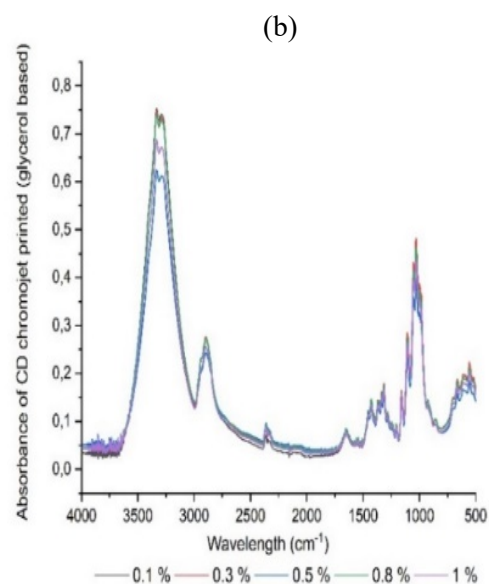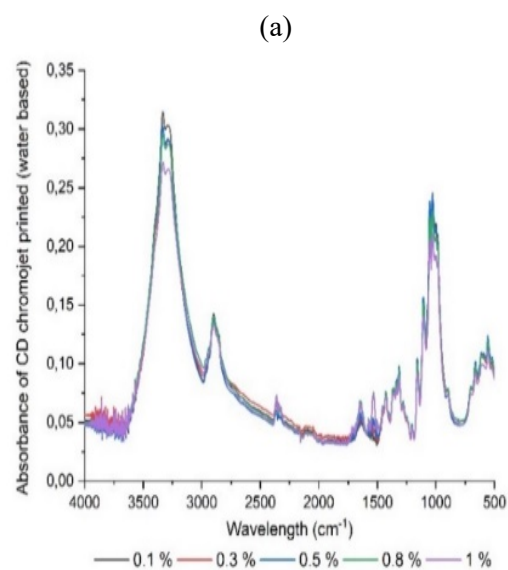
Figure 61. FTIR of chromojet printed textile (a) and (b) CD printed, (c) and (d) MC printed, (e) and (f) PET printed

4.3.3.3 Sample observation under UV chamber

All the chromojet printed samples were observed in a dark chamber using a UV lamp of 370 nm, as described in section 2.5. Table 29 represents the images of the FMN inkjet printed textile samples for the cotton white duck (CD), mercerized cotton (MC), and polyester fabric (PET). Table 30 represents the images of the FMN chromojet printed textile samples with water-based formulations (A to E) and glycerol-based formulations (F to J). Samples before irradiation were observed under normal daylight and UV light. Yellow coloration with varying intensities was observed for all the chromojet printed textile samples under daylight. In contrast, yellow to greenish-yellow fluorescence was observed under UV light for all samples, except at low FMN concentrations of PET (sample A and B).

Table 29. Images of inkjet-printed textile samples under *UV lamp 370 nm, #day light

No. of print pass	CD printed textile	MC printed textile	PET printed textile
Untreated #			
Untreated *			
2 *			
4 *			
6 *			

109
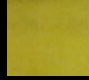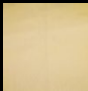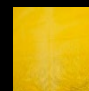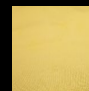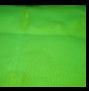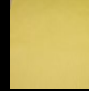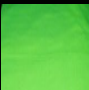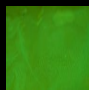
| 8 * | | | |
| 10 * | | | |

Table 30. Images of chromojet printed CD, MC, and PET textile samples under UV lamp 370 nm.

Cotton duck	A	B	C	D	E	F	G	H	I	J
After print under daylight										
After print under UV chamber	524 nm, 4.2*	534 nm, 5.8*	537 nm, 3.7*	537 nm, 5.1*	543 nm, 3.1*	530 nm, 9.4*	531 nm, 6.3*	533 nm, 8.2*	538 nm, 8.3*	537 nm, 7.6*

Merc Cotton	A	B	C	D	E	F	G	H	I	J
After print under daylight										
After print under UV chamber	526 nm, 3.9*	540 nm, 3.2*	547 nm, 2.3*	547 nm, 2.6*	547 nm, 2.1*	529 nm, 9.2*	534 nm, 9.3*	532 nm, 8.5*	536 nm, 10.0*	537 nm, 9.0*

PET	A	B	C	D	E	F	G	H	I	J
After print under daylight										
After print under UV chamber	398 nm, 0.7*	398 nm, 0.4*	566 nm, 0.4*	572 nm, 0.9*	539 nm, 5.6*	566 nm, 0.4*	535 nm, 5.5*	532 nm, 4.4*	536 nm, 6.1*	533 nm, 5.2*

4.3.3.4　　Color strength evaluation

The color strength (K/S) of chromojet printed textile samples are presented in Table 31. An increase in the color strength value was observed with the increase in FMN concentration for both cotton (CD, MC) and polyester (PET) textile samples using water based (A to E) and glycerol based (F to J) formulations.

Table 31. K/S values of CD, MC, and PET chromojet printed textile.

Sample details	K/S of CD at		K/S of MC at		K/S of PET at		Sample details	K/S of CD at		K/S of MC at		K/S of PET at	
	370 nm	450 nm	370 nm	450 nm	360 nm	450 nm		370 nm	450 nm	370 nm	450 nm	360 nm	450 nm
A	0.48	0.35	0.82	0.86	0.97	0.74	F	0.52	0.55	1.03	0.93	1.73	1.69
B	1.44	1.53	2.58	2.91	1.71	1.94	G	0.39	0.36	1.24	1.25	2.10	2.47
C	1.94	2.12	1.88	2.09	1.88	2.11	H	0.79	0.84	1.82	1.97	2.26	2.78
D	2.93	3.05	3.92	4.46	2.88	2.21	I	0.82	0.82	2.86	3.28	2.17	2.56
E	1.99	2.27	6.30	7.75	4.12	5.37	J	0.87	0.85	2.75	3.20	2.53	2.92

Note: The lighter color shades indicate water-based formulations and the darker color shade indicates glycerol-based formulations
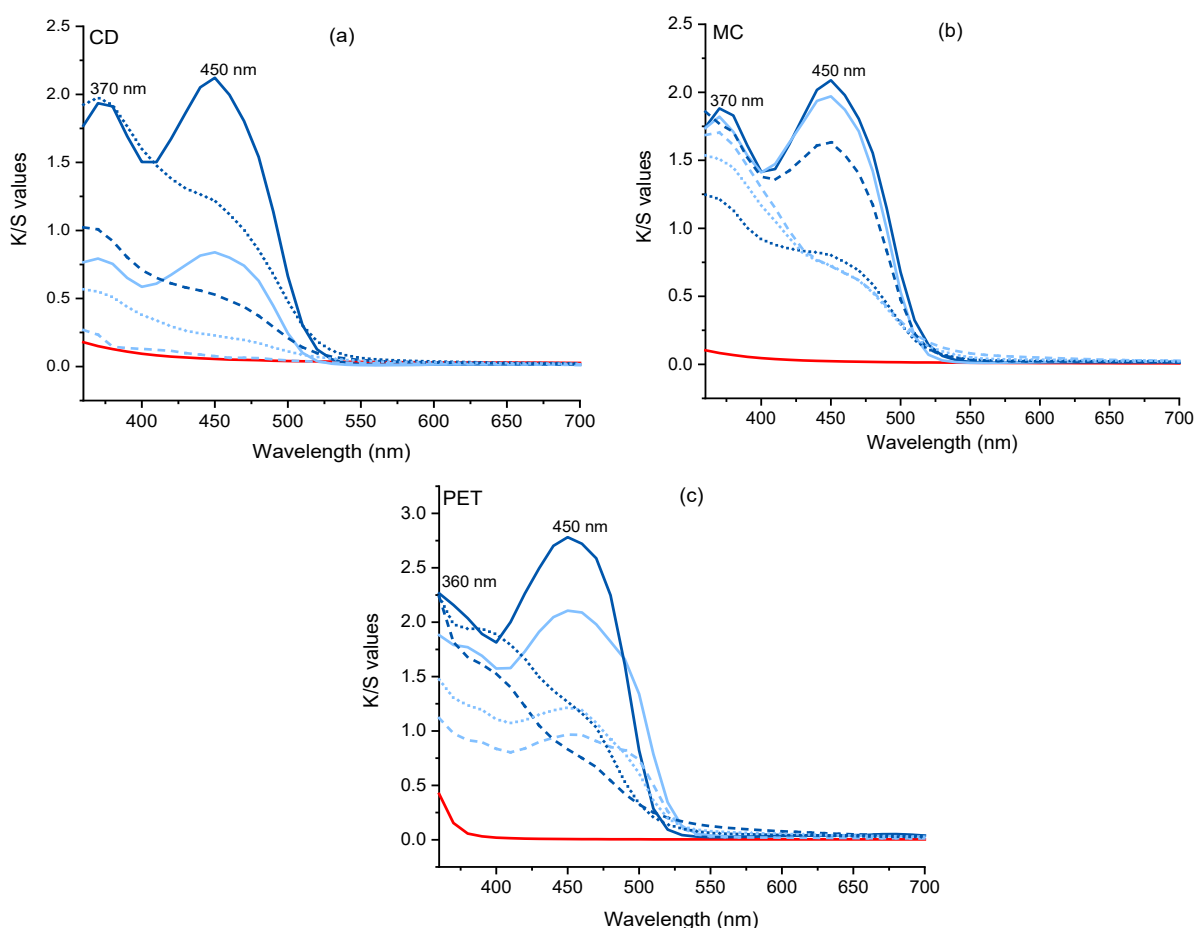
Note: Red line denotes untreated textile, dark blue denotes textile printed with *0.5% FMN water-based and light blue denotes 0.5% FMN glycerol-based*

Figure 62. K/S values before (solid line) and after UVI (dash) VISI light (dots) irradiation for samples, C (0.5% FMN water-based, dark blue curve), H (0.5% FMN glycerol-based, light blue curve) of (a) CD printed, (b) MC printed, (c) PET printed textile samples

Two prominent absorption peaks at 370 and 450 nm were observed for the cotton textiles (CD and MC) printed using both water and glycerol-based formulations before irradiation. Figure 62 represents the color strength value for both cotton textiles (CD and MC) possessing similar values for sample H (glycerol-based) before irradiation. However, a decrease in K/S values at both maxima absorbance of 370 and 450 nm was observed in the case of sample C (water-based) of both cotton textiles (CD and MC). Further, as shown in Table 32, after UV and visible light irradiation on both cotton textiles (CD and MC), overall, a prominent decrease in color strength value at 450 nm was observed for both water and glycerol-based formulations.

The PET printed textile samples showed maximum absorption peaks at 360 and 450 nm before irradiation. However, after UV and visible light irradiation, the PET textile samples using glycerol-based formulation showed a sharp decrease in K/S value at 450 nm. However, PET textile printed using water-based formulation showed absorbance at both 360 and 450 nm even after UV and visible light irradiation, but the K/S values were comparatively lower than that observed before the irradiation of PET textile samples. Although the K/S value for untreated cotton textile (MC) was 0, both cotton (CD) and polyester (PET) untreated textiles possessed minor color strength value at 360 nm.

The color strength (K/S) of chromojet printed textile samples after irradiation for 24 hours under UV light (UVI A to J) and to normal daylight (VISI A to J) are presented in Table 32. Overall, the color strength values were comparatively higher in water-based formulations (A to E) for all textile (CD, MC, PET) samples, as shown in Figure 63. Maximum color strength values were observed for mercerized cotton textile (MC) samples in both water and glycerol-based formulations followed by polyester (PET) and cotton (CD) textile samples. The difference in color strength value between the two different cotton textiles could be due to morphological differences such as round shaped mercerized cotton (MC) fiber cross-section as compared to the bean-shaped cotton duck white (CD), which can allow higher deposition of FMN on MC textile surface [198].

Table 32. K/S values of CD, MC, and PET chromojet printed textile after UV (UVI) and visible light (VISI) irradiation. A to E are water-based formulations, and F to J are glycerol-based formulations

Sample details	K/S of CD at		K/S of MC at		K/S of PET at		Sample details	K/S of CD at		K/S of MC at		K/S of PET at	
	370 nm	450 nm	370 nm	450 nm	360 nm	450 nm		370 nm	450 nm	370 nm	450 nm	360 nm	450 nm
UVI A	0.38	0.19	0.39	0.19	0.65	0.24	UVI F	0.36	0.20	0.37	0.18	1.10	0.22
UVI B	0.49	0.24	2.13	1.24	1.04	0.86	UVI G	0.26	0.15	0.79	0.42	1.91	0.64
UVI C	1.01	0.53	1.77	1.63	1.12	0.97	UVI H	0.23	0.1	1.21	0.80	2.24	0.83
UVI D	2.93	1.96	3.97	2.52	3.03	3.04	UVI I	0.67	0.42	1.95	1.39	2.09	0.67
UVI E	1.64	1.02	7.55	5.59	3.26	2.90	UVI J	0.67	0.40	1.85	1.22	2.19	0.90

VISI A	0.33	0.12	0.54	0.24	0.72	0.34	**VISI F**	0.40	0.16	0.59	0.21	1.52	0.50
VISI B	0.72	0.28	2.41	1.22	1.10	0.99	**VISI G**	0.31	0.12	0.79	0.30	1.96	0.86
VISI C	1.97	1.22	1.70	0.72	1.47	1.21	**VISI H**	0.55	0.23	1.51	0.72	2.23	1.27
VISI D	3.00	2.03	4.09	2.09	2.58	2.23	**VISI I**	0.77	0.36	1.99	0.91	2.11	1.05
VISI E	1.99	1.15	8.25	6.89	2.70	2.98	**VISI J**	0.77	0.34	1.93	0.83	2.28	1.43

Note: The lighter color table background shades correspond to water-based formulations and the darker color shades to glycerol-based formulations.
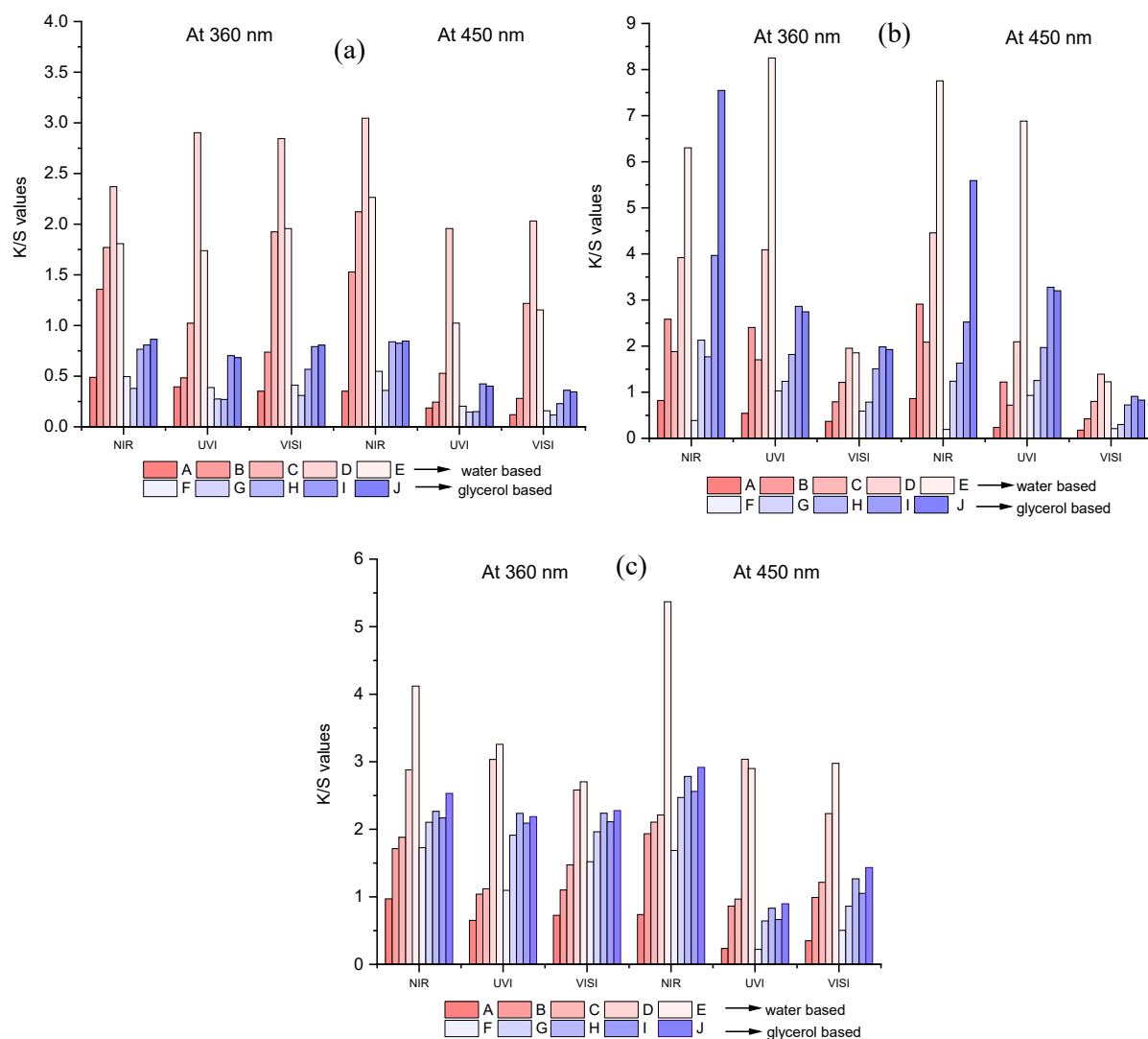
Figure 63. K/S values before and after UV and visible light irradiation for sample C (0.5 % FMN water-based) and H (0.5 % FMN glycerol-based) of (a) CD printed textiles, (b) MC printed textiles, (c) PET printed textiles

4.3.3.5   Fluorolog test

At first, the fluorescence effect in the FMN solution was analyzed to observe the light emission wavelength and their respective intensities at different FMN concentrations using both water-based and glycerol-based

formulations. The fluorescence emission spectra were evaluated at excitation wavelengths of 370 nm over the emission spectra range of 385 – 700 nm. At excitation wavelength of 370 nm, the maximum fluorescence emission wavelength of all printed textiles was observed around 540 nm for both water-based and glycerol-based formulation at all FMN concentrations for samples before irradiation. The fluorescence intensity values varied depending upon the FMN concentration and also the type of solvent used for printing. In the case of water-based formulations, the maximum fluorescence intensity obtained was 3×10^6 CPS / MicroAmps for 0.3 % FMN. This intensity value decreased with an increase in FMN concentration (Figure 64), probably explained by the fluorescence quenching effect. Further, in the case of glycerol-based formulations, the intensity values were higher. However, they did not vary significantly as compared to water-based formulations indicating a lower quenching effect in glycerol: water mixture system.
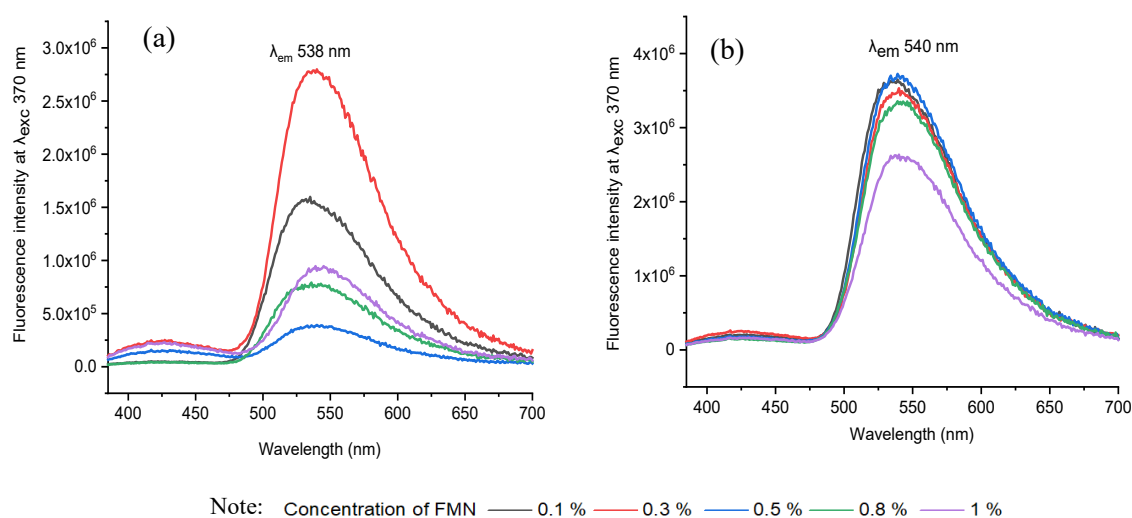
Figure 64. Fluorescence emission spectra of solutions (a) water-based formulation at λex 370 nm (b) glycerol-based formulation at λex 370 nm.

The fluorescence effect of FMN on all chromojet printed textiles (before UV and visible light irradiation) at λexc 370nm was analyzed by evaluating the emission spectra Figure 65. Indeed, without FMN, the untreated cotton (CD, MC) textile samples showed maximum intensity at 435 and 430 nm with intensity values of 1.4×10^6 and 1.2×10^6 CPS / MicroAmps, respectively. The polyester (PET) untreated textile showed a maximum fluorescence emission peak at 397 nm with a shoulder peak observed at 418 nm with similar intensities around 2×10^6 cps/microamps. Under UV light, all the three untreated textiles showed blueish fluorescence, as shown in Table 29. All the chromojet printed textile showed maximum intensity in

the range of 520-570 nm at 370 excitation wavelength (Figure 65 a to c), confirming the FMN fluorescence [199] [178].
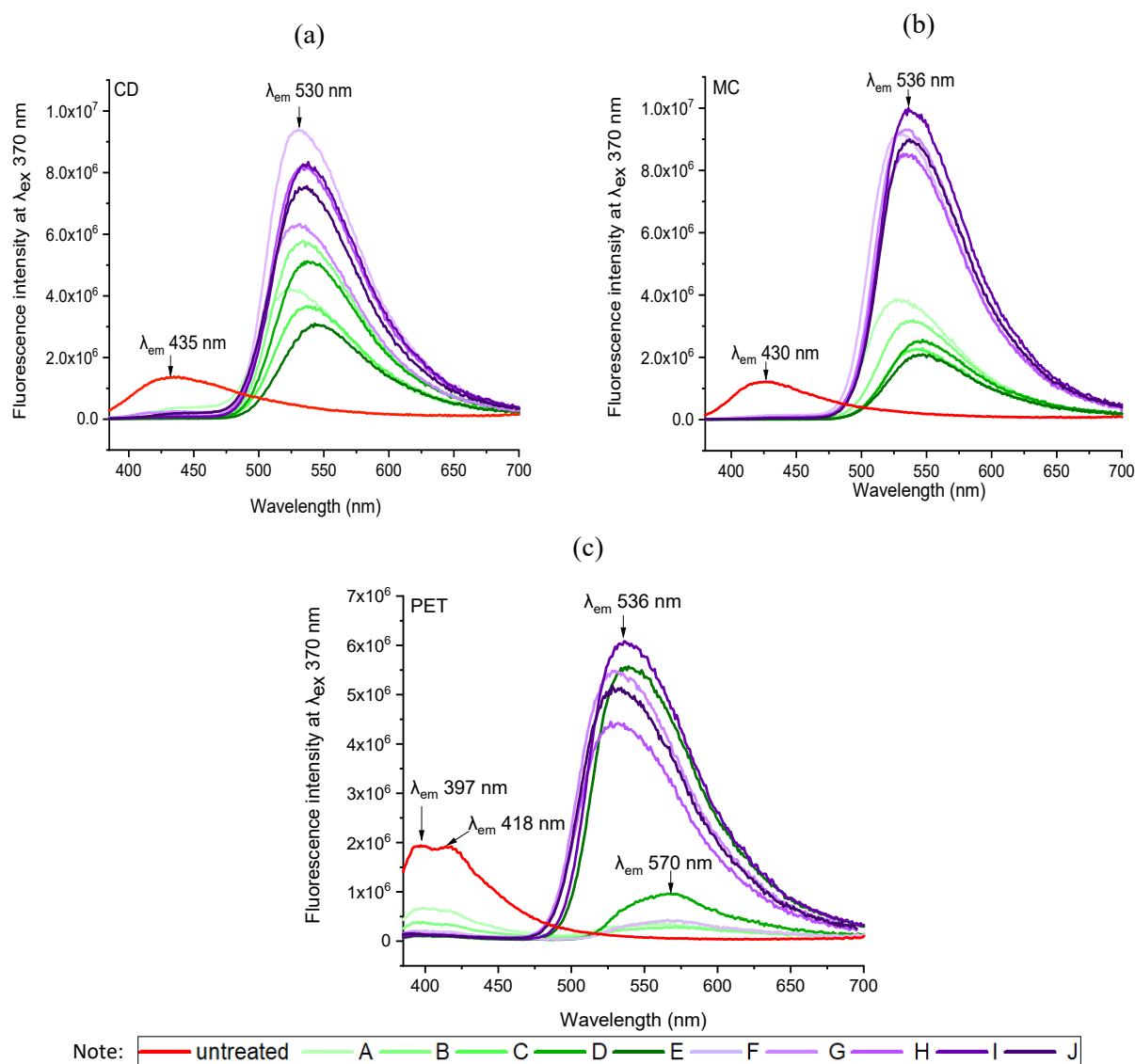
Figure 65. Fluorescence emission spectra of chromojet printed textile samples before irradiation (a) CD printed, (b) MC printed, (c) PET printed at λ_{exc} 370nm wavelength. A to E are water-based formulations, and F to J are glycerol-based formulations

By virtue of inherent fluorescence property of FMN, overall, both the cotton-based textiles (CD and MC) printed using water and glycerol-based formulations displayed greenish-yellow emission in the wavelength range 520 – 550 nm [200][201]. Besides, the maximum fluorescence intensity observed at wavelength range 550-570 nm corresponds to the yellow fluorescence emission region [176]. Both cotton-based textiles (CD and MC) printed using water-based formulations (A-E) showed greenish-yellow fluorescence emission with varying intensity values ranging from 2×10^6 to 6×10^6 CPS / MicroAmps depending upon the concentration. Besides, CD and MC, glycerol-based (F – J) printed textiles also exhibited greenish-yellow fluorescence with intensity values ranging from 6×10^6 to 10×10^6 CPS / MicroAmps. Comparatively,

higher fluorescence intensity values were observed for glycerol-based formulations. However, the intensity values either remained the same or decreased with an increase in concentration for both cotton (CD, MC) water and glycerol-based printed textiles. The tendency of decrease in fluorescence with an increase in FMN concentration was observed in solution as well as in textiles due to the quenching effect seen in FMN [173][172].

Furthermore, the PET printed textiles using water-based formulations showed inherent fluorescence as that of untreated with maximum intensity around 398 nm (samples A, B) along with shoulder peak observed in the range 560 – 570 nm (Figure 65c), which indeed was due to lower amount of FMN deposited on the textile surface. In the case of PET printed textile using water-based formulation (samples C, D, and E), due to the increased FMN concentration, a greenish-yellow to yellow fluorescence emission at a wavelength around 570 nm and 539 nm was observed.

However, when glycerol-based formulations (F to J) were used, the fluorescence intensity value of 0.43×10^6 CPS/MicroAmps was observed for PET textile (sample F) at 566 nm revealing yellow fluorescence emission. Likewise, intensities ranging from 4×10^6 to 6×10^6 CPS / MicroAmps at around 535 nm were observed for PET textiles (samples G – J), thus exhibiting greenish-yellow emission. Hence, the comprehensive quantitative analysis study resembled that of qualitative observations, as shown in Table 30.

4.3.3.6　Degradation property

Both the qualitative and quantitative fluorescence analysis of all the chromojet printed textile samples after UV (UVI), and visible (VISI) light irradiation was evaluated, as shown in Figure 66. Even after 24 h irradiation of UV and visible light, the printed samples showed yellow to blueish-green fluorescence emissions. The intensity values, however, varied depending upon the FMN concentration in the printing formulations and type of irradiation to which the printed samples were subjected.

(a) Water based (A-E) / Glycerol based (F-J)
UVI irradiated CD textile samples

(b) Water based (A-E) / Glycerol based (F-J)
VISI irradiated CD textile samples

(c) Water based (A-E) / Glycerol based (F-J)
UVI irradiated MC textile samples

(d) Water based (A-E) / Glycerol based (F-J)
VISI irradiated MC textile samples
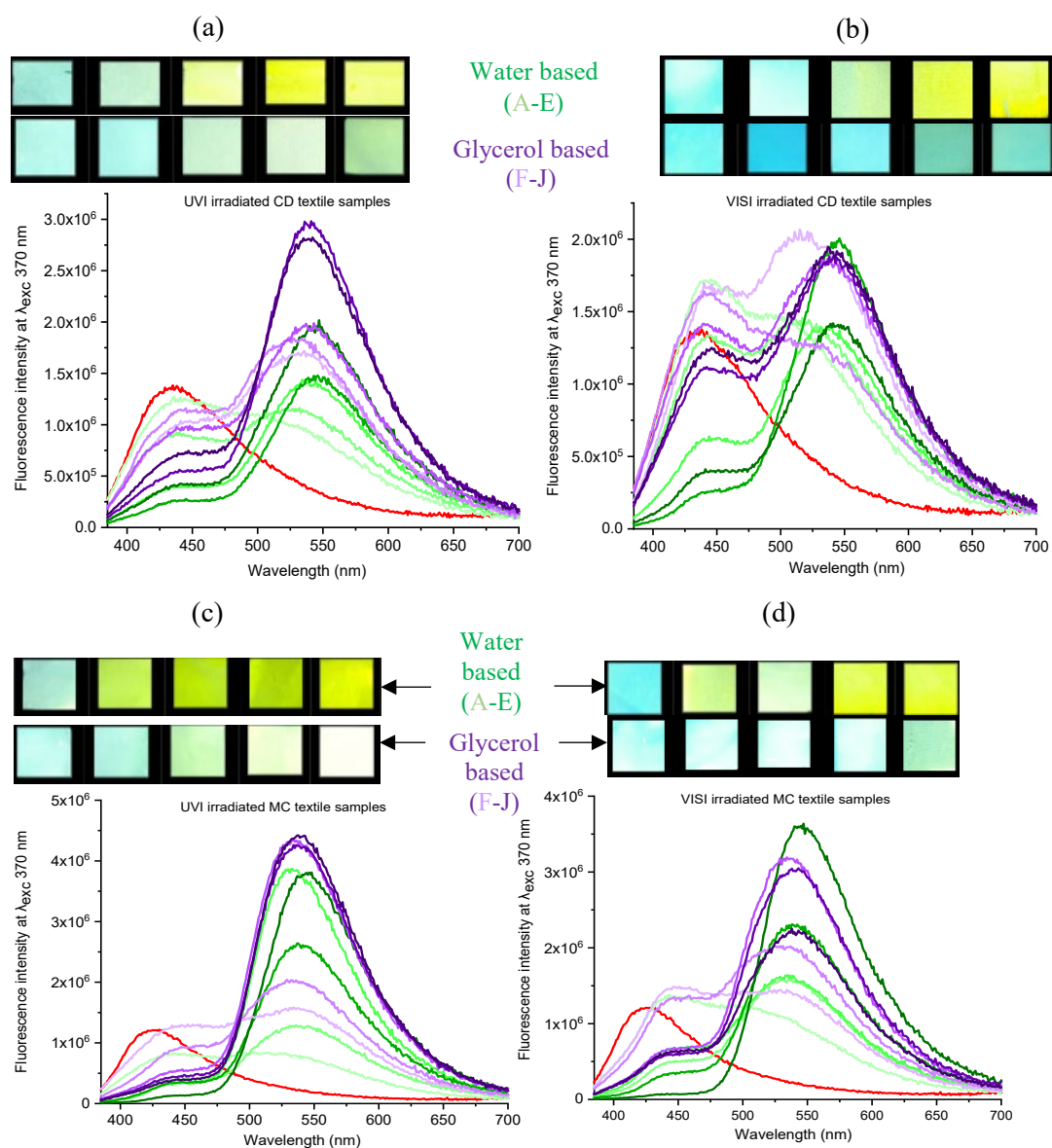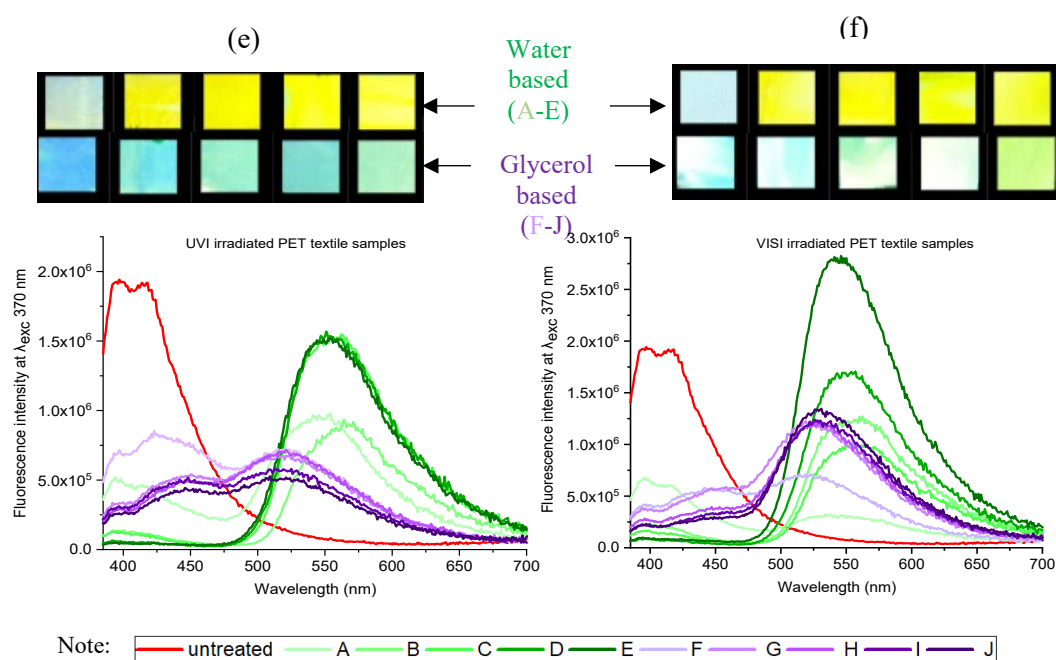
Figure 66. Fluorescence emission spectra of chromojet printed textile sample, (a) and (b) CD printed, (c) and (d) MC printed, (e) and (f) PET printed after UV and visible light irradiation at λ_{exc} 370nm wavelength. A to E are water-based formulations, and F to J are glycerol-based formulations

Majority of all the cotton duck (CD) printed textile samples using both glycerol and water-based formulations possessed maximum fluorescence emission around 530 – 540 nm even after UVI and VISI light irradiation and intensity values ranging from minimum 1×10^6 to maximum 3×10^6 CPS/Microamps. The inherent fluorescence of the cotton duck (CD) textile was also seen at 435 nm. However, the intensity values decreased with an increase in FMN concentration. The CD textile printed using lower FMN concentration (UVI-A) showed relatively high intensity at 435 nm due to inherent blue fluorescence. However, a shoulder peak around 500 nm was also observed, which might be due to a trace amount of surface FMN. A 6-folded decrease in fluorescence intensities at 530 nm was observed for low FMN concentrations (UVI-B, C, D, F, G) and around 3-folded decrease for high FMN concentrations (UVI-E, H, I, J). A similar observation was made for the visible light irradiated printed CD textiles. However, most of the cotton duck textile samples after visible light irradiation exhibited two main fluorescence peaks obtained around 540 nm and 440 nm, respectively, except at higher FMN concentrations (water-based formulations: VISI-C, D, E) the fluorescence intensity around 540 nm was higher possessing yellow fluorescence. Further, for samples (VISI-A, G), the fluorescence intensities at 440 nm were either higher or equivalent to that of the untreated CD along with shoulder peak observed around 500 nm that explains blue fluorescence observed for some samples.

The mercerized cotton (MC) textile samples at higher FMN concentrations (water-based) possessed high fluorescence intensity values ranging from 1×10^6 to maximum 4×10^6 CPS/Microamps around 540 nm

even after UV and visible light irradiation (UVI and VISI- B to E), thus exhibiting greenish-yellow fluorescence. However, at low FMN concentrations (UVI-A and VISI-A), a broad peak with low-intensity values about 0.84 and 1.38 × 10^6 CPS/Microamps were observed at 505 and 443 nm respectively, thus explaining the blue turquoise coloration. At low FMN concentrations (glycerol-based), a broad peak with low fluorescence intensity at 451 nm (VISI F) was observed. At higher FMN concentration, the fluorescence intensity values did not vary significantly for MC textile printed using water-based formulations. However, a 3-folded decrease in intensities was observed in the case of glycerol printed textiles. UV light irradiated PET printed textiles with water-based showed one central fluorescence emission peak around 560 nm exhibiting yellow fluorescence. Except at a low concentration of FMN, the intensity shift of 20 nm was observed, and the fluorescence emission wavelength was observed at 540 nm along with shoulder peak observed around 400 nm for UVI-A sample.

Further, the glycerol-based PET printed textile showed one main peak around 520 nm, with two shoulder peak around 440 nm and 400 nm for almost all UV irradiated samples, except for UVI-F sample (low FMN concentration) showing the main peak at 423 nm along with shoulder peak around 520 nm, thus corresponding to the blue fluorescence observed [202]. The PET printed samples after visible light irradiation (water-based) showed one major absorbance peak around 550-560 nm, except at low FMN concentration (VISI – A), possessing maximum emission at 400 nm. Further, the glycerol-based also showed one major absorbance peak around 525 nm, exhibiting around 10 nm shift in fluorescence emission from 535 nm observed before irradiation. A significant 5-folded decrease in intensities of glycerol-based PET printed textile samples were observed except for low FMN concentration (UVI and VISI-F). However, water-based PET printed textile samples did not show a significant difference in intensity values.

4.3.3.7 Quantum efficiency

Fluorescence quantum efficiency (FQE) of all the chromojet printed textile sample was theoretically evaluated using the extended Kubelka-Munk theory. The quantum efficiency value of flavin mononucleotide varies from 0.20 to 0.32, depending on the solvent that has been studied [203][181][204]. Further, the quantum efficiency values for FMN dyed textile samples using conventional dyeing technique ranging from 0.1 upto 0.3 has been reported in previous studies [169]. Thus, in this study, the FQE values for the chromojet printed samples (water based-A to E and glycerol based-F to J) before and after UV (UVI) and visible light irradiation (VISI) were evaluated at maximum absorbance of 370 and 450 nm for cotton textiles and 360, 450 nm for PET textiles as shown in Table 33.

Table 33. Quantum efficiencies for CD, MC, and PET printed textile sample

| Sample details | Fluorescence quantum efficiency of | | | | | | Sample details | Fluorescence quantum efficiency of | | | | | |
| | CD | | MC | | PET | | | CD | | MC | | PET | |
(water based)	370 nm	450 nm	370 nm	450 nm	360 nm	450 nm	(glycerol based)	370 nm	450 nm	370 nm	450 nm	360 nm	450 nm
A	0.32	0.30	0.19	0.17	0.58	0.38	F	0.27	0.21	0.17	0.17	0.19	0.15
B	0.18	0.16	0.14	0.13	0.49	0.35	G	0.36	0.27	0.17	0.16	0.18	0.14
C	0.16	0.15	0.15	0.14	0.52	0.38	H	0.22	0.19	0.16	0.15	0.18	0.14
D	0.15	0.14	0.13	0.13	0.50	0.37	I	0.21	0.18	0.14	0.13	0.18	0.14
E	0.16	0.15	0.13	0.12	0.20	0.17	J	0.20	0.18	0.14	0.13	0.18	0.15
UVI A	0.64	0.84	0.50	0.66	0.59	0.33	UVI F	0.52	0.57	0.50	0.68	0.43	0.63
UVI B	0.36	0.46	0.17	0.19	0.31	0.19	UVI G	1.03	1.00	0.27	0.33	0.25	0.29
UVI C	0.22	0.27	0.17	0.17	0.27	0.17	UVI H	0.83	0.58	0.20	0.22	0.23	0.27
UVI D	0.16	0.17	0.15	0.16	0.19	0.16	UVI I	0.27	0.29	0.17	0.18	0.25	0.31
UVI E	0.19	0.21	0.14	0.14	0.19	0.17	UVI J	0.27	0.29	0.18	0.19	0.24	0.27
VISI A	0.66	1.24	0.33	0.47	0.78	0.50	VISI F	0.57	0.93	0.28	0.44	0.27	0.31
VISI B	0.27	0.40	0.17	0.20	0.27	0.17	VISI G	0.31	0.45	0.25	0.37	0.24	0.25
VISI C	0.19	0.21	0.19	0.26	0.25	0.19	VISI H	0.25	0.33	0.19	0.24	0.21	0.20
VISI D	0.16	0.17	0.16	0.18	0.19	0.17	VISI I	0.25	0.34	0.18	0.22	0.21	0.21
VISI E	0.17	0.20	0.14	0.15	0.19	0.16	VISI J	0.24	0.22	0.18	0.22	0.21	0.20

Both cotton textiles (CD and MC) showed quantum efficiency values in the range of 0.1 – 0.3 for most of the printed samples (water and glycerol-based) before and after UV and visible light irradiation. However, at a lower concentration of FMN, the efficiency values varied from 0.4 to 1, mainly for irradiated samples (UVI and VISI-A, B, F, G). In the case of PET chromojet printed samples (water based-A to E), higher quantum efficiency values from 0.3 to 0.6 were observed for samples before UV and visible light irradiation, and FQE values of 0.1 to 0.3 were observed after UV and visible light irradiation. With low FMN concentrations (UVI-A and VISI-A), higher quantum efficiency values of 0.3 to 0.7 were obtained.

Besides, the glycerol-based PET printed textiles revealed 0.1 to 0.3 FQE values for almost all samples before and after UV and visible light irradiation, except for the UVI-F sample, which showed higher quantum efficiency value at both absorbance wavelength.

4.3.3.8 Antibacterial effect

The antibacterial finishes are typically applied to textiles to prevent undesirable effects such as the generation of unpleasant odor, discoloration, and contaminations [205]. The antibacterial performances of samples were tested against *E. coli,* according to ASTM 2149, and results are summarized in Table 34. Firstly, FMN powder exhibits good biocidal activity [206], and the same effect can be prominently seen

from the activation zones in Figure 67. However, all untreated samples and FMN printed on PET fabric did not exhibit bacterial inactivation, especially CD and MC wherein they supported the bacterial growth (sample no. 2,3,4 and 7 in Figure 67 b and c). Otherwise, FMN printed on cotton textile E and J samples (sample no. 5 and 6 in Figure 67 b) caused a significant reduction in bacterial growth. It was also found that mercerized textile E and J samples (sample no. 8 and 9 in Figure 67 c) had the maximum antibacterial activity. Overall, the cotton samples MC and CD showed the good antibacterial property. However, the PET chromojet treated samples did not show any antibacterial effect. It can be concluded from these results that FMN could be an effective antibacterial compound in textile treatments.

Table 34. Antibacterial activity of CD, MC, and PET chromojet printed textile samples

| Sample no. | Sample name | 24 hour | |
| | | Antibacterial activity | |
		(%)	log
1	Control	99.1	2.04
2	PET Untreated	-6.45	-0.03
3	PET J	-18.28	-0.07
4	CD Untreated	-30.11	-0.11
5	CD E	92.47	1.12
6	CD J	94.84	1.29
7	MC Untreated	-41.94	-0.15
8	MC E	98.87	1.95
9	MC J	99.94	3.19
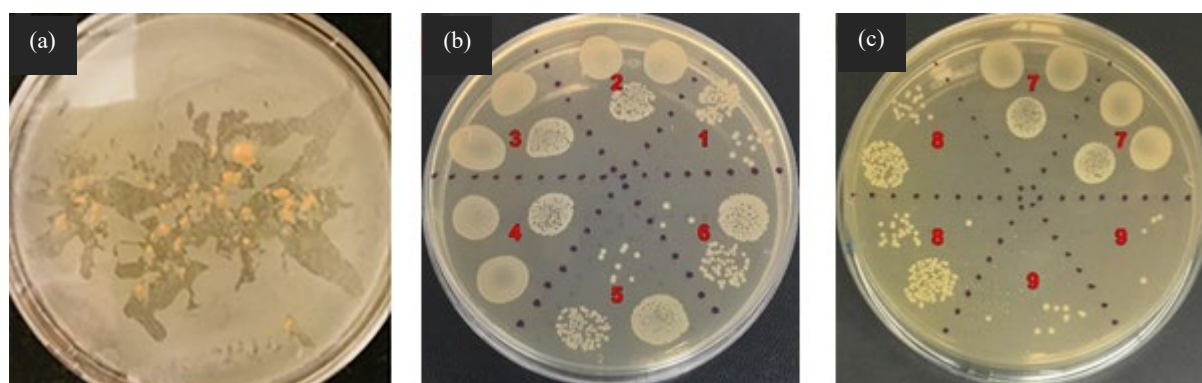
The positive values (%) demonstrate a decrease in bacterial growth, and negative values (%) demonstrate an increase in bacterial growth. The value of (+) 100% indicates that all the bacteria on the surface were killed.* CFU: Colony-forming units.µ

Figure 67. Antibacterial activities against *E. coli* (ATCC 25922) according to ASTM E2149 method for (a) FMN powder (b) chromojet printed textile sample no. 1 to 6 (c) chromojet printed textile sample no.7 to 9.

4.3.3.9   UV protection

In recent days, the demand for textiles with UV protection property is increasing due to the threat caused by ozone layer depletion. The textiles dyed with natural colorants exhibit better UV blocking ability [207][208][209]. The UPF values range from 15 – 24, 25- 35, above 40, can be rated as useful, very good, and excellent UV protection property as per the standard GB/T 18830-2009. In general, UV radiation can be further subdivided into UVA (320-400 nm), UVB (290-320 nm), and UVC (100-290 nm). As shown in Figure 68, improved UPF values were obtained for chromojet printed textile samples.

The untreated CD textile showed UPF mean value of 22. In contrast, CD chromojet printed textile samples A to E (water-based formulation) and F to J (glycerol-based formulation) showed UPF mean value higher than 50 revealing excellent UV protection. Untreated MC textile showed UPF value 8, and an increase in UPF value was obtained for MC samples A to E and F to J, respectively. A maximum UPF value greater than 50 was obtained for MC-D and MC-E samples revealing excellent UV protection. In the case of PET treated samples A to J, the UPF values obtained were higher than 50.

The untreated synthetic PET textile itself showed UPF mean value higher than 50 exhibiting inherent UV protection property. However, the UPF values increased due to the printing of the FMN molecule, which allowed more deposition of FMN on the textile surface. The UV protection value varies due to different conditions such as the physical or chemical type of fiber, textile construction, thickness, and porosity can have different UV protection ability depending on the interaction between the textile material and UV radiation. Exposure to UVA and UVB region is associated with skin-related issues such as aging and cancer. Among all three different types of radiation, UVC is the most dangerous and lethal even in moderate conditions. But, as most of the UVC radiation is filtered by the ozone layer and does not penetrate the surface of the earth, UV protection majorly contributes UVA and UVB region.

The UPF factor increases as a function of % FMN especially for water-based (A to E) printed textile samples. For glycerol-based (F to J) printed textile samples, the increase in FMN showed only a slight increase in UV protection.
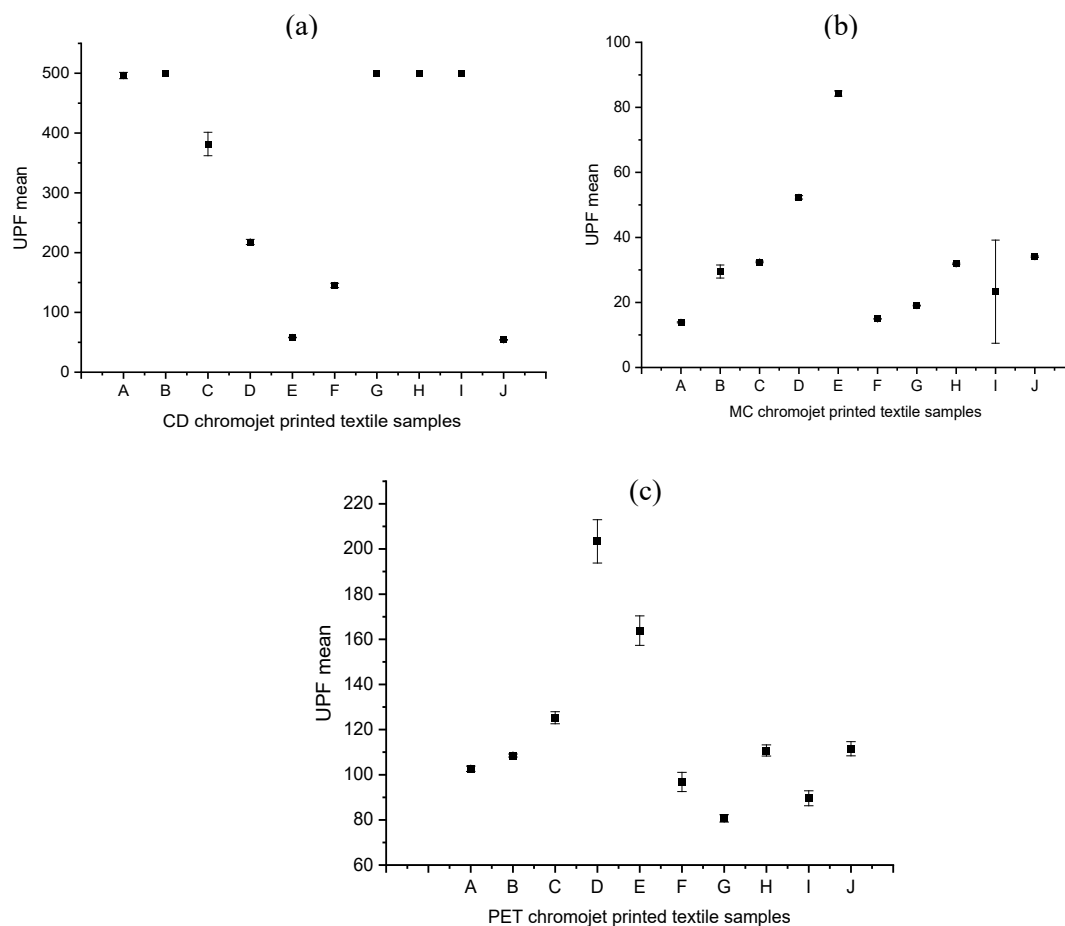
Figure 68. UPF mean values for (a) CD chromojet printed textile, (b) MC chromojet printed textile, (c) PET chromojet printed textile. A to E are water-based formulations, and F to J are glycerol-based formulations.

The study of fabricating photoluminescent textiles using an inkjet printer allowed a higher amount of FMN deposition on the textile/fiber surface with an increase in the number of the print pass from 2 to 10. Hence, appropriate conditions were attained by maintaining and assessing the viscosity of the ink formulation, which allowed printing FMN on both cotton (CD and MC) as well as PET textiles using the inkjet printing technique. Further studies carried using chromojet printing technique was comparatively better as it allowed more surface deposition of the FMN molecule with optimum quantity and a single print, which sufficed due to the large nozzle size. Also, the advantage of the chromojet technology is the possibility of using formulations with a high range of viscosity, surface tension, water-based liquids, pH ranging from 2 to 13, and high quantities of liquids that could be ejected. Particle size can go up to 7 μm, and nozzle diameter range is 120 to 280 μm, hence has broader tolerance of ink viscosity and particle size. The chromojet printing study was done using both water and glycerol-based formulations as the chromojet technique does not possess viscosity restriction for jetting compared to an inkjet printer. Photophysical properties of the ink

molecule and all the treated textile samples were investigated in the wavelength range of λ = 350 to 700 nm using UV-visible, fluorescence, and IR spectroscopy.

The photo, thermal, and chemical degradation properties of both FMN solutions have already been studied in the literature [168] [167]. The UV-visible spectrum of non-irradiated textile samples showed two main peaks 370 nm, 450 nm for cotton printed (CD, MC), and 360, 450 nm for PET printed textiles that can be attributed to the FMN molecule. However, after UV and visible light irradiation, the FMN has undergone photodegradation, and a dominant product, probably lumichrome was formed, showing maximum absorbance around 350 nm [210]. The spectral and the intensity changes indicated that flavin mononucleotide suffers chemical transformations upon UV and visible light irradiation. The isoalloxazine ring of FMN undergoes intramolecular photoreduction wherein the ribityl side-chain serves as the electron donor, and due to oxidation of the side chain, fragmentation may occur, resulting in photoproduct such as lumichrome [211]. The enhancement in the degradation rate of FMN can be a consequence of the reaction of the excited states of FMN subject to interference by molecular oxygen. Thus, loss of the absorption band at 450 nm reflects the formation of lumichrome, a photolysis product formed after UV and visible light irradiation under aerobic conditions.

Furthermore, the fluorescence analysis study of cellulose-based textile after UV and visible light irradiation revealed a spectral peak in the range of 440-460 nm, which is consistent with the work described of lumichrome on cellulose [212]. Also, the shift of fluorescence observed around 520-525 nm for glycerol-based FMN printed PET textile after UV and visible light irradiation can be due to the formation of crystals of lumichrome, which shows fluorescence at 525 nm [166]. In the case of cellulose, the shift of fluorescence towards 525 nm could not be observed due to the probable formation of bonds between lumichrome and cellulose as described in previous work [212], which might not be feasible in the case of PET textile fiber.

The evaluation of color strength values for both cotton (CD, MC) and PET textiles showed an increase in K/S values with an increase in FMN concentrations for both water and glycerol-based formulations at respective maxima absorbance wavelength. FMN printed textiles irradiated under UV light with a lower concentration of FMN exhibited degradation but to a much lesser extent than the visible light irradiated textiles. Overall, the K/S values were highest for mercerized cotton-MC chromojet printed textiles, both with glycerol and water-based formulations followed by polyester-PET and cotton duck white-CD printed textiles.

All treated textiles showed fluorescence emission intensity at around 535 nm as expected for FMN in aqueous solution. The color strength value and the fluorescence intensity varied with an increase in FMN concentration for all chromojet printed textiles. Although the K/S obtained was comparatively low in the glycerol-based formulation, the fluorescence intensity obtained was higher for a glycerol-based formulation, which may be due to FMN being slightly polarized when water is the only solvent. However, the addition

of glycerol suppresses rotational diffusion of the molecule, which, in turn, increases the degree of horizontal polarization and increases the fluorescence intensity [176]. Also, in the case of a glycerol-based solution, the fluorescence intensity was observed to be at a constant level, even at varying concentrations. It must be due to the stability of the formulation attained in the presence of glycerol water mixture, as represented in Figure 64b. Thus, the study reveals the relationship between water-based and glycerol-based formulations used for printing. The results indicated that the FMN dye was adsorbed onto the textile fiber surface through hydrogen bonding and Van der Waals force of attraction. The OH group present in the cotton substrate can with the phosphate group of FMN, as shown in Figure 69.
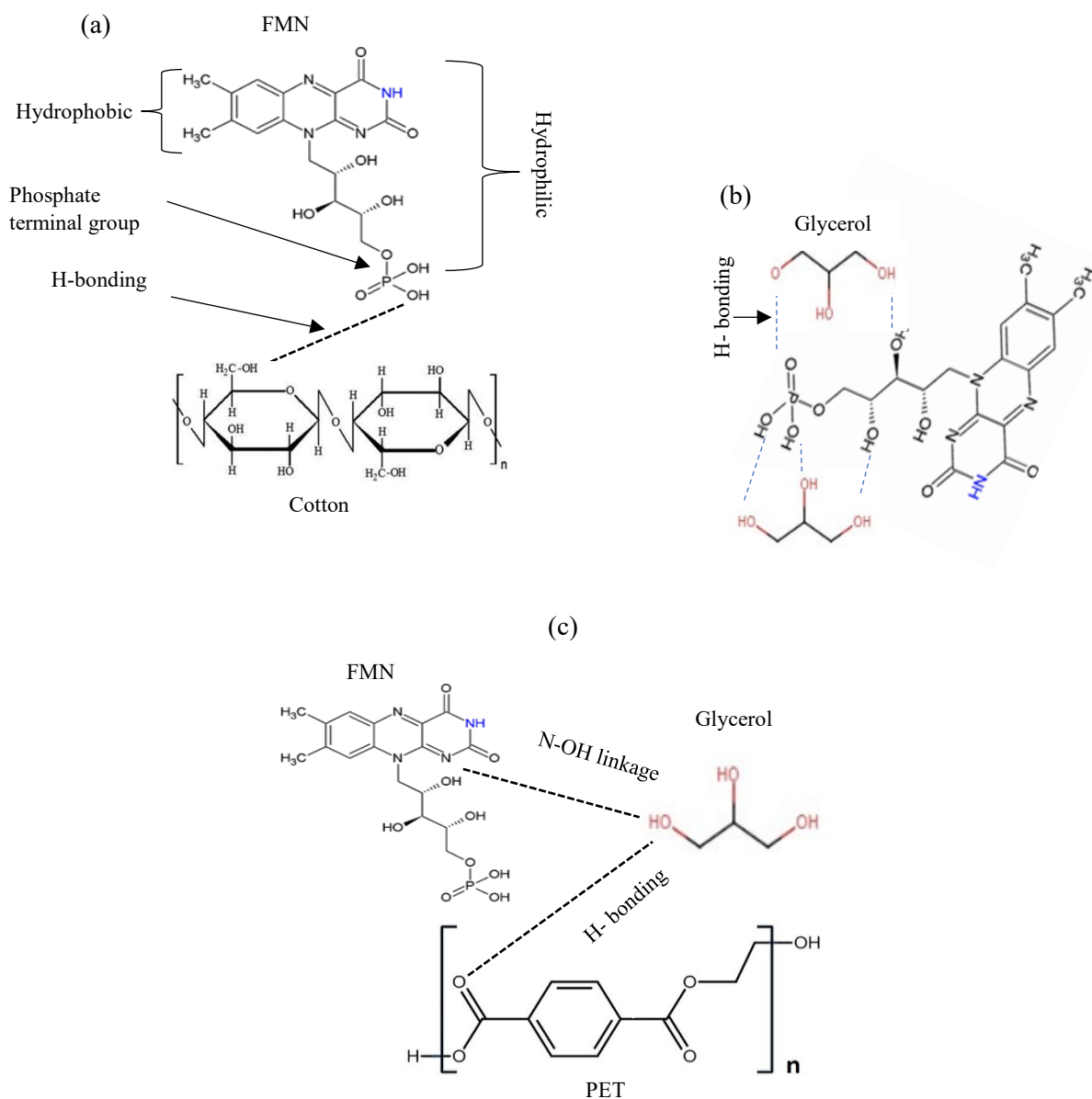
Figure 69. Schematic illustration of the reaction of (a) FMN with the cotton textile surface, (b) FMN with glycerol, (c) FMN with PET textile surface

The absorption and the fluorescence phenomena in aqueous solutions and glycerol-based solutions can be explained through hydrogen bonding and intermolecular interactions of the chromophore dyes. Based on the glycerol interaction study with FMN, the hydrogen bonding seems stronger in the presence of FMN: glycerol system (Figure 69b) than the FMN: water system. The possible N-OH linkage between the –OH of glycerol and the `N´ terminal group of FMN could contribute to a more stable system (Figure 69 c). It further depended upon the textile such as –OH terminal of cotton and C=O of PET can either link with –OH of glycerol and also –OH of the phosphate group in FMN (Figure 69). The fastness properties have to be worked upon, as indicated the FMN molecules are linked through weak hydrogen bonds only. The photodegradation of FMN using different radiation sources also reflects the influence of light intensity (number of quanta s^{-1}) and wavelengths (UV or visible) depending on the photodegradation reactions [213] [214].

The fluorescence intensity data were in agreement with the changes in the fluorescence effect seen visually under the UV chamber. Although specific UV and visible irradiated samples showed low fluorescence intensity, the samples printed using a higher concentration of FMN (0.8 and 1 %) still exhibited fluorescence effect irrespective of prolonged UV and visible light irradiation. The photodegradation property of the riboflavin solution has been studied [213], however in this study we could determine the light intensity effect of FMN on the textile substrate, wherein the range of fluorescence from greenish-yellow to yellow and blue fluorescence [202] as well as white fluorescence [215] could be attained on textiles after UV and visible irradiation. Further, the fluorescence quantum efficiency values also supported the fluorescence effect exhibited by FMN printed textile samples before and after UV and visible light irradiation. Almost all the yellow to greenish-yellow fluorescent textile samples showed FQE values in the range of 0.1 to 0.3. However, higher quantum efficiency values in the range of 0.4 to 1 were observed for blue to white fluorescent samples [215]. In addition, the antibacterial property was observed mainly for cotton textiles (CD, MC) and not polyester-based (PET) textile samples which may be due to the nature of the fiber, as synthetic fiber tend to retain more bacteria compared to natural fibers as it has poor adsorbing properties [216].

4.3.4. Conclusion

Photoluminescent material has gained much attention due to broad application fields, such as biosensors. Various biobased materials are exhibiting photophysical properties due to the presence of conjugated chains serving as light-emitting units, and flavin mononucleotide is one such interesting biobased molecule. It has wide applications in medical, health, and other fields. In this study, by maintaining the appropriate conditions for inkjet printing, photoluminescent textiles were obtained using an inkjet printer. Further, chromojet printing was used to enhance the multifunctional properties of the FMN molecule.

In addition, after irradiation of the FMN printed textiles by UV and visible light for prolonged hours, shifts in fluorescence wavelength(s) were observed. In combination with FMN and lumichrome, a different color variation on textiles was observed, depending upon the irradiation and shift in fluorescence from green, yellow, turquoise to white. These combinations of intensities of blue and yellow variety of colored fluorescence could be interesting for certain smart textile applications, artistic perspectives related to scientific data [217]. Globally, polyester (PET) and cotton are the most widely used textiles [135] due to major industrial applications based upon them. Hence, the photoluminescent effect was studied on both cotton and polyester textile material. All textile samples CD, MC, and PET showed greenish-yellow fluorescence at emission wavelength in the range of 520-550 nm after print. The textile industries today are pursuing the development of digital printing technology to make changes from the conventional techniques which consume large quantities of water and energy. Digital printing processes are efficient due to less energy consumption and can bridge design as well as technology.

Further, the use of the printing technique allowed the deposition of FMN molecule in a sufficient amount on the textile fiber surface, which enabled to impart of multifunctional properties such as antibacterial and UV protection along with photoluminescent effect. Further, the use of biomordants as studied in the diffusion technique can improve the wash fastness of photoluminescent textiles. Also, crosslinking with acrylate and biopolymer coating and printing on PET could be an alternative for improvement of washfastness and its use in other application sectors.

CHAPTER 5: GENERAL CONCLUSION AND FUTURE STUDIES

5.1. General conclusion

This thesis aimed to establish luminescent textiles using a bio-inspired approach. Riboflavin and flavin mononucleotide is biobased molecules, naturally occurring in a variety of animals and plants. Both molecules possess photoluminescence property and, in the presence of an enzyme(s), exhibits bioluminescence property seen in nature. The luminescence characteristics of biobased RF and FMN allowed its potential application in textiles. Therefore, this Ph.D. work aimed to investigate the potential use of biobased FMN for the development of luminescent textiles. A 100% PET nonwoven was used as a textile substrate for the development of bioluminescent textiles. Furthermore, different textile materials such as cellulose, PET, silk, and wool were explored to investigate the fluorescence property of FMN to obtain photoluminescent textiles.

This thesis has two main parts: development of biomimetic/bio luminescent textiles using bioluminescence reaction system and functionalization. The second part was to study the potential of RF and FMN as photoluminescent multifunctional textiles. The development of photoluminescent textiles has three subparts, wherein the photoluminescent behavior has been studied using conventional dyeing techniques, digital printing, and coating techniques, respectively.

Figure 70 summarizes the main finding of the thesis. The study revealed the functionalization of the luminous bacteria reaction system on textiles, which has not been studied until now on textiles. Furthermore, the inherent fluorescence property of riboflavin and flavin mononucleotide were studied on textiles for the first time for the development of photoluminescent multifunctional textiles. The study was performed using both conventional and eco-technologies.

In Chapter 1, the brief overview of luminescence, classification, and the selection of the bioluminescent reaction system to be incorporated on textiles for the thesis research study was highlighted.

Further, to acquire luminescent textiles based on bioinspired strategy, it was necessary to review different functionalization and ecotechnological methods to implement the same. The materials and the detailed methods, equipment, and respective protocols used for obtaining the biobased photoluminescent and bioluminescent textiles, respectively, were described in Chapter 2.

Chapter 3 revealed the analyses results of bioinspired strategy to obtain biomimetic or bioluminescent textiles. The chosen enzymatic bioluminescent reaction system was studied on nonwoven PET textiles to investigate the luminescence attained onto textiles. Cold remote plasma treatment with a mixture of N_2 and O_2 gases and air atmospheric plasma treatment was used to modify the textile surfaces without any additional chemical crosslinker. The plasma treatment process was completed within a confined and short time. The Luc and FMN reductase enzyme(s) involved in the bioluminescent bacterial system was efficiently

immobilized on the nonwoven PET textile surface resulting in luminescence intensity as high as that of LED standard luminescence plate.

Chapter 4 included the results obtained from three specified approaches on different textile substrate materials to investigate and optimize the use of RF and FMN as a fluorescent dye to obtain photoluminescent textiles.

At first, the potential use of RF and FMN as a fluorescent dye on cellulosic fabrics was explored using the conventional diffusion technique. The use of biomordants can improve the wash fastness of photoluminescent textiles. The study allowed to obtain photoluminescent cellulosic textiles along with additional functional property such as UV protection. The RF and FMN also possessed inherent antibacterial property. However, the dyed fabric did not exhibit the antibacterial effect, which may be due to insufficient surface molecule onto textiles to inhibit the growth of bacteria. Hence, to incorporate a higher amount of FMN molecules on the textile surface, digital printing techniques such as inkjet and chromojet were used, which allowed more surface deposition of the molecule. Thus in the second part of the study, along with the investigation of fluorescence property for the printed textile, the other important study was done by analyzing the photodegradation property of the FMN printed textile surface. In addition to the inherent greenish-yellow fluorescence, the investigation allowed facile development of blue to white fluorescence on FMN printed textiles upon prolonged irradiation of UV and visible light.

Moreover, the surface deposition of molecules attributed to the antibacterial property of FMN printed cellulosic textiles in addition to the UV protection and coloration properties. Moreover, silk and wool fabrics were also treated with RF and FMN using diffusion techniques. Both silk and wool possessed enhanced coloration and photoluminescence properties; however, the photoluminescence was better for silk dyed fabric even after wash. The third part of the photoluminescent textile study was to create a glow in the dark patterned on nonwoven PET textile. PET being hydrophobic, plasma treatment was used to make it hydrophilic. The photoluminescence and color strength variation was observed for PET nonwoven before and after plasma treatment. Methods such as coating and screen printing were used to incorporate FMN in the presence of a gelatin biopolymer. Overall, the study revealed different methods to obtain PET photoluminescent textiles along with different designs and patterns that can be used for aesthetic purposes.
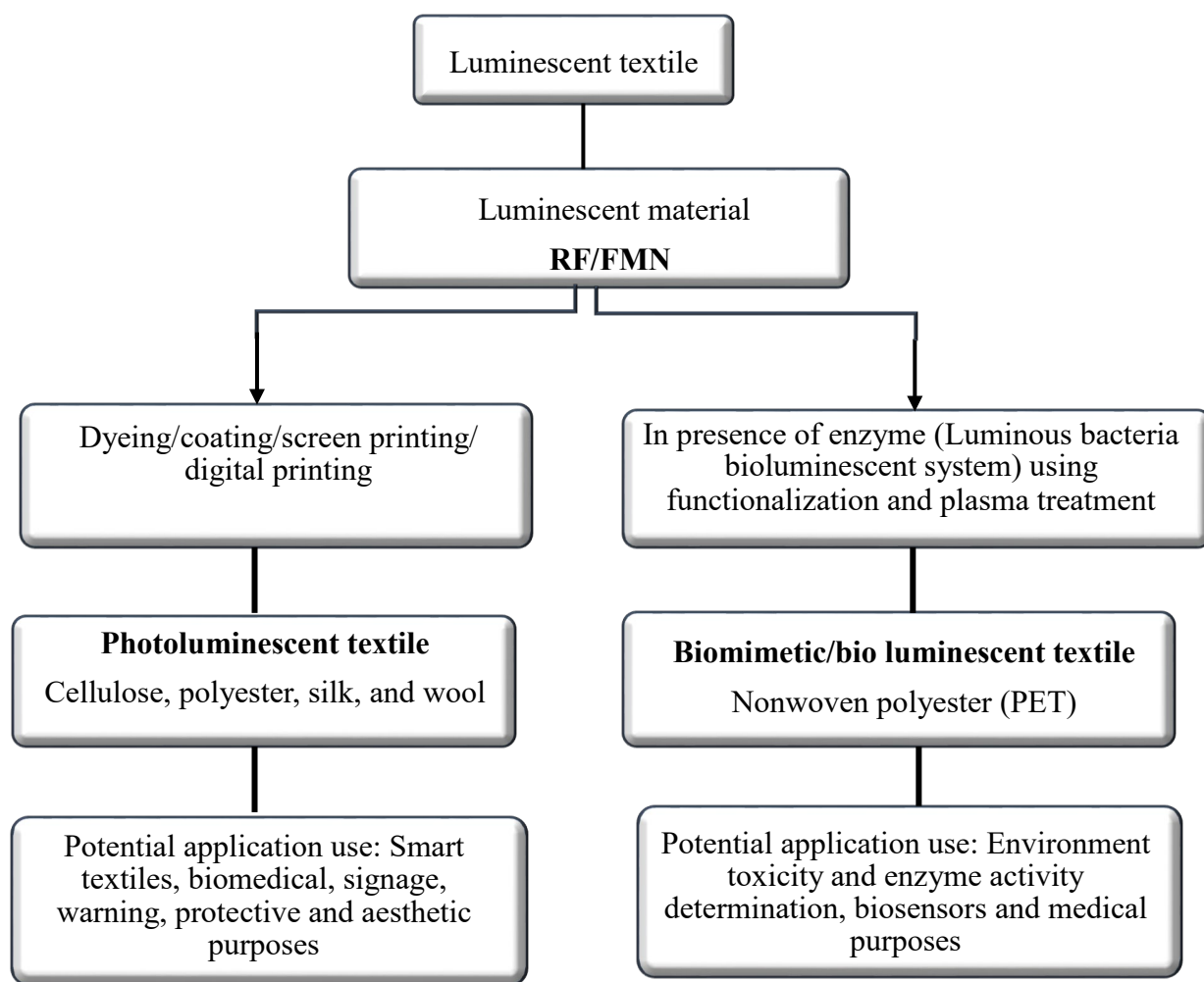
Figure 70: Summary of research and contributions

5.2. Key Contributions and Highlights

Combining the ability to design bioinspired molecules from nature's ingenious paths to produce luminescent textiles with emergent luminescent properties and being able to obtain multifunctional properties are the main highlight of the thesis. The proof-of-concept was demonstrated for the fabrication of biomimetic/bio luminescent textiles using immobilization and functionalization of the enzyme(s) and substrate molecules. The significant advantage of using a bioluminescent system is their high specificity to emit light at their characteristic wavelength without the requirement of any bulky excitation source. Luminescence on textiles is gaining research interest with its broad scope of applications in various sectors, such as biomedical. These new concepts and bioinspired strategies could be an added value for future development and practical contribution in different fields. The first attempt of bioluminescent reaction study onto textiles was reported in this thesis, which is usually studied in immobilized glass rods or within biopolymer or hydrogel state. The study enabled the provision of different types of luminescence on textiles, biomimetic/bio luminescent,

131

and photoluminescent based textiles. Moreover, sustainable methodologies for fabricating luminescent textiles are reported.

5.3. Future studies

Although exploration of luminescent textiles using the luminous bacteria reaction system and biobased resource RF and FMN have been studied in this thesis, several aspects need to be investigated further to improve the luminescent properties for its use in various application fields such as smart textiles, biomedical, biosensors, aesthetic and safety. Both of the attempts to develop biomimetic/bio luminescent and photoluminescent textiles using the proposed system being first of its attempt in this thesis provides a wide scope of future research studies. The outcome of the thesis motivates further to conduct future research activities, and specific aspects of future research interest are elaborated below.

Biomimetic/bio luminescent textiles

- ❖ Further research work is required to stabilize the system and optimize the luminescence in the presence of specified enzyme concentration with an excess substrate concentration of luminous bacteria system, along with more efficient enzyme adsorption for its continuous reaction mechanism process.
- ❖ Previous research work done to immobilize specific enzymes on textiles with the use of a biobased crosslinker 'genipin' [218] motivates its use for immobilization of luminous bacteria system. Genipin, which is a naturally occurring crosslinking agent, could be beneficial due to its low toxicity.
- ❖ Most of the enzymes that are proteins are all water-soluble, enzyme immobilization required to facilitate enzyme recovery. Reuse of support needs to be a key focus and can be a promising material for various biomedical applications.
- ❖ Durability and washability should be further studied depending upon various applications.

Photoluminescent textiles

- ❖ The use of a crosslinking method to functionalize textile material with the biobased flavin molecules RF and FMN could enhance the photoluminescence property.
- ❖ Improved durability and wash fastness studies need to be carried
- ❖ The different photoluminescent effects and persistence of yellow-green, white, and blue fluorescence can be focused in future studies.
- ❖ Correlation between the coloration and photoluminescence effect by focusing on stabilizers, quenchers, and the effect of the solvent of the biobased flavin formulation onto textiles could be studied.

References

[1] L. Eadie and T. K. Ghosh, "Biomimicry in textiles: Past, present and potential. An overview," *J. R. Soc. Interface*, vol. 8, no. 59, pp. 761–775, 2011.

[2] J. F. V. Vincent, "Biomimetics - A review," *Proc. Inst. Mech. Eng. Part H J. Eng. Med.*, vol. 223, no. 8, pp. 919–939, 2009.

[3] O. Speck, D. Speck, R. Horn, J. Gantner, and K. P. Sedlbauer, "Biomimetic bio-inspired biomorph sustainable? An attempt to classify and clarify biology-derived technical developments," *Bioinspiration and Biomimetics*, vol. 12, no. 1, 2017.

[4] N. F. Lepora, P. Verschure, and T. J. Prescott, "The state of the art in biomimetics," *Bioinspiration and Biomimetics*, vol. 8, no. 1, 2013.

[5] D. U. Weerasinghe, S. Perera, and D. G. K. Dissanayake, "Application of biomimicry for sustainable functionalization of textiles: review of current status and prospectus," *Text. Res. J.*, vol. 89, no. 19–20, pp. 4282–4294, 2019.

[6] Y. Liu *et al.*, "Artificial lotus leaf structures from assembling carbon nanotubes and their applications in hydrophobic textiles," *J. Mater. Chem.*, vol. 17, no. 11, pp. 1071–1078, 2007.

[7] S. Das, M. Bhowmick, S. K. Chattopadhyay, and S. Basak, "Application of biomimicry in textiles," *Curr. Sci.*, vol. 109, no. 5, pp. 893–901, 2015.

[8] A. V. Singh *et al.*, "Bio-inspired approaches to design smart fabrics," *Mater. Des.*, 2012.

[9] I *et al.*, "We are IntechOpen , the world ' s leading publisher of Open Access books Built by scientists , for scientists TOP 1 %," *Intech*, vol. i, no. tourism, p. 13, 2012.

[10] S. U. Patwary, K. Farhana, and S. Ahmed, "Smart Textiles and Nano-Technology : A General Overview Textile Science & Engineering Smart Textiles and Nano-Technology : A General Overview," no. February, 2015.

[11] U. Möhring, S. Gimpel, A. Neudeck, W. Scheibner, and D. Zschenderlein, "Conductive, sensorial and luminescent features in textile structures," *Appl. Wearable Comput. (IFAWC), 3rd Int. Forum*, no. January, pp. 1–6, 2006.

[12] M. Kooroshnia, "Designing a two-phase glow-in-the-dark pattern on textiles," *Shapeshifting A Conf. Transform. Paradig. Fash. Text. Des.*, no. April, pp. 1–16, 2014.

[13] A. Büsgen, "New product development in interior textiles," 2012.

[14] M. Yan *et al.*, "Biofabrication Strategy for Functional Fabrics," *NANO Lett.*, vol. 18, no. 9, pp. 6017–6021, Sep. 2018.

[15] X. Guo, K. Zhang, H. Zhang, and M. Ge, "Working Conditions on the Afterglow Characteristics of Rare-earth Luminous Fibers," *FIBERS Polym.*, vol. 19, no. 3, pp. 531–537, Mar. 2018.

[16] K. Baatout *et al.*, "Luminescent cotton fibers coated with fluorescein dye for anti-counterfeiting applications," *Mater. Chem. Phys.*, vol. 234, no. June, pp. 304–310, 2019.

[17] M. Van Parys, "Development and Research of Smart Functional Clothing Textiles," p. 9.

[18] T. A. Khattab, M. Rehan, and T. Hamouda, "Smart textile framework: Photochromic and fluorescent cellulosic fabric printed by strontium aluminate pigment," *Carbohydr. Polym.*, vol. 195, no. November 2017, pp. 143–152, 2018.

[19] "No Title." [Online]. Available: https://en.wikipedia.org/wiki/File:Luminol2006.jpg.

[20] "No Title." [Online]. Available: https://en.wikipedia.org/wiki/File:Fluorescence_rainbow.JPG#filelinks.

[21]   "No Title." [Online]. Available: https://www.dreamstime.com/photos-images/electroluminescence.html.

[22]   Https://wonderfulengineering.com/how-firefly-light-butt/, "firefly." .

[23]   K. Nealson, W. Hastings, and J. W. Hastings, "Yearly review bioluminescence and chemiluminescence," vol. 23, pp. 461–473, 1976.

[24]   M. I. Latz, "The artistry of dinoflagellate bioluminescence," *Mater. Today Proc.*, vol. 4, no. 4, pp. 4959–4968, 2017.

[25]   S. Sharifian, A. Homaei, R. Hemmati, and K. Khajeh, "Light emission miracle in the sea and preeminent applications of bioluminescence in recent new biotechnology," *J. Photochem. Photobiol. B Biol.*, vol. 172, 2017.

[26]   M. Yusuf, M. Shabbir, and F. Mohammad, "Natural Colorants: Historical, Processing and Sustainable Prospects," *Nat. Products Bioprospect.*, vol. 7, no. 1, pp. 123–145, 2017.

[27]   S. Martini and S. H. D. Haddock, "Quantification of bioluminescence from the surface to the deep sea demonstrates its predominance as an ecological trait," *Sci. Rep.*, vol. 7, no. April, pp. 1–11, 2017.

[28]   T. Nakatsu *et al.*, "Structural basis for the spectral difference in luciferase bioluminescence," *Nature*, vol. 440, no. 7082, pp. 372–376, 2006.

[29]   J. Lee, "Bioluminescence: the First 3000 Years (Review)," *J. Sib. Fed. Univ. Biol.*, vol. 1, no. 3, pp. 194–205, 2008.

[30]   R. Capelletti, "Luminescence."

[31]   A. Fleiss and K. S. Sarkisyan, "A brief review of bioluminescent systems (2019)," *Curr. Genet.*, vol. 65, no. 4, pp. 877–882, 2019.

[32]   J. W. Eckstein, J. W. Hastings, and S. Ghisla, "Mechanism of Bacterial Bioluminescence: 4a,5-Dihydroflavin Analogs as Models for Luciferase Hydroperoxide Intermediates and the Effect of Substituents at the 8-Position of Flavin on Luciferase Kinetics," *Biochemistry*, vol. 32, no. 2, pp. 404–411, 1993.

[33]   K. V. Purtov *et al.*, "The Chemical Basis of Fungal Bioluminescence," *Angew. Chemie - Int. Ed.*, vol. 54, no. 28, 2015.

[34]   Y. Ohmiya and T. Hirano, "Shining the light: the mechanism of the bioluminescence reaction of calcium-binding photoproteins."

[35]   M. Vacher *et al.*, "Chemi- and Bioluminescence of Cyclic Peroxides," *Chem. Rev.*, vol. 118, no. 15, pp. 6927–6974, 2018.

[36]   N. V. Belogurova, N. S. Kudryasheva, R. R. Alieva, and A. G. Sizykh, "Spectral components of bioluminescence of aequorin and obelin," *J. Photochem. Photobiol. B Biol.*, 2008.

[37]   S. Medvedeva, "3 Bacterial bioluminescence and its application," no. January 2009, 2014.

[38]   S. Sharifian, A. Homaei, R. Hemmati, R. B. Luwor, and K. Khajeh, "The emerging use of bioluminescence in medical research," *Biomed. Pharmacother.*, vol. 101, no. March, pp. 74–86, 2018.

[39]   G. S. Erzinger *et al.*, "Bioluminescence systems in environmental biosensors," *Bioassays Adv. Methods Appl.*, pp. 242–262, 2017.

[40]   E. A. Widder and B. Falls, "Review of bioluminescence for engineers and scientists in biophotonics," *IEEE J. Sel. Top. Quantum Electron.*, vol. 20, no. 2, 2014.

[41] J. Lee, C. L. Murphy, G. J. Faini, and T. L. Baucom, "BACTERIAL BIOLUMINESCENCE AND ITS APPLICATION TO ANALYTICAL PROCEDURES."

[42] A. Roda, M. Guardigli, E. Michelini, and M. Mirasoli, "Bioluminescence in analytical chemistry and in vivo imaging," *TrAC - Trends Anal. Chem.*, vol. 28, no. 3, pp. 307–322, 2009.

[43] H. Karatani and T. Konaka, "In vitro bacterial bioluminescence coupled with a mediated electrochemical process of flavin on a viologen polymer electrode," *Bioelectrochemistry Bioenerg.*, 1998.

[44] R. Chen and D. J. Lockwood, "Developments in Luminescence and Display Materials Over the Last 100 Years as Reflected in Electrochemical Society Publications," *J. Electrochem. Soc.*, vol. 149, no. 9, p. S69, 2002.

[45] A. Karabchevsky, A. Mosayyebi, and A. V Kavokin, "Tuning the chemiluminescence of a luminol flow using plasmonic nanoparticles," *Light Sci. Appl.*, vol. 5, no. 11, pp. e16164–e16164, 2016.

[46] L. Yang *et al.*, "Study on enhancement principle and stabilization for the luminol-H2O2-HRP chemiluminescence system," *PLoS One*, vol. 10, no. 7, pp. 1–14, 2015.

[47] Dr. Thomas G. Chasteen, "Jablonski diagram." [Online]. Available: https://www.tissuegroup.chem.vt.edu/chem-ed/quantum/jablonsk.html.

[48] J. R. Lakowicz and B. R. Masters, "Principles of Fluorescence Spectroscopy, Third Edition," *J. Biomed. Opt.*, vol. 13, no. 2, p. 029901, 2008.

[49] I. B. Cohen, "A History of Luminescence From the Earliest Times Until 1900. By E. Newton Harvey. [Memoirs of the American Philosophical Society, Volume 44]. (Philadelphia: the Society. 1957. Pp. xxiv, 692. \\$6.00.)," *Am. Hist. Rev.*, vol. 63, no. 4, pp. 937–939, 1958.

[50] 2011 Karl-Dietrich Gundermann, "Early investigations Phosphorescence and uorescence Luminescence excitation Chemiluminescence and bioluminescence," *Encyclopædia Britannica*. Encyclopædia Britannica, inc., pp. 2–9.

[51] I. Obodovskiy, "Chapter 12 - Luminescence," in *Radiation*, I. Obodovskiy, Ed. Elsevier, 2019, pp. 207–220.

[52] D. H. Sliney, "What is light? the visible spectrum and beyond," *Eye*, vol. 30, no. 2, pp. 222–229, 2016.

[53] O. Shimomura, *Bioluminescence*, Revised. WORLD SCIENTIFIC, 2012.

[54] W. W. C. Topley, "Luminescent materials history," *Nature*, vol. 148, no. 3743, p. 118, 1941.

[55] A. Edgar, "Springer Handbook of Electronic and Photonic Materials," *Springer Handb. Electron. Photonic Mater.*, pp. 997–1012, 2017.

[56] G. H. Dieke, 1901-1965, H. M. Crosswhite, 1919-, and H. Crosswhite, "Spectra and energy levels of rare earth ions in crystals." Interscience.

[57] C. Ronda, "Challenges in application of luminescent materials, a tutorial overview," *Prog. Electromagn. Res.*, vol. 147, no. May, pp. 81–93, 2014.

[58] C. Samuel, V. Vakunseh, and D. S. Masson-meyers, "Since January 2020 Elsevier has created a COVID-19 resource centre with free information in English and Mandarin on the novel coronavirus COVID- 19 . The COVID-19 resource centre is hosted on Elsevier Connect , the company ' s public news and information ," no. January, 2020.

[59] A. J. Lees, "Luminescence Properties of Organometallic Complexes," *Chem. Rev.*, vol. 87, no. 4, pp. 711–743, 1987.

[60] R. Dcd, "Chapter 12 Chapter 12," no. page 114, pp. 46–48, 2007.

[61] M. Pope, H. P. Kallmann, and P. Magnante, "Electroluminescence in Organic Crystals," *J. Chem. Phys.*, vol. 38, no. 8, pp. 2042–2043, 1963.

[62] C. W. Tang and S. A. VanSlyke, "Organic electroluminescent diodes," *Appl. Phys. Lett.*, vol. 51, no. 12, pp. 913–915, 1987.

[63] M. S. Sarif Ullah Patwary, "Smart Textiles and Nano-Technology: A General Overview," *J. Text. Sci. Eng.*, vol. 05, no. 01, pp. 1–7, 2015.

[64] T. A. Khattab, M. Rehan, Y. Hamdy, and T. I. Shaheen, "Facile Development of Photoluminescent Textile Fabric via Spray Coating of Eu(II)-Doped Strontium Aluminate," *Ind. Eng. Chem. Res.*, vol. 57, no. 34, pp. 11483–11492, 2018.

[65] E. Lempa, A. Kitzig, E. Naroska, M. Rabe, and B. Neukirch, "Alternative light therapy with luminescent textiles," *Curr. Dir. Biomed. Eng.*, vol. 3, no. 2, pp. 461–463, 2017.

[66] L. Szuster, M. Kaźmierska, and I. Król, "Fluorescent dyes destined for dyeing high-visibility polyester textile products," *Fibres Text. East. Eur.*, vol. 12, no. 1, pp. 70–75, 2004.

[67] S. Rossi, A. Quaranta, L. Tavella, F. Deflorian, and A. M. Compagnoni, *Innovative Luminescent Vitreous Enameled Coatings*. Elsevier Inc., 2015.

[68] S. N. Iyer, N. Behary, J. Guan, and V. Nierstrasz, "Toward Bioluminescent Materials by Plasma Treatment of Micro fi brous Nonwovens , Followed by Immobilization of One or Both Enzyme (s) (Luciferase and FMN Reductase) Involved in Luminescent Bacteria," 2020.

[69] J. W. Lee, "BIOLUMINESCENCE ," no. January, 2017.

[70] 2 and James F. Case3 Steven H.D. Haddock,1 Mark A. Moline, "Bioluminescence in the Sea," *Ann. Rev. Mar. Sci.*, vol. 5, no. 9, pp. 207–236, 2010.

[71] O. Shimomura, "BIOLUMINESCENCE - Chemical Principles and Methods," *Biolumin. - Chem. Princ. Methods*, pp. 1–29, 2006.

[72] T. Kahlke and K. D. L. Umbers, "Bioluminescence," *Curr. Biol.*, vol. 26, no. 8, pp. R313–R314, 2016.

[73] I. Lin, T. Shih, and T. Chan, "BIOLUMINESCENT EMISSIONS OF THE DEEP-WATER PANDALID SHRIMP , HETEROCARPUS SIBOGAE DE MAN , 1917 (DECAPODA , BY In the marine environment , a variety of organisms is able to produce light , a phenomenon known as bioluminescence (see review in Herring , 1," vol. 1917, no. 3, pp. 341–350, 1917.

[74] S. Inoue, H. Kakoi, and T. Goto, "Oplophorus luciferin, bioluminescent substance of the decapod shrimps, Oplophorus spinosus and Heterocarpus laevigatus," *J. Chem. Soc. Chem. Commun.*, no. 24, pp. 1056–1057, 1976.

[75] O. SHIMOMURA, F. H. JOHNSON, and Y. SAIGA, "Extraction, purification and properties of aequorin, a bioluminescent," *J. Cell. Comp. Physiol.*, vol. 59, no. 165, pp. 223–239, 1962.

[76] J. M. Kendall and M. N. Badminton, "Aequorea victoria bioluminescence moves into an exciting new era," *Trends in Biotechnology*. 1998.

[77] https://microbewiki.kenyon.edu/index.php/Vibrio_fischeri, "firefly." .

[78] Y. Nakajima, K. Kobayashi, K. Yamagishi, T. Enomoto, and Y. Ohmiya, "cDNA cloning and characterization of a secreted luciferase from the luminous Japanese ostracod, Cypridina noctiluca," *Biosci. Biotechnol. Biochem.*, vol. 68, no. 3, pp. 565–570, 2004.

[79] Http://awesomeocean.com/guest-columns/beautiful-electrifying-jellyfish-earth/, "jellyfish." .

[80] S. Hosseinkhani, "Molecular enigma of multicolor bioluminescence of firefly luciferase," *Cellular and Molecular Life Sciences*. 2011.

[81] W. Duane and J. W. Hastings, "Flavin mononucleotide reductase of luminous bacteria," *Molecular and Cellular Biochemistry*. 1975.

[82] R. Rawat and D. D. Deheyn, "Evidence that ferritin is associated with light production in the mucus of the marine worm Chaetopterus," *Sci. Rep.*, 2016.

[83] H. B. Park *et al.*, "Bright Green Biofluorescence in Sharks Derives from Bromo-Kynurenine Metabolism," *iScience*, vol. 19, no. August, pp. 1291–1336, 2019.

[84] T. L. Danielson, S. Obeidat, G. D. Rayson, D. M. Anderson, E. L. Fredrickson, and R. E. Estell, "Photoluminescent distinction among plant life forms using phosphate buffered saline extract solutions," *Appl. Spectrosc.*, vol. 60, no. 7, pp. 800–807, 2006.

[85] A. V. Moroz, V. V. Davydov, V. Y. Rud, Y. V. Rud, V. C. Shpunt, and A. P. Glinushkin, "Photoluminescence of plant leaves during high-temperature treatment," *J. Phys. Conf. Ser.*, vol. 1135, no. 1, 2018.

[86] P. Lamichhane, P. N. Paudel, and B. P. Kafle, "Optical absorbance and fluorescence of natural dyes: Prospect of application in dye sensitized solar cell and OLEDs," *Res. J. Pharm. Biol. Chem. Sci.*, vol. 6, no. 5, pp. 823–828, 2015.

[87] R. M. Christie, K. M. Morgan, and M. S. Islam, "Molecular design and synthesis of N-arylsulfonated coumarin fluorescent dyes and their application to textiles," *Dye. Pigment.*, vol. 76, no. 3, pp. 741–747, 2008.

[88] E. H. Anouar, C. P. Osman, J. F. F. Weber, and N. H. Ismail, "UV/Visible spectra of a series of natural and synthesised anthraquinones: Experimental and quantum chemical approaches," *Springerplus*, vol. 3, no. 1, pp. 1–12, 2014.

[89] S. Bhattacharyya, S. Datta, B. Mallick, P. Dhar, and S. Ghosh, "Lutein content and in vitro antioxidant activity of different cultivars of Indian marigold flower (Tagetes patula l.) extracts," *J. Agric. Food Chem.*, vol. 58, no. 14, pp. 8259–8264, 2010.

[90] S. Siriamornpun, O. Kaisoon, and N. Meeso, "Changes in colour, antioxidant activities and carotenoids (lycopene, β-carotene, lutein) of marigold flower (Tagetes erecta L.) resulting from different drying processes," *J. Funct. Foods*, vol. 4, no. 4, pp. 757–766, 2012.

[91] M. Šivel, S. Kráčmar, M. Fišera, B. Klejdus, and V. Kubáň, "Lutein content in marigold flower (Tagetes erecta L.) concentrates used for production of food supplements," *Czech J. Food Sci.*, vol. 32, no. 6, pp. 521–525, 2014.

[92] O. Pes, A. Midlik, J. Schlaghamersky, M. Zitnan, and P. Taborsky, "A study on bioluminescence and photoluminescence in the earthworm Eisenia lucens," *Photochem. Photobiol. Sci.*, vol. 15, no. 2, pp. 175–180, 2016.

[93] P. Perego, L. Fanara, M. Zilli, and M. Del Borghi, "Applications of Luminous Bacteria on Environmental Monitoring," *Chem. Biochem. Eng. Q.*, vol. 16, no. 2, pp. 87–92, 2002.

[94] I. Denisov, K. Lukyanenko, A. Yakimov, I. Kukhtevich, E. Esimbekova, and P. Belobrov, "Disposable luciferase-based microfluidic chip for rapid assay of water pollution," *Luminescence*, pp. 1–17, 2018.

[95] Q. Gui, T. Lawson, S. Shan, L. Yan, and Y. Liu, "The Application of Whole Cell-Based Biosensors for Use in Environmental Analysis and in Medical Diagnostics," *Sensors*, 2017.

[96] G. Shama and D. J. Malik, "The uses and abuses of rapid bioluminescence-based ATP assays," *Int. J. Hyg. Environ. Health*, vol. 216, no. 2, pp. 115–125, 2013.

[97] M. Kobayashi *et al.*, "Establishment and Characterization of Transplantable, Luminescence Labeled Rat Renal Cell Carcinoma Cell Lines," *J. Urol.*, vol. 183, no. 5, pp. 2029–2035, 2010.

[98] S. A. Hasson *et al.*, "Chemogenomic profiling of endogenous PARK2 expression using a genome-edited coincidence reporter," *ACS Chem. Biol.*, vol. 10, no. 5, p. 1188—1197, May 2015.

[99] J. Vieira, L. P. Da Silva, and J. C. G. E. Da Silva, "Advances in the knowledge of light emission by firefly luciferin and oxyluciferin," *Journal of Photochemistry and Photobiology B: Biology*. 2012.

[100] S. Sharifian, A. Homaei, R. Hemmati, R. B. Luwor, and K. Khajeh, "The emerging use of bioluminescence in medical research," *Biomed. Pharmacother.*, vol. 101, no. January, pp. 74–86, 2018.

[101] R. Sharma, "The Role of Photoluminescent Pigments in Textiles," *Trends Text. Eng. Fash. Technol.*, vol. 2, no. 2, pp. 1–7, 2018.

[102] K. Jia and R. E. Ionescu, "Measurement of Bacterial Bioluminescence Intensity and Spectrum : Current Physical Techniques and Principles," no. May 2015, pp. 19–45, 2016.

[103] U. Tamayo and G. Vargas, "Biomimetic economy: human ecological-economic systems emulating natural ecological systems," *Soc. Responsib. J.*, vol. 15, no. 6, pp. 772–785, 2019.

[104] O. Speck and T. Speck, "An Overview of Bioinspired and Biomimetic Self-Repairing Materials," *Biomimetics*, vol. 4, no. 1, p. 26, 2019.

[105] A. Mohamed *et al.*, "Activity of enzymes immobilized on plasma treated polyester," *J. Mol. Catal. B Enzym.*, vol. 134, no. December, pp. 261–272, 2016.

[106] X. Zhang, *Antistatic and conductive textiles*. Woodhead Publishing Limited, 2011.

[107] R. Morent and N. De Geyter, *Improved textile functionality through surface modifications*. Woodhead Publishing Limited, 2011.

[108] M. Neisius, T. Stelzig, S. Liang, and S. Gaan, *Flame retardant finishes for textiles*. Woodhead Publishing Limited, 2015.

[109] S. Giraud *et al.*, "Flame retarded polyurea with microencapsulated ammonium phosphate for textile coating," *Polym. Degrad. Stab.*, vol. 88, no. 1, pp. 106–113, 2005.

[110] J. C. Roy, A. Ferri, S. Giraud, G. Jinping, and F. Salaün, "Chitosan–carboxymethylcellulose-based polyelectrolyte complexation and microcapsule shell formulation," *Int. J. Mol. Sci.*, vol. 19, no. 9, 2018.

[111] L. J. Zheng, H. D. Zheng, B. Du, J. Wei, S. H. Gao, and J. Zhang, "Dyeing Procedures of Polyester Fiber in Supercritical Carbon Dioxide Using a Special Dyeing Frame," *J. Eng. Fiber. Fabr.*, vol. 10, no. 4, pp. 37–46, 2015.

[112] L. Miah, N. Ferdous, and M. M. Azad, "Textiles Material Dyeing with Supercritical Carbon Dioxide (CO2) without using Water," *Chem. Mater. Res.*, vol. 3, no. 5, pp. 2224–2226, 2013.

[113] S. M. Shang, *Process control in dyeing of textiles*. Woodhead Publishing Limited, 2012.

[114] M. Clark, *Handbook of Textile and Industrial Dyeing: Principles, Processes and Types of Dyes Volume 1,Principles, processes and types of dyes*, vol. 1. Woodhead Publishing Ltd, 2011.

[115] N. R. Haddaway, J. McConville, and M. Piniewski, "How is the term 'ecotechnology' used in the research literature? A systematic review with thematic synthesis," *Ecohydrol. Hydrobiol.*, vol. 18, no. 3, pp. 247–261, 2018.

[116] A. Zille, F. R. Oliveira, and P. A. P. Souto, "Plasma treatment in textile industry," *Plasma Process. Polym.*, vol. 12, no. 2, pp. 98–131, 2015.

[117] A. Sparavigna, "Plasma treatment advantages for textiles."

[118] S. K. Malik, S. Kadian, and S. Kumar, "Advances in ink-jet printing technology of textiles," *Indian

J. Fibre Text. Res., vol. 30, no. 1, pp. 99–113, 2005.

[119] B. Tawiah, E. K. Howard, and B. K. Asinyo, "the Chemistry of Inkjet Inks for Digital Textile Printing - Review," *Int. J. Manag. Inf. Technol. Eng.*, vol. 4, no. 5, pp. 61–78, 2016.

[120] X. Li, J. Chen, B. Liu, X. Wang, D. Ren, and T. Xu, "Inkjet Printing for Biofabrication," *3D Print. Biofabrication*, pp. 283–301, 2018.

[121] T. T. Biswas, J. Yu, and V. A. Nierstrasz, *Inkjetting of enzymes*. Elsevier Ltd, 2019.

[122] J. Li, F. Rossignol, and J. Macdonald, "Inkjet printing for biosensor fabrication: Combining chemistry and technology for advanced manufacturing," *Lab Chip*, vol. 15, no. 12, pp. 2538–2558, 2015.

[123] M. Singh, H. M. Haverinen, P. Dhagat, and G. E. Jabbour, "Inkjet printing-process and its applications," *Adv. Mater.*, vol. 22, no. 6, pp. 673–685, 2010.

[124] B. Derby, "Inkjet Printing of Functional and Structural Materials: Fluid Property Requirements, Feature Stability, and Resolution," *Annu. Rev. Mater. Res.*, vol. 40, no. 1, pp. 395–414, 2010.

[125] J. C. É Soares, P. R. Í Cia Moreira, A. Catarina Queiroga, J. É Morgado, F. Xavier Malcata, and M. E. Pintado, "Application of immobilized enzyme technologies for the textile industry: a review."

[126] M. M.M., "The Art of Immobilization Using Biopolymers, Biomaterials and Nanobiotechnology," *Biotechnol. Biopolym.*, no. June 2011, 2011.

[127] H. Mohamed, T. Tamer M, and O. Ahmed M, "Methods of Enzyme Immobilization," *Int. J. Curr. Pharm. Rev. Res.*, vol. 7, no. 6, pp. 385–392, 2016.

[128] A. A. Homaei, R. Sariri, F. Vianello, and R. Stevanato, "Enzyme immobilization: An update," *J. Chem. Biol.*, vol. 6, no. 4, pp. 185–205, 2013.

[129] "Comparative study of immobilized and soluble NADH_FMN-oxidoreductase-luciferase coupled enzyme system."

[130] S. Opperskalski, S. Siew, E. Tan, and L. Truscott, "Preferred Fiber & Materials Market Report 2019," 2019.

[131] C. Vigneswaran, M. Ananthasubramanian, and P. Kandhavadivu, "Bioprocessing of synthetic fibres," *Bioprocess. Text.*, pp. 189–250, 2014.

[132] C. W. Kan, *Plasma treatments for sustainable textile processing*. Elsevier Ltd., 2015.

[133] A. Pourmohammadi, "Nonwoven materials and joining techniques," *Join. Text. Princ. Appl.*, pp. 565–581, 2013.

[134] I. Holme, *Coloration of Technical Textiles*, Second Edi., vol. 1. Elsevier Ltd., 2016.

[135] J. W. S. Hearle, "Textile Fibers: A Comparative Overview," *Encycl. Mater. Sci. Technol.*, pp. 9100–9116, 2001.

[136] T. O. Baldwin *et al.*, "Structure of bacterial luciferase," *Curr. Opin. Struct. Biol.*, 1995.

[137] H. Koike *et al.*, ."8 A Ê Crystal Structure of the Major NAD(P)H:FMN Oxidoreductase of a Bioluminescent Bacterium, Vibrio fischeri: Overall Structure, Cofactor and Substrate-analog Binding, and Comparison with Related Flavoproteins."

[138] V. Takke, N. Behary, A. Perwuelz, and C. Campagne, "Studies on the Atmospheric Air – Plasma Treatment of PET (Polyethylene Terephtalate) Woven Fabrics : Effect of Process Parameters and of Aging," 2009.

[139] L. G. B. Mutel, P. Goudmand, "DESIGN OF LARGE VOLUME COLD REMOTE PLASMA REACTOR. RELATION BETWEEN THE FUNCTIONALIZATION AND THE ADHESION

QUALITY OF POLYPROPYLENE SURFACES TREATED BY A REMOTE NITROGEN PLASMA," 1995, pp. 167–172.

[140] K. Gotoh, A. Yasukawa, and K. Taniguchi, "Water contact angles on poly(ethylene terephthalate) film exposed to atmospheric pressure plasma," *J. Adhes. Sci. Technol.*, vol. 25, no. 1–3, pp. 307–322, 2011.

[141] T. Homola, L. Y. L. Wu, and M. Černák, "Atmospheric plasma surface activation of poly(ethylene Terephthalate) film for roll-to-roll application of transparent conductive coating," *J. Adhes.*, vol. 90, no. 4, pp. 296–309, 2014.

[142] F. Leroux, A. Perwuelz, C. Campagne, and N. Behary, "Atmospheric air-plasma treatments of polyester textile structures," *J. Adhes. Sci. Technol.*, vol. 20, no. 9, pp. 939–957, 2006.

[143] Z. austria 2018 chromojet tabletop Printer, "Leitfaden Rezepturen Herstellung Chromo-Jet HSV800 for digital functionalization," 2020.

[144] T. Shakespeare and J. Shakespeare, "A fluorescent extension to the Kubelka-Munk model," *Color Res. Appl.*, vol. 28, no. 1, pp. 4–14, 2003.

[145] L. Rong, G. Feng, C. Jiangnin, and C. Donghui, "Quantum efficiency of fluorescent dyes in cloth Coloration Technology," *Color. Technol.*, vol. 118, no. 5, pp. 250–255, 2002.

[146] L. J. Kricka, G. K. Wienhausen, J. E. Hinkley, and M. [De Luca], "Automated bioluminescent assays for NADH, glucose 6-phosphate, primary bile acids, and ATP," *Anal. Biochem.*, vol. 129, no. 2, pp. 392–397, 1983.

[147] K. A. Lukyanenko *et al.*, "Analytical Enzymatic Reactions in Microfluidic Chips," *Appl. Biochem. Microbiol.*, vol. 53, no. 7, 2017.

[148] R. Szittner, G. Jansen, D. Y. Thomas, and E. Meighen, "Bright stable luminescent yeast using bacterial luciferase as a sensor," *Biochem. Biophys. Res. Commun.*, vol. 309, no. 1, pp. 66–70, Sep. 2003.

[149] S. E. Medvedeva, N. A. Tyulkova, A. M. Kuznetsov, and E. K. Rodicheva, "Bioluminescent Bioassays Based on Luminous Bacteria," *J. Sib. Fed. Univ. (Biol.)*, vol. 2, no. 4, pp. 418–452, 2009.

[150] E. N. Esimbekova, R. Ranjan, I. G. Torgashina, and V. A. Kratasyuk, "Bioluminescent System of Luminous Bacteria for Detection of Microbial Contamination," vol. 11, no. 2, pp. 174–180, 2018.

[151] E. Brodl, A. Winkler, and P. Macheroux, "Molecular Mechanisms of Bacterial Bioluminescence," *Comput. Struct. Biotechnol. J.*, vol. 16, pp. 551–564, 2018.

[152] E. Jablonski and M. DeLuca, "Immobilization of bacterial luciferase and FMN reductase on glass rods.," *Proc. Natl. Acad. Sci. U. S. A.*, vol. 73, no. 11, pp. 3848–51, 1976.

[153] E. N. Esimbekova, V. A. Kratasyuk, and I. G. Torgashina, "Disk-shaped immobilized multicomponent reagent for bioluminescent analyses: Correlation between activity and composition," *Enzyme Microb. Technol.*, vol. 40, no. 2, pp. 343–346, 2007.

[154] F. Jia, B. Narasimhan, and S. Mallapragada, "Materials-Based Strategies for Multi-Enzyme Immobilization and Co-Localization : A Review," vol. 9999, no. xxx, pp. 1–14, 2013.

[155] N. Behary, A. Perwuelz, C. Campagne, D. Lecouturier, P. Dhulster, and A. S. Mamede, "Adsorption of surfactin produced from Bacillus subtilis using nonwoven PET (polyethylene terephthalate) fibrous membranes functionalized with chitosan," *Colloids Surfaces B Biointerfaces*, vol. 90, pp. 137–143, 2012.

[156] J. C. Makemson and J. W. Hastings, "Bovine serum albumin interacts with bacterial luciferase.," *J. Biolumin. Chemilumin.*, vol. 6, no. 2, pp. 131–136, 1991.

[157] A. Bezrukikh, E. Esimbekova, E. Nemtseva, V. Kratasyuk, and O. Shimomura, "Gelatin and starch as stabilizers of the coupled enzyme system of luminous bacteria NADH:FMN-oxidoreductase-luciferase," *Anal. Bioanal. Chem.*, 2014.

[158] J. M. Guisan, J. M. Bolivar, F. López-Gallego, and J. Rocha-Martín Editors, *Immobilization of Enzymes and Cells Methods and Protocols Fourth Edition Methods in Molecular Biology 2100*. 2020.

[159] E. N. Esimbekova, A. E. Govorun, V. I. Lonshakova-Mukina, and V. A. Kratasyuk, "Gelatin and Starch: What Better Stabilizes the Enzyme Activity?," *Dokl. Biol. Sci.*, vol. 491, no. 1, pp. 43–46, 2020.

[160] N. N. Ugarova and O. V. Lebedeva, "Immobilized bacterial luciferase and its applications," *Appl. Biochem. Biotechnol.*, vol. 15, no. 1, pp. 35–51, 1987.

[161] M. Fischer and A. Bacher, "Biosynthesis of vitamin B_2 in plants," *Physiol. Plant.*, vol. 126, pp. 304–318, 2006.

[162] W. D. Lienhart, V. Gudipati, and P. MacHeroux, "The human flavoproteome," *Arch. Biochem. Biophys.*, vol. 535, no. 2, pp. 150–162, 2013.

[163] T. Udhayabanu, A. Manole, M. Rajeshwari, P. Varalakshmi, H. Houlden, and B. Ashokkumar, "Riboflavin Responsive Mitochondrial Dysfunction in Neurodegenerative Diseases," *J. Clin. Med.*, vol. 6, no. 5, p. 52, 2017.

[164] K. Hitomi *et al.*, "Functional motifs in the (6-4) photolyase crystal structure make a comparative framework for DNA repair photolyases and clock cryptochromes," *Proc. Natl. Acad. Sci. U. S. A.*, vol. 106, no. 17, pp. 6962–6967, 2009.

[165] K. P. Stahmann, J. L. Revuelta, and H. Seulberger, "Three biotechnical processes using Ashbya gossypii, Candida famata, or Bacillus subtilis compete with chemical riboflavin production," *Appl. Microbiol. Biotechnol.*, vol. 53, no. 5, pp. 509–516, 2000.

[166] M. Sikorski, E. Sikorska, F. Wilkinson, and R. P. Steer, "Studies of the photophysics and spectroscopy of alloxazine and related compounds in solution," no. March 2014, 1999.

[167] W. Holzer *et al.*, "Photo-induced degradation of some flavins in aqueous solution," *Chem. Phys.*, vol. 308, no. 1–2, pp. 69–78, 2005.

[168] M. A. Sheraz, S. H. Kazi, S. Ahmed, Z. Anwar, and I. Ahmad, "Photo, thermal and chemical degradation of riboflavin," *Beilstein J. Org. Chem.*, vol. 10, pp. 1999–2012, 2014.

[169] S. N. Iyer, N. Behary, V. Nierstrasz, and J. Guan, "Study of photoluminescence property on cellulosic fabric using multifunctional biomaterials riboflavin and its derivative Flavin mononucleotide," *Sci. Rep.*, no. February, pp. 1–16, 2019.

[170] H. Sigel, B. Song, G. Liang, R. Halbach, M. Felder, and M. Bastian, "Acid-base and metal ion-binding properties of flavin mononucleotide (FMN2-). Is a 'dielectric' effect responsible for the increased complex stability?," *Inorganica Chim. Acta*, vol. 240, no. 1–2, pp. 313–322, 1995.

[171] A. Bennick, "I NTERACTION OF P LANT P OLYPHENOLS," vol. 13, no. 2, pp. 184–196, 2002.

[172] I. Ahmad, M. A. Sheraz, S. Ahmed, S. H. Kazi, T. Mirza, and M. Aminuddin, "Stabilizing effect of citrate buffer on the photolysis of riboflavin in aqueous solution," *Results Pharma Sci.*, vol. 1, no. 1, pp. 11–15, 2011.

[173] S. Astanov, M. Z. Sharipov, A. R. Fayzullaev, E. N. Kurtaliev, and N. Nizomov, "Spectroscopic study of photo and thermal destruction of riboflavin," *J. Mol. Struct.*, vol. 1071, no. 1, pp. 133–138, 2014.

[174] M. Y. Berezin and S. Achilefu, "Fluorescence Lifetime Measurements and Biological Imaging,"

Chem. Rev., vol. 110, no. 5, pp. 2641–2684, 2010.

[175] I. Iqbal and M. M. Rahman, "OPTIMIZATION OF PARAMETERS OF COTTON FABRIC WHITENESS," no. December, 2014.

[176] J. A. Rivera and J. G. Eden, "Flavin mononucleotide bio[1] J. A. Rivera and J. G. Eden, 'Flavin mononucleotide biomolecular laser: longitudinal mode structure, polarization, and temporal characteristics as probes of local chemical environment,' Opt. Express, vol. 24, no. 10, p. 10858," *Opt. Express*, vol. 24, no. 10, p. 10858, 2016.

[177] I. Ahmad, Z. Anwar, S. A. Ali, K. A. Hasan, M. A. Sheraz, and S. Ahmed, "Ionic strength effects on the photodegradation reactions of riboflavin in aqueous solution," *J. Photochem. Photobiol. B Biol.*, vol. 157, pp. 113–119, 2016.

[178] H. Grajek, I. Gryczynski, P. Bojarski, Z. Gryczynski, S. Bharill, and L. Kułak, "Flavin mononucleotide fluorescence intensity decay in concentrated aqueous solutions," *Chem. Phys. Lett.*, vol. 439, no. 1–3, pp. 151–156, 2007.

[179] G. Coppel, M. Andersson, P. Edström, and J. Kinnunen, "Limitations in the efficiency of fluorescent whitening agents in uncoated paper," *Nord. Pulp Pap. Res. J.*, vol. 26, no. 3, pp. 319–328, 2012.

[180] S. Salzmann, V. Martinez-junza, B. Zorn, S. E. Braslavsky, C. M. Marian, and W. Gärtner, "Photophysical properties of structurally and electronically modified flavin derivatives determined by spectroscopy and theoretical calculations Supporting Information (SI) Molecular orbitals and vertical absorption energies in vacuum and different solve," vol. 145, pp. 9365–9375, 2009.

[181] W. M. Moore, J. C. McDaniels, and J. A. Hen, "the Photochemistry of Riboflavin—Vi. the Photophysical Properties of Isoalloxazines," *Photochem. Photobiol.*, vol. 25, no. 6, pp. 505–512, 1977.

[182] D. Saravanan, "UV PROTECTION TEXTILE MATERIALS," vol. 7, no. 1, pp. 11–18, 2007.

[183] D. Machado *et al.*, "Irradiated Riboflavin Diminishes the Aggressiveness of Melanoma In Vitro and In Vivo," *PLoS One*, vol. 8, no. 1, pp. 1–12, 2013.

[184] M. Ge, X. Guo, and Y. Yan, "Preparation and study on the structure and properties of rare-earth luminescent fiber," *Text. Res. J.*, vol. 82, no. 7, pp. 677–684, 2012.

[185] Y. Yu, J. Wang, Y. Zhu, and M. Ge, "Researches on preparation and properties of polypropylene nonwovens containing rare earth luminous materials," *J. Rare Earths*, 2014.

[186] F. Logerfo, "Chapter 7 MODIFICATION OF POLYESTER FOR MEDICAL USES," pp. 91–92, 2006.

[187] C. R. Madhu and M. C. Patel, "Reactive Dye Printing on Cotton with Natural and Synthetic Thickeners," *Int. Res. J. Eng. Technol.*, vol. 3, no. 3, p. 1418, 2016.

[188] S. M. R. Billah, *Textile Coatings*. 2019.

[189] D. V. Gulnov, E. V. Nemtseva, and V. A. Kratasyuk, "Contrasting relationship between macro- and microviscosity of the gelatin- and starch-based suspensions and gels," *Polym. Bull.*, vol. 73, no. 12, pp. 3421–3435, 2016.

[190] H. N. Shsh and a V Rao, "Rheological Properties of Sodium Alginate," *Indian J. Technol.*, vol. 7, no. 8, p. 261, 1969.

[191] G. H. Elgemeie, K. A. Ahmed, E. A. Ahmed, M. H. Helal, and D. M. Masoud, "A simple approach for the synthesis of coumarin fluorescent dyes under microwave irradiation and their application in textile printing," *Pigment Resin Technol.*, vol. 45, no. 4, pp. 217–224, 2016.

[192] V. Popescu *et al.*, "Sustainable and cleaner microwave-assisted dyeing process for obtaining eco-

friendly and fluorescent acrylic knitted fabrics," *J. Clean. Prod.*, vol. 232, pp. 451–461, 2019.

[193] I. Dumitrescu, P. S. Vankar, J. Srivastava, A. N. A. Maria Mocioiu, and O. G. Iordache, "Dyeing of cotton, silk and wool with Bixa orellana in the presence of enzymes," *Ind. Textila*, vol. 63, no. 6, pp. 327–333, 2012.

[194] R. Morent, N. De Geyter, J. Verschuren, K. De Clerck, P. Kiekens, and C. Leys, "Non-thermal plasma treatment of textiles," vol. 202, pp. 3427–3449, 2008.

[195] Y. Zhou, J. Yu, T. T. Biswas, R. C. Tang, and V. Nierstrasz, "Inkjet Printing of Curcumin-Based Ink for Coloration and Bioactivation of Polyamide, Silk, and Wool Fabrics," *ACS Sustain. Chem. Eng.*, vol. 7, no. 2, pp. 2073–2082, 2019.

[196] H. A. El-Wahab, M. M. El-Molla, and L. Lin, "Preparation and characterisation of ink formulations for jet printing on nylon carpet," *Pigment Resin Technol.*, vol. 39, no. 3, pp. 163–169, 2010.

[197] R. A. Sheldon, "Metrics of Green Chemistry and Sustainability: Past, Present, and Future," *ACS Sustain. Chem. Eng.*, vol. 6, no. 1, pp. 32–48, 2018.

[198] I. Holme, "9 - Coloration of technical textiles," in *Handbook of Technical Textiles (Second Edition)*, Second Edi., A. R. Horrocks and S. C. Anand, Eds. Woodhead Publishing, 2016, pp. 231–284.

[199] S. Ghisla, V. Massey, J. M. Lhoste, and S. G. Mayhew, "Fluorescence and Optical Characteristics of Reduced Flavines and Flavoproteins," *Biochemistry*, vol. 13, no. 3, pp. 589–597, 1974.

[200] J. R. Albani, "Chapter 2 - Fluorescence: Principles and Observables," in *Structure and Dynamics of Macromolecules: Absorption and Fluorescence Studies*, J. R. Albani, Ed. Amsterdam: Elsevier Science, 2004, pp. 55–98.

[201] M. Abramowitz and M. W. Davidson, "Overview of Fluorescence Excitation and Emission Fundamentals," *Olympus Microsc. Resour. Cent.*, vol. 1, no. 01 December 2008, pp. 1–4, 2008.

[202] Y. L. Pan *et al.*, "Dynamics of photon-induced degradation and fluorescence in riboflavin microparticles," *Appl. Phys. B Lasers Opt.*, vol. 72, no. 4, pp. 449–454, 2001.

[203] I. Ahmad and F. H. M. Vaid, "Chapter 2 Photochemistry of Flavins in Aqueous and Organic Solvents," in *Flavins: Photochemistry and Photobiology*, vol. 6, The Royal Society of Chemistry, 2006, pp. 13–40.

[204] K. Makdoumi, *Ultraviolet Light A (UVA) Photoactivation of Riboflavin as a Potential Therapy for Infectious Keratitis*. 2011.

[205] D. S. Morais, R. M. Guedes, and M. A. Lopes, "Antimicrobial approaches for textiles: From research to market," *Materials (Basel).*, vol. 9, no. 6, pp. 1–21, 2016.

[206] A. Ahgilan, V. Sabaratnam, and V. Periasamy, "Antimicrobial properties of vitamin B2," *Int. J. Food Prop.*, vol. 19, no. 5, pp. 1173–1181, 2016.

[207] G. SM and H. HM, "UV Protection Properties of Cotton, Wool, Silk and Nylon Fabrics Dyed with Red Onion Peel, Madder and Chamomile Extracts," *J. Text. Sci. Eng.*, vol. 6, no. 4, 2016.

[208] A. K. Sarkar, "An evaluation of UV protection imparted by cotton fabrics dyed with natural colorants," *BMC Dermatol.*, vol. 4, pp. 1–8, 2004.

[209] T. Agnhage *et al.*, "Bioactive and multifunctional textile using plant-based madder dye: Characterization of UV protection ability and antibacterial activity," *Fibers Polym.*, vol. 18, no. 11, pp. 2170–2175, 2017.

[210] S. G. Baldursdóttir, A. L. Kjøniksen, J. Karlsen, B. Nyström, J. Roots, and H. H. Tønnesen, "Riboflavin-photosensitized changes in aqueous solutions of alginate. Rheological studies,"

Biomacromolecules, vol. 4, no. 2, pp. 429–436, 2003.

[211] A. M. Edwards, "Structure and General Properties of Flavins," in *Flavins and Flavoproteins: Methods and Protocols*, S. Weber and E. Schleicher, Eds. New York, NY: Springer New York, 2014, pp. 3–13.

[212] M. Sikorski, E. Sikorska, I. V Khmelinskii, R. Gonzalez-moreno, J. L. Bourdelande, and A. Siemiarczuk, "Photophysics of lumichrome on cellulose," vol. 156, pp. 267–271, 2003.

[213] I. Ahmad, Q. Fasihullah, and F. H. M. Vaid, "Effect of light intensity and wavelengths on photodegradation reactions of riboflavin in aqueous solution," *J. Photochem. Photobiol. B Biol.*, vol. 82, no. 1, pp. 21–27, 2006.

[214] I. Ahmad, Z. Anwar, S. A. Ali, K. A. Hasan, M. A. Sheraz, and S. Ahmed, "Ionic strength effects on the photodegradation reactions of riboflavin in aqueous solution," *J. Photochem. Photobiol. B Biol.*, vol. 157, pp. 113–119, Apr. 2016.

[215] L. G. Coppel, M. Andersson, and P. Edström, "Determination of quantum efficiency in fluorescing turbid media," *Appl. Opt.*, vol. 50, no. 17, pp. 2784–2792, 2011.

[216] C. Callewaert, E. De Maeseneire, F. M. Kerckhof, A. Verliefde, T. Van de Wiele, and N. Boon, "Microbial odor profile of polyester and cotton clothes after a fitness session," *Appl. Environ. Microbiol.*, vol. 80, no. 21, pp. 6611–6619, 2014.

[217] L. Affatato and C. Carfagna, "Smart Textiles: A Strategic Perspective of Textile Industry," *Adv. Sci. Technol.*, vol. 80, pp. 1–6, 2012.

[218] M. Kahoush, *Eco-Technologies for Immobilizing Redox Enzymes on Conductive Textiles , for Sustainable Development Doctoral dissertation by*. .